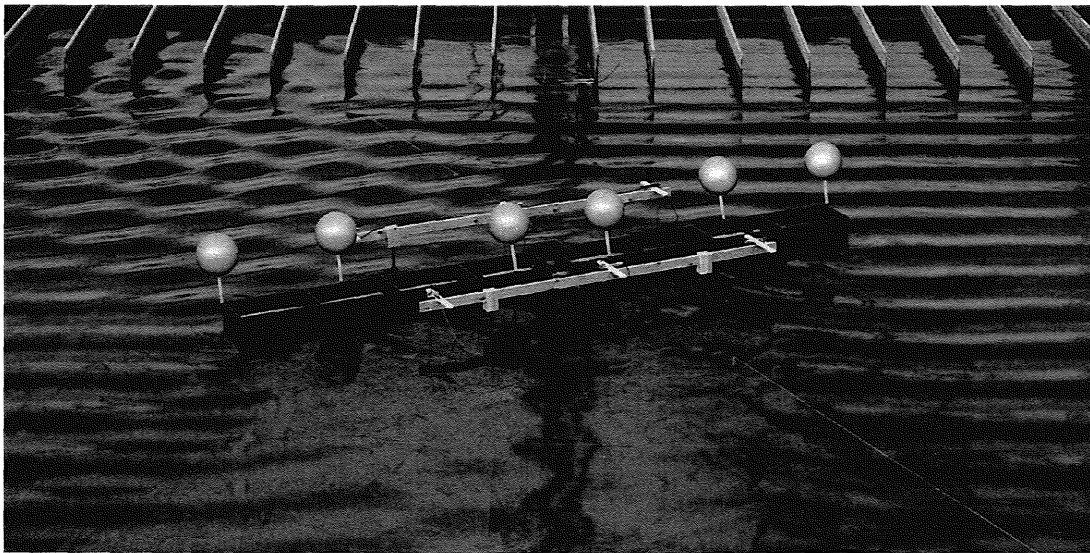


CHALMERS



Wave-Induced Loads and Ship Motions

Lars Bergdahl

Department of Civil and Environmental Engineering
Division of Water Environment Technology
CHALMERS UNIVERSITY OF TECHNOLOGY
Göteborg, Sweden, 2009
Report No. 2009:1

CHALMERS
Water Environment Technology

Wave-Induced Loads
and
Ship Motions

by
Lars Bergdahl

Department of Civil and Environmental Engineering
Division of Water Environment Technology
CHALMERS UNIVERSITY OF TECHNOLOGY
Report No. 2009:1
ISSN 1652-9162

Postal address: Chalmers, 412 96 Göteborg, Sweden
Visiting address: Sven Hultins gata 8
Telephone: +46 31 772 2155
Fax: +46 31 772 2128
email: lars.bergdahl@chalmers.se

| | | |
|------|---|-----|
| 6.4 | The Pitch Problem Using Strip Theory..... | 84 |
| 6.5 | The Roll Problem..... | 89 |
| 6.6 | Forward-Speed Effect..... | 97 |
| 6.7 | Resonance Frequencies..... | 98 |
| 6.8 | Derived Responses..... | 99 |
| 6.9 | Coupled Linear Pitch and Heave Motion at Forward Speed. | 106 |
| 6.10 | Coupled Pitch and Heave Motion at Zero Speed Including Non-Linear Viscous Damping..... | 108 |
| 6.11 | Equivalent Linearised Drag Damping | 111 |
| 7 | WIND WAVES..... | 113 |
| 7.1 | Characteristics of Wind Waves..... | 114 |
| 7.2 | Fourier Analysis..... | 117 |
| 7.3 | Amplitude Spectra and Phase Spectra | 119 |
| 7.4 | Synthesised Waves | 131 |
| 7.5 | Short Term Statistics..... | 134 |
| 7.6 | Extremes in a Sea State..... | 138 |
| 8 | Wave statistics..... | 141 |
| 8.1 | The Concept of Risk | 141 |
| 8.2 | Design Approaches | 143 |
| 8.3 | Long term wave statistics | 146 |
| 9 | RESPONSES OF A SHIP IN IRREGULAR WAVES | 155 |
| 9.1 | The ship as a mechanical filter | 155 |
| 9.2 | The Heave Motion in Irregular Waves | 155 |
| 9.3 | The Pitch Response..... | 160 |
| 9.4 | The Response of Vertical Motion at Station x..... | 161 |
| 9.5 | Accelerations, seasickness and human performance | 163 |
| 9.6 | Motions of moored ships in harbours | 165 |
| | Recommended allowed limits of motions for safe mooring conditions | 165 |
| | Recommended allowed limits of motions for safe working conditions | 166 |
| 9.7 | Green water and propeller or bottom emergence..... | 167 |
| 9.8 | Probability of Slamming..... | 169 |
| 10 | References | 173 |

1. INTRODUCTION

Traditionally the sea keeping properties of ships have been considered of second importance to the fuel consumption for cargo ships and forward speed for faster passenger ships. Knowledge of vertical motions and accelerations are however important for estimating loads on cargo and equipment as well as the possibility for the crew to work safely. The accelerations may also cause seasickness to crew and passengers. The relative motion between the ship and the water surface is important, especially in severe sea states, to investigate the risk of "green water" on deck, propeller emergence and slamming. In the offshore industry, on the other hand, the sea-keeping properties are the most important properties, as these properties are decisive for the usefulness of floating platforms. The "downtime" when one cannot drill, have oil-exporting lines (risers) connected to the sea floor, moor service or living quarters platforms close to fixed or other floating production platforms, exchange cargo with supply ships nor even stay on station must be as short as possible. Therefore, over the past decades, considerable advances have been achieved in the theoretical prediction of motions of floating platforms and ships, and in computer algorithms. The development of computer processing capacity has made this development also useful in practice.

Three-dimensional approaches were thus first developed for the analysis of large fixed or floating offshore structures with complex shapes (Faltinsen and Michelsenⁱ, 1974) and has later been extended to predicting the motion of ships travelling at forward speed in deep or shallow water. However, for traditional ship problems the faster two-dimensional "strip theory", which was initially put forward by Korvin-Kroukovsky and Jacobs, 1957ⁱⁱ and was later developed by other authors, is still used extensively and has been proven by both model tests and full scale trials to predict ship motions in a seaway with acceptable accuracy. It is especially used for conceptual design and risk assessment procedures (Jensen *et al.* 2004ⁱⁱⁱ). Since it is relatively simple and easy to understand this strip theory approach is used for the assignments in this course while some insight is given in the 3D approach. Much of the framework is common for the two methods.

The first part of the course will be devoted to the theory of regular waves and responses to these. However the natural seaway is always irregular, and an irregular wave system can approximately be thought of as a superposed sum of an infinite number of regular sinusoidal waves, each of which is characterized by frequency, amplitude, direction of propagation and a random phase angle. Under the assumption that the motion response to the waves is linear, the superposition method can be utilized also for the sea loads and the ship motions. This assumption is valid for moderately steep waves. Thus once the response to regular waves has been assessed, the response of the ship in an irregular seaway can be determined.

The irregular seaway or sea state is often represented by a spectrum and by multiplication of this, for each frequency, with the linear response ratio in that frequency for e.g. motion a response spectrum of the motion can be produced. Thereafter statistical methods can be utilized to assess characteristics of responses in each sea state or in all anticipated sea states during e.g. 30 years.

For large or steep waves and large relative motions non-linear time-domain or non-linear frequency-domain methods^{iv} must be used, which is out of scope of this course. For completeness, however, some essential effects like viscous quadratic damping (very important in roll motion of ships and heave motion of offshore platforms), slamming and drift forces will be accounted.

The goal of the course is that the participants shall be able to self-dependently analyse wave-induced loads and sea-keeping properties of ships by help of advanced modern software. Necessary prerequisite to attain that goal are understanding of the physical phenomena, knowledge about used simplifying assumptions and some insight into the available mathematical or numerical tools. The means are lectures, literature study and foremost tutored exercises, relying on the conviction that what one just hears is easily forgotten, listening keenly might help to remember but what you do is understood.

The goal of this compendium is to inform about the background of the physics and mathematics of surface gravity waves, wave induced forces and motions. Some information of current and wind loads on moored ships or structures will also be added later, while the resistance to forward speed belongs to another field.

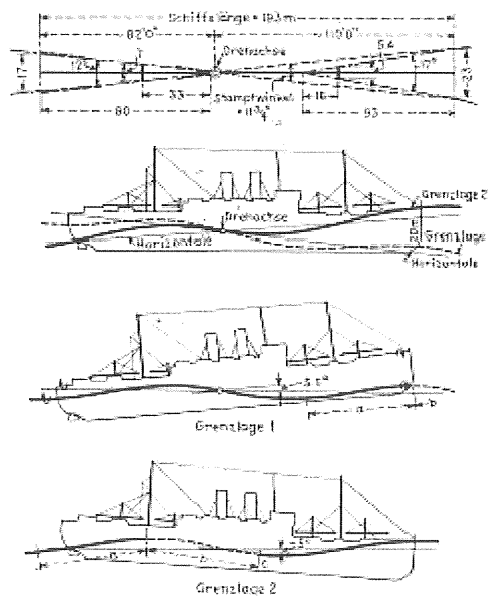


Figure 1.1 Maximum pitching and heaving of SS Hamburg in wave conditions that caused a speed reduction from 16 to 12 knots. (From Kempf and Hoppe, 1926)

1.1 Ship Motions in Waves

A ship with steady forward speed in irregular short-crested sea will oscillate in six degrees of freedom. In the simplified case of steady speed in meeting or following regular waves the ship will heave (vertical motion), pitch (tilting motion) and surge (bow-aft motion) around its mean forward advancing position. In very long waves its motion will just follow the sea surface motion but for shorter waves – near the vertical heave and pitch resonances of respective motion – the motion will be strongly amplified and out of phase with sea surface motion. For somewhat shorter waves the motions will be opposed to the wave motion but less amplified, so when the crest of the wave passes the ship the ship will be at its lowest position, and when the wave

slopes forward the ship will slope backwards with obvious consequences for risk of green water and propeller emergence. See Fig 1.1.

1.2 Calculation Chain

The chain of calculations to assess the sea-keeping properties of a ship is outlined in Figure 1.2.

- a) Gathering of wave data for the route where the ship will operate. Weather data may be taken from archived observations, satellite observations or be “hindcasted” by wave generation models from historical meteorological data. New measurements may be started to check the results from the wave-generation models.
- b) Settling design-weather conditions.
- c) Choosing and applying some adequate wave theory.
- d) Applying an adequate method for the hydrodynamic forces and reactions of the ship or structure.
- e) Calculate the response motions
- f) And finally derive the load effects i.e. sectional forces and moments, tensions, risk for propeller emergence, slamming and green water. For moored ships and structures also the mooring-line tensions are derived.

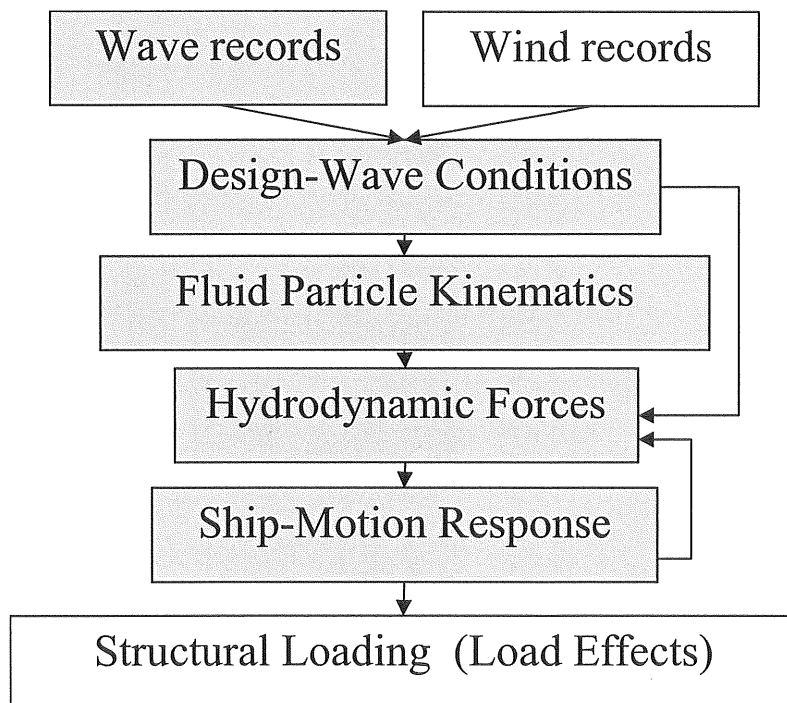


Figure 1.2 Calculation Chain

1.3 On Wave-Induced Forces

One may say that there are two fundamentally different ways to calculate wave-induced forces on structures in the sea. In one method one considers the structure as a whole and assesses the total wave force from empirical or computed coefficients applied on water velocities and accelerations in the undistorted wave motion. In the other method the pressure distribution around the surface of the structure is computed with due consideration to the water motion distorted by the structure itself, and subsequently integrated around the structure.

In both cases some mathematical model for describing the wave properties is necessary. For instance, by making the simplified assumption that the wave motion can be regarded as potential flow, velocities, accelerations and water motion can be computed in any point under a gravity surface wave by a scalar quantity, the velocity potential. In Chapter 4 some basics of potential flow theory will be given and in Chapter 5 it will be used to derive kinematics of linear waves.

2 EQUATION OF MOTION

For hydrodynamic purposes a floating body can mostly be regarded as rigid but moving. It then exhibits six motional degrees of freedom. See Figure 2.1, where also the co-ordinate system used in this compendium is shown. Such a space-fixed, right-handed co-ordinate system is usually oriented with respect to the position of the body in rest. Its origin is either placed in the centre of gravity of the body or in the still water surface vertically above the centre of gravity as is chosen here. Usually the z-axis is vertical and points upwards, the x-axis points horizontally forward, as in Figure 2.1. Some authors and computer codes defines the z-axis vertical but pointing downwards and the x-axis pointing horizontally forwards. In both these cases the y-axis is pointing to portside. For large displacements one may need also body-fitted moving co-ordinate systems.

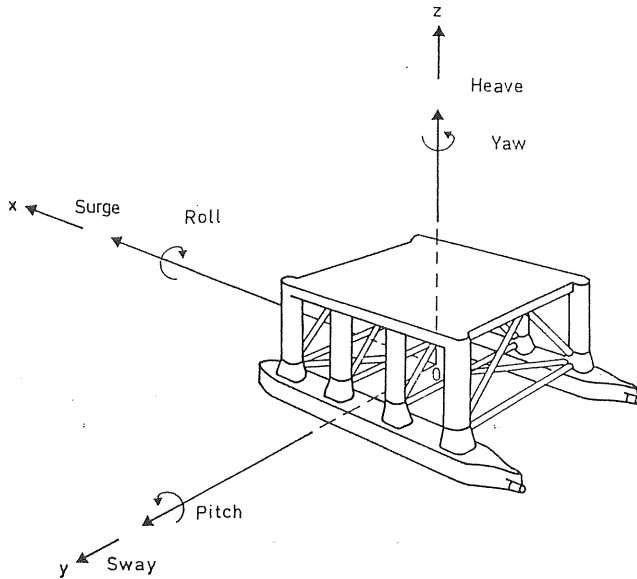


Figure 2.1 Motional degrees of freedom. (Courtesy GVAC)

The six oscillating motions of a floating body have established names in English but lack this in some other languages, see Figure 2.1 and Table 2.1.

Table 2.1 Names of the motional degrees of freedom

| Legend | English | Swedish | Norwegian | Dutch |
|----------|---------|---------|-----------|-----------|
| η_1 | surge | | jage | schrikken |
| η_2 | sway | (svaja) | svaie | verzetten |
| η_3 | heave | håva | hive | dompen |
| η_4 | roll | rulla | rulle | slingeren |
| η_5 | pitch | stampa | stampe | stampen |
| η_6 | yaw | (gira) | (gire) | (gieren) |

Symbolically the equation of motion of a floating body can be written

$$\mathbf{M}\ddot{\underline{\eta}} = \underline{F} \quad \dots(2.1)$$

where \mathbf{M} is a mass matrix

$\underline{\eta} = (\eta_1 \ \eta_2 \ \eta_3 \ \eta_4 \ \eta_5 \ \eta_6)^T$ a vector of positions in the six degrees of freedom
 $\underline{\ddot{\eta}} = d^2 \underline{\eta} / dt^2$ body acceleration and
 $\underline{F} = (F_1 \ F_2 \ F_3 \ F_4 \ F_5 \ F_6)^T = (F_x \ F_y \ F_z \ M_x \ M_y \ M_z)^T$ vector forces and moments acting on the body.

Usually the 6×6 mass matrix for a ship has the structure:

$$\mathbf{M} = \begin{bmatrix} m & 0 & 0 & 0 & mz_G & 0 \\ 0 & m & 0 & -mz_G & 0 & 0 \\ 0 & 0 & m & 0 & 0 & 0 \\ 0 & -mz_G & 0 & I_4 & 0 & -D_{46} \\ mz_G & 0 & 0 & 0 & I_5 & 0 \\ 0 & 0 & 0 & -D_{64} & 0 & I_6 \end{bmatrix} \quad \dots(2.2)$$

where m is the mass of the ship

z_G the vertical coordinate of the centre of gravity of the ship
 $I_4, I_5,$ and I_6 the moments of inertia around the x, y and z axes and
 $D_{46},$ and D_{64} the moments of deviation of the ship.

Normally the masses of the ship should be arranged so that the moments of deviations are approximately zero.

The force vector \underline{F} can be split into the exciting forces, the reaction forces from the water and from moorings if any. Neglecting, for the time being, other exciting forces than the wave excited forces a convenient split of the forces are:

$$\underline{F} = \underline{F}_e + \underline{F}_r + \underline{F}_{rs} \quad \dots(2.3)$$

where \underline{F}_e contains the wave-excited forces on the fixed structure

\underline{F}_r the hydrodynamic reaction forces from the water on the moving body in the absence of the waves

\underline{F}_{rs} reaction forces from the mooring system

The hydrodynamic reaction forces \underline{F}_r i.e. the hydrodynamic properties of the body is in the linear approximation characterised by three properties, namely:

- A hydrodynamic mass or added mass
- B hydrodynamic damping or radiation damping coefficients
- C hydrostatic stiffness

The hydrodynamic reaction force can then be written:

$$\underline{F}_r = -\mathbf{A}\underline{\ddot{\eta}} - \mathbf{B}\underline{\dot{\eta}} - \mathbf{C}\underline{\eta} \quad \dots(2.4)$$

Substituting Eq. (2.3) and Eq. (2.4) into Eq. (2.1) the following simple expression results:

$$(\mathbf{M} + \mathbf{A})\ddot{\underline{\eta}} + \mathbf{B}\dot{\underline{\eta}} + \mathbf{C}\underline{\eta} = \underline{F}_e + \underline{F}_{rs} \quad \dots(2.5)$$

\mathbf{M} , \mathbf{A} , \mathbf{B} and \mathbf{C} in Eq. (2.5) are all 6×6 matrices with the elements M_{ij} , A_{ij} , B_{ij} och C_{ij} ($i = 1, 2, \dots, 6, j = 1, 2, \dots, 6$).

A floating body with arbitrary form can exhibit hydrodynamic reactions in all degrees of freedom i caused by motion in any direction j . For bodies at zero speed the hydrodynamic reaction matrices are symmetrical. For bodies with starboard/port-side symmetry, approximate fore/aft symmetry and the origin of the coordinate system in the water surface above the centre of gravity of the displacement as in Figure 2.1, the matrices \mathbf{A} , \mathbf{B} and \mathbf{C} containing respectively the added masses, radiation-damping coefficients and hydrostatic stiffnesses have the structures

$$\mathbf{A} = \begin{bmatrix} A_{11} & 0 & 0 & 0 & A_{15} & 0 \\ 0 & A_{22} & 0 & A_{24} & 0 & 0 \\ 0 & 0 & A_{33} & 0 & 0 & 0 \\ 0 & A_{42} & 0 & A_{44} & 0 & 0 \\ A_{51} & 0 & 0 & 0 & A_{55} & 0 \\ 0 & 0 & 0 & 0 & 0 & A_{66} \end{bmatrix} \quad \dots(2.6)$$

$$\mathbf{B} = \begin{bmatrix} B_{11} & 0 & 0 & 0 & B_{15} & 0 \\ 0 & B_{22} & 0 & B_{24} & 0 & 0 \\ 0 & 0 & B_{33} & 0 & 0 & 0 \\ 0 & B_{42} & 0 & B_{44} & 0 & 0 \\ B_{51} & 0 & 0 & 0 & B_{55} & 0 \\ 0 & 0 & 0 & 0 & 0 & B_{66} \end{bmatrix} \quad \dots(2.7)$$

$$\mathbf{C} = \begin{bmatrix} 0 & 0 & 0 & 0 & 0 & 0 \\ 0 & 0 & 0 & 0 & 0 & 0 \\ 0 & 0 & C_{33} & 0 & C_{53} & 0 \\ 0 & 0 & 0 & C_{44} & 0 & 0 \\ 0 & 0 & C_{53} & 0 & C_{55} & 0 \\ 0 & 0 & 0 & 0 & 0 & 0 \end{bmatrix} \quad \dots(2.8)$$

Linear reaction forces from e.g. the mooring system can be included in the coefficient matrices \mathbf{A} , \mathbf{B} and \mathbf{C} above, while non-linear reaction forces must be included in the right-hand side of the equation of motion.

For bodies floating in the water surface or bodies being submerged but close to the water surface, the hydrodynamic properties **A** and **B** are functions of the frequency of the motion, which is caused by the generation of waves around the body. Then Eq. (2.5) can be easily solved only for cases when the excitation is a harmonic function.

2.1 The Motion of a Point on a Body

The motion of a point $\underline{r}^T = (x, y, z)$ on a body can for small rotations $\underline{\Omega}^T = (\eta_4, \eta_5, \eta_6)$ (less than 10 degrees or 0.2 rad) be written:

$$\underline{s} = \begin{pmatrix} \eta_1 \\ \eta_2 \\ \eta_3 \end{pmatrix} + \underline{\Omega} \times \underline{r} \quad \dots(2.9)$$

which explicitly in the chosen co-ordinate system is

$$\underline{s} = \begin{pmatrix} \eta_1 + z\eta_5 - y\eta_6 \\ \eta_2 - z\eta_4 + x\eta_6 \\ \eta_3 + y\eta_4 - x\eta_5 \end{pmatrix} \quad \dots(2.10)$$

The velocities and accelerations of the same point is likewise

$$\underline{\dot{s}} = \begin{pmatrix} \dot{\eta}_1 \\ \dot{\eta}_2 \\ \dot{\eta}_3 \end{pmatrix} + \underline{\dot{\Omega}} \times \underline{r} \quad \text{and} \quad \underline{\ddot{s}} = \begin{pmatrix} \ddot{\eta}_1 \\ \ddot{\eta}_2 \\ \ddot{\eta}_3 \end{pmatrix} + \underline{\ddot{\Omega}} \times \underline{r} \quad \dots(2.11) \text{ and } (2.12)$$

For large angles of rotation these simple expressions are not valid but more complicated expressions must be made like those in the manoeuvring compendium.

Example 2.1

Assume that a ship is moving in a closed elliptical orbit in the x-z plane without pitching.

($\eta_2 = \eta_4 = \eta_5 = \eta_6 = 0$). The orbit is described by

$$\underline{\eta} = \begin{pmatrix} \eta_1 \\ \eta_3 \end{pmatrix} = \begin{pmatrix} \hat{\eta}_1 \cos(\omega t) \\ \hat{\eta}_3 \sin(\omega t) \end{pmatrix}$$

The constant buoyancy force is balanced by the weight of the body. The sum of all varying forces acting on the platform must then be given by the following simple equation of motion.

$$\underline{F} = \begin{bmatrix} m & 0 \\ 0 & m \end{bmatrix} \frac{d^2}{dt^2} \begin{pmatrix} \eta_1 \\ \eta_3 \end{pmatrix}$$

Assume that the displacement of the ship is 2 500 tonnes (1 tonne = 1000 kg) the heave amplitude 2.5 m, the surge amplitude 5 m and the wave period 17 s.

Determine the exciting force as a function of time.

3 MOTION RESPONSE TO THE LOADING

The loads on a platform or ship can be constant in time, transient i.e. of short duration or harmonic. Irregular or random loads from e.g. sea waves can to a first, linear approximation be treated as a superposition of harmonic loads. The responses are fundamentally different for the three types of loads.

To clearly illustrate this we will in this chapter use a simple, one-degree-of-freedom system as in Figure 3.1.

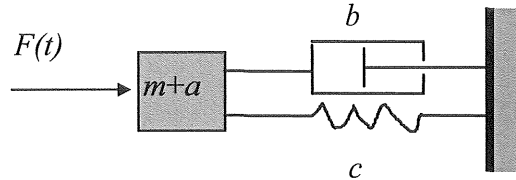


Figure 3.1 A mechanical system with one degree of freedom, mass, m , added mass, a , damping coefficient, b , and spring stiffness, c .

The equation of motion for this system can be written

$$(m + a)\ddot{x} + b\dot{x} + cx = F(t) \quad \dots(3.1)$$

For bodies in water the mass inertia is increased by an "added mass", a , or hydrodynamic mass. This is a result of the fact that to accelerate the body it is also necessary to accelerate the water surrounding the body. For submerged bodies close to the water surface the added mass can be negative, but for deeply submerged bodies it is always positive.

The content in this chapter is meant as a repetition of fundamental mechanics of vibration, more thoroughly given in some fundamental textbooks e.g. books by Craig^v, Roberts and P. D. Spanos^{vi} or Thompson^{vii}. Some application on six-degree-of-freedom floating systems is given in the end of the chapter.

3.1 Free Vibration of a Floating Ship in Heave

Before the discussion of response to different types of loading we will repeat a little about the free vibrations of the one-degree-of-freedom system. The equation of motion for a ship in heave can be written

$$(m + a)\ddot{x} + b\dot{x} + cx = 0, \quad \dots(3.2)$$

which follows directly from Eq. (3.1) setting $F(t) = 0$.

Assuming a solution of the form

$$x = Ce^{st} \quad \dots(3.3)$$

we get the characteristic equation

$$\kappa^2 + 2\xi\omega_N\kappa + \omega_N^2 = 0 \quad \dots(3.4)$$

where

$\omega_N = \sqrt{c/(m+a)}$ is the “natural” angular frequency, that is, the undamped angular frequency and
 $\xi = b/(2\sqrt{c(m+a)})$ the damping factor.

The roots of Eq. (3.4) are

$$\kappa_{1,2} = -\xi\omega_N \pm \omega_N\sqrt{\xi^2 - 1}. \quad \dots(3.5)$$

These roots are complex, zero or real depending on the value of ξ . The damping factor can thus be used to distinguish between three cases: underdamped ($0 < \xi < 1$), critically damped ($\xi = 1$) and overdamped ($\xi > 1$). See Fig. 3.2 for the motion of a body released from the position $x(0) = 1$ m at $t = 0$ s. The underdamped case displays an attenuating vertical oscillation, while the other cases display motions monotonously approaching the vertical equilibrium position. A floating ship in heave, roll and pitch would normally display underdamped characteristics with a damping factor of the order of 10^{-1} in heave and pitch and of the order of 10^{-2} in roll. In the horizontal degrees of freedom there are no stiffnesses so the horizontal motions do not exhibit resonant characteristics.

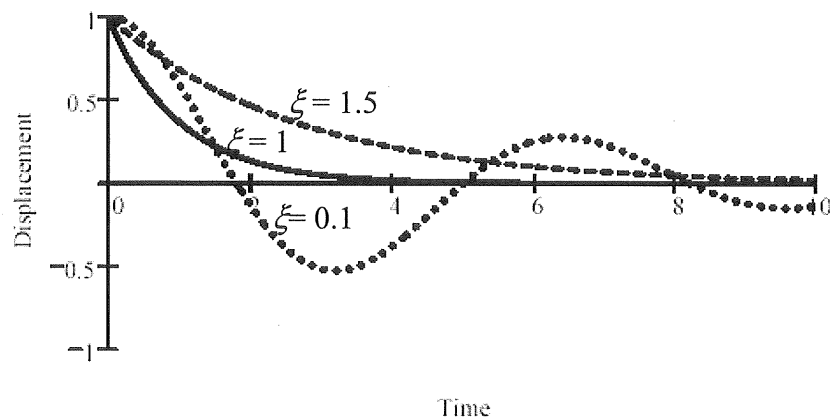


Figure 3.2 Response of a damped SDOF system with various damping ratios.

The damping factor is often called the damping ratio, as it is equal to the ratio between the current damping coefficient b and the critical damping coefficient $2\sqrt{c(m+a)}$.

3.2 Response to Constant Loads

A constant or static load F_o (see Figure 3.3) acting on the system in Figure 3.1 gives as response a displacement to a static equilibrium position, $x = x_o$, because the equation of motion Equation (3.1) gives $cx = F_o \Rightarrow x = F_o/c = x_o$ if F_o is constant, as \ddot{x} and \dot{x} must be identically zero.

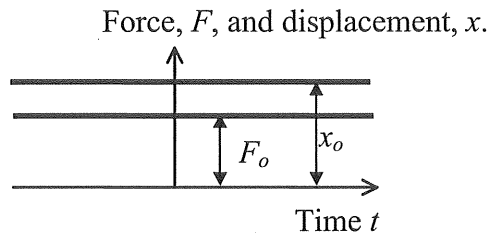


Figure 3.3 Static displacement or response x_o to a constant load F_o .

In dynamic problems one usually calculates the equilibrium position for constant, static loads first, and thereafter, new co-ordinates are defined from this static equilibrium position. Static loads can for instance be the weight of a ship in calm water balanced by the equally constant buoyancy to yield a specific draught, or wind and current forces acting on a moored platform giving a constant offset balanced by the mooring arrangement.

3.3 Response to Harmonic Loads

A harmonic load

$$F(t) = F_o \cos(\omega t) \quad \dots(3.6)$$

as from regular waves for instance gives a response of the same harmonic type:

$$x(t) = \hat{x} \cos(\omega t - \varepsilon). \quad \dots(3.7)$$

The motion $x(t)$ is the stationary response to the harmonic load and is the particular solution to Equation (3.1) with the right hand side $F(t)$ given by (3.6).

In (3.6) and (3.7)

F_o is the force amplitude

$\omega = 2\pi/T$ the angular frequency

T the time period

\hat{x} the amplitude of the displacement

and

ε the phase lag between the force and displacement.

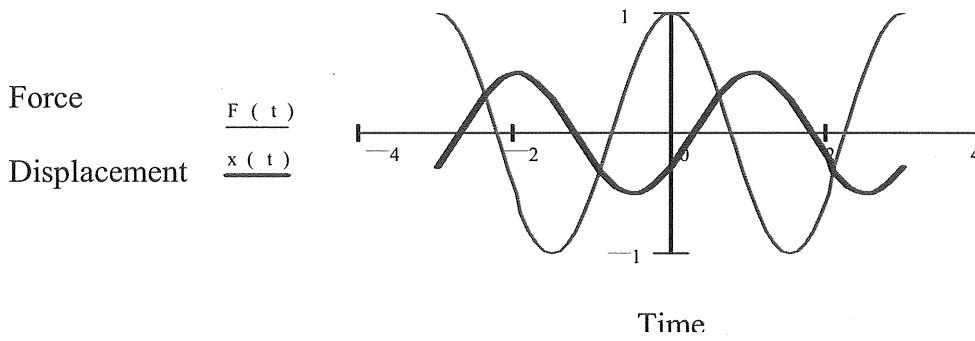


Figure 3.4 The exciting harmonic load $F(t)$ and the stationary Response, $x(t)$, for a linear system.

We can solve Equation (3.1) for the given harmonic load, Equation (3.6), simply by substituting the particular solution Equation (3.7) into it

$$(m+a)\ddot{x} + b\dot{x} + cx = F_o \cos(\omega t)$$

$$x = \hat{x} \cos(\omega t - \varepsilon)$$

$$\dot{x} = -\omega \hat{x} \sin(\omega t - \varepsilon)$$

$$\ddot{x} = -\omega^2 \hat{x} \cos(\omega t - \varepsilon)$$

The substitution gives

$$(c - (m+a)\omega^2)\hat{x} \cos(\omega t - \varepsilon) - b\omega \hat{x} \sin(\omega t - \varepsilon) = F_o \cos(\omega t)$$

Using the trigonometric expressions for sine and cosine of angle differences then yields:

$$(c - (m+a)\omega^2)\hat{x}(\cos(\omega t)\cos(\varepsilon) + \sin(\omega t)\sin(\varepsilon)) - b\omega \hat{x}(\sin(\omega t)\cos(\varepsilon) - \cos(\omega t)\sin(\varepsilon)) = F_o \cos(\omega t)$$

Identification and separation of terms with $\sin(\omega t)$ and $\cos(\omega t)$ gives

$$(c - (m+a)\omega^2)\hat{x} \sin(\varepsilon) - b\omega \hat{x} \cos(\varepsilon) = 0 \quad \dots(3.8)$$

and

$$(c - (m+a)\omega^2)\hat{x} \cos(\varepsilon) - b\omega \hat{x} \sin(\varepsilon) = F_o \quad \dots(3.9)$$

From Equation (3.8) follows directly

$$\tan(\varepsilon) = \frac{b\omega}{(c - (m+a)\omega^2)} \quad \dots(3.10)$$

i.e.

$$\varepsilon = \arctan \frac{b\omega}{c - (m+a)\omega^2}, \quad \dots(3.11)$$

where also the correct quadrant must be decided.

Squaring and adding Equation (3.8) and (3.9) gives after using the trigonometric unity

$$\hat{x}^2 \left\{ \left[c - (m+a)\omega^2 \right]^2 + b^2\omega^2 \right\} = F_o^2, \quad \dots(3.12)$$

and finally, as the amplitude, \hat{x} , by definition is positive,

$$\hat{x} = \frac{F_o}{\sqrt{\left\{ \left[c - (m+a)\omega^2 \right]^2 + b^2\omega^2 \right\}}} \quad \dots(3.13)$$

Amplitude response function, response amplitude operator and transfer function

The ratio \hat{x}/F_o is an amplitude response function and gives the ratio between the amplitude of the harmonic response to the amplitude of the harmonic disturbance that excited it. It is often denoted $T(\omega)$ and has in this example the dimension length/force (m/N).

$$T(\omega) = \frac{\hat{x}}{F_o} = \frac{1}{\sqrt{\left\{ \left[c - (m+a)\omega^2 \right]^2 + b^2\omega^2 \right\}}} \quad \dots(3.14)$$

It is sometimes also called transfer function, but the name transfer function should also encompass the phase lag. See further under complex notation. In sea keeping the special name *response amplitude operator*, RAO, is often used and denotes the ratio between the response amplitude of any studied variable to the wave amplitude. In some literature the RAO is defined as the square of the quantity used here. The word operator is used because the RAO is used to operate on the frequency spectrum of a sea state to produce a spectrum of motion, moment, stress etc.

Amplification factor

The ratio between the amplitude \hat{x} of the calculated harmonic response and the displacement, x_o , which the mass would have got under the constant load the same as the load amplitude, F_o , is known as the amplification factor and is always dimensionless.

$$Y(\omega) = \frac{\hat{x}}{x_o} = \frac{\hat{x}}{F_o/c} = \frac{\hat{x}c}{F_o} = \frac{c}{\sqrt{\left\{ \left[c - (m+a)\omega^2 \right]^2 + b^2\omega^2 \right\}}} \quad \dots(3.15)$$

This amplification factor is illustrated in Figure 3.5 together with the corresponding phase lag ε . In the Figure the frequency axis is nondimensionalised by the natural frequency, $N = \omega_N/(2\pi)$, which by definition is the frequency of the undamped

eigenvibration. Thus the abscissa, frequency axis, in Figure 3.5 is scaled in the nondimensionalised frequency

$$\Omega = f/N = \omega/\omega_N \quad \dots(3.16)$$

The Equation (3.15) can now be written

$$Y(\Omega) = \frac{c}{\sqrt{\left\{c - (m+a)(\omega_N \Omega)^2\right\}^2 + b^2(\omega_N \Omega)^2}} = \frac{1}{\sqrt{\left\{(1 - \Omega^2)^2 + \frac{b^2}{c^2}(\omega_N \Omega)^2\right\}}} \quad \dots(3.17)$$

and finally introducing also the damping ratio defined in Pragraph 3.1

$$Y(\Omega, \xi) = \frac{1}{\sqrt{\left\{(1 - \Omega^2)^2 + 4(\xi \Omega)^2\right\}}} \quad \dots(3.18)$$

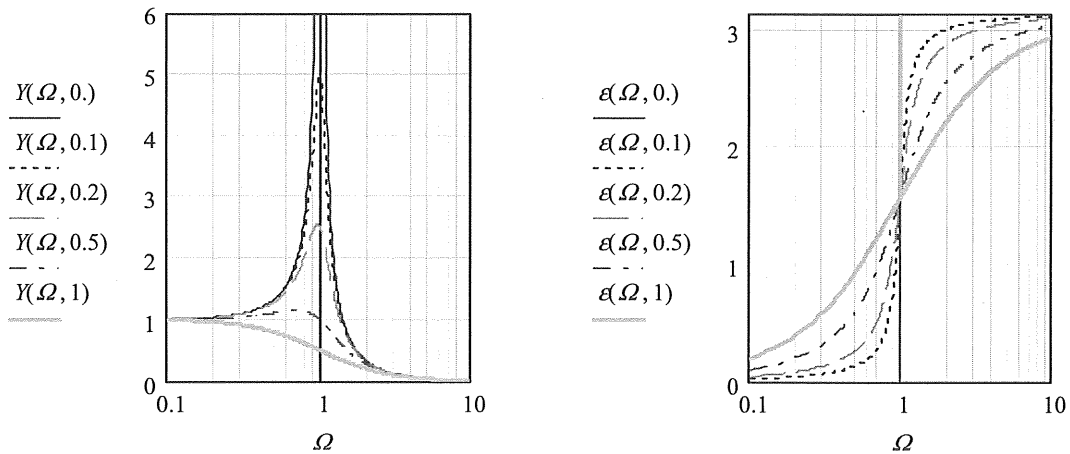


Figure 3.5 Amplification factor, $Y(\Omega, \xi)$, and phase lag, $\epsilon(\Omega, \xi)$, for a system with one degree of freedom. Ω is the non-dimensional frequency and ξ is the damping ratio.

Complex notation

It is often very convenient to use complex notation when treating harmonic oscillatory motion. In the equation of motion (3.1) the real valued driving force, $F(t)$, is then substituted by

$$F_c(t) = F_o e^{j\omega t} \quad \dots(3.19)$$

where thus the real driving force is

$$F(t) = \text{Re}(F_o e^{j\omega t}) = F_o \cos(\omega t) \quad \dots(3.20)$$

because

$$e^{j\omega t} = \cos(\omega t) + j \sin(\omega t) \quad \dots(3.21)$$

Observe that when analysing performed work, power etc. the real valued quantity, $F(t)$, must be used. Sticking to complex notation then the sum of, $F_c(t)$, and its complex conjugate can be used, which sum equals $2F(t)$. Here we will use $\text{Re}(F(t))$ when necessary.

The complex motion, $x_c(t)$, is then set to

$$x_c(t) = \hat{x}_c e^{j\omega t} = \hat{x} e^{-j\varepsilon} e^{j\omega t} = \hat{x} e^{j(\omega t - \varepsilon)}, \quad \dots(3.22)$$

with the complex “amplitude” containing the phase angle

$$\hat{x}_c = \hat{x} e^{-j\varepsilon}$$

and where as before the real motion is

$$x(t) = \text{Re}(x_c(t)) = \hat{x} \cos(\omega t - \varepsilon) \quad \dots(3.23)$$

The complex velocity and acceleration are

$$\dot{x}_c(t) = j\omega \hat{x}_c e^{j\omega t} \quad \dots(3.24)$$

$$\ddot{x}_c(t) = -\omega^2 \hat{x}_c e^{j\omega t} \quad \dots(3.25)$$

The equation of motion (3.1) was

$$(m+a)\ddot{x} + b\dot{x} + cx = F(t) \quad \dots(3.26)$$

Substituting (3.19) and (3.23) to (3.25) into (3.26) yields

$$-(m+a)\omega^2 \hat{x}_c e^{j\omega t} + jb\omega \hat{x}_c e^{j\omega t} + c\hat{x}_c e^{j\omega t} = F_o e^{j\omega t} \quad \dots(3.27)$$

Here we can divide both sides with $e^{j\omega t}$ and extract \hat{x}_c .

$$\hat{x}_c (c - (m+a)\omega^2 + jb\omega) = F_o \quad \dots(3.28)$$

$$\hat{x}_c(\omega) = \frac{F_o}{(c - (m+a)\omega^2 + jb\omega)} \quad \dots(3.29)$$

The complex amplification factor will now become

$$Y_c(\omega) = \frac{c}{c - (m+a)\omega^2 + jb\omega} = Y(\omega)e^{-j\varepsilon}, \quad \dots(3.30)$$

which includes both the amplification factor, $Y(\omega)$, and the phase lag, $\varepsilon(\omega)$. The amplification factor is given by the modulus of $Y_c(\omega)$ ($Y(\omega) = |Y_c(\omega)|$) and the phase lag by its argument ($\varepsilon(\omega) = \arg(Y_c(\omega))$)

Exercise 3.1

Confirm that this gives the same result as Equations (3.15) and (3.11).

The transfer function

The complex motion, $x_c(t)$, can now, with the use of Equations (3.22) and (3.29), be written:

$$x_c(t) = \hat{x}_c e^{j\omega t} = \frac{F_o e^{j\omega t}}{c - (m+a)\omega^2 + jb\omega}, \quad \dots(3.31)$$

but $F_c(t) = F_o e^{j\omega t}$ and thus

$$x_c(t) = \frac{1}{c - (m+a)\omega^2 + jb\omega} F_c(t) = T_c(\omega) F_c(t), \quad \dots(3.32)$$

i.e. the motion is for any regular frequency of excitation given by a complex multiplication of a transfer function, $T_c(\omega)$, and the driving force, $F_c(t)$.

A comparison with Equation (3.14) reveals that

$$T_c(\omega) = T(\omega)e^{-j\varepsilon} \quad \dots(3.33)$$

and thus the amplitude response function equals the modulus of the complex transfer function and the phase lag equals $\varepsilon(\omega) = \arg(T_c)$, i.e. $\arctan(\text{Im } T_c / \text{Re } T_c)$ with additional information of into which quadrant $T_c(\omega)$ points.

Response of a harmonic load on an initially fixed body

Note that the response to harmonic loads described above is valid only under the condition that the excitation and the response have been going on a long time, strictly speaking infinitely long time. If the body is let loose at time zero the response of the body will be composed of the transient response to the release and gradually approach the steady oscillatory motion as time goes by. Equivalently, the force can start abruptly at time zero, which will give exactly the same response. In Fig. 3.6 below the transient motion caused by a cosine excitation $F_o \cos(\omega t)$ started at time zero is illustrated. To make the difference even more clear a comparison between the steady-state oscillation and the transient response is shown in Fig. 3.7.

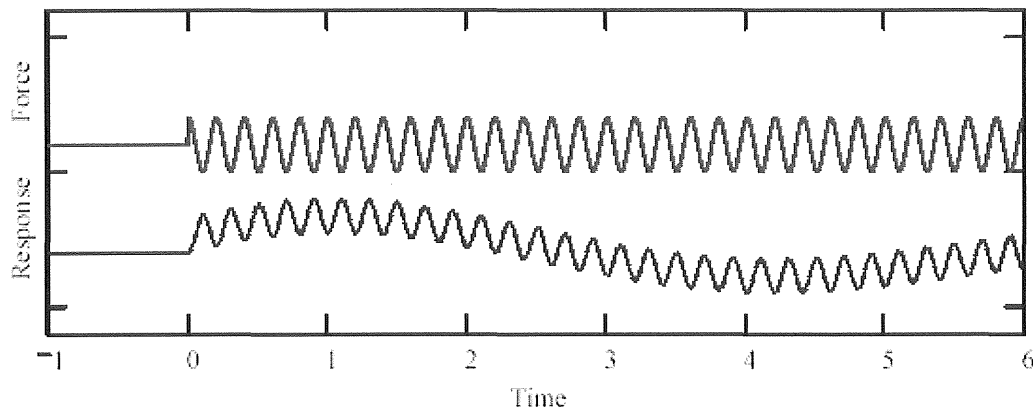


Figure. 3.6 The transient motion response of a one-degree-of-freedom system caused by a cosine excitation $F_o \cos(\omega t)$ started at time zero.

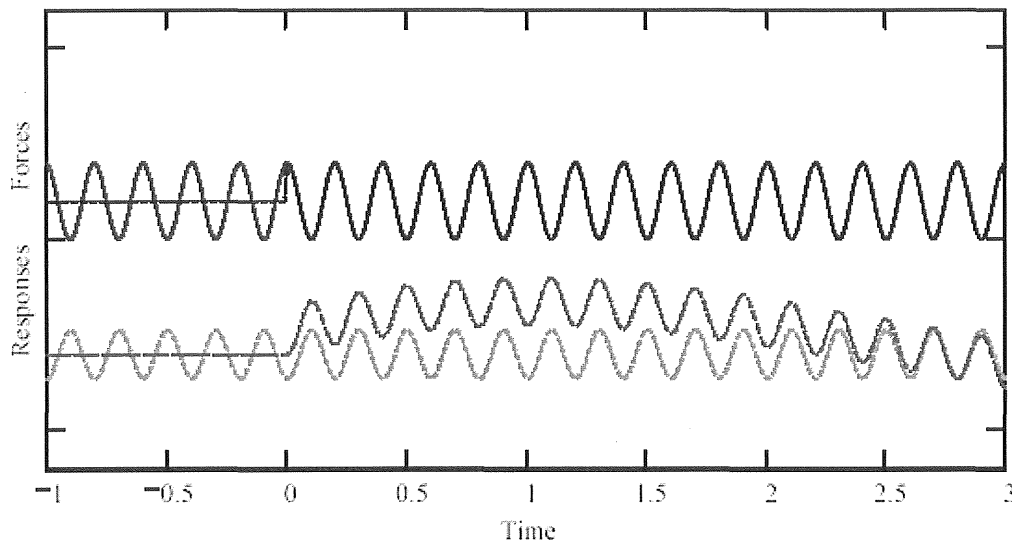


Figure. 3.7 Comparison in the time domain between the transient motion of Fig. 3.6 and steady-state oscillation for the same load amplitude.

The implication of the difference is that – strictly speaking – harmonic, frequency-domain responses must be applied with some caution for sea states of short duration. E.g. in tank tests for assessing “response amplitude operators” the transient in the test must be taken away by filtering the measuring signal. For ships this is most important for roll, and for moored ships or platforms it is also important in the horizontal degrees of freedom, for which resonances of the moored system may influence the response. For transient loads, it is thus important to be able to solve the problem in the time domain also. This can be done by direct time-integration methods as is illustrated for the six degree of freedom system in the end of this chapter, (Eq. 3.34), or by convolution techniques described in the next paragraph. Also for problems where non-linear damping or non-linear mooring characteristics are important time-domain solutions are necessary as will be shown later in Chapter XXX.

3.4 Transient Loads

A method to calculate the response motion, $x(t)$, caused by a transient excitation force, $F(t)$, is by use of the impulse response function, $w(t)$. Then any excitation can be treated that can be described by any finite function of time. For a floating body, where the added mass and radiation damping are functions of the oscillating frequency the result will be approximate but often useful if the characteristic frequency of the motion is selected with care.

The motion, $x(t)$, caused by an impulse, $F\Delta t$, is written

$$x(t) = w(t)F\Delta t \quad \dots(3.34)$$

where $w(t)$ is the transient motion due to a unit impulse, $F\Delta t = 1 \text{ Ns}$, as is illustrated in Figure 3.8.

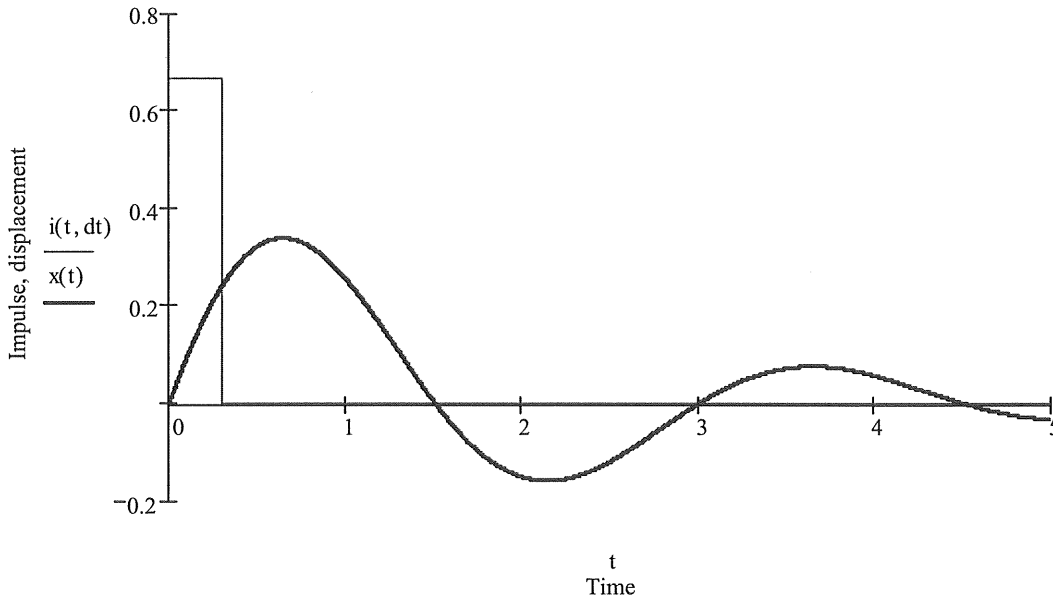


Figure 3.8 Sketch of a motion caused by a unit impulse.

The impulse is equivalent to giving the mass, $m + a$, the momentum, $\dot{x}_o(m + a) = F\Delta t$, at the point of time, $t = 0$. Thus with the initial condition, $\dot{x}_o = F\Delta t / (m + a)$, the solution to the homogeneous equation of motion, $(m + a)\ddot{x} + b\dot{x} + cx = 0$, is:

$$x(t) = \frac{\dot{x}_o}{\omega_r} e^{-bt/2(m+a)} \sin(\omega_r t) \quad \dots(3.35)$$

where ω_r is the damped frequency at resonance

$$\omega_r = \sqrt{c/(m+a) - b^2/4(m+a)^2} .$$

By comparison with (3.34) it is seen that

$$w(t) = \frac{1}{(m+a)\omega_r} e^{-bt/2(m+a)} \sin(\omega_r t) \quad \dots(3.36)$$

for $t \geq 0$ and $w(t) = 0$ for $t < 0$.

The motion caused by an arbitrary varying excitation function can be imagined as composed of a sum of responses, $F_i \Delta t w(t-i\Delta t)$, from a series of impulses, $F_i \Delta t$, approximating the excitation function, $F(t)$, i.e.

$$x(t) \approx \sum_{i=1}^k w(t-i\Delta t) F_i \Delta t \quad \dots(3.37)$$

In Figure 3.9 an approximation of a half-sine excitation by four impulses is shown and the sum of their response in Figure 3.10.

Now if Δt is allowed to be infinitely short $F_i (i \Delta t)$ approaches the continuous function, $F(t)$, and the response, Equation (3.27), approaches the integral

$$x(t) = \int_0^t w(t-\tau) F(\tau) d\tau, \quad \dots(3.38)$$

which is a convolution integral, hereditary integral or Duhamel's integral. In Figure 3.11 the result of an addition of 50 responses instead of four for the same approximated excitation function as in Figure 3.9. As can be seen the result is an almost smooth function, which can be shown to be close to that given by Equation (3.38).

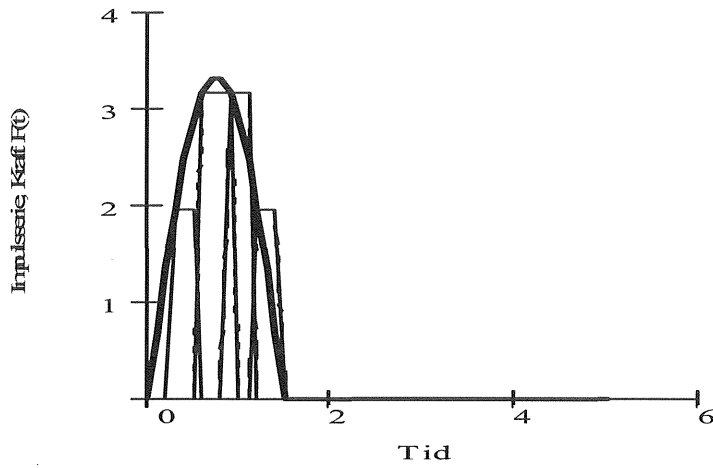


Figure 3.9 Approximation of $F(t)$ by four impulses.

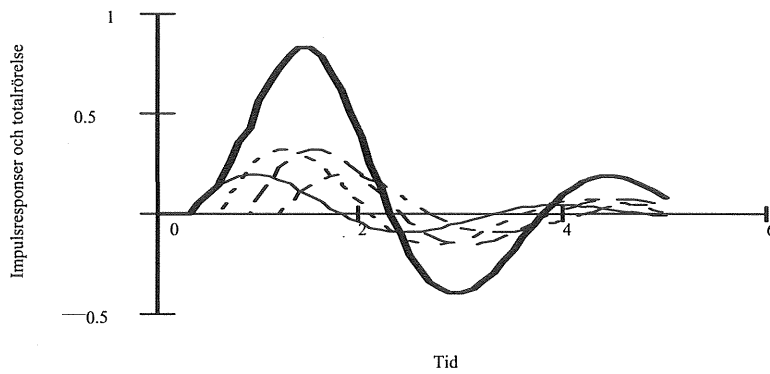


Figure 3.10 Illustration of how the responses of the four impulses are added to a resulting motion.

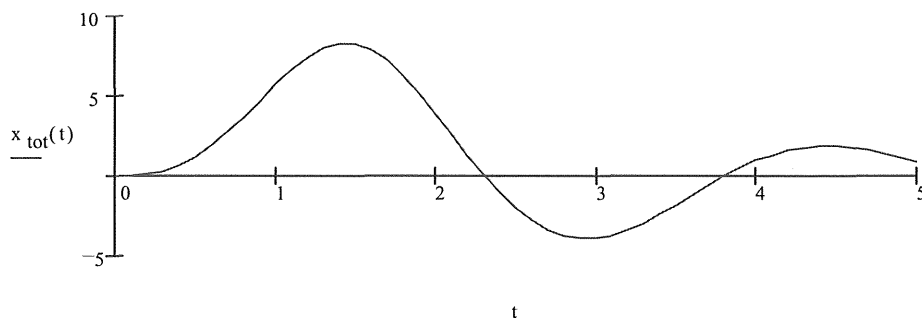


Figure 3.11 The result of the addition of fifty impulse responses to a resulting motion.

One can show that the impulse response function, $w(t)$, and the transfer function, $T_c(\omega)$, is related to each other in the following way

$$T_c(\omega) = \int_0^{\infty} w(t) e^{-j\omega t} dt \quad \dots(3.39)$$

and

$$w(t) = \frac{1}{2\pi} \int_{-\infty}^{\infty} T_c(\omega) e^{-j\omega t} d\omega \quad \dots(3.40)$$

$T_c(\omega)$ and $w(t)$ is then said to constitute a Fourier transform couple. If you know T_c then you can calculate $w(t)$ or vice versa.

Exercise 3.2

Show that Equation (3.39) gives T_c according to Equation (3.32) if $w(t)$ is given by Equation (3.36). Utilise that $\sin(\alpha) = j \sinh(j\alpha)$.

3.5 System with Six Degrees of Freedom

The motion in six degrees of freedom of a ship at zero speed can be described by the following six coupled equations of motion, which looks the same as (2.4):

$$(\mathbf{M} + \mathbf{A})\ddot{\underline{\eta}} + \mathbf{B}\dot{\underline{\eta}} + \mathbf{C}\underline{\eta} = \underline{F} \quad \dots(3.41)$$

Here \mathbf{M} , \mathbf{A} , \mathbf{B} and \mathbf{C} are 6×6 matrices, $\underline{\eta}$ a 6×1 vector with the six motions and \underline{F} a 6×1 vector with the three forces and the three moments. See Figure 2.1. The forces and moments, \underline{F} , are functions of time which implies that the motions, $\underline{\eta}$, also are so.

If the coefficients, the elements of the matrices, in this equation all are constants, it can be solved directly in the time domain for arbitrary loads by methods equivalent to those in Paragraph 3.3. For large motions the elements of damping matrix, \mathbf{B} , is however depending on the quadratic drag forces and the velocity amplitudes relative to the water motion. For floating bodies the matrices \mathbf{A} and \mathbf{B} are functions of the frequency of the motion and Equation (3.41) can only be solved for one harmonic motion at a time.

Solution in the time domain

For constant coefficients one can integrate numerically in the time domain by e.g. a central-difference method according to the following:

- $\underline{\eta}_n$ is the position and rotational angles at the point of time $n\Delta t$
- n a positive integer
- $\dot{\underline{\eta}}_n$ the linear and angular velocities at the point of time $n\Delta t$
- $\ddot{\underline{\eta}}_n$ the accelerations and angular accelerations at the point of time $n\Delta t$.

Using three consecutive points of time, then the velocities or first derivatives with respect to time can be approximated by:

$$\dot{\underline{\eta}}_n = \frac{\underline{\eta}_{n+1} - \underline{\eta}_{n-1}}{2\Delta t} \quad \dots(3.42)$$

$$\ddot{\underline{\eta}}_n = \frac{\underline{\eta}_{n+1} - 2\underline{\eta}_n + \underline{\eta}_{n-1}}{\Delta t^2}. \quad \dots(3.43)$$

As initial values ($n = 0$) all positions and velocities, $\underline{\eta}_0$, can be set to zero. Substitution of (3.42) and (3.43) into the Equation of Motion (3.41) gives

$$\underline{\eta}_{n+1} = \left((\mathbf{M} + \mathbf{A}) + \frac{\Delta t}{2} \mathbf{B} \right)^{-1} \left\{ \left(2(\mathbf{M} + \mathbf{A}) - \Delta t^2 \mathbf{C} \right) \underline{\eta}_n - \left((\mathbf{M} + \mathbf{A}) - \frac{\Delta t}{2} \mathbf{B} \right) \underline{\eta}_{n-1} + \Delta t^2 \underline{F}_n \right\} \quad \dots(3.44)$$

Many numerical methods are described in Bathe^{viii} or Björk and Dahlquist

Solution in the frequency domain

As told above the matrices \mathbf{A} and \mathbf{B} are functions of the frequency of the motion for floating bodies and one cannot make a time integration as simply as above, but one must use a special convolution technology. (Cummins^{ix} 1962, van Oortmerssen^x, or Bergdahl and Johansson^{xi} 1988). This is sometimes used when non-linear terms as fender forces, drag forces, power take-off or mooring reactions are included in the equation of motion. For motion of “small” amplitude in an irregular sea state, however, a technique, where the wave is assumed to be composed of a series of harmonic functions is mostly used. By multiplying each harmonic, sine function, with the transfer function for the response of interest for each frequency a series of harmonic response function are produced, the sum of which makes the total response. This method requires that \mathbf{A} and \mathbf{B} are functions of only the frequency of the wave and not the wave amplitude.

In the equation of motion then the motion, $\underline{\eta}(t)$, is simplest written as a complex position vector, $\underline{\eta}_c(t)$, with the elements ($i=1,2,\dots,6$):

$$\eta_{ic} = \hat{\eta}_{ic} e^{j\alpha} = \hat{\eta}_i e^{-j\epsilon_i} e^{j\alpha} \quad \dots(3.45)$$

and the force vector

$$F_{ic} = \hat{F}_{ic} e^{j\alpha} = \hat{F}_i e^{-j\alpha_i} e^{j\alpha} \quad \dots(3.46)$$

With individual phase lags α_i for the six forces and moments. Compare with Equation (3.19).

If (3.45) and (3.46) is substituted into the equation of motion (3.41) one can divide both sides of the equation system by $e^{j\omega t}$ and thereby eliminate the time dependence except the phase lag between the motions and the forces:

$$\left(-\omega^2(\mathbf{M} + \mathbf{A}) - j\omega\mathbf{B} + \mathbf{C}\right)\underline{\eta}_c e^{j\omega t} = \underline{F}_c e^{j\omega t} \quad \dots(3.47)$$

$$\left(\mathbf{C} - \omega^2(\mathbf{M} + \mathbf{A}) - j\omega\mathbf{B}\right)\underline{\eta}_c = \underline{F}_c \quad \dots(3.48)$$

Equation (3.38) can be solved by help of some standard computer program that can handle complex matrices; alternatively the equation system can be split into two real-valued systems, one for the real part and the other for the imaginary part.

Symbolically the solution can be written

$$\underline{\eta}_c = \left(\mathbf{C} - \omega^2(\mathbf{M} + \mathbf{A}) - j\omega\mathbf{B}\right)^{-1} \underline{F}_c \quad \dots(3.49)$$

The decomposition of the irregular load into harmonic components, solution of the equation of motion for each component as above and superposition of the resulting harmonic motion components makes it possible to fast predict statistical properties of the studied motion without knowing its course in detail. Se Figure 3.12 below. Starting out from pseudo-random irregular waves characterised by a wave spectrum, the response will be the same going from the wave spectrum over the time domain integration and back to the response spectrum as going directly down on the frequency-domain side for a linear system. This will be described in connection with ship motions in irregular waves later in this compendium. First, however, we will explain the mechanics of regular, surface gravity waves of finite amplitude.

Alternative roads of action

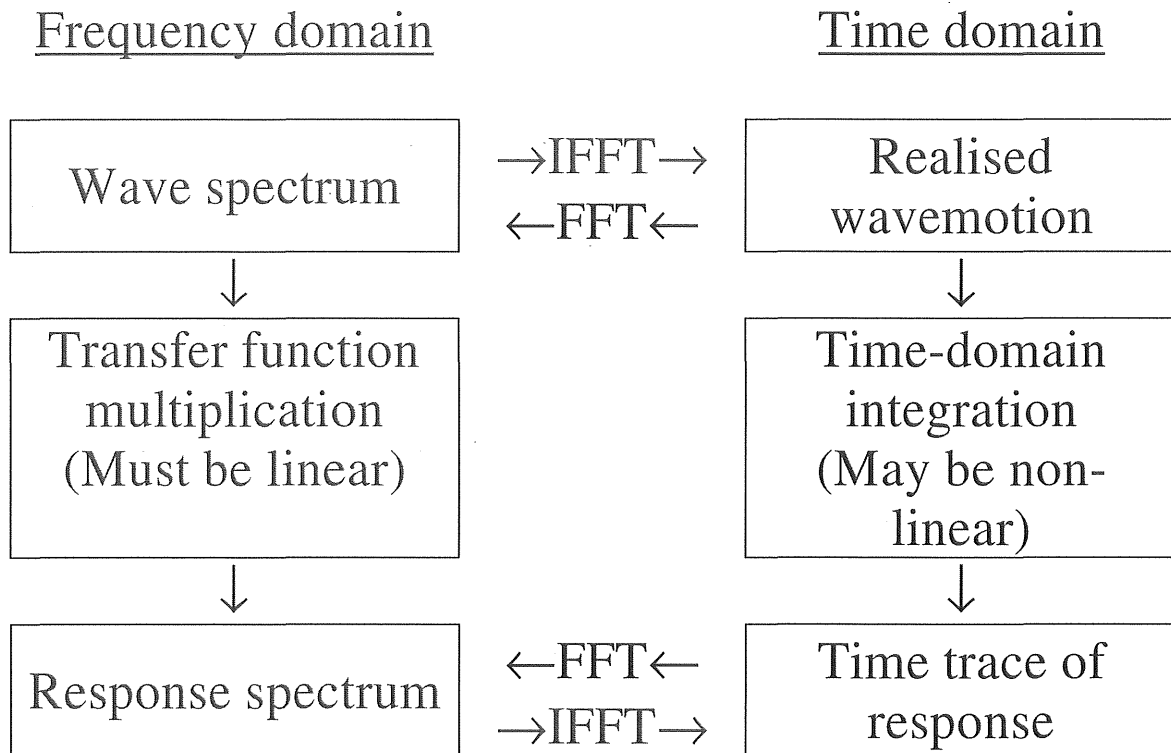


Figure 3.12 Alternative roads of calculating response of a body subjected to pseudo-random irregular waves characterised by a wave spectrum. For a linear system the response will be the same going from the wave spectrum over the time domain integration and back to the response spectrum as going directly down on the frequency-domain side. FFT denotes fast Fourier transformation, which is an efficient numerical technique of transforming a time signal to a frequency-domain representation in the form of a Fourier transform (similar to a Fourier series). IFFT is the inverse fast Fourier transformation from the frequency domain to the time domain.

4 POTENTIAL FLOW THEORY – AN INTRODUCTION

Many flow problems are elegantly solved by help of potential flow theory. It is then assumed that the fluid is *incompressible* and the flow *irrotational*. Irrotational flow is a flow where any selected fluid packed does not rotate around its centre. It may, however be strongly deformed..

4.1 The Equation of Continuity

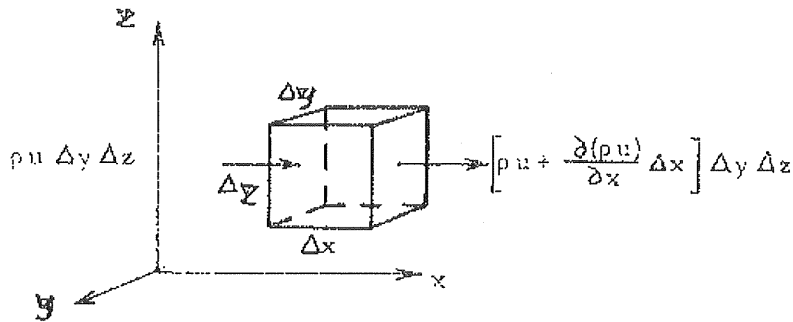


Figure 4.1 The continuity of flow of an infinitesimal control volume

Look at an infinitesimal control volume of fluid with the density, ρ , in a flow with a co-ordinate system (x, y, z) and corresponding velocity components (u, v, w) . From Figure 4.1 it is evident that to first order the resulting inflow of mass can be written

$$- \frac{\partial(\rho u)}{\partial x} + \frac{\partial(\rho v)}{\partial y} + \frac{\partial(\rho w)}{\partial z} \Delta x \Delta y \Delta z \quad \dots(4.1)$$

But this mass inflow must equal the increase of mass in the infinitesimal control volume. $\Delta x \Delta y \Delta z$, i.e.

$$- \frac{\partial(\rho u)}{\partial x} + \frac{\partial(\rho v)}{\partial y} + \frac{\partial(\rho w)}{\partial z} \Delta x \Delta y \Delta z = \frac{\partial \rho}{\partial t} \Delta x \Delta y \Delta z \quad \dots(4.2)$$

which also can be expanded to

$$\frac{\partial \rho}{\partial t} + u \frac{\partial \rho}{\partial x} + v \frac{\partial \rho}{\partial y} + w \frac{\partial \rho}{\partial z} + \rho \left(\frac{\partial u}{\partial x} + \frac{\partial v}{\partial y} + \frac{\partial w}{\partial z} \right) = 0 \quad \dots(4.4)$$

or written

$$\frac{d\rho}{dt} + \rho \left(\frac{\partial u}{\partial x} + \frac{\partial v}{\partial y} + \frac{\partial w}{\partial z} \right) = 0. \quad \dots(4.5)$$

For a homogeneous incompressible fluid each of the derivatives of ρ is zero, and if the fluid is incompressible it is easily understood that the total derivative, $d\rho/dt = 0$,

i.e. that the density of a chosen control volume of fluid is not changed during its motion. Observe, on the other hand, that various parts of the fluid may have different density due to e.g. varying salinity or temperature. The fact that $d\rho/dt = 0$ leads to the continuity conditions for both three-dimensional and two-dimensional flow.

$$\begin{aligned}
 3-D \quad \frac{\partial u}{\partial x} + \frac{\partial v}{\partial y} + \frac{\partial w}{\partial z} &= 0 \\
 2-D \quad \frac{\partial u}{\partial x} + \frac{\partial w}{\partial z} &= 0
 \end{aligned}
 \tag{4.6}$$

4.2 Irrotational Flow

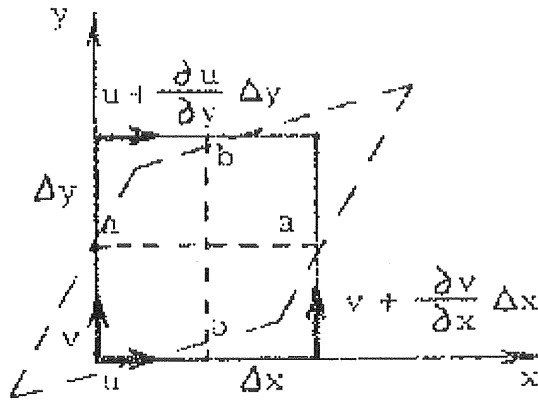


Figure 4.2 Rotation and deformation of an infinitely small fluid element

The rotation of a fluid element around its centre can be expressed by the spatial gradients of the local fluid velocities in the x-, y- and z-directions. For the two-dimensional case sketched in Figure 4.2 we find that the gradients generally would deform the element, because the sections a – a and b – b rotates counter clockwise with the angular velocities

$$\begin{aligned}
 \frac{v + \Delta x \frac{\partial v}{\partial x} - v}{\Delta x} &= \frac{\partial v}{\partial x} \\
 -\frac{u + \Delta y \frac{\partial u}{\partial y} - u}{\Delta y} &= -\frac{\partial u}{\partial y}
 \end{aligned}
 \tag{4.7}$$

The rotation of the element per unit of time, ω_z , around the z-axis is defined as the mean of the two angular velocities above, i.e.

$$\omega_z = \frac{1}{2} \frac{\partial v}{\partial x} - \frac{\partial u}{\partial y}
 \tag{4.8}$$

The rotation around the x- and y-axes, ω_x and ω_y , are similarly

$$\omega_x = \frac{1}{2} \left(\frac{\partial w}{\partial y} - \frac{\partial v}{\partial z} \right) \quad \dots(4.9)$$

$$\omega_y = \frac{1}{2} \left(\frac{\partial u}{\partial z} - \frac{\partial w}{\partial x} \right) \quad \dots(4.10)$$

The flow is said to be irrotational or free from circulation if

$$\omega_x = \omega_y = \omega_z = 0 \quad \dots(4.11)$$

i.e. it does not rotate around its centre.

The equations (4.8) to (4.11) then give

$$\begin{aligned} \frac{\partial w}{\partial y} &= \frac{\partial v}{\partial z} \\ \frac{\partial u}{\partial z} &= \frac{\partial w}{\partial x} \\ \frac{\partial v}{\partial x} &= \frac{\partial u}{\partial y} \end{aligned} \quad \dots(4.12)$$

Note that even in irrotational flow the fluid element can be strongly deformed, e.g. be deformed from a cube to a diamond. For examples of irrotational and rotational flows see Figure 4.3 and 4.4.

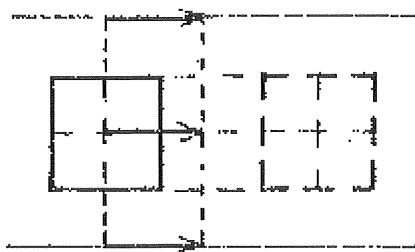
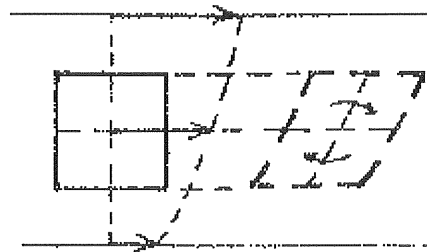


Figure 4.3 Irrotational parallel flow.



Rotational parallel flow



Figure 4.4 Curved irrotational flow



Curved rotational flow

4.3 The Velocity Potential and Laplace Differential Equation

Under which conditions does a continuous and differentiable function, $\phi(x, z, t)$, exist such that

$$\begin{aligned} u &= \frac{\partial \phi}{\partial x} \\ v &= \frac{\partial \phi}{\partial y} \\ w &= \frac{\partial \phi}{\partial z} \end{aligned} \quad \dots(4.13)$$

Equation (4.13) means that the spatial gradient of ϕ in each point shall give the velocity vector of the flow, $\underline{U} = \nabla \phi = \text{grad}(\phi)$. The function, ϕ , is therefore named the velocity potential. Observe that the sign in Equation (4.13) as well could be set to - as it is a pure definition, and so is also the convention in many civil engineering textbooks and some other scientific literature, which one has to note when studying different sources. A rational motive for choosing a negative sign is that a minus sign corresponds to the analogy that the gravity force acts downhill when going uphill i.e. in opposite direction to the slope. Here we will follow the less intuitive convention according to (4.13) as this is most common in naval architecture.

If the flow is irrotational then in e.g. in the x-z plane according Equation (4.12) $\bar{\partial}u/\bar{\partial}z = \bar{\partial}w/\bar{\partial}x$ and thus that

$$\frac{\partial u}{\partial z} = \frac{\partial^2 \phi}{\partial z \partial x} = \frac{\partial w}{\partial x} = \frac{\partial^2 \phi}{\partial x \partial z} \quad \dots(4.14)$$

i.e. that the mixed second derivatives are equal, which in turn proves that ϕ is continuous and differentiable with respect to x and z . The same is true in the other two orthogonal planes. The potential function ϕ exists thus if the flow is irrotational and irrotational flow is therefore also called potential flow.

Further for an incompressible fluid the condition of continuity Equation (4.6) is true and $\partial u/\partial x + \partial v/\partial y + \partial w/\partial z = 0$ which with (4.13) substituted gives Laplace' differential equation:

$$\begin{aligned} \text{in 3 D} \quad & \frac{\partial^2 \phi}{\partial x^2} + \frac{\partial^2 \phi}{\partial y^2} + \frac{\partial^2 \phi}{\partial z^2} = 0 \\ \text{and in 2 D} \quad & \frac{\partial^2 \phi}{\partial x^2} + \frac{\partial^2 \phi}{\partial z^2} = 0 \end{aligned} \quad \dots(4.15)$$

or symbolically $\Delta \phi = 0$ or $\nabla^2 = 0$.

Irrotational flow for an incompressible flow can thus be described by the differential equation (4.15), which is a linear differential equation of second order. A surface water wave motion with “small” amplitude in relation to its wavelength and the water depth can with good precision be described as potential flow. The deviation from the true physical wave motion for higher waves depends on approximations of the boundary condition and on viscous and rotational effects. Due to the linearity of the differential equation (4.15) a wave motion decomposed into many harmonic wave components with different amplitudes, frequencies and phase lags first the flow for each component can be solved and then linearly be added to a total solution which gives all velocities and accelerations anywhere in the fluid.

4.4 Bernoulli’s Equation for Potential Flow

Velocities and accelerations in potential flow can thus be obtained directly from the velocity potential, ϕ , by taking the derivatives with respect to space and time. To calculate pressures and water levels it is, however, necessary to use an additional condition, namely the Bernoulli Equation for incompressible, irrotational flow. Most of us have met it before in the context of one-dimensional pipe flow, but the version here is somewhat different and valid in three dimensions. In the next paragraph we will derive it for two dimensions from Navier-Stokes’ Equation for an incompressible fluid.

Navier-Stokes’ Equations in two dimensions

Navier-Stokes’ Equations for two-dimensional flow (See e.g. Rouse^{xii}, Daily-Harleman^{xiii} or M^{xiv}) can be written:

$$\frac{\partial u}{\partial t} + u \frac{\partial u}{\partial x} + w \frac{\partial u}{\partial z} = -g \frac{\partial h}{\partial x} - \frac{1}{\rho} \frac{\partial p}{\partial x} + \frac{\mu}{\rho} \left[\frac{\partial^2 u}{\partial x^2} + \frac{\partial^2 u}{\partial z^2} \right]$$

...(4.16)

$$\frac{\partial w}{\partial t} + u \frac{\partial w}{\partial x} + w \frac{\partial w}{\partial z} = -g \frac{\partial h}{\partial z} - \frac{1}{\rho} \frac{\partial p}{\partial z} + \frac{\mu}{\rho} \left[\frac{\partial^2 w}{\partial x^2} + \frac{\partial^2 w}{\partial z^2} \right]$$

where t is time
 x and z space coordinates
 u and w velocities in x - and z -directions
 g the earth acceleration
 h height, a coordinate in negative g -direction i.e. h is positive upwards
 ρ density of the fluid
and μ the dynamic viscosity of the fluid.

Deduction of the Bernoulli Equation

Substituting the conditions for irrotational flow Equation (4.12), $\partial u/\partial z = \partial w/\partial x$, into Equation (4.16) gives

$$\frac{\partial u}{\partial t} + u \frac{\partial u}{\partial x} + w \frac{\partial w}{\partial x} = -g \frac{\partial h}{\partial x} - \frac{1}{\rho} \frac{\partial p}{\partial x} + \frac{\mu}{\rho} \left(\frac{\partial^2 u}{\partial x^2} + \frac{\partial^2 w}{\partial z \partial x} \right) \quad \dots(4.17)$$

$$\frac{\partial w}{\partial t} + u \frac{\partial u}{\partial z} + w \frac{\partial w}{\partial z} = -g \frac{\partial h}{\partial z} - \frac{1}{\rho} \frac{\partial p}{\partial z} + \frac{\mu}{\rho} \left(\frac{\partial^2 u}{\partial x \partial z} + \frac{\partial^2 w}{\partial z^2} \right)$$

As both u and w are continuous and differentiable the order of differentiation can be changed and $\partial^2 / \partial x \partial z = \partial^2 / \partial z \partial x$. Introduce also the fact that $u \partial u / \partial x = \partial(\frac{1}{2}u^2) / \partial x$ etc. and then:

$$\frac{\partial u}{\partial t} + \frac{\partial}{\partial x} \left(\frac{u^2}{2} + \frac{w^2}{2} + \frac{p}{\rho} + gh \right) = \frac{\mu}{\rho} \frac{\partial}{\partial x} \left(\frac{\partial u}{\partial x} + \frac{\partial w}{\partial z} \right) \quad \dots(4.18)$$

$$\frac{\partial w}{\partial t} + \frac{\partial}{\partial z} \left(\frac{u^2}{2} + \frac{w^2}{2} + \frac{p}{\rho} + gh \right) = \frac{\mu}{\rho} \frac{\partial}{\partial z} \left(\frac{\partial u}{\partial x} + \frac{\partial w}{\partial z} \right)$$

But the continuity condition (4.6) is $\partial u / \partial x + \partial w / \partial z = 0$, and therefore the right hand sides of the equations (4.18) are identically zero for a continuous, incompressible fluid.

The velocity potential, ϕ , according to the definition (4.13) gives the accelerations expressed as:

$$\begin{aligned} \frac{\partial u}{\partial t} &= \frac{\partial}{\partial t} \left(\frac{\partial \phi}{\partial x} \right) = \frac{\partial^2 \phi}{\partial x \partial t} \\ \frac{\partial w}{\partial t} &= \frac{\partial}{\partial t} \left(\frac{\partial \phi}{\partial z} \right) = \frac{\partial^2 \phi}{\partial t \partial z} = \frac{\partial^2 \phi}{\partial z \partial t} \end{aligned} \quad \dots(4.19)$$

Substitution of these into Equation (4.18) and integration with respect to x and z then gives:

$$\begin{aligned} \frac{\partial \phi}{\partial t} + \frac{u^2}{2} + \frac{w^2}{2} + \frac{p}{\rho} + gh &= f_1(t, z) \\ \frac{\partial \phi}{\partial t} + \frac{u^2}{2} + \frac{w^2}{2} + \frac{p}{\rho} + gh &= f_2(t, x) \end{aligned} \quad \dots(4.20)$$

The equations (4.20) must be satisfied simultaneously in all points (x, z) in the flow, and therefore

$$f_1(t, z) = f_2(t, x) = f(t) \quad \dots(4.21)$$

and the result is one single equation, the Bernoulli Equation, for an incompressible fluid in irrotational two-dimensional flow:

$$\frac{\partial\phi}{\partial t} + \frac{u^2}{2} + \frac{w^2}{2} + \frac{p}{\rho} + gh = f(t) \quad \dots(4.22)$$

The time-dependant part of $f(t)$ can be included in $\partial\phi/\partial t$, and then

$$\frac{\partial\phi}{\partial t} + \frac{u^2}{2} + \frac{w^2}{2} + \frac{p}{\rho} + gh = C. \quad \dots(4.23)$$

where C is a constant.

For three-dimensional flow the Bernoulli Equation is written:

$$\frac{\partial\phi}{\partial t} + \frac{1}{2}(u^2 + v^2 + w^2) + \frac{p}{\rho} + gh = C \quad \dots(4.24)$$

For stationary flow $\partial\phi/\partial t = 0$, and then we recognise the Bernoulli Equation familiar from stationary one-dimensional pipe flow.

5 REGULAR WAVES

5.1 The Velocity Potential

If the motion in a water mass due to a surface gravity wave can be approximated by potential flow, we can derive the properties of the wave motion from the Laplace Differential Equation as stated in Chapter 4,

$$\Delta\phi = 0, \quad \dots(5.1)$$

where ϕ is the velocity potential. From ϕ we can then derive i.e. velocities, accelerations and pressures everywhere in the water mass.

The Laplace Differential Equation is widely applicable for field problems i.e. treating heat, sound, electromagnetism and structural mechanics. In civil engineering we meet it for description of ground water flow and for diffusion of heat and chemical matters in structures. Note, however, that potential flow is free from losses caused by viscosity, which ground water flow is not.

In this chapter we will treat “small-amplitude” wave theory, also called first order wave theory or linear wave theory, which well describes waves with the wave amplitude much smaller than the wavelength and the water depth. For steep waves or finite amplitude waves in shallow water, higher-order wave theories and non-linear wave theories for shallow water must be used. See e.g. Wiegel^{xv}, Dean and Dalrymple^{xvi}, LeMéhauté^{xvii}, Skjelbreja and Henriksen^{xviii}.

The small-amplitude wave theory is, in spite of the underlying simplified assumptions, very useful for many applications. It functions well for wave steepness¹ up to $H/\lambda = 0.03$ and furthermore, as it is linear, one can superpose solutions for different frequencies and with varying direction of propagation and thus calculate motion in irregular sea states.

5.2 Boundary Conditions

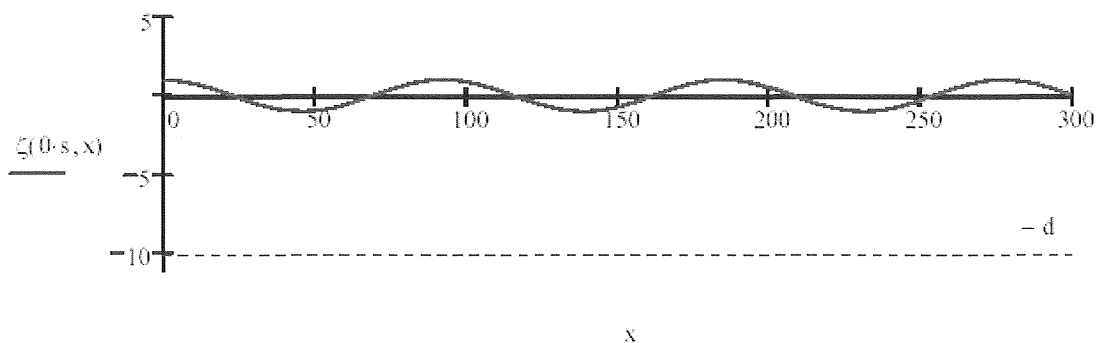


Figure 5.1 A progressive gravity wave, $T = 10$ s and $d = 10$ m.

¹ Note the difference between the wave steepness $H/\lambda = 2a/\lambda$ and the wave slope, which latter is the slope of the water surface $\partial\zeta/\partial x$ and sometimes the maximum slope which is $ak = 2\pi a/\lambda$ for a sinusoidal wave.

The waveform of a plane harmonic wave progressing in the x-direction as illustrated in Figure 5.1 can be written as a cosine function:

$$\zeta(x, t) = a \cos(kx - \omega t) \quad \dots(5.2)$$

The most obvious and also the simplest boundary condition is that the velocity perpendicular to the bottom must be zero. Thus the Bottom Boundary Condition

$$\frac{\partial \phi}{\partial z} = w_{z=-d} = 0. \quad \dots(5.3)$$

The Free Surface Kinematic Boundary Condition states that a particle on the surface will stay at the surface:

$$\frac{\partial \zeta}{\partial t} + u \frac{\partial \zeta}{\partial x} - w = \frac{\partial \zeta}{\partial t} + \frac{\partial \phi}{\partial x} \frac{\partial \zeta}{\partial x} - \frac{\partial \phi}{\partial z} = 0 \quad \dots(5.4)$$

The Free Surface Dynamic Boundary Condition derives from the Bernoulli Equation on the assumption that the pressure is constant on the free surface. Then, especially, if the atmospheric pressure is set to the reference pressure 0:

$$\frac{\partial \phi}{\partial t} + \frac{1}{2}(u^2 + w^2) + g\zeta = \frac{\partial \phi}{\partial t} + \frac{1}{2} \left(\left(\frac{\partial \phi}{\partial x} \right)^2 + \left(\frac{\partial \phi}{\partial z} \right)^2 \right) + g\zeta = 0 \quad \dots(5.5)$$

The velocity potential, ϕ , of the wave, Equation (5.2) must satisfy the Laplace Equation (5.1) and the boundary conditions (5.3) to (5.5). The solution of this problem is not easy because the free-surface boundary conditions are non-linear following the moving free surface.

5.3 Linear Airyix Wave Theory

The simplest, but very useful, wave theory is the linear or small amplitude wave theory, which is based on the assumption that the wave amplitude, a , is small compared to the wavelength, λ .

The linear wave theory is also called the first-order theory because one can neglect terms that are above first order when expanding the solution in a perturbation series. The solution of ϕ and the wave profile are then assumed to be expanded in power series of a non-dimensional perturbation parameter, ε , in terms of the wave slope at the zero down crossing of the wave:

$$\varepsilon = \frac{2\pi a}{\lambda} = ka \quad \dots(5.6)$$

in which λ is the wavelength, a the wave amplitude and k the wave number. Then we can write for the potential

$$\phi = \sum_{n=1}^{\infty} \varepsilon^n \phi_n \quad \dots(5.7)$$

and for the wave profile

$$\zeta = \sum_{n=1}^{\infty} \varepsilon^n \zeta_n \quad \dots(5.8)$$

with index n indicating the n th order term.

Inserting the expansions (5.7) and (5.8) into the free-surface boundary conditions retaining only first order terms gives:

$$\frac{\partial \zeta_1}{\partial t} - \frac{\partial \phi_1}{\partial z} = 0 \quad \dots(5.9)$$

$$\frac{\partial \phi_1}{\partial t} + g \zeta_1 = 0 \quad \dots(5.10)$$

One can show that these, to first order, can be applied at the mean water level. (see e.g. Krogstad and Arntsen 2000^{xx}). For second order Stokes theory see e.g. Chakrabarti^{xxi}.

The wave profile is given at $z = 0$ by (5.10) as

$$\zeta_1 = -\frac{1}{g} \frac{\partial \phi_1}{\partial t} \quad \dots(5.11)$$

The two linearised free-surface boundary conditions can be combined to one by eliminating ζ_1

$$\frac{\partial^2 \phi_1}{\partial t^2} + g \frac{\partial \phi_1}{\partial z} = 0 \quad \dots(5.12)$$

Solution for a progressive wave

The solution for a progressive wave is easiest accomplished by using complex notation:

$$\zeta_c = a e^{j(kx - \omega t)} = a e^{jkx} e^{-j\omega t} = a [\cos(kx - \omega t) + j \sin(kx - \omega t)] \quad \dots(5.13)$$

so that the real progressive wave Equation (5.2) is given by

$$\text{Re}(\zeta_c) = \text{Re}(a [\cos(kx - \omega t) + j \sin(kx - \omega t)]) = a \cos(kx - \omega t). \quad \dots(5.14)$$

We can from Equation (5.13) see that the waveform, which is a function of both time and space, can be separated into a product of two functions each a function of only one independent variable. Assuming the solution can be written as a product of three single-variable functions, the solution could be written

$$\phi = X(x)Z(z)T(t). \quad \dots(5.15)$$

Then the Laplace Equation gives

$$\frac{\partial^2 \phi}{\partial x^2} + \frac{\partial^2 \phi}{\partial z^2} = [X''(x)Z(z) + X(x)Z''(z)]T(t) = 0, \quad \dots(5.16)$$

which can be separated into two equations for $T(t)$ not being identically zero:

$$\frac{X''}{X} = -\frac{Z''}{Z} = k_1^2 \Rightarrow \begin{cases} X'' + k_1^2 X = 0 \\ Z'' - k_1^2 Z = 0 \end{cases} \quad \dots(5.17).$$

The solution to these two second-order differential equations in x and z have the forms

$$\begin{cases} X(x) = Ae^{jk_1x} + Be^{-jk_1x} \\ Z(z) = Ce^{k_1z} + De^{-k_1z} \end{cases} \quad \dots(5.18)$$

where the sign of k_1^2 have been chosen to get a harmonic solution in the x -direction. Thus

$$\phi = (Ae^{jk_1x} + Be^{-jk_1x})(Ce^{k_1z} + De^{-k_1z})T(t) \quad \dots(5.19)$$

where A , B , C and D are constants given by the boundary conditions.

The time function of the complex waveform (5.13) is $e^{-j\omega t}$ and therefore $T(t) = e^{-j\omega t}$. Further the waveform (5.13) progresses to the right as $e^{j(kx - \omega t)}$, and then B must be zero. Further A can arbitrarily be set to 1 by including it into C and D and then $X(x) = e^{jk_1x}$. We then also realise that k_1 must be the same constant as the wave number k otherwise the celerity – the propagation speed of the waveform, ω/k – would be wrong.

There is of course also a solution for waves progressing to the left for $A = 0$ and $B = 1$. Now the problem is reduced to

$$\begin{aligned} \phi &= (Ae^{jkx} + Be^{-jkx})(Ce^{kz} + De^{-kz})T(t) = Ae^{jkx}(Ce^{kz} + De^{-kz})e^{-j\omega t} = \\ &= (Ce^{kz} + De^{-kz})e^{j(kx - \omega t)} = (Ce^{kz} + De^{-kz})X(x)T(t) \end{aligned} \quad \dots(5.20)$$

Two constants remain to be determined from the bottom and free surface boundary conditions.

The bottom boundary condition gives

$$\frac{\partial \phi}{\partial z}_{z=-d} = k(Ce^{-kd} - De^{kd})X(x)T(t) = 0. \quad \dots(5.21)$$

As $X(x)$ and $T(t)$ are not identically zero this can be solved for instance for C ;

$$Ce^{-kd} - De^{kd} = 0 \quad \dots(5.22)$$

$$C = De^{2kd}, \quad \dots(5.23)$$

which gives

$$Z(z) = De^{kd}(e^{k(z+d)} + e^{-k(z+d)}) = D_1 e^{kd} \cosh k(z+d) \quad \dots(5.24)$$

with one unsolved constant $D_1 = 2D$.

The linearised kinematic free surface boundary condition Equation (5.9) and the wave form Equation (5.13) then gives D_1 :

$$\frac{\partial \zeta_c}{\partial t} = -ja\omega e^{jkx} e^{-j\alpha x} = \frac{\partial \phi}{\partial z} = e^{jkx} D_1 e^{kd} k(\sinh kd) e^{-j\alpha x} \quad \dots(5.25)$$

$$D_1 = \frac{-ja\omega}{e^{kd} k \sinh kd} \quad \dots(5.26)$$

which substituted into (5.20) gives one version of the complex velocity potential:

$$\phi = e^{jkx} \frac{-ja\omega}{e^{kd} k \sinh kd} e^{kd} \cosh k(z+d) e^{-j\alpha x} = -j \frac{a\omega \cosh k(z+d)}{k \sinh kd} e^{j(kx-\alpha x)} \quad \dots(5.27)$$

The combined free-surface boundary condition, (5.12),

$$\frac{\partial^2 \phi}{\partial t^2} + g \frac{\partial \phi}{\partial z} = 0$$

will finally yield a functional relation between k and ω . Starting with

$$X(x)Z(z)\ddot{T}(t) + gX(x)Z'(z)T(t) = 0 \quad \dots(5.28)$$

dividing by $X(x)$, and substituting $Z(z)$ (Equation 5.24) and $T(t) = e^{-j\alpha t}$ gives

$$D_1 e^{kd} \cosh k(z+d) (-\omega^2 e^{-j\alpha t}) + gkD_1 e^{kd} \sinh k(z+d) e^{-j\alpha t} = 0. \quad \dots(5.29)$$

Finally

$$\frac{\omega^2}{gk} = \tanh(kd) \quad \dots(5.30)$$

which implicitly gives the wave celerity, $\omega/k = f(k)$, and is called the dispersion relation, because it shows that the wave celerity depends on the wave length, which fact in turn makes groups of waves disperse.

The final complex velocity potential for plane progressive waves in finite water depth is then after having substituted the constants and the dispersion relation:

$$\phi_c = -j \frac{a\omega}{k} \frac{\cosh k(z+d)}{\sinh kd} e^{j(kx-\omega t)} = -j \frac{ag}{\omega} \frac{\cosh k(z+d)}{\cosh kd} e^{j(kx-\omega t)} \quad \dots(5.31)$$

and its corresponding real valued expression is

$$\begin{aligned} \phi &= \text{Re}\left(-j \frac{ag}{\omega} \frac{\cosh k(z+d)}{\cosh kd} e^{j(kx-\omega t)}\right) = \\ &= \text{Re}\left(-j \frac{ag}{\omega} \frac{\cosh k(z+d)}{\cosh kd} [\cos(kx-\omega t) + j \sin(kx-\omega t)]\right) \\ \phi &= \frac{ag}{\omega} \frac{\cosh k(z+d)}{\cosh kd} \sin(kx-\omega t) \quad \dots(5.32) \end{aligned}$$

5.4 The Application of the Velocity Potential

The velocity potentials (5.31) or (5.32) for a progressive plane harmonic wave are very useful, because from one single scalar equation we can derive all particle velocities and pressures in the water mass beneath the still-water level.

According to the definition (4.13) the complex particle velocities will be

$$\begin{aligned} u_c &= \frac{\partial \phi_c}{\partial x} = \frac{agk}{\omega} \frac{\cosh k(z+d)}{\cosh kd} e^{j(kx-\omega t)} \\ w_c &= \frac{\partial \phi_c}{\partial z} = -j \frac{agk}{\omega} \frac{\sinh k(z+d)}{\cosh kd} e^{j(kx-\omega t)} \end{aligned} \quad \dots(5.33)$$

and the complex particle accelerations becomes, after taking the time derivatives,

$$\begin{aligned} \dot{u}_c &= \frac{\partial^2 \phi_c}{\partial t \partial x} = -jagk \frac{\cosh k(z+d)}{\cosh kd} e^{j(kx-\omega t)} \\ \dot{w}_c &= \frac{\partial^2 \phi_c}{\partial t \partial z} = -agk \frac{\sinh k(z+d)}{\cosh kd} e^{j(kx-\omega t)} \end{aligned} \quad \dots(5.34)$$

The pressure above the atmospheric reference pressure can be calculated using the Bernoulli equation (4.21)

$$p_c = -\left[\rho \frac{\partial \phi_c}{\partial t} + \frac{1}{2} \rho (u_c^2 + w_c^2) + \rho g z \right]. \quad \dots(5.35)$$

Here the first and second term are the dynamic fluctuating pressure due to the waves and the third term the hydrostatic pressure. To first order the velocity squared term can be neglected. Thus

$$p_c = -\rho \left[\frac{\partial \phi_c}{\partial t} + g z \right] = \rho a g \frac{\cosh k(z+d)}{\cosh kd} e^{j(kx-\omega t)} - \rho g z. \quad \dots(5.36)$$

The wave form can be retained from the linearised free-surface boundary condition (5.10):

$$\zeta_c = -\frac{1}{g} \frac{\partial \phi_c}{\partial t} = a e^{j(kx-\omega t)}, \quad \dots(5.37)$$

Real-valued expressions

The real valued particle velocities are from (5.33)

$$\begin{aligned} u &= \frac{\partial \phi}{\partial x} = \frac{agk}{\omega} \frac{\cosh k(z+d)}{\cosh kd} \cos(kx - \omega t) \\ w &= \frac{\partial \phi}{\partial z} = \frac{agk}{\omega} \frac{\sinh k(z+d)}{\cosh kd} \sin(kx - \omega t) \end{aligned} \quad \dots(5.38)$$

and the real valued particle accelerations

$$\begin{aligned} \dot{u} &= \frac{\partial^2 \phi}{\partial t \partial x} = agk \frac{\cosh k(z+d)}{\cosh kd} \sin(kx - \omega t) \\ \dot{w} &= \frac{\partial^2 \phi}{\partial t \partial z} = -agk \frac{\sinh k(z+d)}{\cosh kd} \cos(kx - \omega t) \end{aligned} \quad \dots(5.39)$$

The real valued pressure above the atmospheric reference pressure to first order is

$$p = \rho g a \frac{\cosh k(z+d)}{\cosh kd} \cos(kx - \omega t) - \rho g z. \quad \dots(5.40)$$

Furthermore the particle paths in the wave can be calculated from the equations (5.38) by integration with respect to time. The resulting form is elliptic with the largest axis horizontal. Close to the bottom the vertical axis is very short and the water is oscillating horizontally only. In deep water the particle paths are circular.

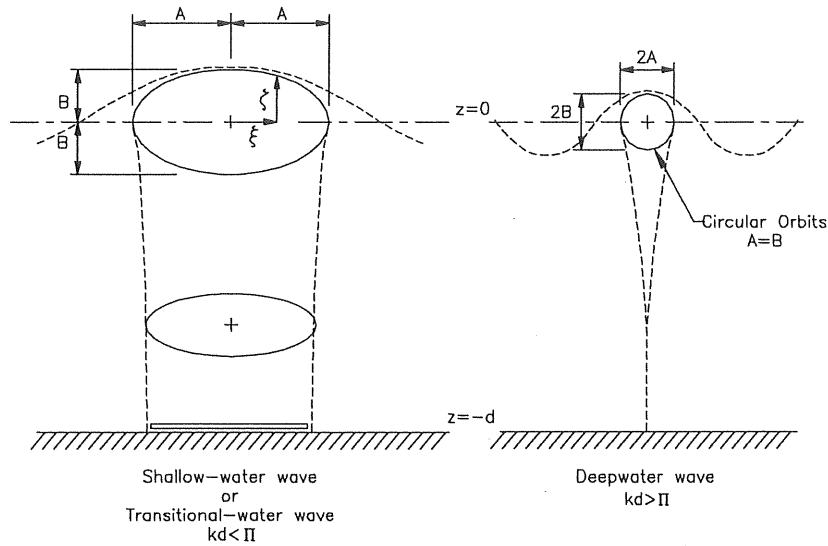


Figure 5.2 Sketch of fluid-particle motion beneath a wave as predicted by linear wave theory. (From CERC^{xxii}, 1984)

5.5 Velocity Potential in Deep Water

By rearranging the velocity potential (5.31) by hyperbolic “trigonometry” and then letting $d \rightarrow \infty$ bringing with it $\tanh(kd) \rightarrow 1$ and $\omega^2 = gk$, expressions for waves in deep water in relation to the wavelength are yielded

$$\begin{aligned}
 \phi_c &= -j \frac{ag}{\omega} \frac{\cosh k(z+d)}{\cosh kd} e^{j(kx-\omega t)} = -j \frac{ag}{\omega} \frac{\cosh k(z+d)}{\cosh kd} e^{j(kx-\omega t)} = \\
 &= -j \frac{ag}{\omega} \left(\cosh(kz) + \frac{\sinh(kz) \sinh(kd)}{\cosh kd} \right) e^{j(kx-\omega t)} = \\
 &= -j \frac{ag}{\omega} (\cosh(kz) + \sinh(kz) \tanh(kd)) e^{j(kx-\omega t)} = \\
 &= -j \frac{a\omega}{k} e^{kz} e^{j(kx-\omega t)}
 \end{aligned} \tag{5.41}$$

which thus gives a simple exponential function of z . Its corresponding real-valued expression is

$$\phi = \frac{a\omega}{k} e^{kz} [\sin((kx - \omega t))] \tag{5.42}$$

The complex velocities in deep water are thus

$$\begin{aligned}
 u_c &= \frac{\partial \phi_c}{\partial x} = a\omega e^{kz} e^{j(kx-\omega t)} \\
 w_c &= \frac{\partial \phi_c}{\partial z} = -ja\omega e^{kz} e^{j(kx-\omega t)}
 \end{aligned} \tag{5.43}$$

and the complex particle accelerations in deep water,

$$\begin{aligned} \dot{u}_c &= \frac{\partial^2 \phi_c}{\partial t \partial x} = -ja\omega^2 e^{kz} e^{j(kx-\omega t)} \\ \dot{w}_c &= \frac{\partial^2 \phi_c}{\partial t \partial z} = -a\omega^2 e^{kz} e^{j(kx-\omega t)} \end{aligned} \quad \dots(5.44)$$

The complex pressure

$$p_c = \rho a g e^{kz} e^{j(kx-\omega t)} - \rho g z. \quad \dots(5.45)$$

Real-valued expressions

The real valued particle velocities are from (5.43)

$$\begin{aligned} u &= a\omega e^{kz} \cos(kx - \omega t) \\ w &= a\omega e^{kz} \sin(kx - \omega t) \end{aligned} \quad \dots(5.46)$$

and the real valued particle accelerations from (5.44)

$$\begin{aligned} \dot{u} &= a\omega^2 e^{kz} \sin(kx - \omega t) \\ \dot{w} &= -a\omega^2 e^{kz} \cos(kx - \omega t) \end{aligned} \quad \dots(5.47)$$

The real valued pressure to first order from (5.45) is

$$p = \rho a g e^{kz} \cos(kx - \omega t) - \rho g z. \quad \dots(5.48)$$

Particle paths

As told above the particle paths in a wave at any depth can be calculated from the equations (5.38) by integration with respect to time. We will do this for the deep-water wave to show the principle. First the horizontal position of a particle as a function of time is

$$\xi = \int u dt = \int a\omega e^{kz} \cos(kx - \omega\tau) d\tau = -ae^{kz} \sin(kx - \omega t) + \xi_0 \quad \dots(5.49)$$

and the vertical position

$$\zeta = \int w dt = \int a\omega e^{kz} \sin(kx - \omega\tau) d\tau = -ae^{kz} \cos(kx - \omega t) + \zeta_0 \quad \dots(5.50)$$

which using the trigonometric unity gives

$$(\xi - \xi_0)^2 + (\zeta - \zeta_0)^2 = a^2 e^{2kz} = r^2(z) \quad \dots(5.51)$$

where $r(z)$ is recognized as the radius of the particle path. Thus in deep water the particles move in circular orbits with radii that decrease exponentially with depth.

How large is the particle radius at the level $z = -\lambda/2$?

5.6 Wave Properties in Shallow Water

In shallow water the general expression for the velocity potential must be used, but the derived velocities, accelerations and pressure can be simplified using the fact that when $d \rightarrow 0$ so $\tanh(kd) \rightarrow kd$

The complex velocities in shallow water are thus

$$\begin{aligned} u_c &= \frac{\omega a}{kd} e^{j(kx - \omega t)} \\ w_c &= -j\omega a \frac{z+d}{d} e^{j(kx - \omega t)} \end{aligned} \quad \dots(5.52)$$

and the complex particle accelerations in shallow water,

$$\begin{aligned} \dot{u}_c &= -j \frac{a\omega^2}{kd} e^{j(kx - \omega t)} \\ \dot{w}_c &= -a\omega^2 \frac{z+d}{d} e^{j(kx - \omega t)} \end{aligned} \quad \dots(5.53)$$

The complex pressure

$$p_c = \rho a g e^{j(kx - \omega t)} - \rho g z . \quad \dots(5.54)$$

Real-valued expressions

The real valued particle velocities are

$$\begin{aligned} u &= \frac{\omega a}{kd} \cos(kx - \omega t) \\ w &= \omega a \frac{z+d}{d} \sin(kx - \omega t) \end{aligned} \quad \dots(5.55)$$

and the real valued particle accelerations are

$$\begin{aligned} \dot{u} &= \frac{a\omega^2}{kd} \sin(kx - \omega t) \\ \dot{w} &= -a\omega^2 \frac{z+d}{d} \cos(kx - \omega t) \end{aligned} \quad \dots(5.56)$$

The real valued pressure is

$$p = \rho a g \cos(kx - \omega t) - \rho g z . \quad \dots(5.57)$$

Table 5.1 Summary - Linear (Airy) wave theory, Wave characteristics, CERF 1984. Here $L = \lambda$.

| RELATIVE DEPTH | SHALLOW WATER $\frac{d}{L} < \frac{1}{25}$ | TRANSITIONAL WATER $\frac{1}{25} < \frac{d}{L} < \frac{1}{2}$ | DEEP WATER $\frac{d}{L} > \frac{1}{2}$ |
|---------------------------------|---|--|---|
| 1. Wave Profile | Some As \rightarrow | $\eta = \frac{H}{2} \cos \left[\frac{2\pi x}{L} - \frac{2\pi t}{T} \right] = \frac{H}{2} \cos \theta$ | Some As \leftarrow |
| 2. Wave Celerity | $C = \frac{L}{T} = \sqrt{gd}$ | $C = \frac{L}{T} = \frac{gT}{2\pi} \tanh \left(\frac{2\pi d}{L} \right)$ | $C = C_0 = \frac{L}{T} = \frac{gT}{2\pi}$ |
| 3. Wave Length | $L = T \sqrt{gd} = CT$ | $L = \frac{gT^2}{2\pi} \tanh \left(\frac{2\pi d}{L} \right)$ | $L = L_0 = \frac{gT^2}{2\pi} = C_0 T$ |
| 4. Group Velocity | $C_g = C = \sqrt{gd}$ | $C_g = nC = \frac{1}{2} \left[1 + \frac{4\pi d/L}{\sinh(4\pi d/L)} \right] \cdot C$ | $C_g = \frac{1}{2} C = \frac{gT}{4\pi}$ |
| 5. Water Particle Velocity | | | |
| a) Horizontal | $u = \frac{H}{2} \sqrt{\frac{g}{d}} \cos \theta$ | $u = \frac{H}{2} \frac{gT}{L} \frac{\cosh[2\pi(z+d)/L]}{\cosh(2\pi d/L)} \cos \theta$ | $u = \frac{\pi H}{T} e^{\frac{2\pi z}{L}} \cos \theta$ |
| b) Vertical | $w = \frac{H\pi}{T} \left(1 + \frac{z}{d}\right) \sin \theta$ | $w = \frac{H}{2} \frac{gT}{L} \frac{\sinh[2\pi(z+d)/L]}{\cosh(2\pi d/L)} \sin \theta$ | $w = \frac{\pi H}{T} e^{\frac{2\pi z}{L}} \sin \theta$ |
| 6. Water Particle Accelerations | | | |
| a) Horizontal | $a_x = \frac{H\pi}{T} \sqrt{\frac{g}{d}} \sin \theta$ | $a_x = \frac{g\pi H}{L} \frac{\cosh[2\pi(z+d)/L]}{\cosh(2\pi d/L)} \sin \theta$ | $a_x = 2H \left(\frac{\pi}{T}\right)^2 e^{\frac{2\pi z}{L}} \sin \theta$ |
| b) Vertical | $a_z = -2H \left(\frac{\pi}{T}\right)^2 \left(1 + \frac{z}{d}\right) \cos \theta$ | $a_z = -\frac{g\pi H}{L} \frac{\sinh[2\pi(z+d)/L]}{\cosh(2\pi d/L)} \cos \theta$ | $a_z = -2H \left(\frac{\pi}{T}\right)^2 e^{\frac{2\pi z}{L}} \cos \theta$ |
| 7. Water Particle Displacements | | | |
| a) Horizontal | $\xi = -\frac{HT}{4\pi} \sqrt{\frac{g}{d}} \sin \theta$ | $\xi = -\frac{H}{2} \frac{\cosh[2\pi(z+d)/L]}{\sinh(2\pi d/L)} \sin \theta$ | $\xi = -\frac{H}{2} e^{\frac{2\pi z}{L}} \sin \theta$ |
| b) Vertical | $\zeta = \frac{H}{2} \left(1 + \frac{z}{d}\right) \cos \theta$ | $\zeta = \frac{H}{2} \frac{\sinh[2\pi(z+d)/L]}{\sinh(2\pi d/L)} \cos \theta$ | $\zeta = \frac{H}{2} e^{\frac{2\pi z}{L}} \cos \theta$ |
| 8. Subsurface Pressure | $p = \rho g (\eta - z)$ | $p = \rho g \eta \frac{\cosh[2\pi(z+d)/L]}{\cosh(2\pi d/L)} - \rho g z$ | $p = \rho g \eta e^{\frac{2\pi z}{L}} - \rho g z$ |

5.7 “Oblique” Waves

For the discussion of motions of ships in obliquely approaching waves, the two-dimensional linear plane wave above can be considered to be a three-dimensional wave train with straight, infinitely long wave crests. If the considered wave is travelling at the angle, μ , contraclockwise to the x-axis it can be described by the equation:

$$\zeta(x, y, t) = a \cos(k(x \cos \mu + y \sin \mu) - \omega t) \quad \dots(5.57b)$$

and, in fact, all the arguments $(kx - \omega t)$ can be exchanged by $(k(x \cos \mu + y \sin \mu) - \omega t)$ in all the equations. In some literature the notations $k_x = kx \cos \mu$ and $k_y = ky \sin \mu$ are used giving

$$\zeta(x, y, t) = a \cos(k_x x + k_y y - \omega t) \quad \dots(5.57c)$$

5.8 Wave Energy

The local mean energy in a regular progressive wave can be estimated by integrating the potential and kinetic energy in the wave over a wavelength

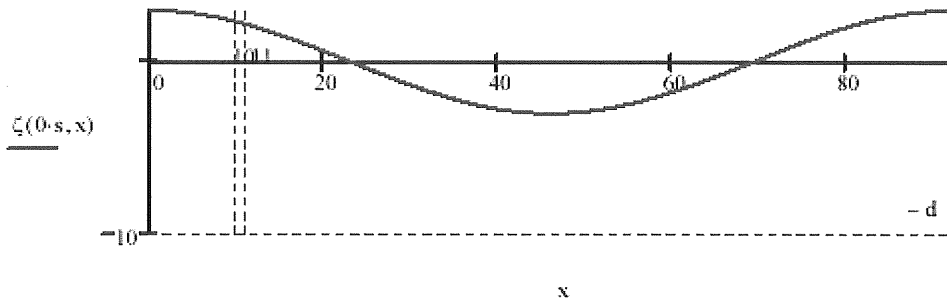


Figure 5.3 The mass of the lifted water mass between the two dashed verticals is $\rho g \zeta dx$ and this mass is lifted the height $\zeta/2$

The potential energy of the wave at a time instant e.g. $t = 0$ can be calculated as the deformation work needed to give the form of the wave $\zeta = a \cos kx$. Thus the mean energy over one wavelength is

$$E_p = \frac{1}{\lambda} \int_0^\lambda \rho g \zeta dx \frac{\zeta}{2} = \frac{\rho g}{2\lambda} \int_0^\lambda \zeta^2 dx = \frac{1}{4} \rho g a^2. \quad \dots(5.58)$$

The kinetic energy is the total kinetic energy contained in all the water from the free water surface to the bottom of the sea. To first order we can only integrate from the mean water surface, as the theory is not valid above the mean water surface, and would in fact give large errors for finite waves. For the wave in deep water it is especially easy to make the integration as the water particle moves with constant speed V along their circular paths with the radius decreasing with the level of submergence, z ,

$$r = r_0 e^{kz} = r_0 e^{\frac{2\pi}{\lambda} z}, \quad \dots(5.59)$$

where $r_0 = a$ is the radius at the mean water level $z = 0$ equal to the wave amplitude. The velocity is thus

$$V(z) = \frac{2\pi r(z)}{T} = \sqrt{u^2 + w^2} \quad \dots(5.60)$$

and the kinetic energy per unit volume is

$$\frac{1}{2} \rho (V(z))^2. \quad \dots(5.61)$$

It is interesting to note that the kinetic energy is constant over the horizontal planes at each level.

Finally integrating from the depth to the mean water level

$$\begin{aligned} E_k &= \frac{1}{2} \rho \int_{-\infty}^0 \left[\frac{2\pi}{T} a e^{kz} \right]^2 dz = \frac{1}{2} \rho \left(\frac{2\pi}{T} \right)^2 a^2 \frac{1}{2k} e^{2kz} \Big|_{-\infty}^0 = \\ &= \frac{1}{2} \rho \omega^2 a^2 \frac{1}{2k} = \frac{1}{4} \rho g a^2 \end{aligned} \quad \dots(5.61)$$

The last equality comes from the dispersion relation in deep water $gk = \omega^2$. The total wave energy follows as

$$E = E_p + E_k = \frac{1}{2} \rho g a^2,$$

which has the unit J/m^2 , shows that the energy content averaged over a horizontal area in a small-amplitude, harmonic wave is proportional to the wave amplitude squared.

5.9 Wave Power

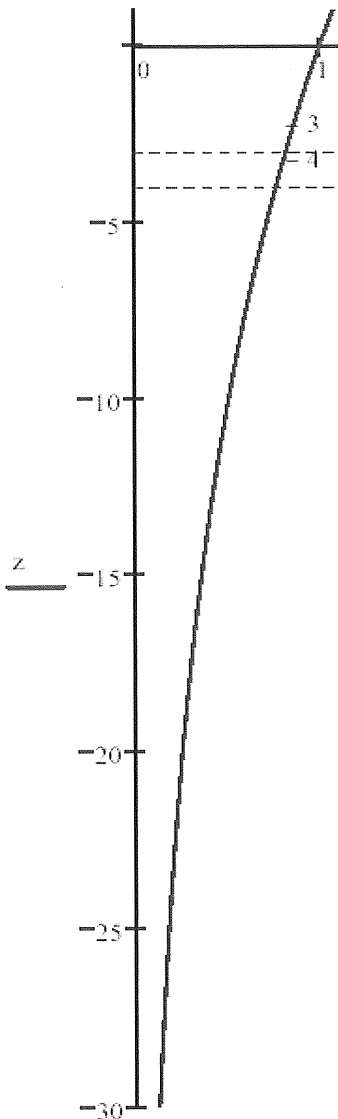
The energy transport or wave power per unit width of a plane wave can be calculated by estimating the work done in the propagation direction on the water mass to the left.

In deep water the work done at the level z in the vertical $x = 0$ m during the time dt is

$$dW = p dx dz \quad \dots(5.62)$$

and per time unit of time

Figure 5.4 Pressure distribution in a deep-water wave



$$\frac{dW}{dt} = p \frac{dx}{dt} dz = p u dz$$

Integrated along the vertical the wave power is

$$\begin{aligned} P(t) &= \int_{-\infty}^0 \rho g (a e^{kz} \cos(-\omega t) - z) a \omega e^{kz} \cos(-\omega t) dz = \\ &= \int_{-\infty}^0 \rho g a^2 \omega e^{2kz} \cos^2(\omega t) dz + \int_{-\infty}^0 \rho g (-z) a \omega e^{kz} \cos(\omega t) dz = \\ &= \rho g a^2 \omega \cos^2(\omega t) \int_{-\infty}^0 e^{2kz} dz - \rho g a \omega \cos(\omega t) \int_{-\infty}^0 z e^{kz} dz = \\ &= \rho g a^2 \omega \frac{1}{2} (1 + \cos(2\omega t)) \int_{-\infty}^0 e^{2kz} dz - \rho g a \omega \cos(\omega t) \int_{-\infty}^0 z e^{kz} dz \end{aligned} \quad \dots(5.63)$$

The first term on the right hand side in the last line in (5.63) thus oscillates with twice the frequency of the wave, but is always larger than zero, while the second term has the same frequency as the wave but gives no net transport as its time average is zero.

The net power energy transport is thus

$$\begin{aligned} \overline{P(t)} &= \frac{1}{T} \rho g a^2 \omega \frac{1}{2} \int_0^T (1 + \cos(2\omega t)) dt \int_{-\infty}^0 e^{2kz} dz = \\ &= \frac{1}{2} \rho g a^2 \omega \frac{1}{2k} = \frac{1}{2} \rho g a^2 \frac{1}{2} \frac{\omega}{k} = \frac{C}{2} E = C_g E \end{aligned} \quad \dots(5.64)$$

from which it is seen that in deep water the wave energy is transported at half the wave celerity C . This transport velocity, C_g , is also called the *group velocity* due to the fact that a group of waves must propagate with this velocity. Otherwise it would leave its energy behind and disappear. See also the next paragraph.

5.10 Wave Celerity, Group Velocity and Particle Velocities

Dispersion and celerity

An important feature of surface gravity waves is that the speed of propagation of the waveform, i.e. the phase speed or the *celerity* depends on the wave period. This has the effect that a group of waves containing components of various frequencies will be spread out or *dispersed* as it propagates.

To illustrate the effect of dispersion a wave train registered at three different points along its route of propagation is shown in Figure 5.5. The composed wave train in the uppermost time trace separates into longer and shorter waves, the longer component waves arriving earlier than the shorter component waves further along the route of propagation.

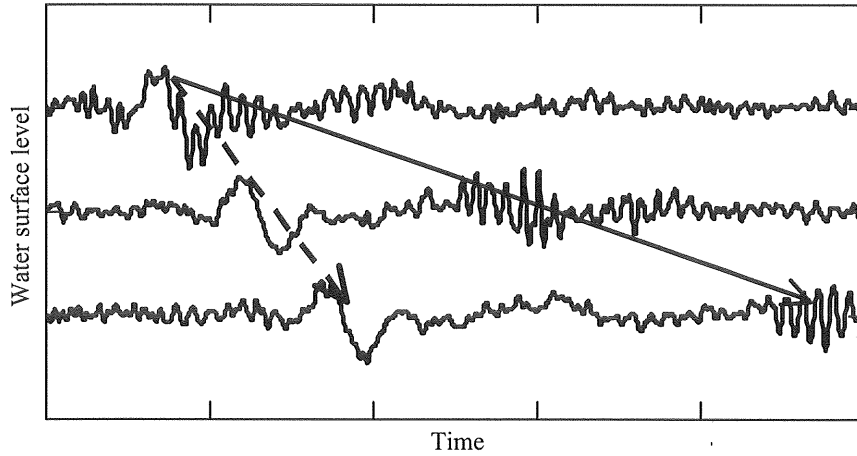


Figure 5.5 The water level as a function of time for a composed wave train at three points along its route of propagation. The uppermost trace is “upwind” and the lower ones are increasingly farther downwind. The arrows indicate how the shorter waves arrive later (solid arrow) downwind than the longer waves (dashed arrow).

The celerity is by definition:

$$C = \frac{\lambda}{T} = \frac{\omega}{k} \quad \dots(5.65)$$

where ω and k are interdependent through an implicit dispersion relation, Equation (5.30), that was derived from the velocity potential

$$\omega^2 = gk \tanh(kd) \quad \dots(5.66)$$

which gives the celerity

$$C = \frac{\omega}{k} = \sqrt{\frac{g}{k} \tanh(kd)} = \frac{g}{\omega} \tanh(kd) \quad \dots(5.67)$$

This expression cannot be solved explicitly for k or C , but must be solved by iteration in k or using approximations. (E.g. a Padé approximation)

In the limits for deep water ($d \gg \lambda$) and shallow water ($d \ll \lambda$), however, explicit expressions for the celerity and wavelength are attained. See Table 5.2 below and Table 5.1.

Table 5.1 Some important relations for linear waves at various relative depths

| | Deep water ($kd > \pi$) | Intermediate water ($\pi/10 < kd < \pi$) | Shallow water ($kd < \pi/10$) |
|--|---|---|------------------------------------|
| Celerity | $C = \frac{g}{\omega}$ | $C = \frac{g}{\omega} \tanh(kd)$ | $C = \sqrt{gd}$ |
| Wavelength | $\lambda = \frac{gT^2}{2\pi}$ | $\lambda = \frac{gT^2}{2\pi} \tanh(kd)$ | $\lambda = T\sqrt{gd}$ |
| Group velocity | $C_g = \frac{C}{2} = \frac{g}{2\omega}$ | $C_g = \frac{1}{2} \left[1 + \frac{2kd}{\sinh(2kd)} \right] C$ | $C_g = C = \sqrt{gd}$ |
| Amplitude of vertical particle velocity at the water surface | $a\omega$ | $a\omega$ | $a\omega$ |

Group velocity

The energy of surface gravity waves is generally propagating slower than the waveform, which means that, except in extremely shallow water, a group of waves will propagate slower than the individual waves. Thus the rearmost wave will progress through the wave group to finally die out at the front of the wave group while “new” waves are continuously developing in the rear.

This phenomenon is illustrated for a deep-water wave in Figure 5.6, where a wave group is snapshot at equally spaced time intervals along its route of propagation. The crest of the rearmost wave in the earliest snapshot is marked with a circle and traced in the consecutive snapshots. It can be seen how it is progressing through the group and how its amplitude first grows and then attenuates to nil when it leaves the group in the front.

The speed of propagation of the energy and the wave group is called the *group velocity* and is half the wave celerity in deep water and equal to the wave celerity in very shallow water. Equations for the group velocity are given in Table 5.2, and the group velocity in deep water was derived from the energy transport in Equation (5.64).

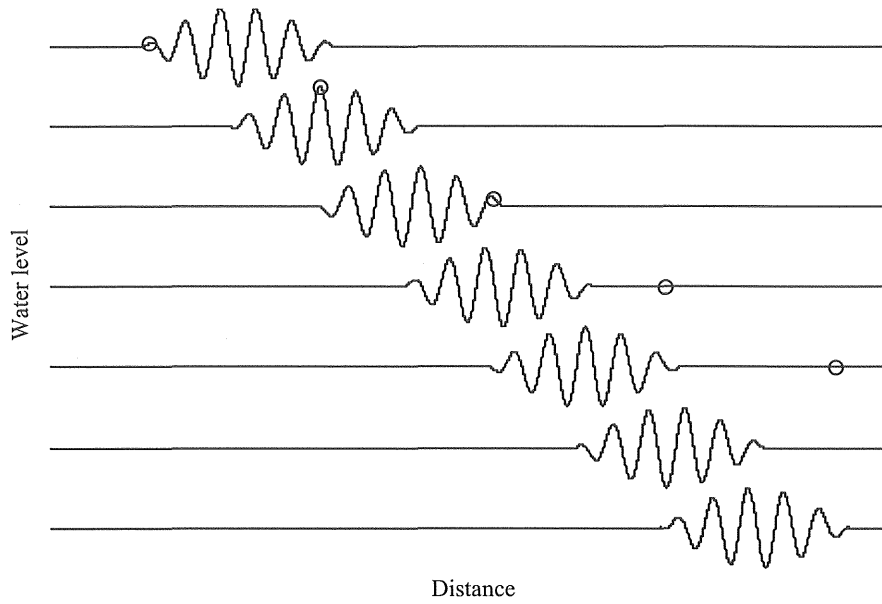


Figure 5.6 Snapshot of a deep-water wave group at equally spaced intervals along its route of propagation. The rearmost wave in the earliest snapshot is marked with a circle and traced in the consecutive snapshots.

An alternative to the calculation of the group velocity from the energy transport is to superpose two progressive waves with almost the same frequencies ω and ω' and consequently almost the same wave numbers k and k' . See Figure 5.7.

$$\begin{aligned}
 \zeta(x, t) &= a(\cos(kx - \omega t) + \cos(k'x - \omega' t)) = \\
 &= a \left[\cos^2\left(\frac{1}{2}(kx - \omega t)\right) - \sin^2\left(\frac{1}{2}(kx - \omega t)\right) \right] + \left[\cos^2\left(\frac{1}{2}(k'x - \omega' t)\right) - \sin^2\left(\frac{1}{2}(k'x - \omega' t)\right) \right] = \dots(5.68) \\
 &= 2a \cos\left(\frac{1}{2}(k'x - \omega' t) + \frac{1}{2}(kx - \omega t)\right) \cos\left(\frac{1}{2}(k'x - \omega' t) - \frac{1}{2}(kx - \omega t)\right) = \\
 &= 2a \cos\left(kx - \omega t + \frac{1}{2}(\delta kx - \delta \omega t)\right) \cos\left(\frac{1}{2}(\delta kx - \delta \omega t)\right)
 \end{aligned}$$

where $\delta k = k' - k$ and
 $\delta \omega = \omega' - \omega$.

As δk and $\delta \omega$ are assumed to be small we can write

$$\zeta(x, t) = 2a \cos(kx - \omega t) \cos\left(\frac{1}{2}(\delta kx - \delta \omega t)\right) \dots(5.69)$$

The “carrier wave” $a \cos(kx - \omega t)$ will thus be modulated by the function

$$\cos\left(\frac{1}{2}(\delta kx - \delta \omega t)\right)$$

which has the phase velocity

$$\frac{\delta\omega}{\delta k}$$

Each group of waves that is contained between the zero-crossings of the modulating function is thus moving with this velocity, and therefore it is denoted the group velocity.

In the limit when $\delta k \rightarrow 0$ the group velocity will be given by the partial derivative of k in Equation (5.30) with respect to ω

$$\lim_{\delta k \rightarrow 0} \frac{\delta\omega}{\delta k} = \frac{\partial k}{\partial \omega} = C_g \quad \dots(5.70)$$

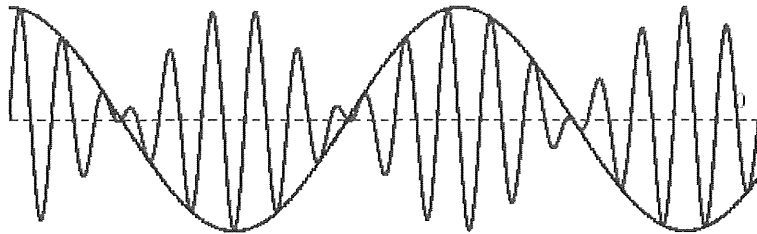


Figure 5.7 Snapshot of a wave composed of two sinusoidal waves of almost the same wavelength. The longer-period wave is the modulated wave and the shorter-period wave is the “carrier” wave.

Water particle motion and dynamic pressure

The water particle velocities were derived from the velocity potential above. The vertical velocity amplitude of a regular linear wave is always $2\pi a/T$ or $a\omega$. In deep water the horizontal velocity amplitude also equals that value, while in shallower water the horizontal velocity amplitude is larger. See Table 5.1. Note also that the particle velocity is generally different from the wave celerity and the group velocity, except for very steep, breaking wave crests, where the particle velocity can approach or even supersede the celerity, thus making the particles leave the wave surface.

5.11 Finite Amplitude Waves and Higher-Order Waves

Recall that the linear wave theory assumes that the wave height is small compared to the wavelength and water depth. In natural wind waves the steepness H/λ seldom exceeds 0.05 to 0.08 in deep water, so the small amplitude theory is often valid. In some applications it is, however, necessary to use non-linear or *finite-amplitude wave theory*. Physically the difference between linear and finite-amplitude theories is that finite amplitude-theories consider the influence of the wave itself on its properties. Therefore the phase speed, wavelength, water surface elevation and other properties are functions of the actual wave height.

There are a number of different finite-amplitude wave theories. For deep to intermediate-depth water ($d/\lambda < 1/8$) the most commonly adopted is the theory by *Stokes* (1847, see e.g. *Wiegel*^{xv} 1964). For shallower water *Cnoidal Wave Theory* (*Korteweg de Vries*, 1895, see e.g. *Wiegel* 1964) or *Stream Function Theory* (See e.g. *Dean and Dalrymple*^{xvi}, 1991) is more applicable. *Williams*^{xxiii} (1985) has produced tables of progressive gravity waves covering the full range of wavelength from solitary to infinite-depth waves, and up to the waves of limiting heights with sharp crests.

Stokes' second order wave in deep water

Linear wave theory predicts sinusoidal waves with equal crest height and trough depth. However, steep real waves in deep water have peaked high crests and flat shallow troughs. For applications such as determining deck elevation of offshore structures this is important, and usually Stokes' 2nd order theory is used for this problem, while for calculating wave forces on fixed structures from extremely large long period waves rather Stokes' 3rd or 5th order theory is applied. Also, linear wave theory predicts no net mass transport, as the water particles move in closed orbits, while finite amplitude theories predict a small net transport in the direction of wave propagation.

In deep water the surface elevation of a second order Stokes' wave with the wave height $H = 2a$ can be written

$$\zeta(x, t) = a \cos(kx - \omega t) + \frac{\pi a^2}{2\lambda} \cos(2(kx - \omega t)) \quad \dots(5.71)$$

Its elevation as a function of the space co-ordinate x is shown in Figure 5.8.

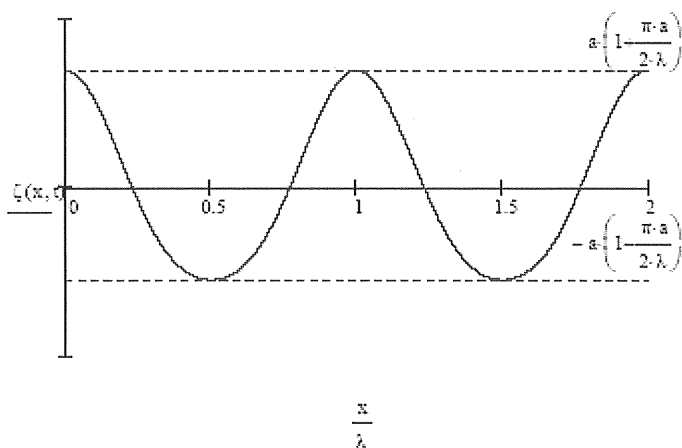


Figure 5.8 An example of a second order Stokes' wave as a function of the horizontal co-ordinate x . The crest and trough elevations are also given.

Finite-height shallow water waves

For real shallow water waves of finite height the flaws of linear theory become still more apparent. E.g. the mass transport is significant, waves may break, the crests get

steeper fronts than backs and the mean water level is elevated above the still water level. In the limit, the whole wave may be above the still water level and the whole water mass of the wave is transported forward for each individual wave passage. In this limit solitary wave theory can be used for non-breaking waves while for waves with steep fronts other depth-integrated theories like the shallow water equation may be more useful describing bores and shocks.

In Figure 5.9 dimensionless wave profiles of 40 cases (Dean^{xxiv}, 1974) as published by CERC^{xxiii} (1984), are shown as an illustration of the fit to the linear, sinusoidal wave profile of the Airy theory. In the figure the parameter, d/gT^2 , is a shallow-water parameter (\sim water-depth to deep-water wavelength) and the parameter, H/H_b , is a kind of steepness parameter (ratio between actual wave height and the breaking wave height for the considered water depth and wavelength). In the left low corner the profile of a moderately steep wave in intermediate water is shown, and it can be seen that this profile is reasonably sinusoidal. As a contrast, in the right high corner a maximally steep wave in very shallow water shows a profile far from sinusoidal.

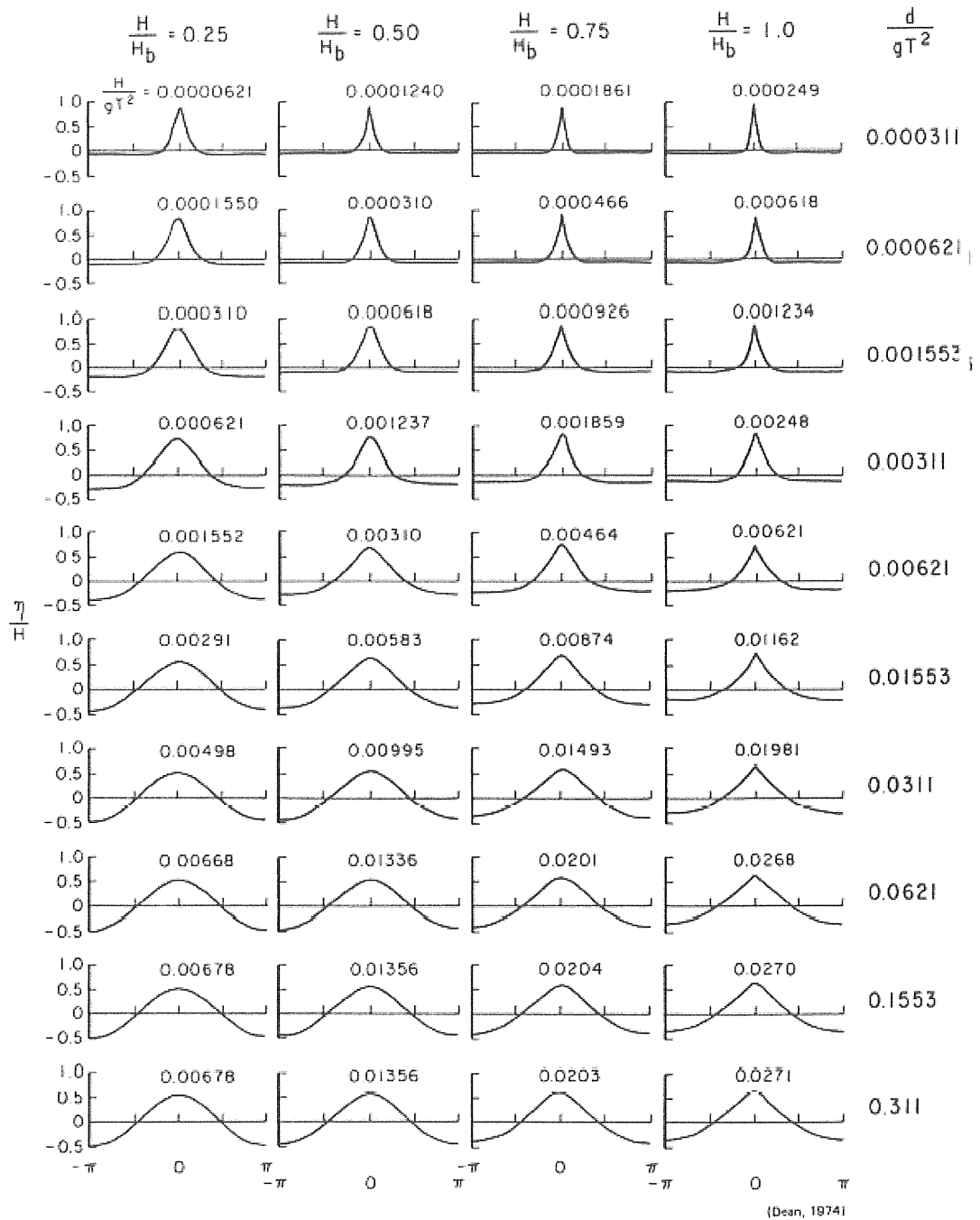
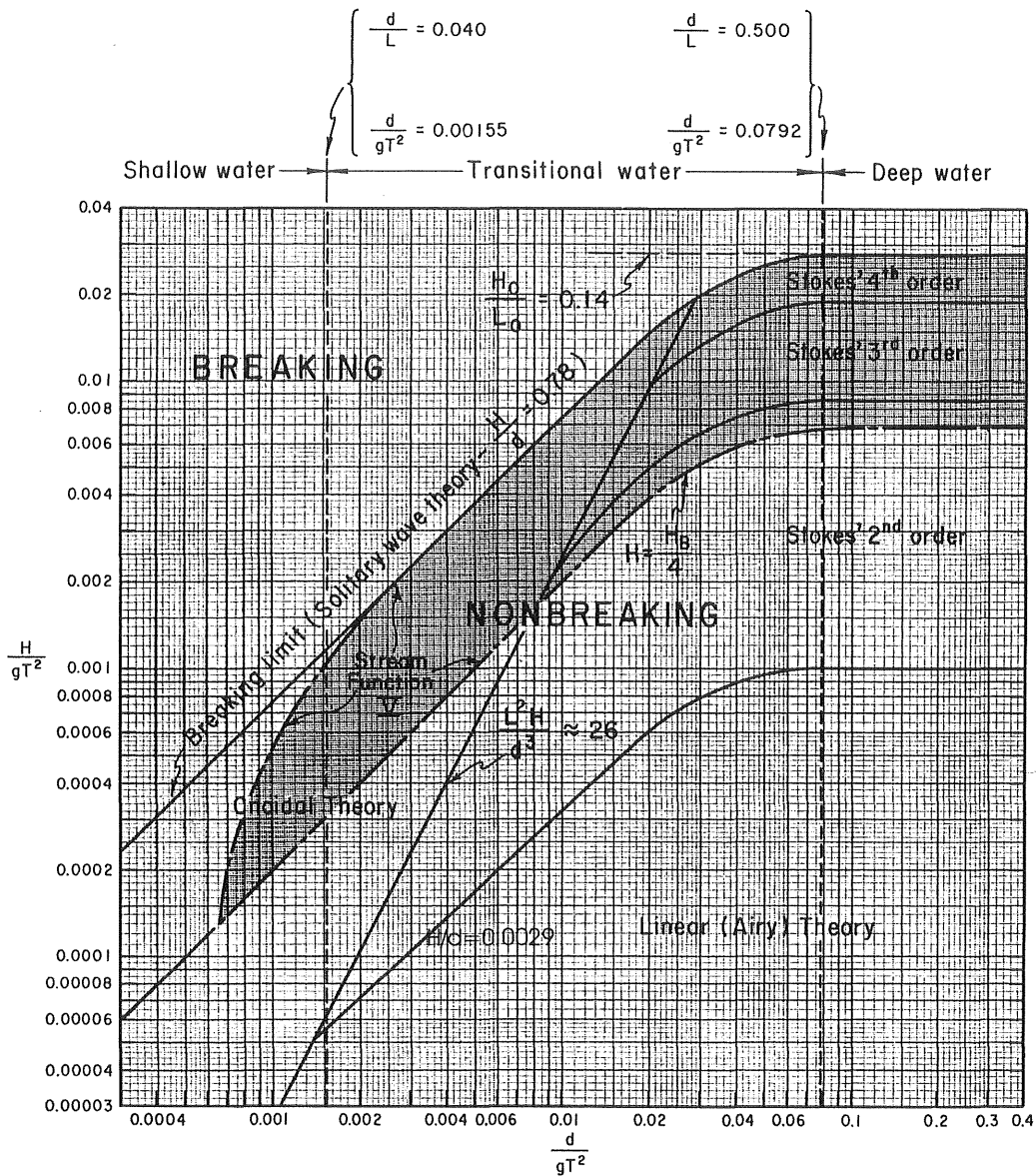


Figure 5.9 Dimensionless wave profiles for 40 cases of steep periodic waves in shallow to intermediate water depth. (Numbers on each plot represent the value of H/gT^2 for each case). (CERC^{xxii}, 1984)
 Here $\eta = \zeta$.

In Figure 5.10 a graph over areas of best fit for wave theories according to Le Méhauté, as published by CERC (1984), is shown. The horizontal axis is a water-depth to deep-water wavelength parameter, d/gT^2 , and the vertical axis a wave height to deep-water wavelength parameter, H/gT^2 .



(after Le Mehaute, 1969)

Figure 5.10 Regions of validity for various wave theories. (CERC^{xxii}, 1984)
 Here $L = \lambda$ and L_0 is the deep water wave length.

Solitary waves

The theories above consider oscillatory or almost oscillatory waves, i.e. the water moves forward and backwards. The linear wave is truly oscillatory, as the water particles will return to their starting position for each cycle. In finite-amplitude waves,

however, the water particles are translated a small net amount forward for each wave passage. When the water particles move only in the direction of wave propagation, the wave is called a wave of translation. The solitary wave is such a wave. A true solitary wave is entirely above the still water level, shows up as a smooth hump of water with no waves behind or in front of it and translates at constant celerity without losing wave-height. It requires finite-depth and it is two-dimensional. It is difficult to form a solitary wave in practice although it is rather easy to form an approximate one with a tail of small dispersive waves. (Wiegel^{xv}, 1964)

For regular waves running up a beach it is recommended to rather use the cnoidal wave theory or the stream function wave theory. The cnoidal wave theory approaches the solitary wave theory for shallow water waves and the linear or Stokes theory for deep-water waves. (CERC^{xxii}, 1984) For a comparison of waveforms see Figure 5.11.

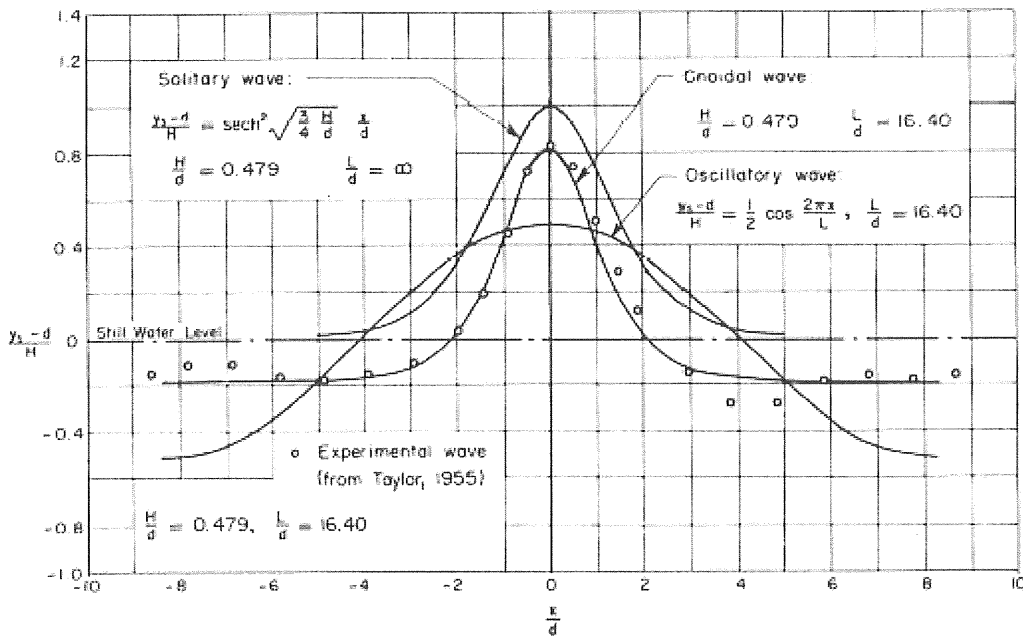


Figure 5.11 Comparison of measured and theoretical wave profiles
 (From Wiegel^{xv}, 1964)

5.12 Propagation and Transformation

Dispersion and transformation to swell

Weather systems usually move at a much slower speed than the wind velocity within them. As the celerity of the waves in a well developed sea state are approximately the same as the wind velocity, and the group velocity is less than that – in deep water only half the celerity – the result will be that the waves run out of the windy area where they are generated. After leaving the generation area they are no longer acted upon by the wind, and rather soon internal friction (viscosity), parasitic capillary waves and air resistance will dissipate the sharp wave crests and the shortest components of the spectrum. Such a free wave system is referred to as swell. Also, due to dispersion the longer faster waves with longer periods will arrive at distant points long before the

shorter waves. The total effect is that at distant points the swell can become almost monochromatic with a wave period slowly decreasing with time, as decreasingly shorter waves continue to arrive. In the low atoll islands of Polynesia, traditionally, the first arriving swell served as an alarming forewarning of approaching hurricanes. (Wiegel^{xxv}, 1964 and Kinsman^{xxv}, 1965)

Shoaling

Consider the two-dimensional problem of regular waves at normal incidence to a shoaling beach. Neglecting dissipation, e.g. bottom friction, the time average energy transport, \bar{P} , must be constant through all vertical sections, and as the energy is transported by the group velocity which varies with the depth, d , the following relation must hold from deep water to finite water depth

$$\bar{P} = C_{go} E_o = C_g E, \quad \dots(5.72)$$

index o denoting deep water, C_g the group velocity and E the wave energy.

With the energy at any depth proportional to amplitude squared, in deep water $E_o = (1/2)\rho g a_o^2$ and in finite-depth water $E = (1/2)\rho g a^2$ the ratio between the wave amplitude or wave height in finite depth water to that in deep water can be solved. This ratio is called the shoaling coefficient,

$$K_s = \frac{a}{a_o} = \frac{H}{H_o} = \sqrt{\frac{C_{go}}{C_g}}. \quad \dots(5.73)$$

As shown in Figure 5.12, going from deep water into shallower water, the shoaling coefficient first decreases slightly below one before increasing rapidly. At the same time the wavelength becomes shorter due to decreasing celerity, and finally the waves may break. See the paragraph on wave breaking below.

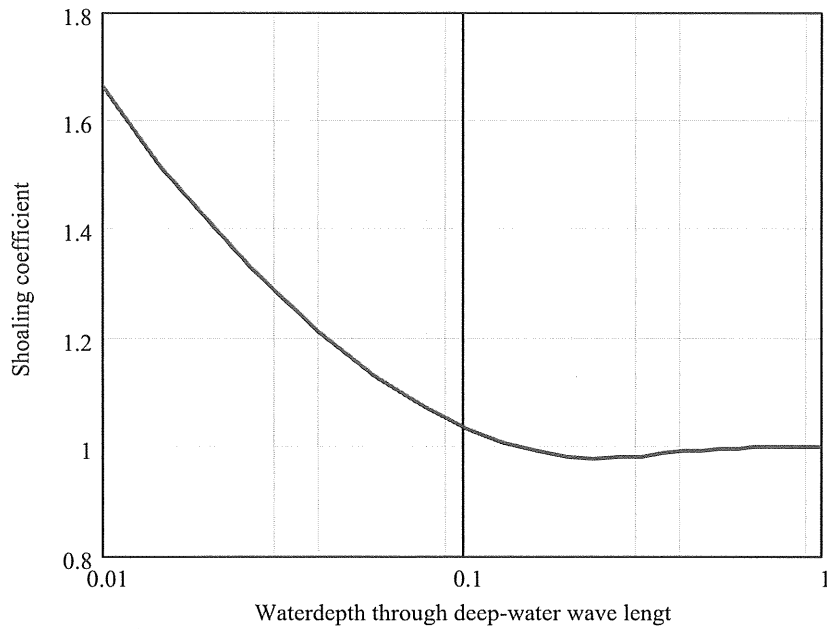


Figure 5.12 Variation of the shoaling coefficient, $K_s = H/H_0$, with the non-dimensional water depth, d/L_0 . L_0 is the deep-water wavelength.

Refraction

As pointed out above, the wave celerity decreases with water depth. Then, if a long-crested wave approaches a uniformly sloped shelf at an oblique angle the wave slows down and the wave crest will bend to become more parallel to the depth contours. This phenomenon is equivalent to the refraction of light in optics.

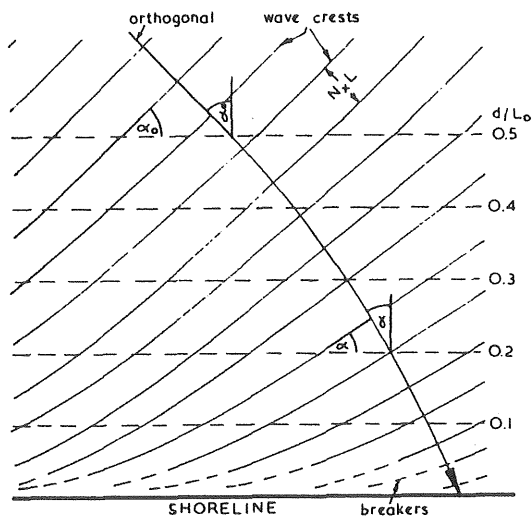


Figure 5.13 Oblique waves traversing a uniformly sloped shelf. (From Silvester^{xxvi}, 1974)

Going into more detail to see how the refraction affects the wave height one can follow wave rays or wave rays normal to the wave crests and parallel to the wave celerity in each point. Being parallel in deep water they will either spread or approach each other approaching land, depending on the bottom topography. Further, assuming that no energy will be transported across the wave rays but be contained between two adjacent wave rays, the effect will be decreasing wave height if they spread and increasing wave height if they approach each other.

Letting them be evenly distributed in deep water at a distance, b_o , the distance will become, b , somewhere closer to land. The result will be a change in wave height by a factor $K_r = \sqrt{b_o/b}$ additional to the shoaling effect. The factor, K_r , is called the refraction coefficient. The total effect of shoaling and refraction will be

$$\frac{a}{a_o} = \frac{H}{H_o} = \sqrt{\frac{C_{go}}{C_g}} \sqrt{\frac{b_o}{b}} = K_s K_r \dots(5.74)$$

On a straight, shoaling coast the wave rays will spread and thus the refraction coefficient will become lower than one: $K_r < 1$. See Figure 5.14.

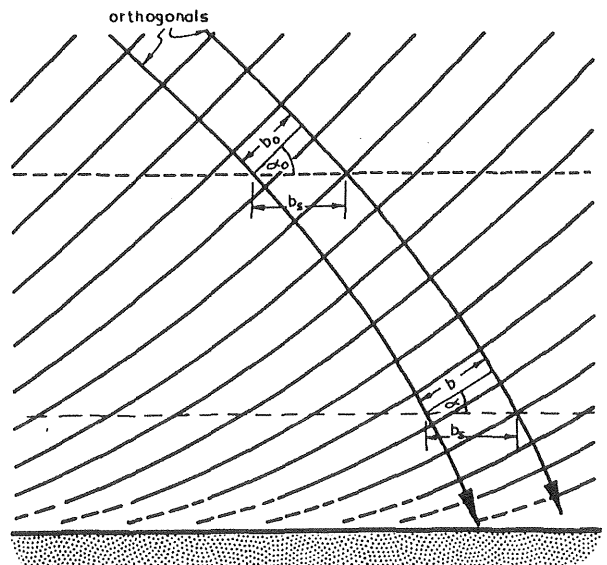


Figure 5.14 Orthogonal spacing over a uniformly sloped beach.
 (From Silvester^{xxvi}, 1974)

On a coastline with headlands and bays the result of refraction and shoaling will be increased wave action on the headlands and decreased action in the bays. See Figure 5.15.

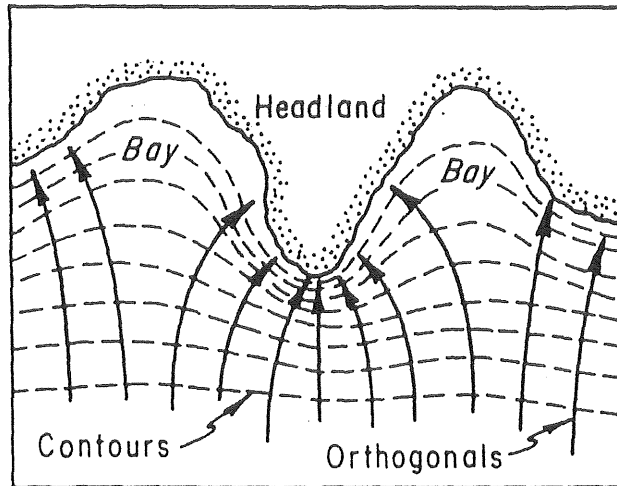


Figure 5.15 Refraction along an irregular shoreline. (From CERC^{xxii}, 1984)

Diffraction and reflection

In water deeper than half the wavelength there is no refraction, but the waves will spread around steep rock peninsulas, piers and structures with steep walls due to diffraction, when energy spreads along the wave crests into “shadow” areas.

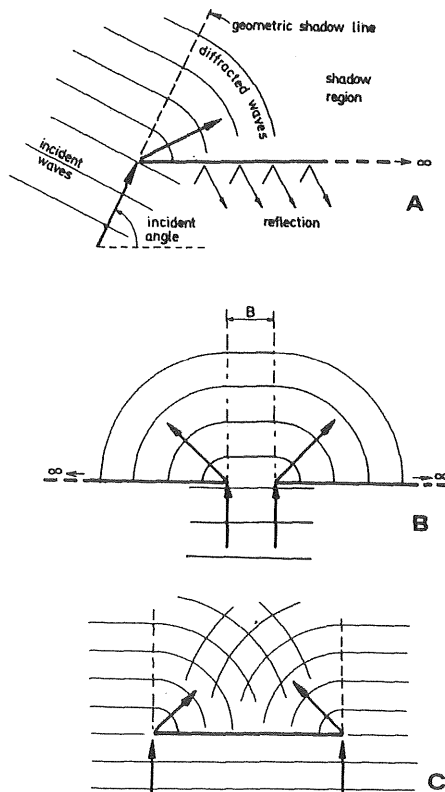


Figure 5.16 A. Wave diffraction behind a semi-infinite breakwater.
B. Diffraction through a breakwater gap
C. Diffraction behind an island or offshore breakwater.
(From Silvester^{xxvi}, 1974)

While waves approaching a gradually shoaling coastline will be absorbed by bottom friction and wave breaking, waves hitting steep rocks, piers or other structures will be reflected. In the examples shown in Figure 5.16 e.g. waves will be reflected on the “wave ward” side of the structures, so that a complicated wave pattern composed of reflected, incident and diffracted reflected waves will set up on the “wave ward” side. An example is shown in Figure 5.17. If thus the bottom is steep or structures dominate an area, where wave propagation shall be modelled, models must be used that can take diffraction and reflection into account, while simpler models may be used for mildly sloping bottom topographies.

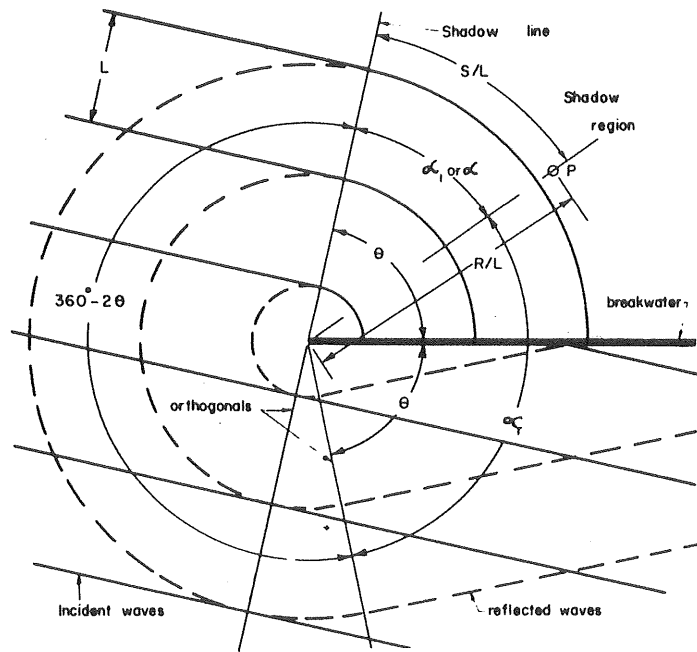


Figure 5.17 Sketch of wave crests of regular waves incident, reflected and diffracted against a semi-infinite breakwater. (From Silvester^{xxvi}, 1974)

Wave breaking

The “white capping” or wave breaking involves dissipation of energy. Regular waves will theoretically break when the wave steepness, H/λ , approaches

$$H_b/\lambda = \gamma \tanh(2\pi d/\lambda), \quad \dots(5.75)$$

with $\gamma = 0.142$ (Miche, 1944). In Fig 5.10 this limit is denoted $H_0/L_0 = 0.14$. In practice however $\gamma = 0.12$. In deep water this means that the steepness will normally not exceed 0.12. See Silvester^{xxvi} (1974) for further details. Although steeper waves than given by Equation (5.75) have been registered now and then, it is not until lately it has been recognised that these rogue or freak waves may be more frequent than anticipated, and thus are responsible for many losses of ships and some unforeseen damage to offshore drilling platforms. Such waves are three-dimensional in character

and just now (2004) subject to much research.² In an irregular sea the steepness breaking will transfer some energy to longer wave components (Silvester^{xxvi}, 1974) but largely involves dissipation of energy of shorter wave components. See Young (1999) for further details.

If the wave does not break before it has entered the sloping beach the slope itself has an influence on the breaking process. One criterion by Collins (1970, cited by Silvester^{xxvi}, 1974) takes this into account:

$$H_b / d = 0.72 + 5.6S, \quad \dots(5.76)$$

Here S is the bottom slope. The breaker height is thus increased at breaking. Often however a simplified expression is used only containing the water depth:

$$H_b / d = 0.78 \quad \dots(5.77)$$

In Fig 5.10 this limit is denoted $H/d = 0.78$. Different types of breakers are shown in Figure 5.18. The breaker type depends on deep-water steepness, beach slope and wave period. See e.g. CERC^{xxii} (1984) or Silvester (1974)

For irregular waves there are some different approaches to depth limited breaking. Battjes and Jansen (1978, as cited by Young, 1999) e.g. look at individual waves assuming them to be Rayleigh distributed, and let all waves with heights above the limiting criterion be dissipated. Young (1999) limits the total energy of the spectrum by a criterion containing the average wave celerity.

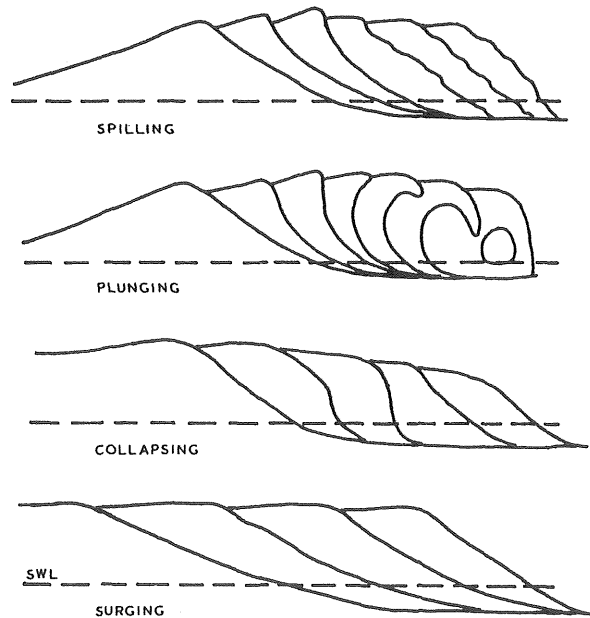


Figure 5.18 Successive profiles of breakers of various types.
 (From Silvester^{xxvi}, 1974)

² http://www.esa.int/esaCP/SEMOKQL26WD_index_0.html

Bottom friction dissipation

The fourth term listed by Young (1999) is the bottom friction dissipation, which for rigid impermeable bottoms depends on the shear just above the bottom. Therefore it is negligible in water deep in relation to the wavelength and increases for shallower waters. It is, however, important for longer waves in rather deep water e.g. for tidal waves, the “Bernoulli wave”, or shoaling secondary ship generated waves. Silvester^{xxvi} (1974) gives an account for regular waves, and Young (1999) for irregular waves. The degree of dissipation is governed by the bottom roughness, which depends on grain diameter of the bottom material, the geometry of ripples or dunes etc. Permeable and soft bottoms increase the dissipation.

The lost wave energy is partly dissipated into heat and partly used for erosion, ripple and dune formation, and net transport of bottom materials.

6 WAVE LOADS ON AND MOTIONS OF A SHIP IN REGULAR WAVES

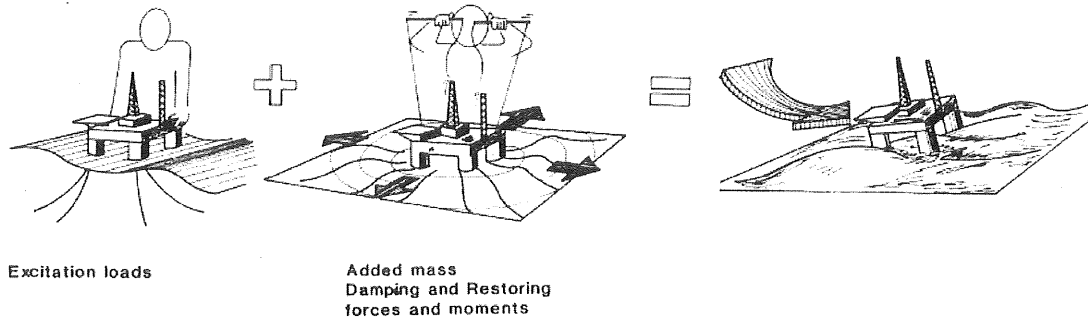


Figure 6.1 Superposition of wave excitation (left); added mass, radiation damping and restoring loads (middle); to the total hydrodynamic problem (right). (From Faltinsen^{xxvii} 1990)

6.1 Decomposition of the Problem³

The six hydrodynamic problems for each degree of freedom of motions in waves can each be solved separately by solving

- 1 the forces on the body when this is forced to oscillate with an arbitrary amplitude in calm water,
- 2 the forces on the body when this is fixed in the incident waves and last
- 3 the dynamic equilibrium or equation of motion when the difference between the forces 1 and 2 is balanced in each time instant by the inertia force of the accelerating body.

See figure 6.1 for an illustration of this. In Figure 6.2 we also define the degrees of freedom and coordinate system again.

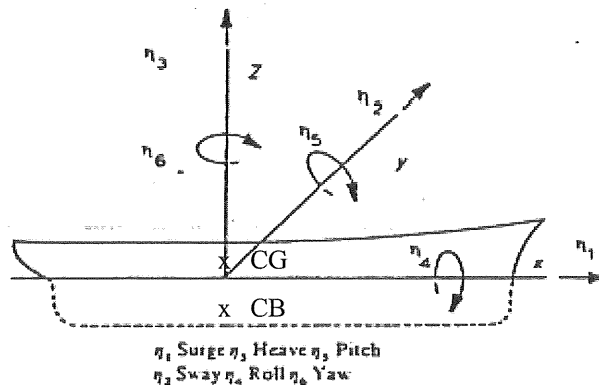


Figure 6.2 Definition of the chosen coordinate system for a ship. The z-axis is drawn vertically through the centre of buoyancy, CB, which must be vertically below the centre of gravity, CG, for a ship floating in equilibrium.

³ This chapter is partly founded on a compendium by professor emeritus Gilbert Dyne

We will first study the problem of wave-induced motions of a two-dimensional floating body in regular sea. With two-dimensional body is meant an infinitely long ship, whose cross-sectional shape is constant in the x-direction, and where all body motions (heave, sway and roll) and the water flow are parallel to the y-z-plane. This problem is fundamental in the much used strip theory, in which two-dimensional slices of mildly different ship shapes are added two form oblong approximately three-dimensional ships, as will be demonstrated later.

6.2 The Two-Dimensional Heave Problem

Forces on the two-dimensional ship heaving in calm water

Assume that the ship is forced to oscillate in heave in calm water with the amplitude, $\hat{\eta}_3$, and the angular frequency, ω .

$$\eta_3 = \hat{\eta}_3 \cos(\omega t) \quad \dots(6.1)$$

The arising forces are due to the vertical position, η_3 , Equation (6.1), vertical velocity

$$\dot{\eta}_3 = -\omega \hat{\eta}_3 \sin(\omega t) \quad \dots(6.2)$$

and vertical acceleration

$$\ddot{\eta}_3 = -\omega^2 \hat{\eta}_3 \cos(\omega t) \quad \dots(6.3)$$

relative the still water.

The vertical reaction force acting on the body from the water can be written

$$f_3 = -a_{33}\ddot{\eta}_3 - b_{33}\dot{\eta}_3 - c_{33}\eta_3 \quad \dots(6.4)$$

where the coefficients a_{33} , b_{33} and c_{33} must be assessed.

The vertical restoring force $-c_{33}\eta_3$ is due to the change of displacement. If the beam (width, breadth) of the body is B then the stiffness, c_{33} , must be

$$c_{33} = \rho g B \quad \dots(6.5)$$

The dynamic forces due to the acceleration and velocity of the body are associated with the forced oscillatory motion of the ambient water. For example the acceleration of a floating body is associated with a local, evanescent wave (standing wave, clapotis) when the water is forced to shift back and forth between the bottom and the sides. See Figure 6.3.

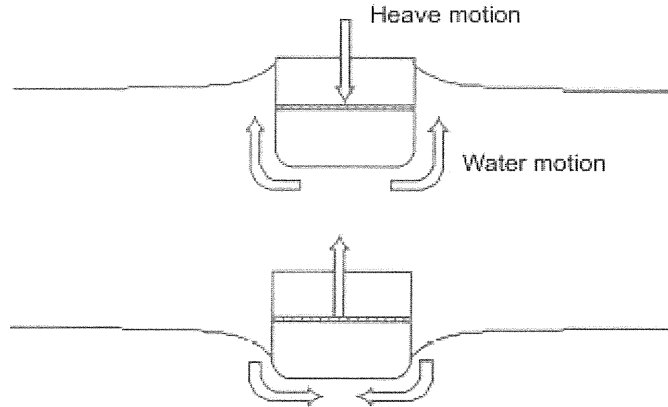


Figure 6.3 A standing or evanescent wave around a heaving ship's cross-section.

Added mass

As the force $a_{33}\dot{\eta}_3$ is in phase⁴ with the force needed to accelerate the body the coefficient a_{33} is often called the “added mass” and sometimes the hydrodynamic mass.

For bodies floating in the water surface or positioned close to the water surface the added mass is a function of the frequency of oscillation due to the evanescent waves and degree of resonance. Far from the free surface the added mass is constant and depends only on the shape of the body and its vicinity to other bodies or fixed boundaries. Also for floating bodies, in the limit, as $\omega \rightarrow \infty$, no waves are formed, and the added mass becomes independent on the frequency. See Figure 6.4b for an example of added-mass coefficients for a rectangular cross section in water shallow compared to the draft.

Radiation damping

The heave motion also causes waves that radiate out from the body, and the force, $b_{33}\dot{\eta}_3$ needed to maintain this oscillation is in phase with the velocity. The radiated waves transport energy away from the body and therefore introduces hydrodynamic or radiation damping. Therefore the coefficient, b_{33} , is called the damping coefficient or radiation damping coefficient, when stressing the phenomenon of the radiated waves. For bodies floating in the water surface or positioned close to the water surface also the radiation damping is a function of the frequency of oscillation due to the generation of waves. For floating bodies, in the limit, as $\omega \rightarrow \infty$, no waves can be formed, and the radiation damping is nil as it is for deeply submerged bodies, that cannot produce surface gravity waves. The radiation damping is actually nil both for $\omega \rightarrow 0$ and $\omega \rightarrow \infty$. There is a maximum somewhere in between where the body has a maximal ability to radiate energy or reciprocally absorb wave energy. See Figure 6.4c for an example of radiation-damping coefficients for a rectangular cross section in water shallow compared to the draft.

⁴ Or sometimes in antiphase for slightly submerged bodies, that is, the added mass a_{33} is negative.

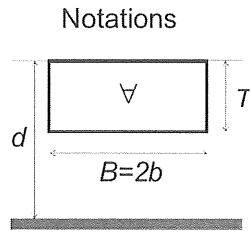


Figure 6.4a Notations for a two-dimensional rectangular hull in shallow water, $2T = B$, $d/T = 2$, $d/B = 1$, $\nabla = TB = \text{displacement}$, $k = \text{wave number}$ and $b = B/2$

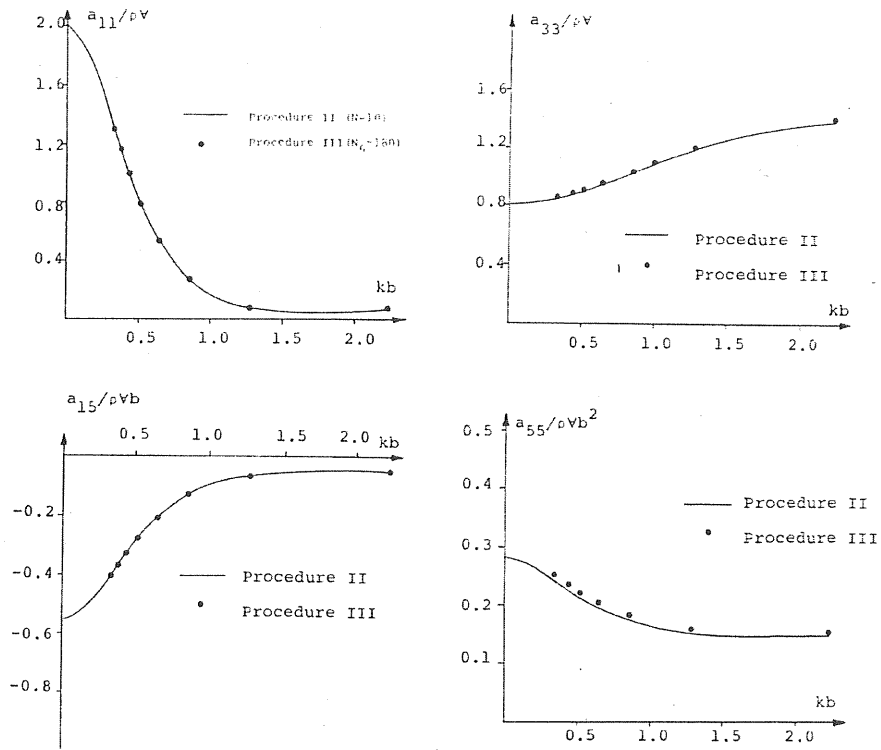


Figure 6.4b Two-dimensional added mass coefficients for the hull in Fig. 6.4a (From Johansson 1989^{xxviii})

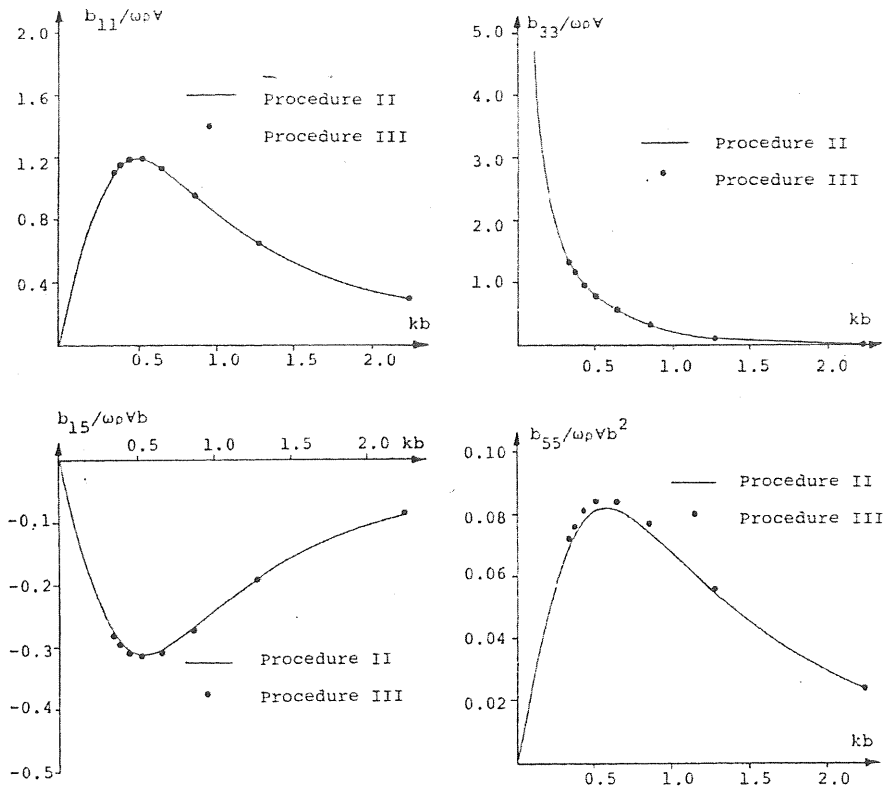


Figure 6.4c Two-dimensional radiation-damping coefficients for the hull in Fig. 6.4a (From Johansson 1989^{xxviii})

As stated above any body forced to oscillate in the water surface will create waves that propagate away from the body thus transporting out or radiating energy. For the two-dimensional case this will be illustrated below. See Figure 6.5.

The damping force in heave for a two-dimensional body can be written

$$f_{rd3} = -b_{33}\dot{\eta}_3 \quad \dots(6.6)$$

During a period, T , of oscillation, the exciting force $-f_{rd3}$ necessary to maintain a harmonic motion at the amplitude $\hat{\eta}_3$ will exert the mean power

$$\frac{1}{T} \int_0^T (-f_{rd3}\dot{\eta}_3) dt = \frac{1}{T} \int_0^T b_{33}\dot{\eta}_3\dot{\eta}_3 dt = \omega^2 b_{33} \frac{(\hat{\eta}_3)^2}{2} \quad \dots(6.7)$$

The body will radiate waves equally to starboard and port side with the amplitude, a , and the radiated power – in deep water – to one side is according to Equation (5.64)

$$\frac{1}{4} \rho g a^2 \frac{\omega}{k} \quad \dots(6.8)$$

Setting twice this radiated power equal to the exerted power – in order to take both starboard and portside wave into account – gives

$$\omega^2 b_{33} \frac{(\hat{\eta}_3)^2}{2} = 2 \frac{1}{4} \rho g a^2 \frac{\omega}{k} \quad \dots(6.9)$$

from which b_{33} can be solved

$$b_{33} = \rho g \left(\frac{a}{\hat{\eta}_3} \right)^2 \frac{1}{k\omega} = \rho \left(\frac{a}{\hat{\eta}_3} \right)^2 \frac{g^2}{\omega^3} \quad \dots(6.10)$$

which is valid for all frequencies and shows that the damping is always positive, which is not necessarily true for the added mass. Remember that according to the used linear assumptions and the potential theory, the given coefficients are only valid for small-amplitude motion and viscous non-linear damping is not taken into account either. In reality the total damping is always larger than the radiation damping.

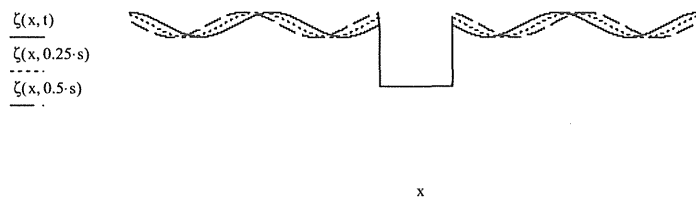


Figure 6.5 Radiated 2D waves

Two-dimensional added-mass and radiation coefficients in heave

In order to calculate the added mass and the radiation-damping coefficient potential problems described by Laplace equation are solved. For heave this is done by adding the solutions for the incident undisturbed wave (Chapter 5), the solution for the scattered (reflected and transmitted) wave from the fixed body and the radiated wave from the body heaving in calm water. The solution should satisfy the boundary conditions on the water surface, the sea bottom and on the wetted part, hull, of the body. The first two conditions were discussed in Chapter 5. The last condition demands that the water velocity perpendicular to the hull must be the same as the velocity of the hull, so that no water passes the hull, that is, the total relative velocity perpendicular to the hull must be nil. Also the radiation condition must be satisfied which for the two-dimensional problem means that the reflected, transmitted and radiated waves must propagate outwards from the body and be bound.

The solution can be attained by simple Rankin sources distributed over all the boundaries of the problem, or by smarter Greens' functions or Havelock sources fulfilling by themselves the free-boundary and radiation conditions. In this chapter we will not describe this further but accept the results calculated by Grim (1959) for various Lewis-form cross sections.^{xxix}

The added mass can then be assessed by reading the coefficient C from the diagrams in Figure 6.7,

$$a_{33} = \rho(\pi/8)B^2C, \quad \dots(6.11)$$

where B as before is the beam of the ship section and C is a function of

the beam to draught ratio B/T ,
the section-area coefficient $\beta = S/(BT)$ and
a dimensionless wave number expressed as $(\omega_e)^2 B/(2g)$.

In Figure 6.5 B and β are indexed n to stress that they are valid for a section No n along the ship. The angular frequency ω_e is the encounter, angular frequency experienced by the ship. At zero speed the encounter frequency is identical to the wave frequency.

Similarly the radiation-damping coefficient can be assessed by reading the coefficient A from the diagrams in Figure 6.8. Here A is the ratio between the amplitude of the radiated waves and the amplitude of the driving heave motion. Compare Equation (6.10).

$$b_{33} = \rho g^2 A^2 / \omega^3 \quad \dots(6.12)$$

A is a function of the same parameters as the added mass, namely B/T , β , and $(\omega_e)^2 B/(2g)$.

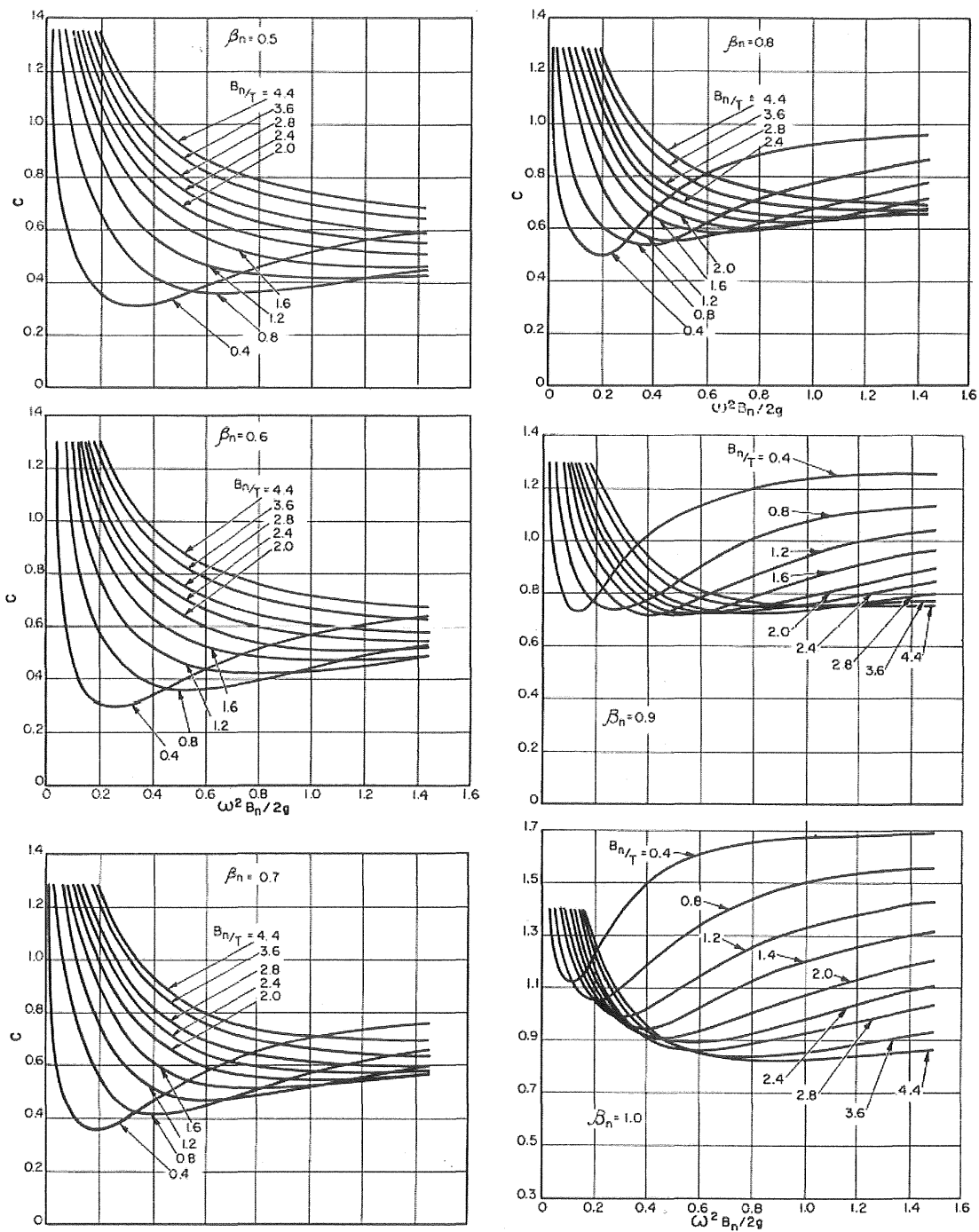


Fig. 37 Grim's (1959) computations of hydrodynamic mass coefficients C for two-dimensional floating bodies in heaving motion (Ref. [26])

Figure 6.7 Coefficient, C , of added mass for two-dimensional floating ship-shaped Lewis-form sections. (Grim, 1959)

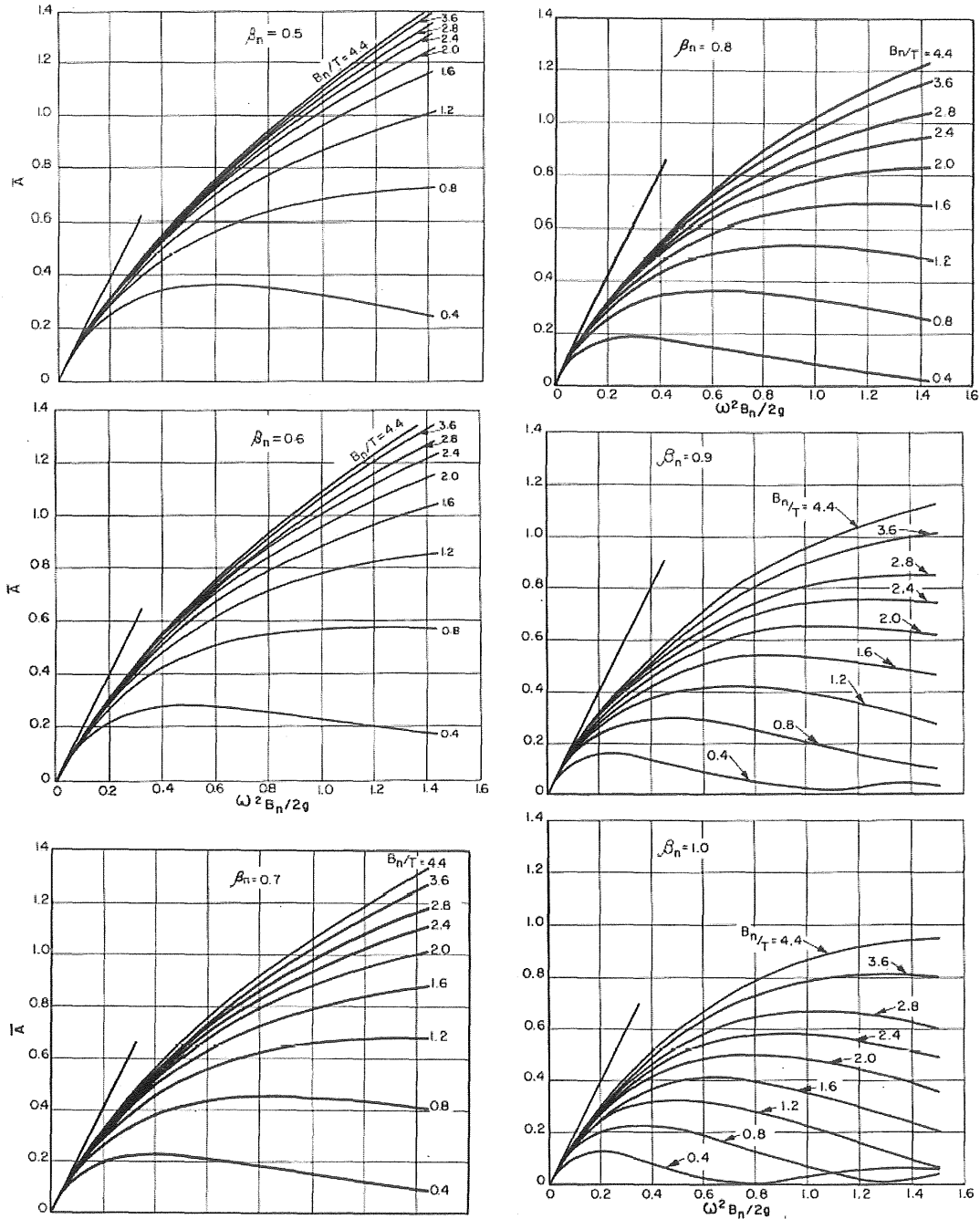


Fig. 40 Grim's (1959) computations of amplitude ratios \bar{A} for two-dimensional floating bodies in heaving motion (Ref. [26])

Figure 6.8 Coefficient, A , of radiation damping for two-dimensional floating ship-shaped Lewis-form sections. (Grim, 1959)

Jensen (2004) simply used for a ship at speed V and heading, θ , the constant added mass, $a_{33} = \rho g B T$, with astonishingly good result, and a somewhat more complicated closed-form expression for b_{33} .

$$b_{33} = \rho g^2 A^2 / (\omega^3 \alpha^3)$$

where

$$A = 2 \sin\left(\frac{\omega_e^2 B}{2g}\right) \exp\left(-\frac{\omega_e^2 T}{g}\right) = 2 \sin\left(\frac{1}{2} kB \alpha^2\right) \exp(-kT \alpha^2)$$

the encounter frequency, $\omega_e = \omega - kV \cos \theta \equiv \alpha \omega$, the parameter $\alpha = 1 - Fn \sqrt{kL} \cos \theta$, Froude number $F_n = V / \sqrt{kL}$ and forward speed V .

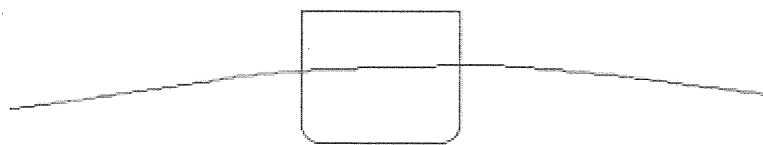
Wave-excited heave force

To set up the wave excited heave force we assume the body to be fixed in a regular beam wave progressing from portside to starboard

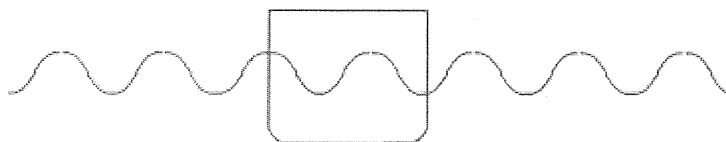
$$\zeta = a \cos(ky + \omega t), \quad \dots(6.13)$$

and ask ourselves which forces that will act on the body. See Figure 6.9. This so-called wave-diffraction or scattering problem can be solved in a similar manner as used for solving the added mass and the radiation-damping coefficient. The difference is now that the boundary condition on the hull states that the water velocities perpendicular to the hull surface should be nil, that is, the water particle velocities of the scattered wave must compensate the normal water particle velocities of the incident wave. This will cause a part of the wave to be reflected and the other part to be transmitted passed the hull.

To make it simple here we will restrict our treatise to using the small-body assumption, which demands that the cross-section width, beam, should be less than a fourth to fifth of a wavelength for producing reasonable results. Then the variation of incident wave properties across the beam can be neglected, which is equivalent of setting $y = 0$ in Equation (6.13). (Some authors use the term long-wave approximation, but this notation is in wave contexts mostly used to denote wave-theory approximations for waves with a longer wavelength than 10 to 20 water depths)



Small-body approximation is valid ($B < \lambda/4$)



Small-body approximation is not valid ($B > \lambda/4$)

Figure 6.9 A ship cross-section in beam waves.

Sticking to the small-body assumption the wave excited force acting on the cross-section can be expressed by help of the same coefficients a_{33} , b_{33} and c_{33} as above.

Assume temporarily the cross-section is rectangular with a flat, horizontal bottom and the draught T , and further that the wave is not distorted by the presence of the ship, which by help of the more complete theory can be shown to be approximately valid. Then the pressure from the incident wave on the ship's bottom is

$$p = \rho g (T + ae^{-kt} \cos(\omega t)), \quad \dots(6.14)$$

where the first term is balanced by the displacement of the ship and can be dismissed in this context, and the wave excited force due to relative displacement will be

$$B\rho gae^{-kt} \cos(\omega t) = c_{33}ae^{-kt} \cos(\omega t) = c_{33}\zeta e^{-kt} \quad \dots(6.15)$$

as

$$c_{33} = B\rho g . \quad \dots(6.16)$$

That is, the wave-excited force depends on the relative motion between the wave and the fixed ship, in the same way as the reaction force on the ship in still water depended on the motion of the ship.

When the wave passes the fixed ship the relative velocity will be

$$\dot{\zeta} = -a\omega e^{-kt} \sin(\omega t), \quad \dots(6.17)$$

and the relative acceleration

$$\ddot{\zeta} = -a\omega^2 e^{-kt} \cos(\omega t), \quad \dots(6.18)$$

The total exciting force can therefore be written

$$f_{3e} = (a_{33}\ddot{\zeta} + b_{33}\dot{\zeta} + c_{33}\zeta)e^{-kt} \quad \dots(6.19)$$

If the ship's cross-section is not full the draught, T , can as an approximation be exchanged by the cross-sectional mean draught $\bar{T} = S/B$.

Heave motion of the two-dimensional ship-section in regular beam waves

If now the two-dimensional ship-section is let free to heave without rolling, the total relative motion at the ship's bottom between the ship's bottom and the incident wave is $\eta_3 - \zeta e^{-kt}$ and the sum of the wave excited force Equation (6.19) and the reaction force Equation (6.4) on the moving ship must be balanced by its inertia force $m\ddot{\eta}_3$.

$$f_{3e} + f_3 = -a_{33}\ddot{\eta}_3 - b_{33}\dot{\eta}_3 - c_{33}\eta_3 + (a_{33}\ddot{\zeta} + b_{33}\dot{\zeta} + c_{33}\zeta)e^{-kt} = m\ddot{\eta}_3 \quad \dots(6.20)$$

Separating this equation so that the dependent unknown variable η_3 is gathered on the left-hand side gives

$$(m + a_{33})\ddot{\eta}_3 + b_{33}\dot{\eta}_3 + c_{33}\eta_3 = (a_{33}\ddot{\zeta} + b_{33}\dot{\zeta} + c_{33}\zeta)e^{-kT} \quad \dots(6.21)$$

which can be solved by the same technology as was demonstrated in Chapter 3.2. The difference from Chapter 3 is now that the “driving force” on the right-hand side displays a phase lag, α , in relation to the wave.

$$f_{3e} = (a_{33}\ddot{\zeta} + b_{33}\dot{\zeta} + c_{33}\zeta)e^{-kT} = \sqrt{(c_{33} - \omega^2 a_{33})^2 + (\omega b_{33})^2} e^{-kT} \hat{\zeta} \cos(\omega t - \alpha) \dots(6.22)$$

Again the easiest way to solve this problem is to use complex notation. Compare Equation (3.27).

Let, here, the complex wave progress from portside to starboard, i.e. in the negative y-direction, compare Equation (5.13)

$$\zeta_c = ae^{j(ky + \omega t)} = ae^{jky} e^{j\omega t} = a[\cos(ky + \omega t) + j \sin(ky + \omega t)] \quad \dots(6.23)$$

so that the real progressive wave is given by

$$\text{Re}(\zeta_c) = \text{Re}(a[\cos(ky + \omega t) + j \sin(ky + \omega t)]) = a \cos(ky + \omega t), \quad \dots(6.24)$$

the vertical displacement, velocity and acceleration of the water at the depth $z = -T$ are

$$\zeta_{c(z=-T)} = ae^{-kT} e^{j\omega t}, \quad \dot{\zeta}_{c(z=-T)} = ja\omega e^{-kT} e^{j\omega t} \quad \text{and} \quad \ddot{\zeta}_{c(z=-T)} = -a\omega^2 e^{-kT} e^{j\omega t} \quad \dots(6.25)$$

The dynamic pressure is, again dismissing the statically balanced mean pressure $-\rho gT$ in Equation (5.45)

$$p_{c(z=-T)} = \rho g a e^{-kT} e^{j\omega t}. \quad \dots(6.26)$$

Let similarly the heave motion be

$$\eta_{3c} = \hat{\eta}_{3c} e^{j\omega t}, \quad \dots(6.27)$$

where now also the amplitude is complex containing the information of the phase angle between the wave and the heave motion. The vertical velocity and acceleration are then

$$\begin{aligned} \dot{\eta}_{3c} &= j\omega \hat{\eta}_{3c} e^{j\omega t} \\ \ddot{\eta}_{3c} &= -\omega^2 \hat{\eta}_{3c} e^{j\omega t} \end{aligned} \quad \dots(6.28)$$

Substitute this into the equation of motion Equation (6.20) and solve for the complex amplitude $\hat{\eta}_{3c}$.

$$\hat{\eta}_{3c} = \frac{c_{33} - a_{33}\omega^2 + j\omega b_{33}}{c_{33} - (m + a_{33})\omega^2 + j\omega b_{33}} a e^{-kT} \quad \dots(6.29)$$

The motion amplitude is finally given by the modulus, $\hat{\eta}_3 = |\hat{\eta}_{3c}|$, the phase angle between wave motion and heave by the argument, $\arg(\hat{\eta}_{3c})$, and the complex transfer function from wave motion to heave motion by $T_c = \hat{\eta}_{3c} / a$. The factor e^{-kT} is often called the Smith effect and shows that the deeper the draught the less are the excitation forces. In Figure 6.10 the response amplitude operator $Rao_3 = |\hat{\eta}_{3c}| / a$ and the wave-excited force normalised by the displacement force ρS are shown as functions of angular frequency. In Figure 6.11 the phase angles between wave and heave motion; and between wave and wave-excited force as functions of angular frequency.

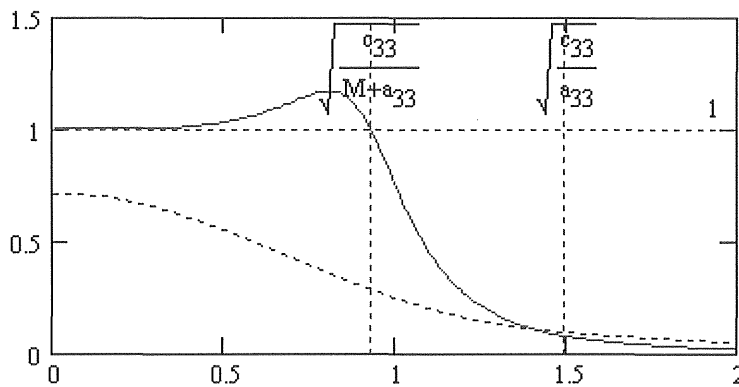


Figure 6.10 The heave-response amplitude operator, Rao_3 , (continuous line) and 10 times the wave-excited force divided by the displacement force (dashed curve) as functions of normalised angular frequency, $\Omega = \omega / \omega_N$. Two-dimensional ship.

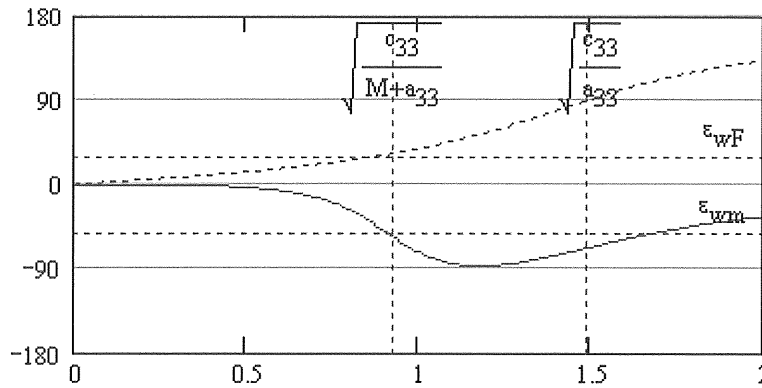


Figure 6.11 The phase angles between wave and heave motion (continuous line) and between wave and wave-excited force (dashed line) as functions of normalised angular frequency, $\Omega = \omega / \omega_N$. Two-dimensional ship.

In Figure 6.10 it is seen that for long waves $\omega \rightarrow 0$ the amplitude of the heave motion is the same as the amplitude of the wave, then grows to a maximum just below the natural angular frequency, $\omega_N = \sqrt{c_{33} / (m + a_{33})}$ and finally attenuates to nil for higher frequencies.

In Figure 6.11 it is seen that for long waves $\omega \rightarrow 0$ the wave-excited force is in phase with the wave, then as the wave frequency increases to $\omega = \sqrt{c_{33} / a_{33}}$ the force is 90° before the wave and for higher frequencies the force becomes in opposition to the waveform. For all frequencies the maximum of the wave-excited force appears before the maximum of the wave elevation, $0 < \epsilon_{wF} < 180^\circ$. The heave motion, on the other hand, appears for all frequencies after both the wave motion and the wave-excited force, $\epsilon_{wm} < 0^\circ < \epsilon_{wF}$.

Note, however, that strictly speaking the small-body assumption in this example is violated for angular frequencies above approximately 1 rad/s. We have furthermore assumed that the added mass and the radiation-damping coefficient are constant. Yet, the features of the response are valid. A more thorough calculation using correct potential forces and coefficients derived from potential theory would give the same result in principle, although with somewhat different graphs, especially for angular frequencies above 1 rad/s.

The sway and roll problem

The sway problem can for a two-dimensional ship be treated similarly but as concerns the roll problem the dynamic equilibrium must be solved for the ship as an entity as the roll stiffness is due to the mass distribution of the entire ship. Therefore we will save the roll problem till later.

6.3 The Uncoupled Three-Dimensional Heave Problem Using Strip Theory

Strip method for a ship

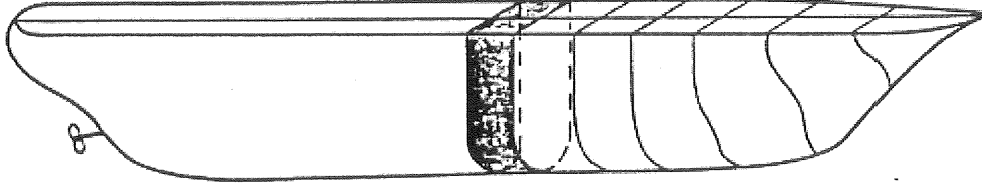


Figure 6.12 In the strip theory the ship is divided into slices or strips of the hull surface. For each strip the two-dimensional hydrodynamic problem is then solved.

The simple method used above for the two-dimensional ship can be used also for real three-dimensional ships, in an approximate variant of the so called *strip theory*, where the ship is divided into slices – or strips of the hull surface – and the two-dimensional flow problem is assumed to hold for each slice or strip. The problem is then reduced to integrating the forces or hydrodynamic characteristics along the ship knowing the added-mass and radiation-damping coefficients for each strip. The ship has to be reasonably slender, at least, $L/B > 5$ to neglect the end effects. The approximation is also better for ships with pointed ends as the three-dimensional end effects are less pronounced for such ships.

Forces on the three-dimensional ship heaving in calm water

Assume that the ship is forced to oscillate without pitching in calm water with the amplitude, $\hat{\eta}_3$, and the angular frequency, ω .

$$\eta_3 = \hat{\eta}_3 \cos(\omega t). \quad \dots(6.30)$$

The vertical reaction force acting on the body from the water can after integrating the two-dimensional reaction force, Equation (6.4), along the ship be written

$$F_3 = -A_{33}\dot{\eta}_3 - B_{33}\ddot{\eta}_3 - C_{33}\eta_3 \quad \dots(6.31)$$

where now the coefficients A_{33} , B_{33} and C_{33} are the integrated or summed quantities along the ship

$$A_{33} = \int_L a_{33}(x) dx = \sum_n a_{33n} \Delta x_n \quad \dots(6.32)$$

$$B_{33} = \int_L b_{33}(x) dx = \sum_n b_{33n} \Delta x_n \quad \dots(6.33)$$

$$C_{33} = \int_L c_{33}(x) dx = \sum_n c_{33n} \Delta x_n = \sum_n \rho g B_n \Delta x_n \quad \dots(6.34)$$

As an example in this compendium we use a box-like ship, which due to the bluff ends is not ideal for the strip-theory approximation, but makes the mathematics simple. Note again that the coefficients a_{33} and b_{33} and thus A_{33} and B_{33} are functions of the oscillation frequency. For simplified estimates a characteristic frequency of the exciting wave can be used and, actually, for each sea state the resulting sea-keeping properties will be astonishingly realistic.

For the box-like ship thus

$$\begin{aligned} A_{33} &= a_{33}L \\ B_{33} &= b_{33}L \\ C_{33} &= c_{33}L = \rho gBL = \rho gA_{WL} \end{aligned} \quad \dots(6.35)$$

where B is the beam and A_{WL} is the water-line area.

Wave-excited force in heave

The heave wave-excited force on the fixed ship in waves can be written

$$F_{3e} = \int_{-L/2}^{L/2} p(x, -T)B dx + \int_{-L/2}^{L/2} \dot{w}(x, -T)a_{33} dx + \int_{-L/2}^{L/2} w(x, -T)b_{33} dx \quad \dots(6.36)$$

where T is the draught
 $p(x, -T)$ the undisturbed pressure at the box bottom $z = -T$
 $\dot{w}(x, -T)$ the water acceleration at the bottom $z = -T$
 $w(x, -T)$ the water velocity at the bottom $z = -T$
 a_{33} the vertical two-dimensional added mass
 b_{33} the vertical two-dimensional radiation damping coefficient
 B the beam (breadth) of the ship section
and L the length of the ship.

Also in this case we have utilised the “small-body” assumption that the beam of the ship should be small in relation to the wavelength, i.e. $B < \lambda / 4$. For following or meeting waves this is not a restrictive assumption as the apparent wavelength for these two conditions is infinitely long.

Again we will, for simplicity use complex notation. Also, because it is more useful and not very complicated we will directly formulate the wave-excited force for waves oblique to the ship in the following example. The potential for such waves in complex notation is

$$\phi_c = j \frac{ag}{\omega} e^{kz} e^{j(k(\cos\theta)x + (\sin\theta)y)} e^{-j\omega t} \quad (6.37)$$

For the ship heading along the x-axis i.e. $y = 0$ it reduces to:

$$\begin{aligned} \phi_c &= j \frac{ag}{\omega} e^{kz} e^{j(k(\cos\theta)x)} e^{-j\alpha t} \\ \text{water vertical motion at bottom: } \zeta_c &= ae^{-kT} e^{j(k(\cos\theta)x)} e^{-j\alpha t}, \\ \text{pressure at bottom } p_c(x, -T) &= \rho g a e^{-kT} e^{j(k(\cos\theta)x)} e^{-j\alpha t}, \\ \text{vertical velocity at bottom } w_c(x, -T) &= -ja\omega e^{-kT} e^{j(k(\cos\theta)x)} e^{-j\alpha t} \\ \text{and vertical acceleration at bottom } \dot{w}_c(x, -T) &= -a\omega^2 e^{-kT} e^{j(k(\cos\theta)x)} e^{-j\alpha t}. \end{aligned}$$

Substituting these expressions into (6.36) gives

$$F_{3e} = \int_{-L/2}^{L/2} (\rho g a e^{-kT} e^{jk(\cos\theta)x} B - a\omega^2 e^{-kT} e^{jk(\cos\theta)x} a_{33} - ja\omega e^{-kT} e^{jk(\cos\theta)x} b_{33}) e^{-j\alpha t} dx \dots (6.38)$$

$$F_{3e} = ae^{-kT} (\rho g B - \omega^2 a_{33} - ja\omega b_{33}) e^{-j\alpha t} \int_{-L/2}^{L/2} (e^{jk(\cos\theta)x}) dx. \dots (6.39)$$

The integral is solved separately as

$$\begin{aligned} \int_{-L/2}^{L/2} (e^{jk(\cos\theta)x}) dx &= \frac{1}{jk \cos\theta} (e^{jk(\cos\theta)L/2} - e^{-jk(\cos\theta)L/2}) = \\ &= \frac{2j \sin(k(\cos\theta)L/2)}{jk \cos\theta} = 2 \frac{\sin(k(\cos\theta)L/2)}{k \cos\theta} \end{aligned} \dots (6.40)$$

which is also valid for beam sea $\theta = \pi/2$, because for small arguments $\cos\theta \rightarrow 0$, $\sin(k(\cos\theta)L/2) \rightarrow k(\cos\theta)L/2$ and

$$2 \frac{\sin(k(\cos\theta)L/2)}{k \cos\theta} = 2 \frac{k(\cos\theta)L/2}{k \cos\theta} = L. \dots (6.41)$$

That is, in beam sea the wave-excited force on the 3-D ship will equal the two-dimensional wave-excited force multiplied by the length of the ship.

If, however the waves progress along the longitudinal direction of the ship, following or meeting sea, for very long waves the force is in principle the same as for beam sea, but when the wavelength decreases the wave-excited force will decrease so that when the wavelength is close to the length of the ship it will be at a minimum. And for still smaller wavelengths, higher frequencies, the force will approach nil. See Figure 6.13.

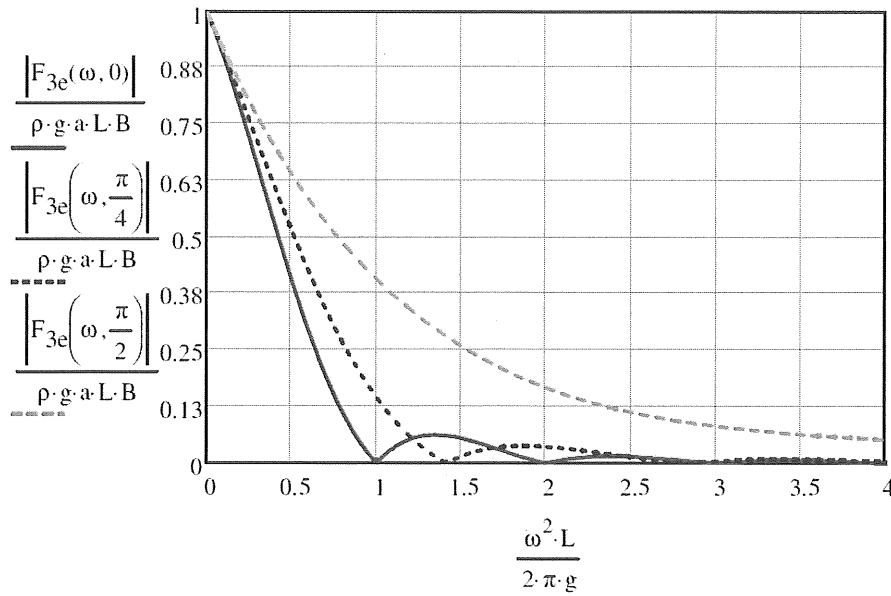


Figure 6.13 Heave wave-excited force as a function of ship length over wavelength, L/λ .

Now set the ship motion to $\eta_{3c} = \hat{\eta}_{3c} e^{-j\alpha}$,
 which gives the vertical velocity and acceleration of the ship

$$\dot{\eta}_{3c} = -j\omega \hat{\eta}_{3c} e^{-j\alpha}$$

$$\ddot{\eta}_{3c} = -\omega^2 \hat{\eta}_{3c} e^{-j\alpha}$$

Using Equation (6.31) with the complex motion above the equation of motion $F_3 + F_{3e} = m\ddot{\eta}_3$ finally gives

$$(C_{33} - (m + A_{33})\omega^2 - j\omega B_{33})\hat{\eta}_{3c} e^{-j\alpha} = a e^{-kT} (\rho g B - \omega^2 a_{33} - j\omega b_{33}) e^{-j\alpha} 2 \frac{\sin(k(\cos\theta)L/2)}{k \cos\theta} \quad \dots(6.42)$$

which can be solved for the complex motion to form a nice closed-form expression

$$\hat{\eta}_{3c} = a e^{-kT} \frac{(\rho g B - \omega^2 a_{33} - j\omega b_{33})}{(\rho g B L - (\rho T B L + a_{33} L)\omega^2 - j\omega b_{33} L)} 2 \frac{\sin(k(\cos\theta)L/2)}{k \cos\theta} \quad \dots(6.43)$$

Inspecting this equation one can see that the amplitude response function $|\hat{\eta}_{3c}|/a$ has one minimum around $\rho g B = \omega^2 a_{33}$, minima in deep water for $\sin(k(\cos\theta)L/2) = \sin((\omega^2/g)(\cos\theta)L/2) = 0$, and a maximum around $\rho g B L = (\rho g T B L + a_{33} L)\omega^2$. Explain why.

The natural angular frequency is obtained by setting the driving force and damping to nil in Equation (6.42), which gives $\omega_{N3} = \sqrt{C_{33}/(m + A_{33})}$.

In Figure 6.14 the heave motion as a function of time at zero speed in head waves are shown, in Figure 6.15 the amplitude response and in Figure 6.16 the phase lag between heave motion and wave are shown as functions of angular frequency.

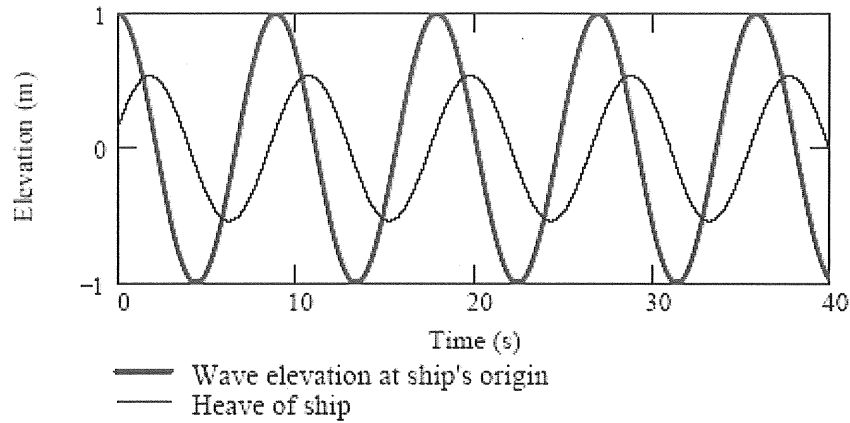


Figure 6.14 Heave motion and water level as a function of time in head waves with the wave amplitude $a = 1$ m.

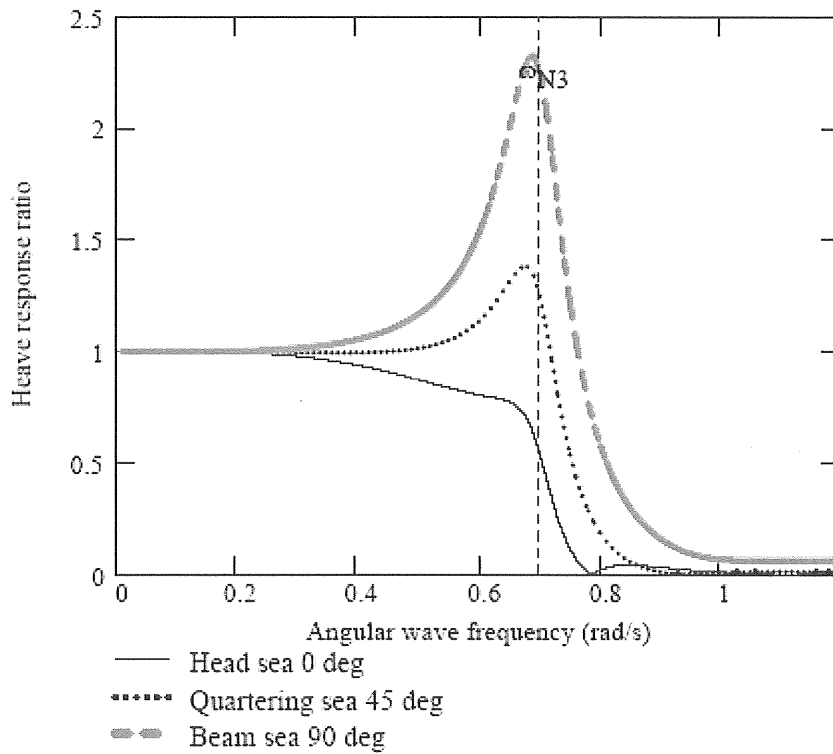


Figure 6.15 Amplitude response function at the headings: 0 , $\pi/4$ and $\pi/2$ rad.

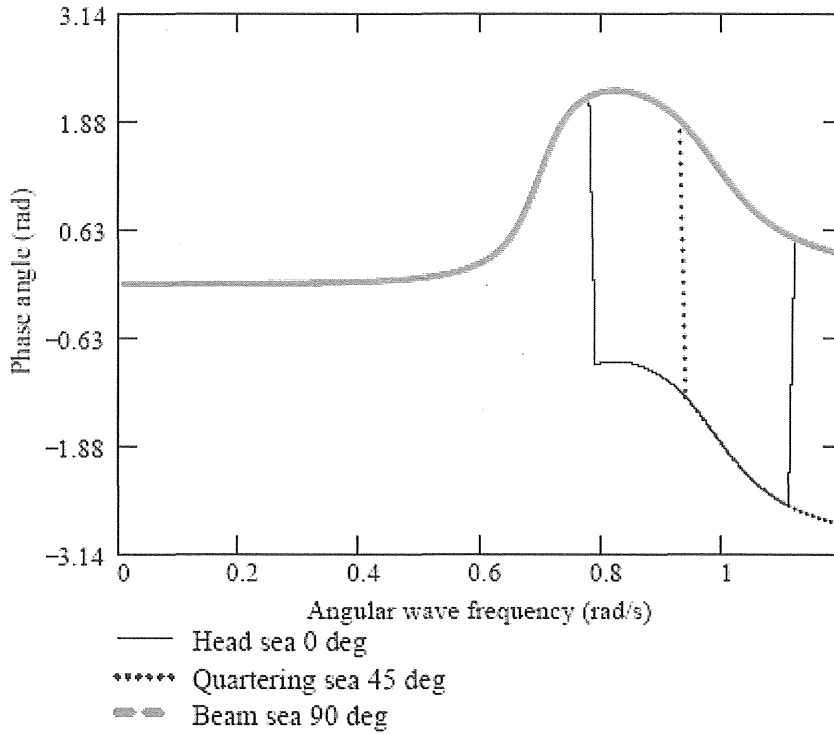


Figure 6.16 Phase lag between heave motion and wave at the headings: 0, $\pi/4$ and $\pi/2$ rad.

6.4 The Pitch Problem Using Strip Theory

Forces on the three-dimensional ship pitching in calm water

Assume now that the ship is forced to oscillate in pitch in still water without heaving with the amplitude, $\hat{\eta}_5$, and the angular frequency, ω :

$$\eta_5 = \hat{\eta}_5 \cos(\omega t). \quad \dots(6.44)$$

The vertical reaction moment acting on the body from the water can by integrating the two-dimensional reaction force, Equation (6.4), along the ship be written

$$F_5 = -A_{55}\ddot{\eta}_5 - B_{55}\dot{\eta}_5 - C_{55}\eta_5 \quad \dots(6.45)$$

where now the coefficients A_{55} , B_{55} and C_{55} are the integrated quantities along the ship:

$$A_{55} = \int_{-L/2}^{L/2} a_{33}(x)x^2 dx - \frac{U^2}{\omega_e^2} A_{33} \quad \dots(6.46)$$

$$B_{55} = \int_{-L/2}^{L/2} x^2 b_{33}(x) dx + \frac{U^2}{\omega_e^2} B_{33}. \quad \dots(6.47)$$

$$C_{55} = \rho g V(z_B - z_G) + \rho g \int_{-L/2}^{L/2} B(x)x^2 dx = \rho g \overline{VGM}_L \quad \dots(6.48)$$

Here the first terms in the added mass and radiation-damping coefficient are caused by the motion in still water as in Equation (6.4) or (6.31) taking into account that the vertical motion due to pitch at each cross section is the pitch motion multiplied by the lever, x , and that the reaction moment also is the sectional reaction force multiplied by the lever, x . From this fact comes the x^2 in the integrations. The second terms, the forward-speed terms, are caused by the forward-speed potential and will not be explained further here. (See Salvesen^{xxx} et al. 1970). U is the speed of the ship and ω_e is the angular frequency of encounter.

For the box-like ship, again the coefficients a_{33} and b_{33} are functions of the oscillation frequency but independent of x , and the beam is $B(x) = B$. For simplified estimates a characteristic frequency of the exciting wave can be used and, actually, for each sea state the resulting sea-keeping properties will be astonishingly realistic.

For the box-like ship at zero speed thus

$$\begin{aligned} A_{55} &= a_{33} \frac{1}{12} L^3 \\ B_{55} &= b_{33} \frac{1}{12} L^3 \\ C_{55} &= \rho g V(z_B - z_G) + \rho g B \frac{1}{12} L^3 = \rho g \overline{VGM}_L \approx \rho g B \frac{1}{12} L^3 \end{aligned} \quad \dots(6.49)$$

Wave-excited moment in pitch

The pitch wave-excited moment on the box-like fixed ship in waves can be written

$$F_{5e} = - \int_{-L/2}^{L/2} p_c(x, -T) B x dx - \int_{-L/2}^{L/2} \dot{w}_c(x, -T) a_{33} x dx - \int_{-L/2}^{L/2} w_c(x, -T) b_{33} x dx \quad \dots(6.50)$$

where T is the draught

$p_c(x, -T)$ the undisturbed pressure at the box bottom $z = -T$

\ddot{w}_c the water acceleration at the bottom $z = -T$

\dot{w}_c the water velocity at the bottom $z = -T$

a_{33} the vertical two-dimensional added mass

b_{33} the vertical two-dimensional radiation damping coefficient

B the beam (breadth) of the ship section

and L the length of the ship.

Again we will, for simplicity use complex notation. Also, because it is more useful and not very complicated we will directly formulate the wave-excited moment for waves oblique to the ship in the following example. The potential and derived properties for such waves in complex notation were given above in connection with the heave problem Equation (6.37). Substituting these expressions into (6.50) gives

$$F_{5e} = - \int_{-L/2}^{L/2} (\rho g a e^{-kT} e^{-jk(\cos\theta)x} B - a \omega^2 e^{-kT} e^{-jk(\cos\theta)x} a_{33} - j a \omega e^{-kT} e^{-jk(\cos\theta)x} b_{33}) e^{-j\alpha x} dx \dots (6.51)$$

$$F_{5e} = -a e^{-kT} (\rho g B - \omega^2 a_{33} - j \omega b_{33}) e^{-j\alpha x} \int_{-L/2}^{L/2} (e^{jk(\cos\theta)x}) dx \dots (6.52)$$

The integral was solved separately by Jensen et al (2004)^{xxxi} as

$$\int_{-L/2}^{L/2} (e^{jk(\cos\theta)x}) dx = \frac{2j}{(k \cos \theta)^2} \left(\sin(k(\cos \theta) \frac{L}{2}) - k(\cos \theta) \frac{L}{2} \cos(k(\cos \theta) \frac{L}{2}) \right) \dots (6.53)$$

which approaches zero in the limit as $\theta \rightarrow \pi/2$, and thus confirms that in beam regular waves the pitch is zero.

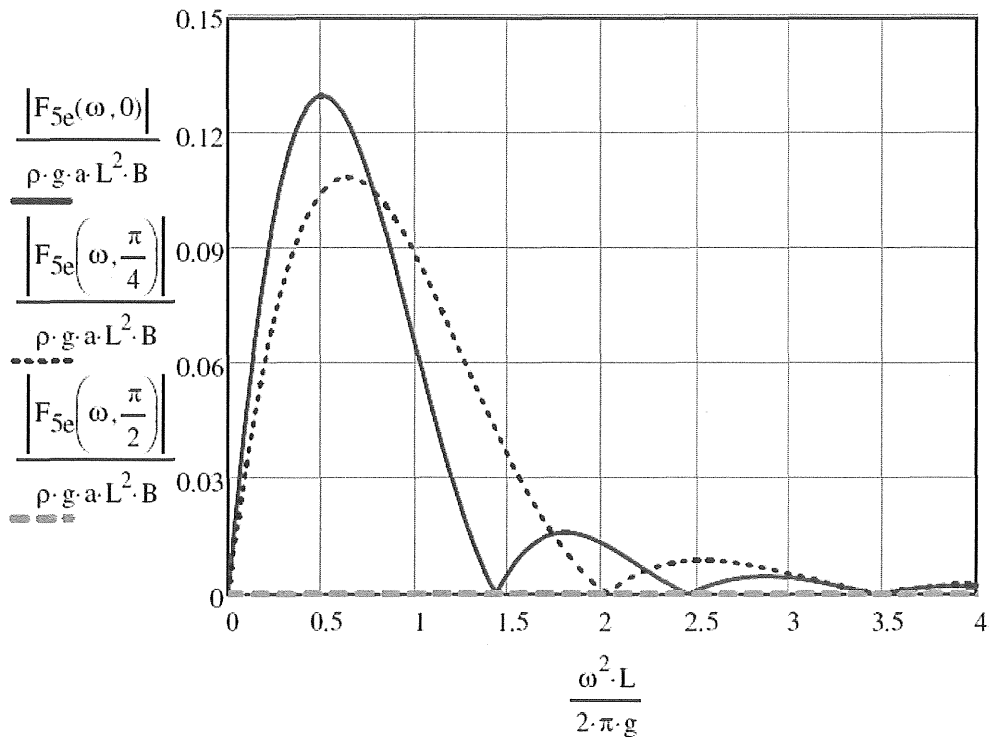


Figure 6.17 The amplitude of the pitch wave excited forces at zero speed as a function of ship length divided by wave length in deep water, L/λ . Why are the forces zero for meeting waves at 1.5, 2.5, 3.5 etc.?

Now set the pitch motion to $\eta_{5c} = \hat{\eta}_{5c} e^{-j\alpha x}$,
which gives the pitch angular velocity and acceleration of the ship to

$$\dot{\eta}_{5c} = -j\omega \hat{\eta}_{5c} e^{-j\alpha x}$$

$$\ddot{\eta}_{5c} = -\omega^2 \hat{\eta}_{5c} e^{-j\alpha x}$$

Using Equation (6.45) with the complex motion above, the equation of motion $F_5 + F_{5e} = I_5 \dot{\eta}_5$ finally gives

$$\begin{aligned} & (C_{55} - (I_5 + A_{55})\omega^2 - j\omega B_{55})\hat{\eta}_{5c}e^{-j\omega t} = \\ & = -ae^{-kt}(\rho gB - \omega^2 a_{33} - j\omega b_{33})e^{-j\omega t} \frac{2j}{(k \cos \theta)^2} \left(\sin(k(\cos \theta)\frac{L}{2}) - k(\cos \theta)\frac{L}{2} \cos(k(\cos \theta)\frac{L}{2}) \right) \end{aligned} \quad \dots(6.54)$$

which can be solved for the complex pitch motion amplitude in a closed-form expression

$$\hat{\eta}_{5c} = -ae^{-kt} \frac{(\rho gB - \omega^2 a_{33} - j\omega b_{33})}{(C_{55} - (I_5 + A_{55})\omega^2 - j\omega B_{55})} \frac{2j}{(k \cos \theta)^2} \left(\sin\left(k(\cos \theta)\frac{L}{2}\right) - k(\cos \theta)\frac{L}{2} \cos\left(k(\cos \theta)\frac{L}{2}\right) \right) \quad \dots(6.55)$$

Inspecting this equation one can see that the amplitude response function $\boxed{\times}$ has one minimum around $\rho gB = \omega^2 a_{33}$, minima for

$$\left(\sin(k(\cos \theta)\frac{L}{2}) = k(\cos \theta)\frac{L}{2} \cos(k(\cos \theta)\frac{L}{2}) \right), \text{ and a maximum around}$$

$$C_{55} = (I_5 + A_{55})\omega^2. \text{ Explain why.}$$

The natural angular frequency is obtained by setting the driving moment and damping to nil in Equation (6.54), which gives $\omega_{N5} = \sqrt{C_{55}/(I_5 + A_{55})}$.

The amplitude response function and the corresponding phase lag as functions of angular wave frequency are shown in Figures 6.18 and 6.19.

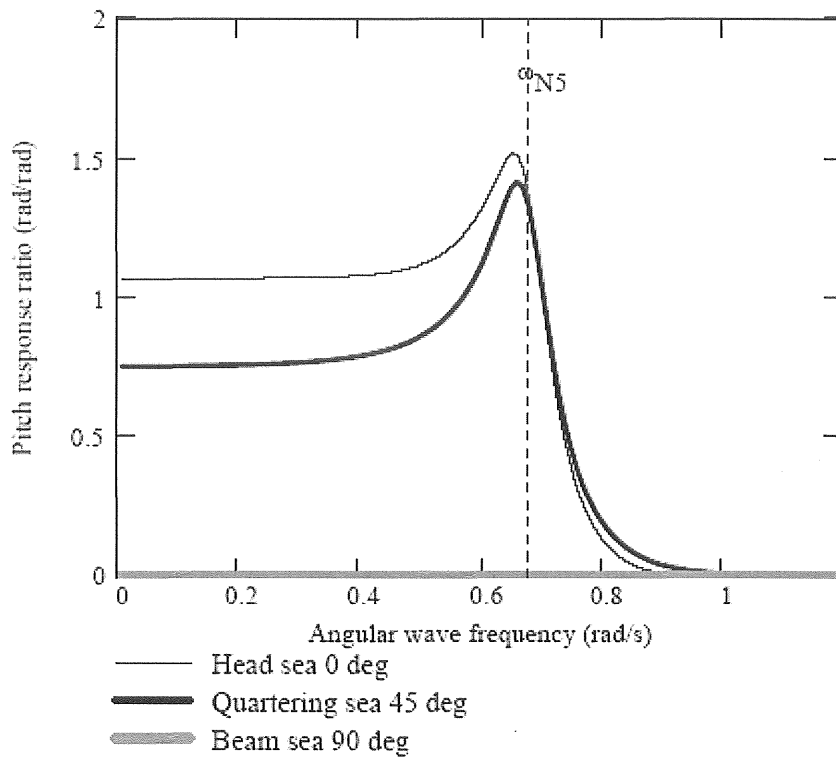


Figure 6.18 Pitch amplitude response functions at the headings: 0, $\pi/4$ and $\pi/2$ rad.

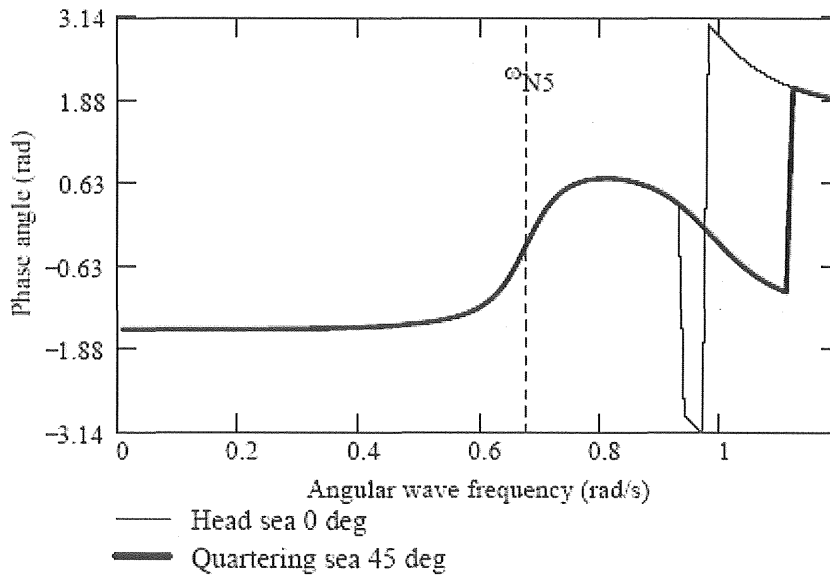


Figure 6.19 Phase lags between pitch motion and wave at the headings: 0, $\pi/4$ and $\pi/2$ rad.

As an example, in Figure 6.20 the pitch motion and wave slope at the origin of a ship as functions of time are shown for a swell with a period around 43 s. For this very long wave the ship will follow the slope of the wave surface almost exactly, but due

to the definitions of slope and pitch angle, the time functions are 180 degrees out of phase.

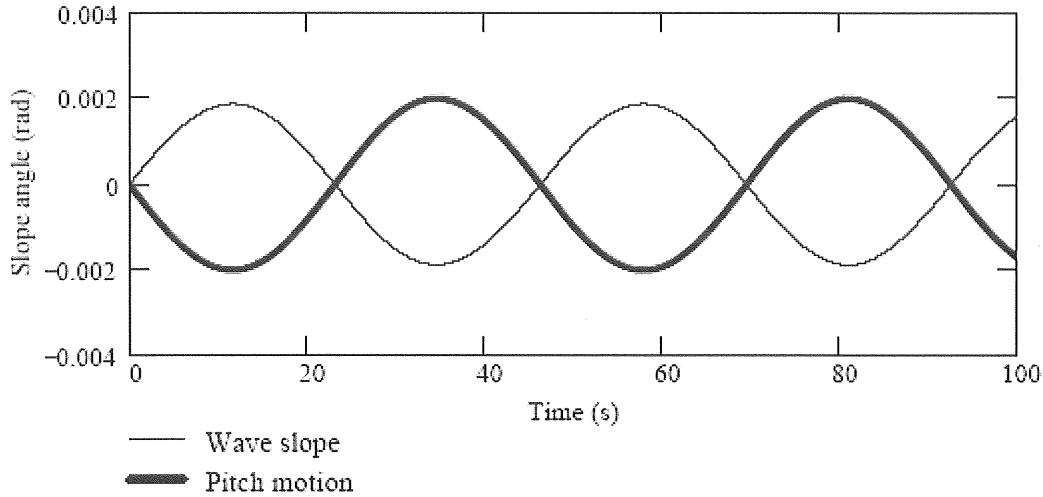


Figure 6.20 Pitch motion and wave slope at the origin of a ship as functions of time in a swell with the period around 43 s. Observe that the ship follows the slope of the wave-surface exactly for this swell, but due to the definitions of slope and pitch angle, the functions are 180 deg out of phase.

6.5 The Roll Problem

To solve the roll-motion problem for a two-dimensional ship, we can – as before – split the hydrodynamic problem into two problems: the problem to assess the moment on the ship caused by the ship rolling in calm water and the problem to assess the moment acting on the fixed ship by the progressing waves.

As most ships are symmetric with respect to their longitudinal axes, the couplings to the heave and pitch motions are negligible, while there are – usually weak – couplings to the sway and yaw motions. Here only uncoupled roll motion is treated.

Moments on the two-dimensional body rolling in calm water

Assume that the body is forced to oscillate in roll in calm water with the amplitude, η_{4c} , and the angular frequency, ω .

$$\eta_{4c} = \hat{\eta}_{4c} e^{-j\alpha} \quad \dots(6.56)$$

The arising forces are due to the roll angle, η_4 , Equation (6.30), roll angular velocity

$$\dot{\eta}_{4c} = -j\omega \hat{\eta}_{4c} e^{-j\alpha} \quad \dots(6.57)$$

and roll angular acceleration

$$\ddot{\eta}_{3c} = -\omega^2 \hat{\eta}_{4c} e^{-j\alpha} \quad \dots(6.58)$$

relative to the horizontal still-water surface.

The roll reaction moment acting on the ship from the water can be written

$$F_{4rc} = -A_{44} \ddot{\eta}_{4c} - B_{44} \dot{\eta}_{4c} - C_{44} \eta_{4c} \quad \dots(6.59)$$

where the coefficients A_{44} , B_{44} and C_{44} must be assessed.

The linear static restoring moment $-C_{44} \eta_4$ is due to the change of the shape of the displacement and the vertical position of the static centre of buoyancy in relation to the centre of gravity of the ship. See the course in “stability and weight”. The restoring moment can then be written in terms of the transverse metacentre height, $h_{m4} = \overline{GM}_T$,

$$C_{44} = \rho g V (z_B - z_G) + \rho g L \frac{1}{12} B^3 = \rho g V \overline{GM}_T \quad \dots(6.60)$$

The dynamic moments due to the roll angular acceleration and roll angular velocity of the ship are – as for the other degrees of freedom – associated with the forced oscillatory motion of the ambient water. The roll acceleration of the ship is thus associated with a local, evanescent wave in which the water is forced to shift back and forth between the bottom and the sides alternately to starboard and portside. The effect is an “added moment of inertia”, which can be calculated by help of two-dimensional potential theory in combination with strip theory or directly from three-dimensional potential theory for short ships or floating objects with complicated shapes like offshore drilling platforms. As, for a ship, the order of magnitude of the added moment of inertia is only 10 to 20 % of the mass moment of inertia of the ship itself, it can suffice here to use an approximate value. Thus

$$A_{44} = 0.15 I_4 \quad \dots(6.61a)$$

For bodies floating in the water surface or positioned close to the water surface this added moment is a function of the frequency of oscillation. Far from the free surface the added moment of inertia is constant and depends only on the shape of the body and its vicinity to other bodies or fixed boundaries. Also for floating bodies, in the limit, as $\omega \rightarrow \infty$, no waves are formed, and the added moment becomes independent of the frequency and is half that of the body mirrored in the water surface and submerged deeply below the free surface.

To have an approximate value of the roll moment of inertia one can use the fact that usually the radius of inertia in roll i_4 is of the order of $0.4B$, where B is the beam of the ship, and thus

$$I_4 = \rho C_B B L T_4^2 = \rho V i_4^2 \approx 0.16 \rho V B^2 \quad \dots(6.61b)$$

where $C_B = V/(BLT)$ is the block coefficient and V the displacement.

Roll damping

As the heave motion causes waves that radiate out from the body, so does the roll motion, and the moment, $B_{44}\dot{\eta}_4$, needed to maintain this radiation is in phase with the angular roll velocity. Only now the waves are anti-symmetric with respect to the axis of the ship. See figure 6.21. Again these radiated waves transport energy away from the body and therefore introduces hydrodynamic or radiation damping. However, in roll motion the damping is not dominated by this radiation damping but depends to a substantial degree on turbulent skin friction, turbulence caused by bilge keels and appendages. Therefore the total damping cannot be calculated by potential theory only, but the also other damping contributions must be taken into account. Traditionally one depends on experiments with obvious problems of scaling, but recently possibilities have been created to use turbulent, viscous flow computations.

In summary the roll-damping moment is caused by

1. radiated waves
2. turbulent skin friction between the hull and the water
3. appendage or bilge-keel vortex shedding and
4. moorings for moored ships or moored offshore platforms.

To make it further complicated the contributions from items 2 to 4 are functions on velocities squared so they depend on the amplitude of roll.

For bodies floating in the water surface or positioned close to the water surface also the radiation roll damping is a function of the frequency of oscillation due to the generation of waves. For floating bodies, in the limit, as $\omega \rightarrow \infty$, no waves can be formed, and the radiation damping is nil as it is for deeply submerged bodies, that cannot produce surface gravity waves. The radiation damping is actually nil both for $\omega \rightarrow 0$ and $\omega \rightarrow \infty$. There is a maximum somewhere in between where the body has a maximal ability to radiate energy or reciprocally absorb wave energy.

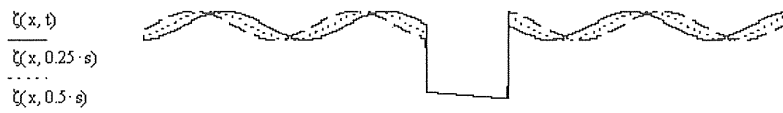


Figure 6.21 Radiated 2D waves caused by roll motion.

Jensen et al. (2004)^{xxxix} could not find simple closed-form solutions for the sectional radiation damping, b_{44} , not even for rectangular shapes. Therefore he determined the coefficient by a 2-D potential method, the Frank close-fit method, for a range of B/T ratios both for triangular sections and for rectangular sections. He then fitted parametric curves, linear in B/T, through the results, Equation (6.62)

$$\frac{b_{44}}{\rho A_c B^2} \sqrt{\frac{B}{2g}} = a\left(\frac{B}{T}\right) \exp\left(b\left(\frac{B}{T}\right) (\omega_e \text{ s/rad})^{-1.3}\right) (\omega_e \text{ s/rad})^{d(B/T)} \quad \dots(6.62)$$

where A_c is the cross-sectional area of the submerged part of the section. For triangular cross-sections the functions $a(\bullet)$, $b(\bullet)$ and $d(\bullet)$ became:

$$\left. \begin{aligned} a(B/T) &= 0.256B/T - 0.286 \\ b(B/T) &= -0.11B/T - 2.55 \\ d(B/T) &= 0.033B/T - 1.419 \end{aligned} \right\} \text{ for } 3 \leq B/T \leq 6 \quad \dots(6.63)$$

For ships with fuller lines, e.g. container ships and tankers, the same procedure was used for rectangular cross-sections.

$$\left. \begin{aligned} a(B/T) &= -3.94B/T + 13.69 \\ b(B/T) &= -2.12B/T - 1.89 \\ d(B/T) &= 1.16B/T - 7.97 \end{aligned} \right\} \text{ for } 1 \leq B/T \leq 3 \quad \dots(6.64)$$

Added viscous roll damping

For assessing the total roll damping one must rely on model tests. One way is then to add a fraction of critical damping to calibrate calculated heave amplitude operators against model tests for a similar ship.

The critical damping in roll is, compare Chapter 3.1,

$$B_{44}^{crit} = 2\sqrt{C_{44}(I_{44} + A_{44})}. \quad \dots(6.65)$$

Jensen (2004) proposed to set the total damping to

$$B_{44}^{TOT} = B_{44} + \xi B_{44}^{crit}. \quad \dots(6.66)$$

For a Panamax container vessel progressing at a speed equivalent to $Fn = 0.245$, Jensen made calculations agree with experiments with values on ξ according to Table.

| Heading (deg) | Added damping ratio ξ | Comments |
|---------------|---------------------------|-------------------------|
| 25 | 0 | Response too low |
| 45 | 3 | OK |
| 65 | 20 | OK |
| 205 | 20 | Responses overpredicted |
| 225 | 20 | Ditto |
| 245 | 20 | Ditto |

180 deg corresponds to head sea

Wave-excited roll moment

The sectional wave-excited moment can approximately be expressed in terms of the hydrodynamic damping, b_{44} . (Newman 1978 cited by Jensen 2004).

$$f_4 = a \sqrt{\frac{\rho g^2}{\omega}} b_{44} e^{jkx \cos \theta} e^{-j\omega x} \sin \theta \quad \dots(6.67)$$

This moment is in phase with the cross-beam slope velocity of the wave because here we have neglected the force in phase with the slope and with the slope acceleration, which are less important when the magnitude of the roll motion shall be assessed.

Integrating along our box-like ship yields the moment

$$\begin{aligned} F_4 &= \int_{-L/2}^{L/2} a \sqrt{\frac{\rho g^2}{\omega}} b_{44} e^{jkx \cos \theta} e^{-j\omega x} \sin \theta dx = \\ &= a \sqrt{\frac{\rho g^2}{\omega}} b_{44} \frac{2 \sin \theta}{k \cos \theta} e^{-j\omega x} \{\sin(k(\cos \theta)L/2)\} \end{aligned} \quad \dots(6.68)$$

In this equation ω can as an approximation be exchanged with the encounter frequency, ω_e , but maintaining $k = f(\omega)$ thus making the expression approximately valid for a ship at speed.

Because $\theta \rightarrow \pi/2$ gives $\sin\{k(\cos \theta)L/2\} \rightarrow k(\cos \theta)L/2$ Equation (6.68) is also valid in the limit for beam sea as

$$F_4 = a \sqrt{\frac{\rho g^2}{\omega}} b_{44} L(\sin \theta) e^{-j\omega x} \quad \text{for } \theta \text{ close to } \pm \pi/2 \quad \dots(6.69)$$

See Figure 6.22

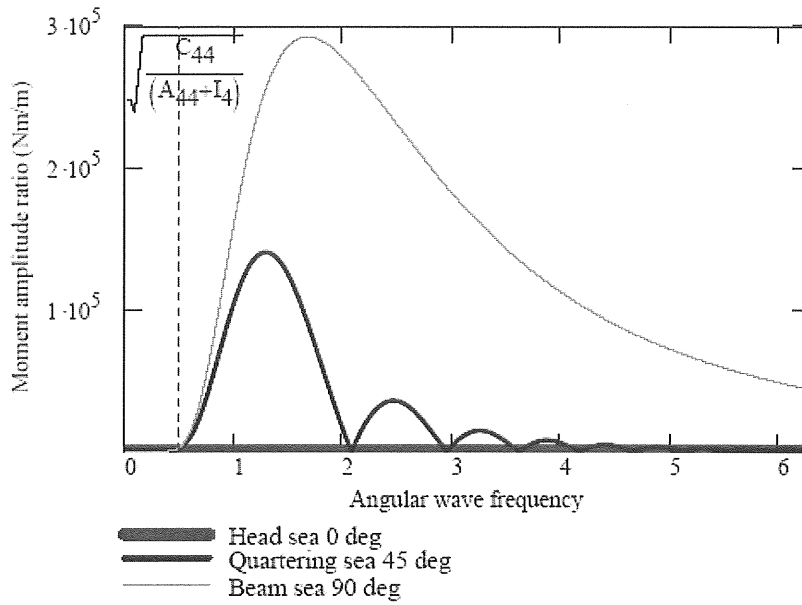


Figure 6.22 The roll-excited wave-moment amplitude ratio \hat{F}_4 / a as a function of angular wave frequency for zero speed forward, $U = 0$ m/s, and some chosen headings.

As the wave excited roll moment should be added to the reaction moment from the water due to the roll of the ship in still water, Equation (6.59), and be balanced by the roll moment of inertia the following equation of roll motion is yielded:

$$(I_4 + A_{44})\ddot{\eta}_{4c} + B_{44}\dot{\eta}_{4c} + C_{44}\eta_{4c} = F_4 \quad \dots(6.70)$$

Roll motion

The ship must roll with the encounter frequency, ω_e . Using complex notation and solving for the amplitude gives the motion amplitude as

$$\hat{\eta}_4 = \left| \frac{F_4}{C_{44} - \omega_e^2(A_{44} + I_4) - j\omega B_{44}^{TOT}(\omega_e, \xi)} \right|, \quad \dots(6.71)$$

which is a function of encountered angular wave frequency, ω_e , ship's heading, θ , and ship speed, U , defined as positive in the propagation direction of the waves. In Figure 6.23 to 6.24, the roll response amplitude operator $\hat{\eta}_4/a$ is illustrated for various combinations of these variables.

The natural angular frequency is obtained by setting the driving moment and damping to nil in Equation (6.70), which gives $\omega_{N4} = \sqrt{C_{44}/(I_4 + A_{44})}$.

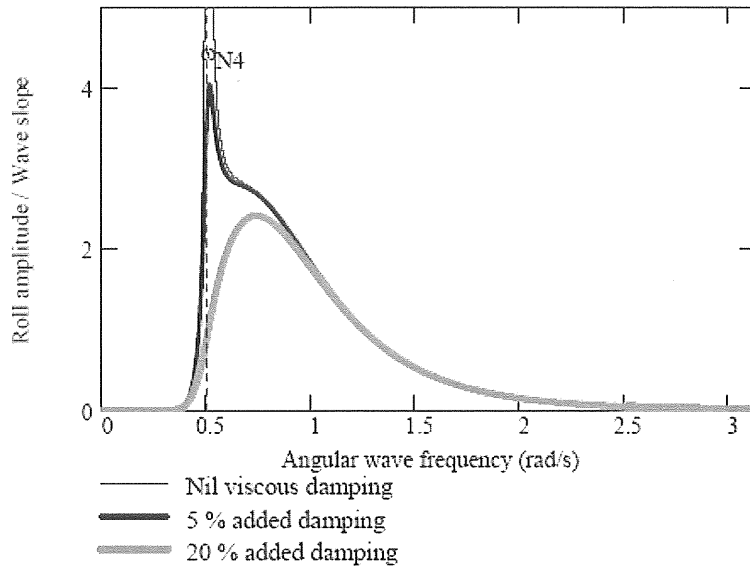


Figure 6.23 The dimensionless roll response slope-amplitude operator $\hat{\eta}_4/(ka)$ (deg/deg) as a function of angular wave frequency for beam sea, $\theta = 90^\circ$, zero speed forward, $U = 0$ m/s and damping ratios $\xi = 0, 0.05$ and 0.2 .

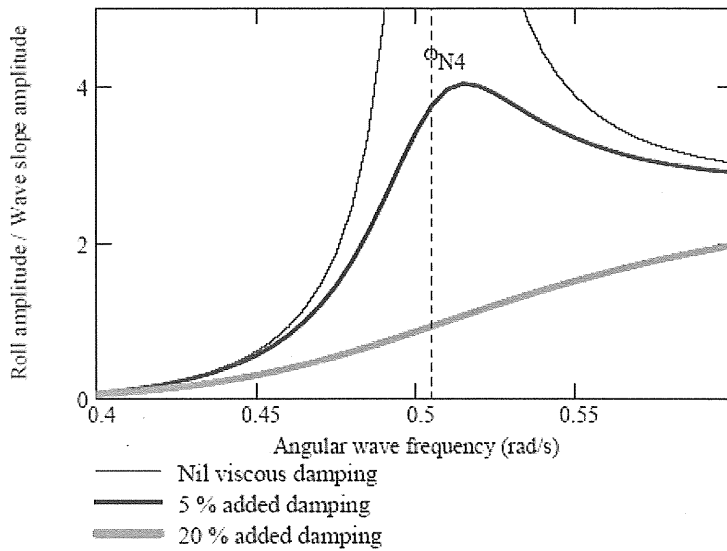


Figure 6.24 The dimensionless roll response slope-amplitude operator $\hat{\eta}_4/(ka)$ (deg/deg) as a function of angular wave frequency for beam sea, $\theta = 90^\circ$, zero speed forward, $U = 0$ m/s and damping ratios $\xi = 0, 0.05$ and 0.2 . A blow up of Fig. 6.23 around the roll resonance frequency.

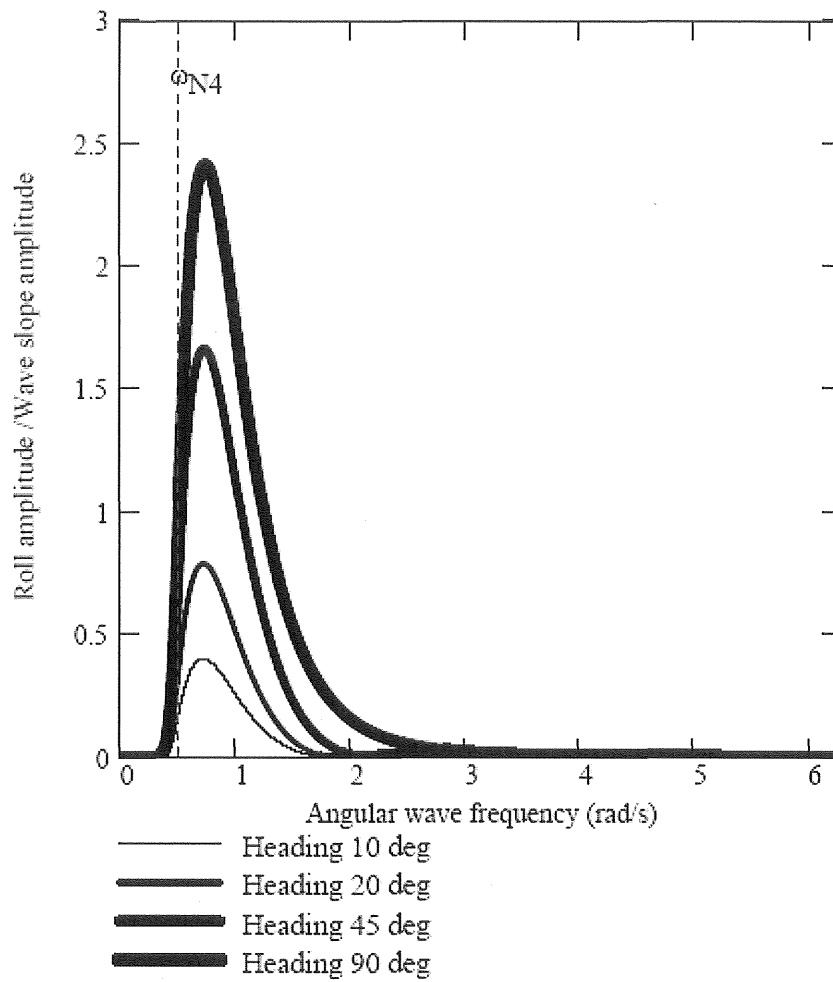


Figure 6.25 The dimensionless roll response slope-amplitude operator $\hat{\eta}_4/(ka)$ (deg/deg) as a function of angular wave frequency for zero speed, damping ratio, $\xi = 0.2$, and different headings. Observe that for 0 deg heading the wave slope projected on the ship is zero and thus is the roll amplitude.

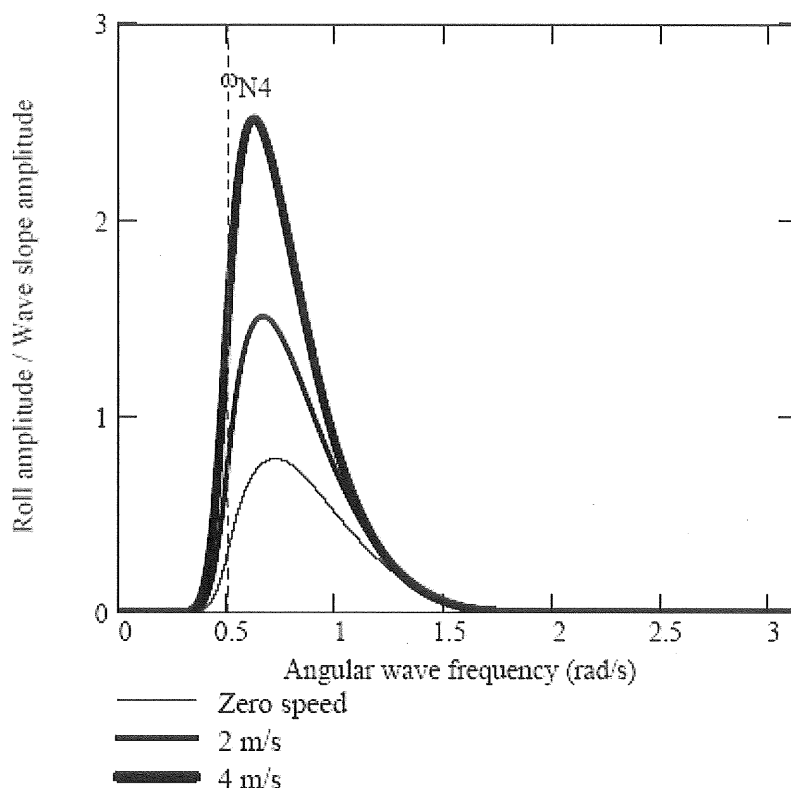


Figure 6.26 The dimensionless roll response slope-amplitude operator $\hat{\eta}_4/(ka)$ (deg/deg) as a function of angular wave frequency for damping ratio, $\xi = 0.2$, heading 20 deg, and different speeds forward.

6.6 Forward-Speed Effect

Although the wave frequency variation in an irregular sea state influence the ship motion at zero speed, the effect of the frequency change due to ship moving through the waves is much more pronounced. A ship progressing through a following wave with the speed, U , at the heading, θ , in relation to the direction of wave propagation, will be passed by a wave crest every encounter period

$$T_e = \frac{\lambda}{C - U \cos(\theta)} \quad \dots(6.72)$$

Negative encounter period means that the ship moves faster than the wave. This can only happen for waves abaft the beam, $-90^\circ < \theta < 90^\circ$. In head waves, meeting (encountered) waves, $90^\circ < \theta < 270^\circ$, the encountered period is always positive and shorter than the wave frequency.

The angular frequency of encounter is thus

$$\omega_e = \frac{2\pi}{T_e} = \frac{2\pi}{\lambda} (C - U \cos(\theta)) \text{ or } \frac{\lambda}{T_e} = (C - U \cos(\theta)), \quad \dots(6.73)$$

which in deep water can be written

$$\omega_e = \omega - \frac{\omega^2 U}{g} \cos(\theta) \quad \dots(6.74)$$

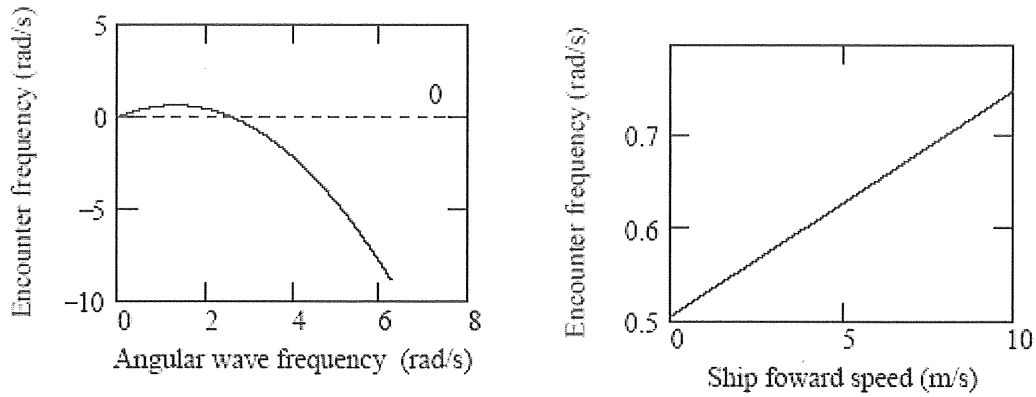


Figure 6.27 Encounter wave frequency
 Left: as a function of wave frequency at zero heading (following waves) and forward speed 4 m/s
 Right: as a function of forward speed at 180 deg heading (meeting waves) and angular wave frequency 0.5 rad/s.

6.7 Resonance Frequencies

The heave, pitch and roll motions are resonant motions, while the horizontal motions sway, surge and yaw are non-resonant because there are no stiffnesses in the latter modes of motion for unmoored ships.

The eigenfrequencies, undamped resonance frequencies or natural frequencies can be written

$$\omega_{N3} = \sqrt{\frac{C_{33}}{\rho V + A_{33}}} = \sqrt{\frac{\rho g A_w}{\rho V + A_{33}}} \text{ in heave}$$

$$\omega_{N4} = \sqrt{\frac{C_{44}}{I_4 + A_{44}}} \text{ in roll and}$$

$$\omega_{N5} = \sqrt{\frac{C_{55}}{I_5 + A_{55}}} \approx \sqrt{\frac{\rho g I_{w5}}{I_5 + A_{55}}} \text{ in pitch.}$$

The last approximation can be used because the hydrodynamic stiffness dominates in pitch. A_w is the water-plane area and $I_{w5} = BL^3/12$ is the area moment in pitch of the water-plane area.

For the box-like ship one can approximately write

$$\omega_{N3} = \sqrt{\frac{C_{33}}{\rho V + A_{33}}} = \sqrt{\frac{\rho g B}{\rho B T + a_{33}}} \text{ in heave}$$

$$\omega_{N4} = \sqrt{\frac{C_{44}}{I_4 + A_{44}}} = \sqrt{\frac{\rho g L B (B^2 + T(z_B - z_G))}{I_4 + a_{44} L}} \text{ in roll and}$$

$$\omega_{N5} = \sqrt{\frac{C_{55}}{I_5 + A_{55}}} \approx \sqrt{\frac{\rho g I_{w5}}{I_5 + A_{55}}} = \sqrt{\frac{\rho g B L^3}{12 I_5 + a_{55} L}} \text{ in pitch.}$$

Typical resonance periods are in heave 10 s, in roll 8 – 12 s and in pitch 10–20 s. For anchored ships the resonance periods in surge may be > 200 s, in sway > 100 s and in yaw > 100 s and are highly dependent on the mooring system.

6.8 Derived Responses

Hitherto we have assessed the global motion of the ship in six degrees of freedom referred to the origin of the chosen co-ordinate system. For applications we have to be able to describe the translational motion in three degrees of freedom at any point of the ship. The aim can be to investigate the freeboard, the risk for propeller emergence out of the water, the risk for slamming and also accelerations for assessing cargo fastenings, comfort and seasickness. These local motions are called derived responses.

The motion at a point

Using Equations (2.9) to (2.12) the motion of a point $\underline{r}^T = (x, y, z)$ on a body can for small rotations $\underline{\Omega}^T = (\eta_4, \eta_5, \eta_6)$ (less than 10 degrees or 0.2 rad) be written:

$$\underline{s} = \begin{pmatrix} \eta_1 \\ \eta_2 \\ \eta_3 \end{pmatrix} + \underline{\Omega} \times \underline{r} \quad \dots(2.9)$$

which explicitly in the chosen co-ordinate system is

$$\underline{s} = \begin{pmatrix} \eta_1 + z\eta_5 - y\eta_6 \\ \eta_2 - z\eta_4 + x\eta_6 \\ \eta_3 + y\eta_4 - x\eta_5 \end{pmatrix} \quad \dots(2.10)$$

As we in the strip theory cannot predict the surge motion with any degree of success the first row of Equation (2.10) describing the horizontal motion in the surge direction is of no interest in this chapter. Furthermore as we in this treatise have not calculated the yaw motion, although it is fully feasible, we cannot use the second row for the crossbeam horizontal motion. The most important motion is, however, the vertical motion described by the third row. Thus

$$s_3 = \eta_3 + y\eta_4 - x\eta_5 \quad \dots(6.75)$$

Here we have retained all the vertical motions heave, pitch and roll (η_3, η_4, η_5) contributing to the vertical motion of a point. It should be warned that as the used method for calculating the roll motion is not phase correct, it should not be included in Equation (6.75) if it lessens the vertical motion. For statistical estimates in irregular waves see Chapter 9.

The vertical velocity and acceleration of the same point are likewise

$$\dot{s}_3 = \dot{\eta}_3 + y\dot{\eta}_4 - x\dot{\eta}_5 \quad \dots(6.76)$$

and

$$\ddot{s}_3 = \ddot{\eta}_3 + y\ddot{\eta}_4 - x\ddot{\eta}_5 \quad \dots(6.77)$$

The vertical motions heave, pitch and roll (η_3, η_4, η_5) are most conveniently introduced into Equation (6.75) to (6.77) in their complex time-domain form. The real motion is then assessed by taking the real part of the derived motion s_3 .

An example of a calculation of the vertical bow motion of the example ship is shown in Figure 6.28. with $y = 0$ m, or no roll motion. The ship is a box 100 m long, 20 m wide and with 10 m draught. In Figure 6.29 and Figure 6.30 the response amplitude operator and phase lag is shown.

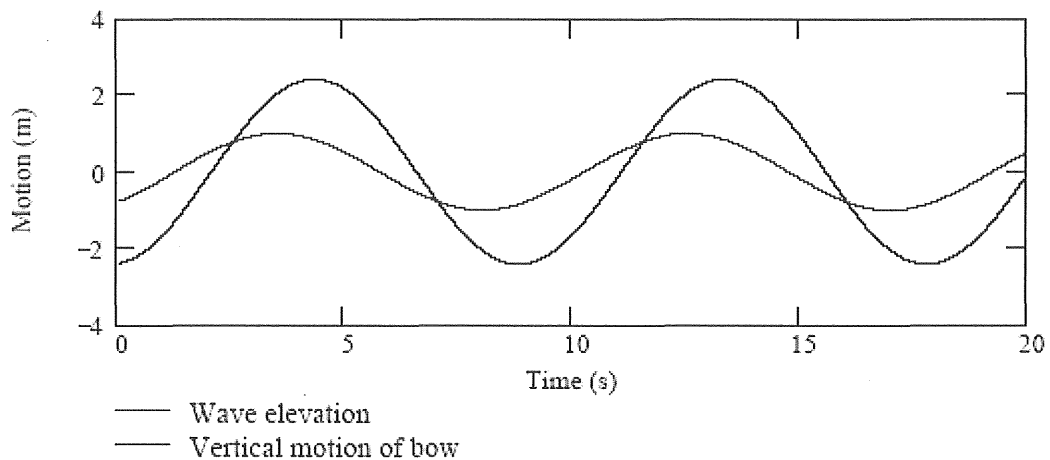


Figure 6.28 Vertical bow motion and wave elevation near pitch and heave resonance

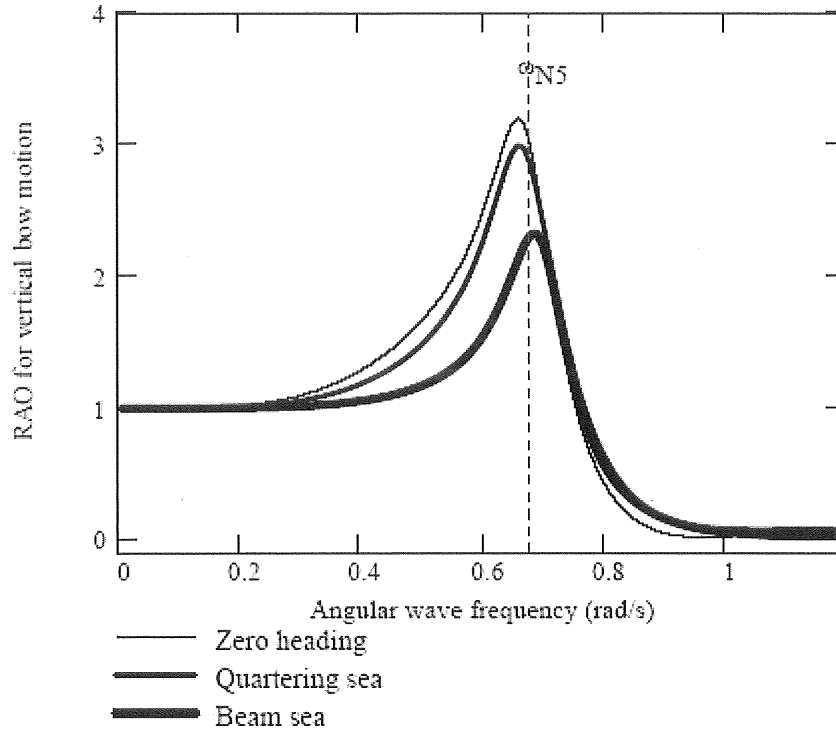


Figure 6.29 The response amplitude operator for the vertical bow motion.

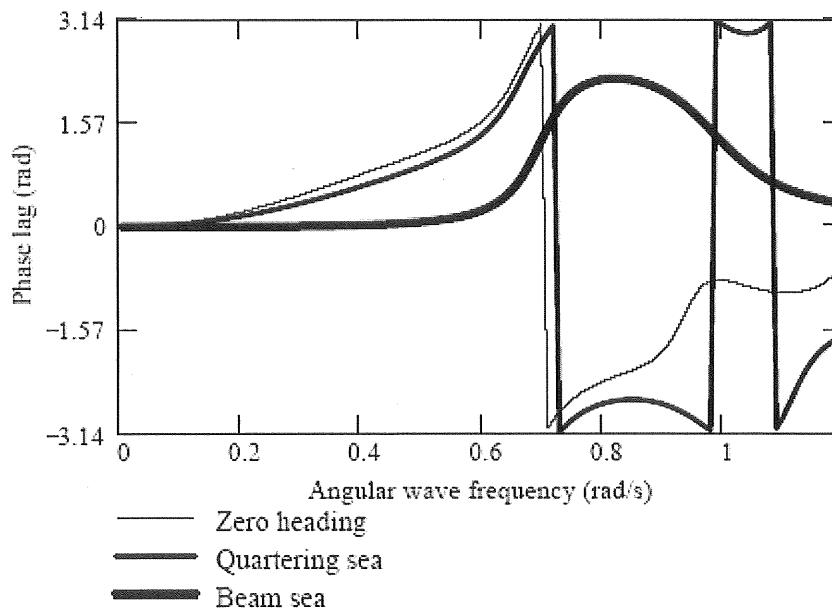


Figure 6.30 The phase lag of the vertical bow motion.

Acceleration

It is important to assess the accelerations of a ship because it is difficult to work if the accelerations are too large, say $g/3$; accelerations at certain frequencies also causes seasickness; cargo may get loose or fastenings must be attached and designed. In the passenger and cruising trade the comfort is important, in the offshore industry the focus is to avoid downtime of operations like drilling or pumping oil and gas, while in

cargo traffic the safety of the goods is most important but also speed reductions should be avoided. In Figures 6.31 to 6.33 the acceleration (Equation (6.77)) at the bow of the example ship is shown.

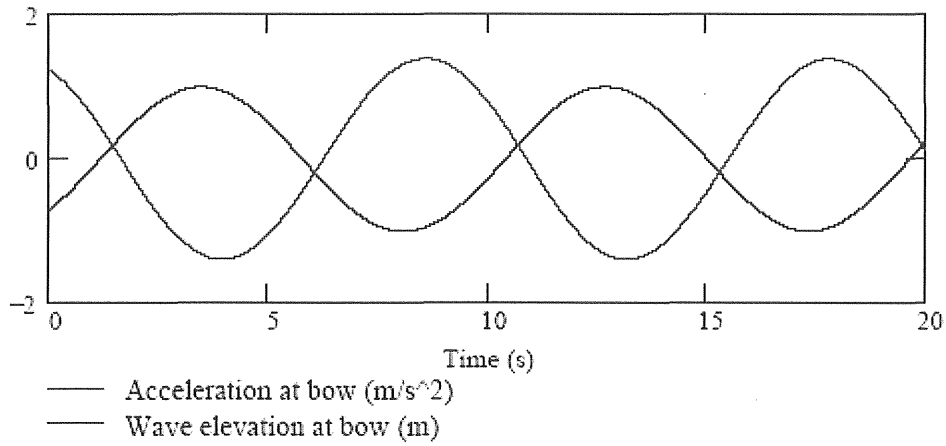


Figure 6.31 Vertical bow acceleration and wave elevation near pitch and heave resonance

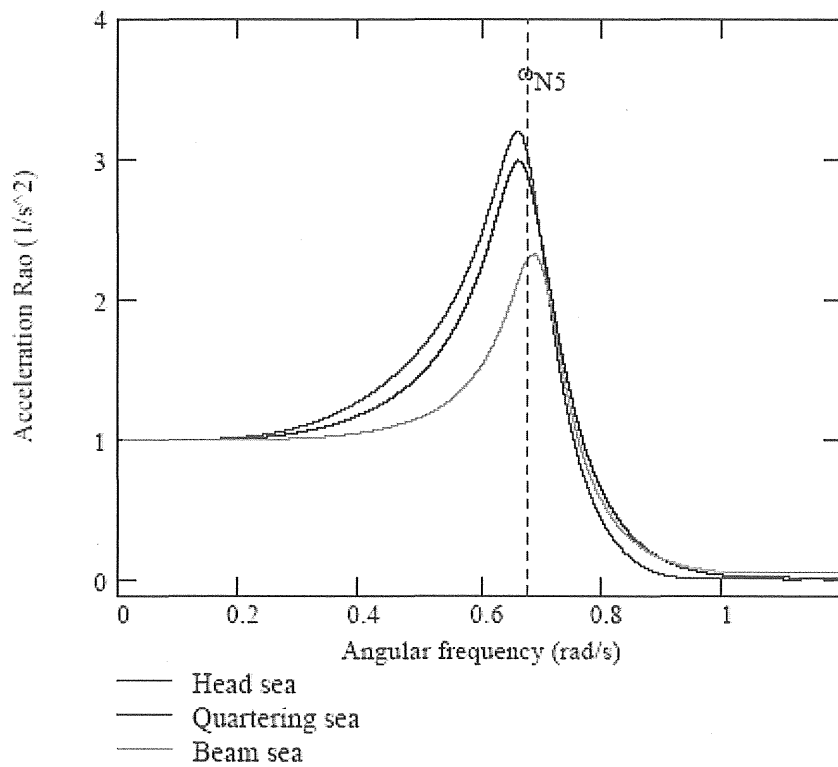


Figure 6.32 The response amplitude operator for the vertical bow acceleration.

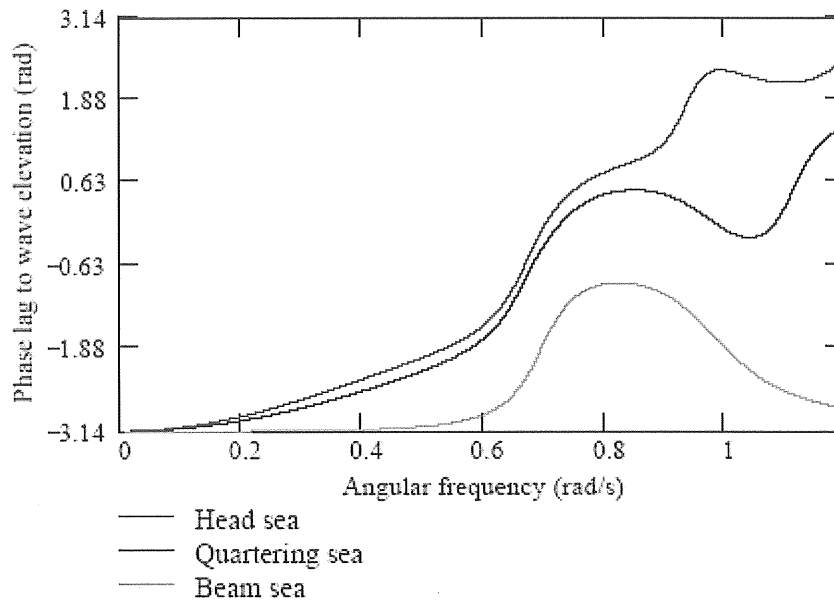


Figure 6.33 The phase lag of the vertical bow acceleration.

Green water

If the wave elevation comes above the instantaneous position of the railing or above the freeboard at any point of the ship this will result in water on deck, so called green water. This can be tested by the following expression for regular plane waves

$$s_{FB}(t) = \eta_3(t) + y\eta_4(t) - x\eta_5(t) + z_{FB} - \zeta(x \cos(\theta), y \sin(\theta), t) > 0 \quad \dots(6.78)$$

where

- $s_{FB}(t)$ is the instantaneous freeboard
- z_{FB} the static freeboard at station x, y and actual trim and
- $\zeta(x \cos(\theta), y \sin(\theta), t)$ the instantaneous wave elevation at station x, y .

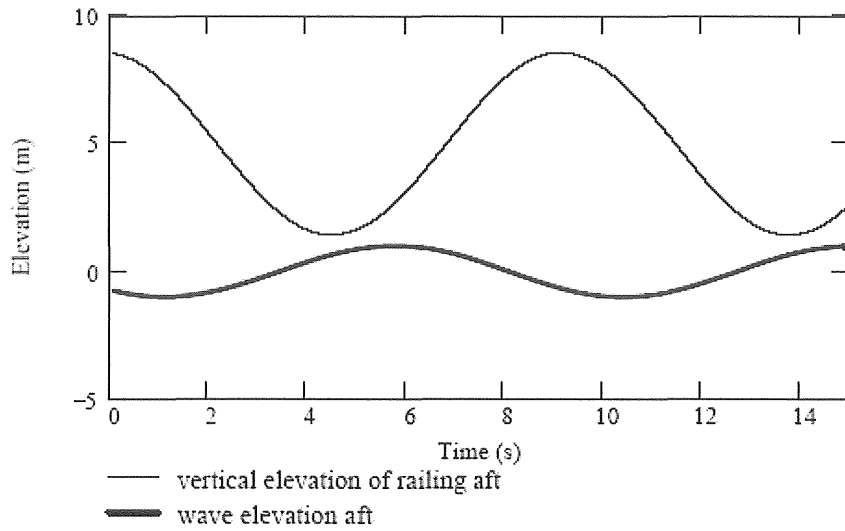


Figure 6.34 Elevation of railing aft and wave elevation at the same place.

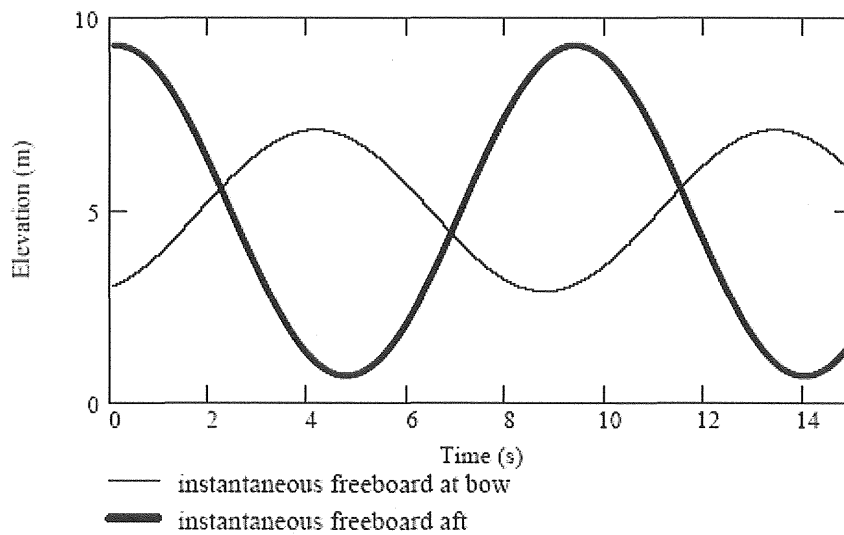


Figure 6.35 Instantaneous freeboard at bow and aft.

Propeller emergence and risk for slamming

The risk for the propeller to emerge out of the water and the risk that the bottom will rise above the water and experience slamming at re-entry must be assessed. This can be tested by a similar expression as was used for assessing the freeboard.

$$s_{BE}(t) = -\eta_3(t) - y\eta_4(t) + x\eta_5(t) + T + \zeta(x \cos(\theta), y \sin(\theta), t) > 0 \quad \dots(6.78b)$$

where

- $s_{BE}(t)$ is the instantaneous submergence of the ship's bottom or propeller
- T the draught at station x, y and actual trim and
- $\zeta(x \cos(\theta), y \sin(\theta), t)$ the instantaneous wave elevation at station x, y .

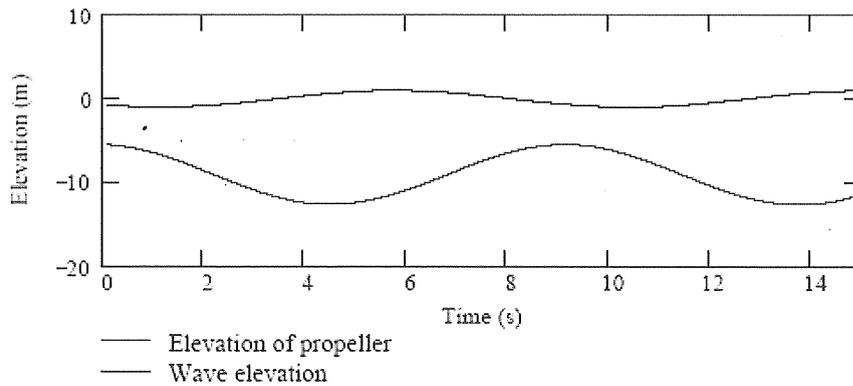


Figure 6.37 The elevation of the propeller centre and the wave surface as a function of time. In this case the propeller is submerged all the time

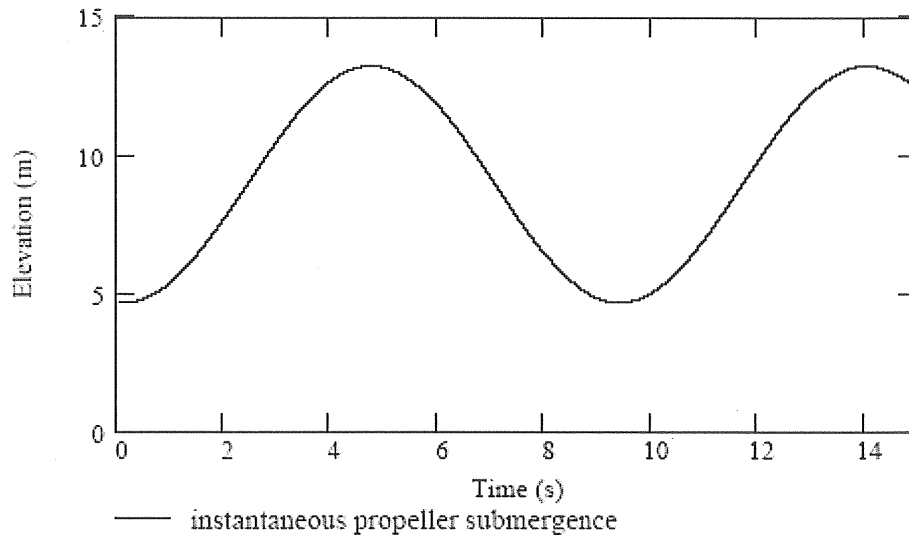


Figure 6.38 The submergence of the propeller centre as a function of time. The difference between the graphs in Figure 6.33.

Slamming

Slamming will appear when the ship's bottom has risen out of the wave and hits back at re-entry. The slamming pressure depends on the relative velocity squared, between the ship's bottom and the water surface, the angle between them, their irregularity and content of air bubbles. The slamming is complicated and it is referred to e.g. Faltinsen (1990) for a deeper description. The slamming pressure can very roughly be approximated by $p_s = const\rho U_{rel}^2$. Then the starting point of assessment is to calculate the relative velocity. If we approximate this by the relative vertical velocity we can just take the time derivative of Equation (6.78b) with $y = 0$:

$$U_{rel}(t) = \frac{\partial}{\partial t}(-\eta_3(t) - y\eta_4(t) + x\eta_5(t) + T + \zeta(x \cos(\theta), y \sin(\theta), t)) = \dots(6.79)$$

$$= -\dot{\eta}_3(t) + x\dot{\eta}_5(t) + \dot{\zeta}(x \cos(\theta), y \sin(\theta), t)$$

This velocity should be evaluated for all moments when Equation (6.78b) is zero

$$-\eta_3(t) - y\eta_4(t) + x\eta_5(t) + T + \zeta(x \cos(\theta), y \sin(\theta), t) = 0 \quad \dots(6.80)$$

and U_{rel} is positive. See further for statistical simplifications in irregular waves in Paragraph 9.6.

6.9 Coupled Linear Pitch and Heave Motion at Forward Speed.

Assume that, in calm water, the ship is forced to oscillate and pitch with the amplitudes, $\hat{\eta}_3$ and $\hat{\eta}_5$, at the angular frequency, ω . The vertical reaction force and pitch reaction moment acting on the body from the water can be written, after integrating the two-dimensional reaction forces along the ship,

$$F_3 = -A_{33}\ddot{\eta}_3 - B_{33}\dot{\eta}_3 - C_{33}\eta_3 - A_{35}\ddot{\eta}_5 - B_{35}\dot{\eta}_5 - C_{35}\eta_5 \quad \dots(6.81)$$

and

$$F_5 = -A_{53}\ddot{\eta}_3 - B_{53}\dot{\eta}_3 - C_{53}\eta_3 - A_{55}\ddot{\eta}_5 - B_{55}\dot{\eta}_5 - C_{55}\eta_5, \quad \dots(6.82)$$

or in matrix form

$$\underline{F}_r = -\underline{A}\ddot{\underline{\eta}} - \underline{B}\dot{\underline{\eta}} - \underline{C}\underline{\eta} \quad \dots(6.83)$$

where A, B and C are 2x2 matrices and $\underline{\eta}$ a 2D vector. To assess the coupled motion due to fore-aft asymmetry of a real ship now the coupling coefficients between heave and pitch are needed:

$$A_{35} = -\int_L x a_{33}(x) dx + \frac{U}{\omega_e^2} B_{33} \quad \dots(6.84)$$

$$A_{53} = -\int_L x a_{33}(x) dx - \frac{U}{\omega_e^2} B_{33} \quad \dots(6.85)$$

$$B_{35} = -\int_L x b_{33}(x) dx - U A_{33} \quad \dots(6.86)$$

$$B_{53} = -\int_L x b_{33}(x) dx + U A_{33} \quad \dots(6.87)$$

and

$$C_{35} = C_{53} = \rho g \iint_{A_{wp}} x ds, \quad \dots(6.88)$$

as well as the diagonal elements defined before:

$$A_{33} = \int_L a_{33}(x) dx = \sum_n a_{33n} \Delta x_n \quad \dots(6.32)$$

$$B_{33} = \int_L b_{33}(x) dx = \sum_n b_{33n} \Delta x_n \quad \dots(6.33)$$

$$C_{33} = \int_L c_{33}(x) dx = \sum_n c_{33n} \Delta x_n = \sum_n \rho g B_n \Delta x_n \quad \dots(6.34)$$

$$A_{55} = \int_{-L/2}^{L/2} a_{33}(x) x^2 dx - \frac{U^2}{\omega_e^2} A_{33} \quad \dots(6.46)$$

$$B_{55} = \int_{-L/2}^{L/2} x^2 b_{33}(x) dx + \frac{U^2}{\omega_e^2} B_{33} \quad \dots(6.47)$$

$$C_{55} = \rho g V (z_B - z_G) + \rho g \int_{-L/2}^{L/2} B(x) x^2 dx = \rho g V \overline{GM}_L \quad \dots(6.48)$$

The coupling between heave and pitch

At zero speed $A_{35} = A_{53}$, $B_{35} = B_{53}$, and $C_{35} = C_{53}$ and the equation system is symmetric. For the chosen coordinate system and the boxlike ship used in the examples with its centre of gravity amidships they are zero. Further, for a merchant ship the coupling between pitch and surge can be ignored, but for an offshore platform it must be taken into account, while the coupling between heave and pitch may be ignored instead.

The 2×2 mass matrix, \mathbf{M} , is diagonal i.e. $M_{35} = M_{53} = 0$, because the origin of the coordinate system is placed above the centre of gravity.

The driving force and moment is somewhat modified due to the forward speed and we can include the dependence on station x of the ship but specialise for following sea (for meeting sea change $-j\omega$ to $+j\omega$):

$$F_{3e} = a e^{-j\omega t} \int_{-L/2}^{L/2} e^{jkx} e^{-kT(x)} [c_{33}(x) - \omega(\omega_e a_{33}(x) - j b_{33}(x))] dx \quad \dots(6.89)$$

$$F_{5e} = -a e^{-j\omega t} \int_{-L/2}^{L/2} e^{jkx} e^{-kT(x)} \left(x + \frac{U}{j\omega_e} \right) [c_{33}(x) - \omega(\omega_e a_{33}(x) - j b_{33}(x))] dx \quad \dots(6.90)$$

Compare Equations (6.38) and (6.51).

With $\underline{F} = (F_{3e}, F_{5e})^T$ then the equation of motion is

$$\mathbf{M} \underline{\ddot{\eta}} = \underline{F}_r + \underline{F} = -\mathbf{A} \underline{\ddot{\eta}} - \mathbf{B} \underline{\dot{\eta}} - \mathbf{C} \underline{\eta} + \underline{F} \quad \dots(6.91)$$

or

$$(\mathbf{M} + \mathbf{A})\dot{\underline{\eta}} + \mathbf{B}\dot{\underline{\eta}} + \mathbf{C}\underline{\eta} = \underline{F}, \quad \dots(6.92)$$

which is recognised as Equation (3.41), and can be solved in the time or frequency domain by methods advised in Section 3.4 of Chapter 3.

6.10 Coupled Pitch and Heave Motion at Zero Speed Including Non-Linear Viscous Damping.

For the box-like ship used in the examples we will investigate the effect of viscous, drag damping, which is quadratic and therefore hinder us from solution in the frequency domain, the use of complex numbers and linear superposition.

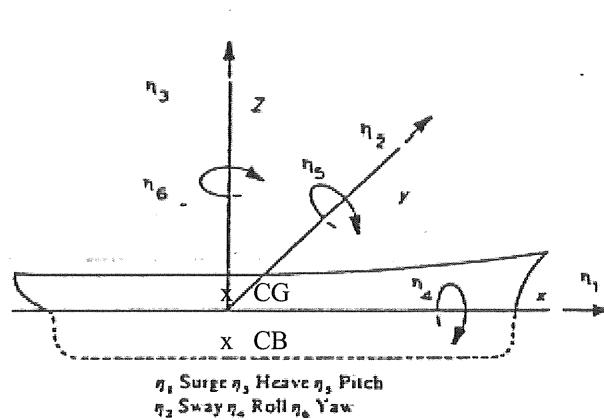


Figure 6.39 Definition of the chosen coordinate system for a ship. The z-axis is drawn vertically through the centre of buoyancy, CB, and the centre of gravity, CG. (From Faltinsen)

We will therefore formulate the problem in the time domain, using the notations we used before.

The wave

Elevation or vertical displacement of a sheet of water particles at the level $z = -T$

$$\zeta(t, x, -T) = ae^{-kT} \cos(kx - \omega t) \quad \dots(6.93)$$

Vertical particle velocity

$$\dot{\zeta}(t, x, -T) = a\omega e^{-kT} \sin(kx - \omega t) = w \quad \dots(6.94)$$

Vertical particle acceleration

$$\ddot{\zeta}(t, x, -T) = -a\omega^2 e^{-kT} \cos(kx - \omega t) = \dot{w} \quad \dots(6.95)$$

Heave

Displacement

$$\eta_3(t) = \hat{\eta}_3 \cos(-\omega t - \varepsilon_3) \quad \dots(6.96)$$

Velocity

$$\dot{\eta}_3(t) = \hat{\eta}_3 \omega \sin(-\omega t - \varepsilon_3) \quad \dots(6.97)$$

Acceleration

$$\ddot{\eta}_3(t) = -\hat{\eta}_3 \omega^2 \cos(-\omega t - \varepsilon_3) \quad \dots(6.98)$$

Pitch

Displacement

$$\eta_5(t) = \hat{\eta}_5 \cos(-\omega t - \varepsilon_5) \quad \dots(6.99)$$

Angular velocity

$$\dot{\eta}_5(t) = \hat{\eta}_5 \omega \sin(-\omega t - \varepsilon_5) \quad \dots(6.100)$$

Acceleration

$$\ddot{\eta}_5(t) = -\hat{\eta}_5 \omega^2 \cos(-\omega t - \varepsilon_5) \quad \dots(6.101)$$

Equations of motion

Fore/aft symmetrical box

Heave

$$\begin{aligned}
 m\ddot{\eta}_3 &= \int_{-L/2}^{L/2} a_{33} (\ddot{\zeta} - \ddot{\eta}_3 + x\ddot{\eta}_5) dx + && \text{(diffraction force)} \\
 &+ \int_{-L/2}^{L/2} b_{33} (\dot{\zeta} - \dot{\eta}_3 + x\dot{\eta}_5) dx + && \text{(linear damping force)} \\
 &+ \int_{-L/2}^{L/2} \frac{1}{2} \rho C_D B |\dot{\zeta} - \dot{\eta}_3 + x\dot{\eta}_5| (\dot{\zeta} - \dot{\eta}_3 + x\dot{\eta}_5) dx + && \text{(viscous drag force)} \\
 &+ \int_{-L/2}^{L/2} \rho g B \left(\underbrace{\zeta}_{\substack{\text{Froude-Krylov} \\ \text{force}}} - \underbrace{\eta_3 + x\eta_5}_{\substack{\text{Buoyancy} \\ \text{force}}} \right) dx && \dots(6.102)
 \end{aligned}$$

Assemble exciting forces on the right hand side and linear reaction terms on the left hand side.

$$(m + A_{33})\ddot{\eta}_3 + B_{33}\dot{\eta}_3 + C_{33}\eta_3 = \int_{-L/2}^{L/2} (a_{33}\ddot{\zeta} + b_{33}\dot{\zeta} + \rho g B \zeta) dx +$$

$$+ \int_{-L/2}^{L/2} \frac{1}{2} \rho C_D B \left| \dot{\zeta} - \dot{\eta}_3 + x \dot{\eta}_5 \right| \left(\dot{\zeta} - \dot{\eta}_3 + x \dot{\eta}_5 \right) dx \quad \dots(6.103)$$

We have then used that

$$A_{33} = \int_{-L/2}^{L/2} a_{33} dx \quad B_{33} = \int_{-L/2}^{L/2} b_{33} dx \quad C_{33} = \int_{-L/2}^{L/2} \rho g B dx \quad \dots(6.104)$$

and e.g. that

$$\int_{-L/2}^{L/2} x \dot{\eta}_5 dx = \dot{\eta}_5 \int_{-L/2}^{L/2} x dx = 0 \quad \dots(6.105)$$

i.e. all linear coupling terms vanish.

We are left with the last non-linear coupling term, which cannot be separated into dependent and non-dependent terms because of the product with its modulus, and therefore must be evaluated in the time domain, which makes the use of the convenient complex variables impossible. Compare e.g. $\zeta|\zeta|$ and $\zeta_c|\zeta_c|$:

$$\begin{aligned} \zeta_c &= a e^{i(kx - \omega t)} & \zeta &= \text{Re}(\zeta_c) = a \cos(kx - \omega t) \\ \zeta_c|\zeta_c| &= a^2 e^{i(kx - \omega t)} = a^2 (\cos(kx - \omega t) + i \sin(kx - \omega t)) \\ \text{Re}(\zeta_c|\zeta_c|) &= a^2 \cos(kx - \omega t) \end{aligned}$$

which is not the same as

$$\zeta|\zeta| = a^2 |\cos(kx - \omega t)| (\cos(kx - \omega t))$$

Pitch

$$\begin{aligned} I_5 \ddot{\eta}_5 &= - \int_{-L/2}^{L/2} a_{33} (\ddot{\zeta} - \ddot{\eta}_3 + x \ddot{\eta}_5) x dx - && \text{(diffraction moment)} \\ &- \int_{-L/2}^{L/2} b_{33} (\dot{\zeta} - \dot{\eta}_3 + x \dot{\eta}_5) x dx && \text{(linear damping moment)} \\ &- \int_{-L/2}^{L/2} \frac{1}{2} \rho C_D B \left| \dot{\zeta} - \dot{\eta}_3 + x \dot{\eta}_5 \right| (\dot{\zeta} - \dot{\eta}_3 + x \dot{\eta}_5) x dx - && \text{(viscous drag moment)} \\ &- \int_{-L/2}^{L/2} \rho g B \left(\underbrace{\zeta}_{\text{Froude-Krylov moment}} \underbrace{-\eta_3 + x \eta_5}_{\text{Buoyancy moment}} \right) x dx && \dots(6.106) \end{aligned}$$

Assemble exciting moments on the right hand side and linear reaction terms on the left hand side.

$$(I_5 + A_{55})\ddot{\eta}_5 + B_{55}\dot{\eta}_5 + C_{55}\eta_5 = - \int_{-L/2}^{L/2} (a_{33}\ddot{\zeta} + b_{33}\dot{\zeta} + \rho g B \zeta) x dx - \int_{-L/2}^{L/2} \frac{1}{2} \rho C_D B |\dot{\zeta} - \dot{\eta}_3 + x \dot{\eta}_5| (\dot{\zeta} - \dot{\eta}_3 + x \dot{\eta}_5) x dx \quad \dots(6.107)$$

We have then used that

$$A_{55} = \int_{-L/2}^{L/2} a_{33} x^2 dx \quad B_{55} = \int_{-L/2}^{L/2} b_{33} x^2 dx$$

$$C_{55} = \int_{-L/2}^{L/2} \rho g B x^2 dx - (z_G - z_B) \rho g V \approx \int_{-L/2}^{L/2} \rho g B x^2 dx \quad \dots(6.108)$$

and e.g. that

$$\int_{-L/2}^{L/2} x \dot{\eta}_3 dx = \dot{\eta}_3 \int_{-L/2}^{L/2} x dx = 0 \quad \dots(6.109)$$

i.e. again all linear coupling terms vanish and we are left with the last non-linear coupling term.

6.11 Equivalent Linearised Drag Damping

The non-linear coupled drag term constitutes a problem, when making assessment of sea-keeping properties in the frequency domain.

In roll, the linear radiation damping is very small and the viscous non-linear drag damping dominates and must therefore be assessed to get realistic motion. Jensen increased the linear damping coefficient, Equation (6.66), by comparing the calculated motion with seakeeping model tests. In this section we will show that such an equivalent linear drag-damping coefficient depends on the amplitude of motion.

Neglecting the coupling between roll and sway we can symbolically write the drag damping moment in beam regular sea as

$$F_{D4} = K |\dot{\zeta}_y - \dot{\eta}_4| (\dot{\zeta}_y - \dot{\eta}_4), \quad \dots(6.110)$$

where K can be set to $(1/2)\rho C_D B^2 L$ and $\dot{\zeta}_y = \partial^2 \zeta / \partial t \partial y$ is the angular velocity of the wave slope in the y direction i.e. in the starboard-portside direction.

When the non-linear roll damping is important usually $\dot{\zeta}_y \ll \dot{\eta}_4$ and then

$$F_{D4} \approx K|\dot{\eta}_4|(\dot{\eta}_4), \quad \dots(6.111)$$

which is simpler but still non-linear.

To assess the equivalent linear coefficient we can compare the dissipated energy over one wave cycle with an equivalent linear expression, assuming harmonic motion with the roll angular velocity amplitude $\hat{\eta}_4$,

$$\dot{\eta}_4 = \hat{\eta}_4 \sin(\omega t) \quad \dots(6.112)$$

The dissipated energy is

$$\int_0^T K|\dot{\eta}_4|(\dot{\eta}_4)^2 dt = \int_0^T B_{e44}(\dot{\eta}_4)^2 dt, \quad \dots(6.113)$$

L.H.S.:

$$K \left(\int_0^{T/2} (\dot{\eta}_4)^3 dt + \int_{T/2}^T (\dot{\eta}_4)^3 dt \right) = 2K \left(\int_0^{T/2} (\dot{\eta}_4)^3 dt \right) = \frac{4K}{3} (\hat{\eta}_4)^3, \quad \dots(6.114)$$

R.H.S.:

$$\int_0^T B_{e44} (\dot{\eta}_4)^2 dt = B_{e44} \frac{\pi}{2} (\hat{\eta}_4)^2, \quad \dots(6.115)$$

L.H.S. = R.H.S.:

$$\frac{4K}{3} (\hat{\eta}_4)^3 = B_{e44} \frac{\pi}{2} (\hat{\eta}_4)^2 \quad \dots(6.116)$$

$$\therefore B_{e44} = \frac{8K}{3\pi} \hat{\eta}_4 \quad \dots(6.117)$$

That is, the equivalent damping coefficient, B_{e44} , depends on the amplitude of the roll motion.

In a harmonic wave motion e.g. roll in beam swell iteration on the roll amplitude must be performed, guessing the roll amplitude, calculating it from the equation of motion and then repeat with this new value until it converges. In an irregular sea a guess of the significant roll amplitude is made, then this is calculated from the equation of motion and then fed as input for consecutive rounds of iteration.

7 WIND WAVES

In this chapter some properties of real wind waves are described, it is shown how they can be looked upon as a linear combination, superposition, of regular waves, and how realistic wind waves can be synthesised or simulated. Last some basic wave statistics are given. For broader information, see the classical book by Kinsman (1965) or a recent book by Dean and Dalrymple (1991).

Waves at sea show a constantly changing, never repeated pattern. They grow under the action of the wind, and during the growth phase the wave-height, wave period and wavelength are due to the wind force (wind speed), the duration of the wind and the length, *fetch*, of which the wind can act on the waves. On the high seas the possible wave height is thus limited by the strength, diameter and motion of the low-pressures, in lakes and landlocked seas of the wind speed and distance to the upwind shore. At *Fully Arisen Sea, FAS*, the celerity of dominating waves approach the wind speed and as a result the wind cannot transfer more energy to the waves. The exact mechanisms for the generation of waves from a smooth wave-surface are still not completely explained, but there are hypothetical models describing the energy transfer from the wind to the waves, e.g. Jeffreys' and Phillips-Miles' modeller (See Massel, 1996). Based on these, empirical functions were developed during the first half of the 20th century notably by Sverdrup, Munk och Bredtschneider (See SPM 1983). Later more sophisticated models have been developed, that in some countries are run on a daily basis to give wave prognoses. An orientation over recent models is given by Young (1999).

Under the progression towards coasts and beaches the waves will be affected by the bottom so that their height, wavelength and direction of propagation are changed due to variation in depth, bottom friction and currents still under the influence of the wind. These effects, refraction, reflection, diffraction and wavebreaking are equivalent to those of regular waves and were explained in Chapter 5.

If the waves progress out of the low-pressure where they are generated by the strong wind into areas of little or low wind, the shortest waves will gradually be dissipated and the longer waves will due to their higher celerity overtake the shorter waves, so as a result, at a place far away from the low-pressure, they will be almost regular but with a frequency gradually increasing with time. Such waves are called swell.

An example of a time trace of a wave is shown in Figure 7.1. In the figure also some basic, fundamental definitions are illustrated. The wave height, H , is the difference in level between a wave crest and the following wave trough, the positive amplitude, a^+ , is the crest height above the still-water level, the negative amplitude, a^- , is the trough depth below the still-water level, and the wave period, T , is the time lapse between the up-crossings of the still-water level. (In some treatises the down-crossings are used instead of the up-crossings. Note that an up-crossing in time corresponds to a down-crossing in space.)

crest

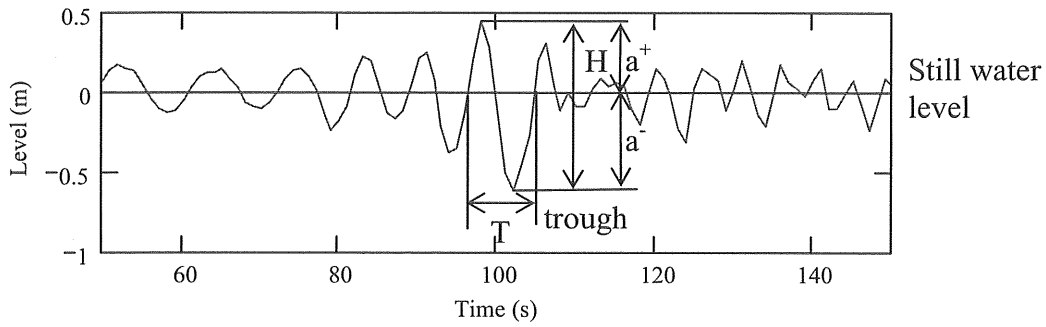


Figure 7.1 Some fundamental definitions of wave properties.

In space, the wavelength, λ , corresponding to the wave period is defined as the horizontal distance between two consecutive up-crossings in the direction of wave advance, and the wave height and amplitude within a wavelength are defined in analogy to those in time. For an irregular wave as in Figure 7.1 the wave heights and amplitudes in space are normally not the same as those in time, due to the dispersive properties of the wave.

In this compendium we will not delve further on the generation of the wind waves, but direct our interest towards the description of different sea states and statistics for calculating of design waves. Wave generation is described thoroughly by e.g. Kinsman (1965).

7.1 Characteristics of Wind Waves

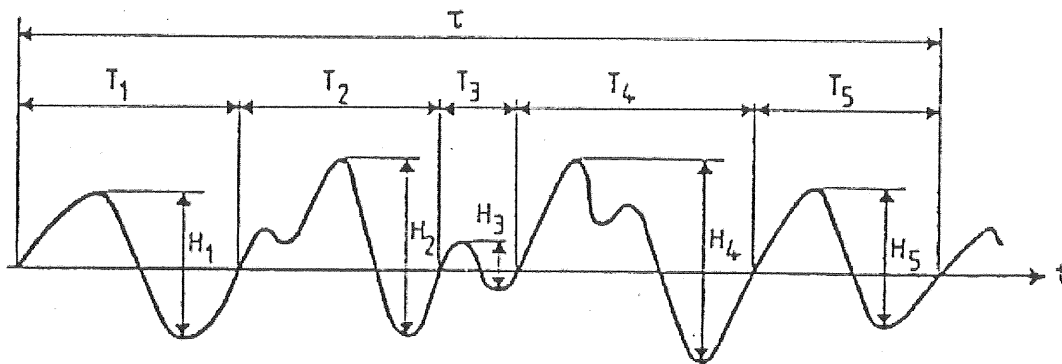


Figure 7.2 Point record of a wave elevation. The wave periods defined as zero up-crossing periods.

In Figure 7.2 an example of a time trace of a wave elevation in a point is shown. The wave periods are there defined as the times between the *zero up-crossings*. Before the advance of computers such traces were in the form of paper graphs and were evaluated by hand. The result of such an evaluation was a list of wave periods, T_i , and connected wave heights, H_i . From that a series of characteristics of the wave can be defined and is still used, although nowadays the methods of evaluation are different, which will be described later. One used to say that the analysed wave record should contain at least 200 waves for the analysis to be meaningful.

Mean zero up-crossing period, often called only zero up-crossing period:

$$T_z = \frac{1}{N_z} \sum_{i=1}^{N_z} T_{zi} = \frac{\tau}{N_z} \quad \dots(7.1)$$

where N_z is the number of waves in the record, T_{zi} the individual zero-crossing periods of Figure 7.2 and τ the length of the record. This definition leaves shorter small waves riding on the long waves uncouned.

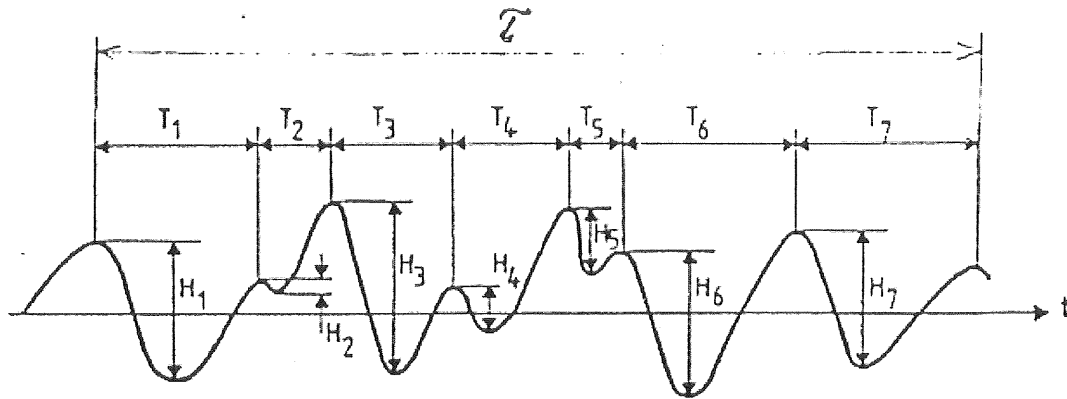


Figure 7.3 The same point record of a wave elevation as in Figure 7.2. The wave periods defined as wave crest periods.

For certain purposes we also need to define periods between local time maxima or crests, the crest periods, (See Figure 7.3) from which the mean crest period is defined as

Mean crest period:

$$T_c = \frac{1}{N_c} \sum_{i=1}^{N_c} T_{ci} = \frac{\tau}{N_c} \quad \dots(7.2)$$

where N_c is the number of waves in the record, T_{ci} the individual crest periods of Figure 7.3 and τ the length of the record.

In the example case $T_z = \tau/5$, $T_c = \tau/7$ and generally $N_c \geq N_z$ and $T_c \leq T_z$.

The wave heights are normally referred to the zero crossing definition, and the zero-crossing wave heights and number of waves are used from here and onwards without index. There are many possibilities to characterise the wave height. The most common are defined below.

Mean wave height:

$$\bar{H} = \frac{1}{N} \sum_{i=1}^N H_i \quad \dots(7.3)$$

Root mean square wave height H_{rms} or the sample variance

$$H_{rms}^2 = \frac{1}{N} \sum_{i=1}^N H_i^2 \quad \dots(7.4)$$

Significant wave height, the mean of the highest 1/3 of the N wave heights.

$$H_{1/3} = H_s \quad \dots(7.5)$$

It can be noted that using down-crossings or up-crossings gives somewhat different values on $H_{1/3}$. It can be shown that $H_{1/3} \approx \sqrt{2}H_{rms}$. Experience shows also that H_s is approximately equal to the wave height, H_v , that is visually estimated by an experienced observer. In Figure 7.4 a confirmation of this from a Swedish investigation (Wahl, 1974) is given. Different light-house keepers may however have different calibration factors.

For visual observations from ships Nordenström (1969) gave the following relations between visually observed and measured wave height and wave period after analysis of data from Hogben and Lumb.

$$\begin{aligned} H_{1/3} &= 1.68H_v^{0.75} \\ T_z &= 0.82T_v^{0.96} \end{aligned} \quad \dots(7.6)$$

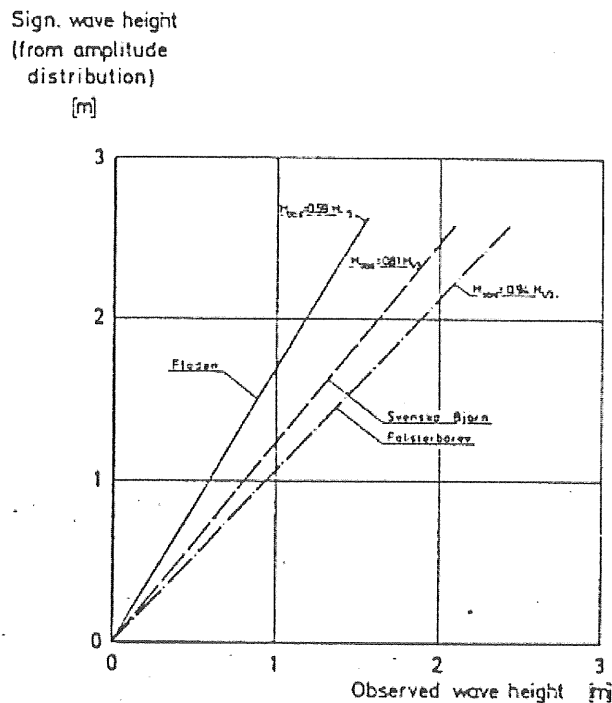


Figure 7.4 Comparisons between by light-house keepers visually observed wave heights and by pressure wave probes measured significant wave heights. (From Wahl, 1974).

A measure to assess the irregularity or broadbandness of the wave could be to count the total number of crest maxima and the number of zero-crossing maxima. The ratio between these two numbers is T_c/T_z , and can be used to estimate “spectral-width parameter”, ε :

$$\varepsilon = \sqrt{1 - \left(\frac{T_c}{T_z}\right)^2} \quad \dots(7.7)$$

Assessment of wave characteristics directly from time traces is not very reproducible, mostly because the number of waves and consequently T_z are very much depending on how small undulations of the time trace that is taken into account. Due to modern computer processing and algorithms developed for Fast Fourier Transformation, FFT, this latter Fourier technology is used in stead, which makes possible objective, reproducible filtering.

7.2 Fourier Analysis

Fourier series

From analysis we know that every piecewise continuous function can on a finite interval be approximated by a sum of sine and cosine functions. A point registration of the wave elevation, $\zeta(t) = f(t)$, can thus be written on $(0 < t < T)$:

$$f(t) \approx \frac{1}{2}a_0 + \sum_{i=1}^N \left(a_i \cos\left(i\frac{2\pi}{T}t\right) + b_i \sin\left(i\frac{2\pi}{T}t\right) \right) \quad \dots(7.8)$$

It is then implicitly assumed that the point registration is repeated for the registration period, T . See figure 7.19 for a simulated point registration of a wave elevation.

The coefficients a_i and b_i can be calculated by

$$a_i = \frac{2}{T} \int_{t_0}^{t_0+T} f(t) \cos\left(i\frac{2\pi}{T}t\right) dt \quad i = 0,1,2\dots N \quad \dots(7.10)$$

$$b_i = \frac{2}{T} \int_{t_0}^{t_0+T} f(t) \sin\left(i\frac{2\pi}{T}t\right) dt \quad i = 1,2,3\dots N \quad \dots(7.11)$$

Alternatively (7.8) can be written

$$f(t) \approx \frac{1}{2}a_0 + \sum_{i=1}^N \left(c_i \cos\left(i\frac{2\pi}{T}t + \varepsilon_i\right) \right), \quad \dots(7.12)$$

where

$$c_i = \sqrt{a_i^2 + b_i^2} \quad \dots(7.13)$$

and

$$\varepsilon_i = \arctan\left(-\frac{b_i}{a_i}\right) \quad \dots(7.14)$$

The Fourier series (7.8) or (7.12) approximates $f(t)$ well if the number of components in the series is sufficient. Observe also that the longest wave that can be detected by a record with the length, T , is a wave with the period, T . The measurement must thus be long enough in relation to the wave periods contained in the seastate to give any relevant information. Usually 100 to 200 components are sufficient to approximate a smooth function such as a train of non-breaking waves.

Parseval's equation, orthogonality

In Chapter 5 the energy in a harmonic water gravity wave was shown to be proportional to the square of its amplitude, $(1/2)\rho g a^2$. For a Fourier series with zero mean, ($a_0 = 0$), the sum of the square of the component amplitudes equals the variance of the function itself.

$$\frac{1}{4}a_o^2 + \frac{1}{2}\sum_{i=1}^N c_i^2 = \frac{1}{4}a_o^2 + \frac{1}{2}\sum_{i=1}^N (a_i^2 + b_i^2) = \frac{1}{T} \int_{t_0}^{t_0+T} (f(t))^2 dt = \text{Var}(f(t)) \dots(7.15)$$

This equation is a form of Parseval's equation.

The consequence for water waves, where we only take the elevation in relation to the mean water level into account, is then that the waves are not only geometrically additive but that also the sum of the energy of the components equals the energy of the composed sea state, at least over one period of analysis, T . Also, all wave-induced forces and resulting motions are orthogonal and can be calculated for each component frequency independently of the motions at other frequencies. Then the resultant irregular motions are given by superposition of the component motions with due respect to the random phases of the wave components.

The derivation of Fourier series and Parseval's equation is based on the orthogonality of the trigonometric functions:

$$\int_{t_0}^{t_0+T} 1 \cos\left(\frac{2\pi}{T} t\right) dt = \int_{t_0}^{t_0+T} 1 \sin\left(\frac{2\pi}{T} t\right) dt = 0 \quad \dots(7.16)$$

$$\int_{t_0}^{t_0+T} \sin\left(i \frac{2\pi}{T} t\right) \sin\left(j \frac{2\pi}{T} t\right) dt = \begin{cases} 0 & \text{if } i \neq j \\ T/2 & \text{if } i = j \end{cases} \quad \dots(7.17)$$

$$\int_{t_0}^{t_0+T} \cos\left(i \frac{2\pi}{T} t\right) \cos\left(j \frac{2\pi}{T} t\right) dt = \begin{cases} 0 & \text{if } i \neq j \\ T/2 & \text{if } i = j \end{cases} \quad \dots(7.18)$$

$$\int_{t_0}^{t_0+T} \sin\left(i\frac{2\pi}{T}t\right) \cos\left(j\frac{2\pi}{T}t\right) dt = 0 \quad \dots(7.19)$$

where i and j are positive integers. For a more exhaustive treatise on Fourier analysis see e.g. Hildebrand (1962), or other textbooks in calculus.

7.3 Amplitude Spectra and Phase Spectra

The Fourier series, resulting from the analysis of the wave records can be illustrated graphically as amplitude and phase spectra. To illustrate this we will analyse a sample wave record.

Wave record

In Figure 7.5 a 3 hour record of a wave in the Norwegian sea is shown. In Figure 7.6 a blow up of the 3 hour record is shown to see the shape of the waves.

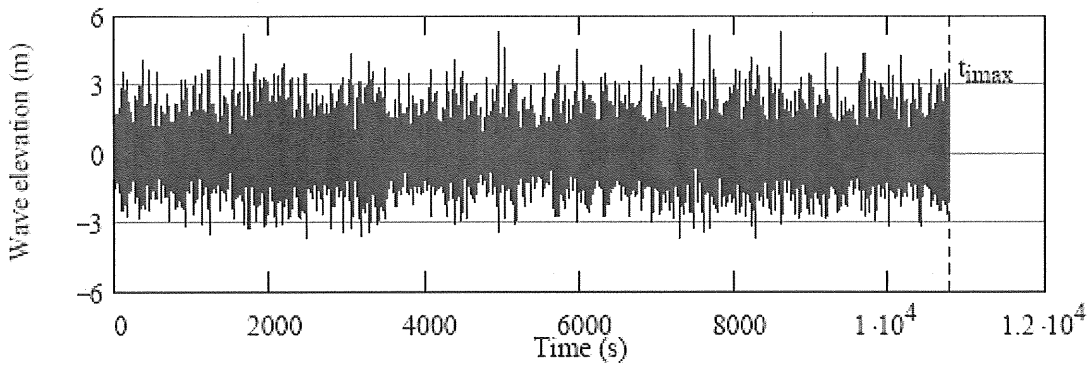


Figure 7.5 A 3 hour record of a wave in the Norwegian sea

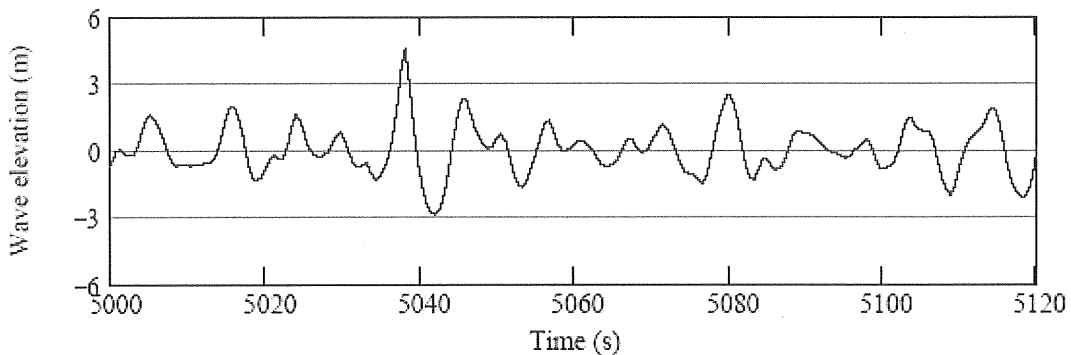


Figure 7.6 A blow up of the 3 hour record in Figure 7.5

Amplitude, variance and energy spectra

We will now show the result of an FFT analysis of the wave record. The wave record contains 19,051 discrete values at the time interval 0.556 s. The used FFT demands the number of values to be 2^n where n is an integer. The nearest number of is $2^{14} = 16,384$ which gives the useful time-length to $T_R = 2.5744$ h. The maximum resolution of the discrete variance spectrum is then $\Delta f = 1/T_R$, where T_R is the length of the

record, and the resulting amplitude, variance or energy spectra will in this case contain 8192 discrete amplitudes. In Figure 7.7 the resulting component amplitudes as a function of angular frequency or the *amplitude spectrum* is shown and in Figure 7.8 the corresponding component phases. The graphs reveal that the amplitudes, although having stochastic magnitudes, show some kind of pattern with the dominant amplitudes around 0.7 rad/s, period around 8 s, but that the phases seem to be completely random.

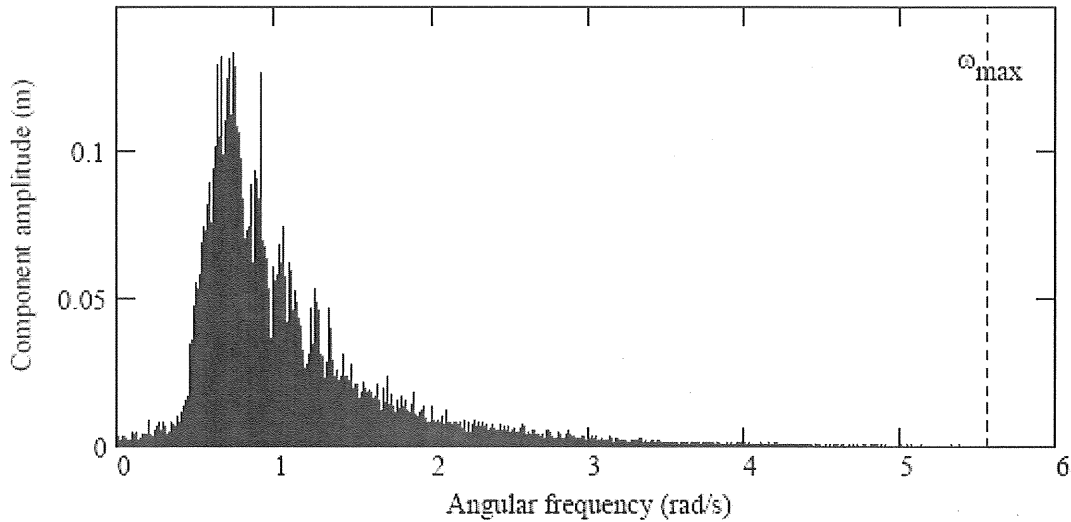


Figure 7.7 Component amplitudes as a function of angular frequency or *amplitude spectrum*

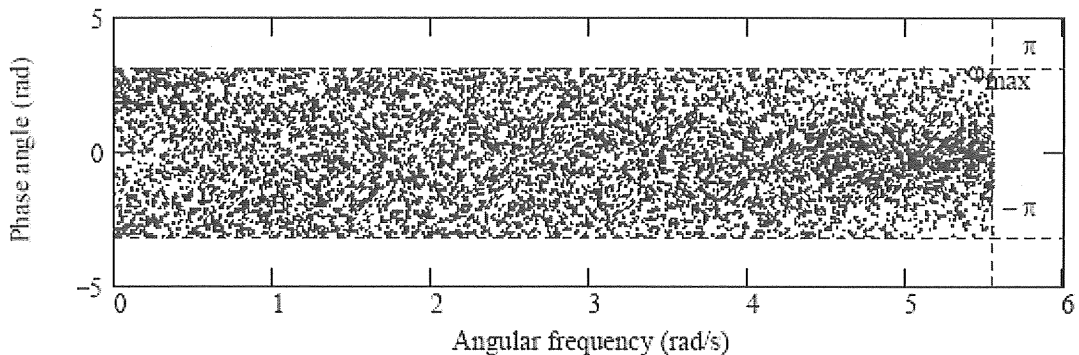


Figure 7.8 Component phases as a function of angular frequency.

If the original time record should be reconstructed both the amplitudes and phases must be saved. However, mostly only the component amplitude spectra are saved, as any particular wave record is seen as one realisation of many possible. Even a few wavelengths downwind or upwind the shape of the elevation graph would have been different due to the different celerity, dispersion, of the component waves.

Traditionally the information is saved as a variance spectrum or “wave-energy spectrum”. Recall that the variance of each component is $\frac{1}{2}a_i^2$ and the energy $\frac{1}{2}\rho g a_i^2$.

Such a discrete variance spectrum of the sample wave record is shown in Figure 7.9. To make the further discussion more clear the variance spectrum is blown up in Figure 7.10.

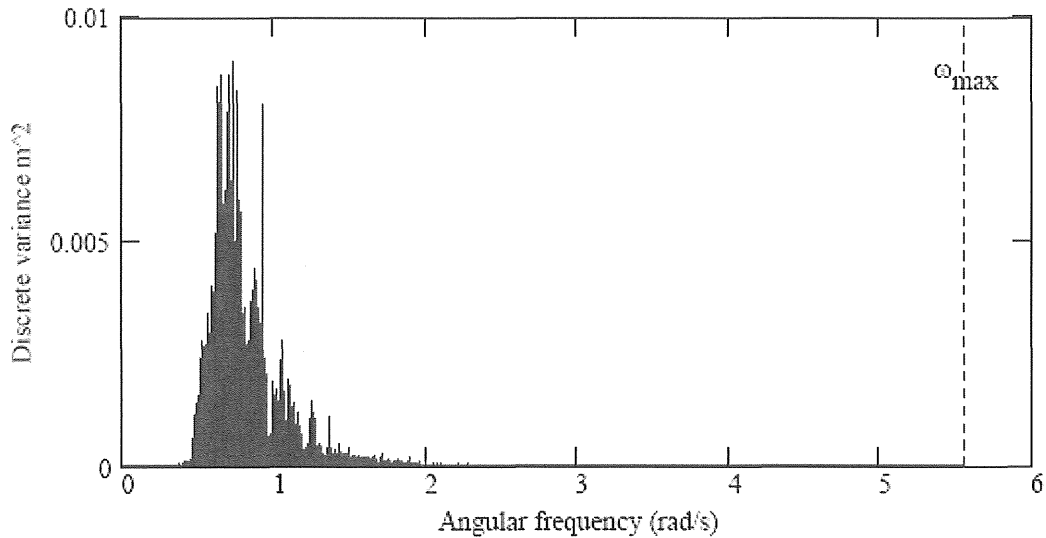


Figure 7.9 Discrete variance as a function of angular frequency.

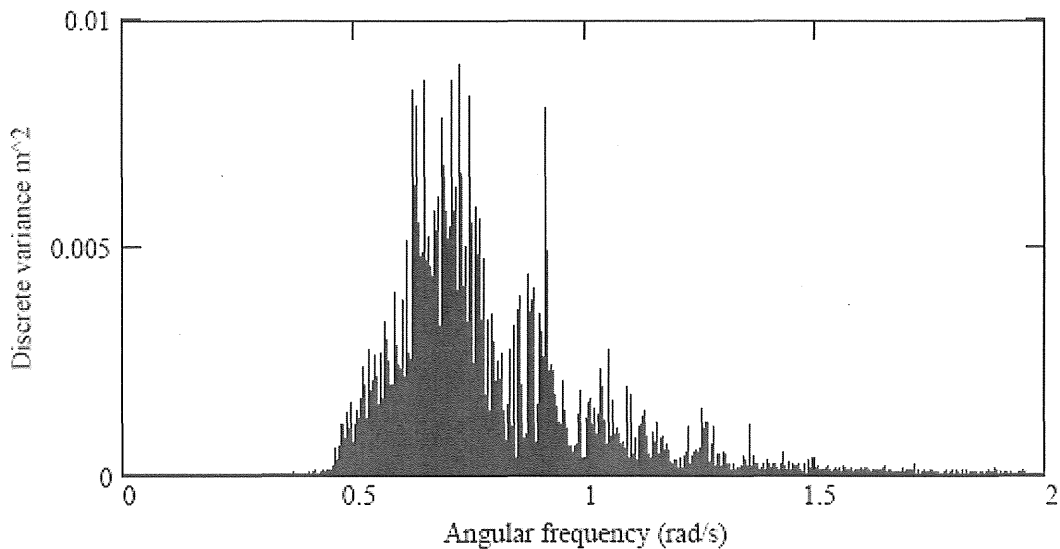


Figure 7.10 The discrete variance spectrum of Figure 7.9, blown up between 0 and 2 rad/s, as a function of angular frequency.

To make the appearance of the discrete variance spectrum look more “deterministic” and be able to compare it to other spectra or standard spectra it can be smoothed. The sample record here was, after some trials, smoothed by taking a centred arithmetic mean of 201 discrete variances. The result of this smoothing is shown in Figure 7.11.

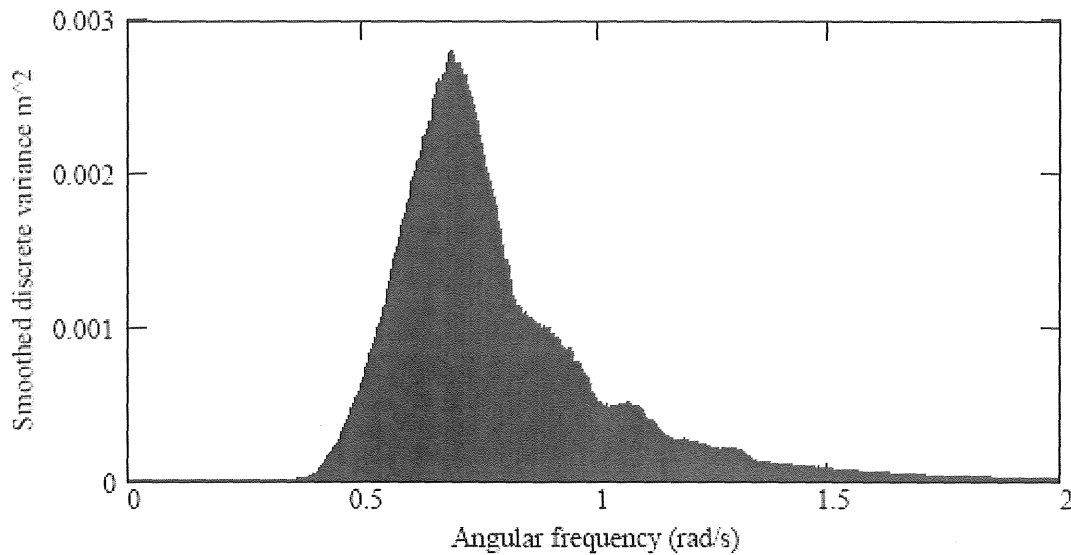


Figure 7.11 The smoothed discrete variance spectrum, blown up between 0 and 2 rad/s, as a function of angular frequency.

For the comparison between spectra, deduced from records of various record lengths T_R , sampling intervals, Δt , etc., the discrete variance spectrum has to be transformed to a continuous density, spectrum. This is done by dividing the discrete variances by the frequency division $\Delta\omega$:

$$S_i = \frac{a_i^2}{2\Delta\omega} \quad \dots(7.20)$$

The result of this action is shown in Figure 7.12, and we now have a spectrum that resembles the standard, empirical spectra used in the ship industry. Such standard spectra are the result of assembling and taking the mean of many measured spectra. We will try to fit some standard spectrum to the smoothed measured spectrum. But to do that we will describe the standard spectra, and how wave characteristics are derived from spectra by using spectral moments.

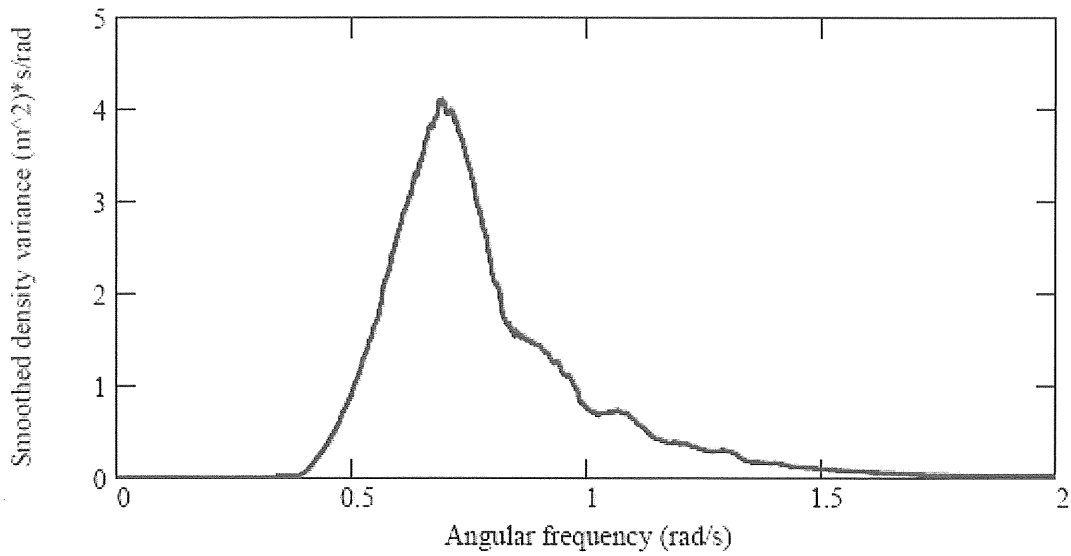


Figure 7.12 The smoothed density variance spectrum or “wave energy spectrum” of the sample record.

Standard spectra

A fundamental spectrum is the Pierson-Moscowitz spectrum, which should describe wave spectra for fully developed sea, or fully arisen sea (FAS), when a constant wind blowing infinitely long cannot increase the energy in the waves, but the energy transfer is balanced by dissipation. This spectrum is a one-parameter spectrum completely described by the wind speed:

$$S_{PM}(\omega) = \alpha g^2 \omega^{-5} e^{-0.74(\omega_o/\omega)^4} \quad \dots(7.21)$$

where $\alpha = 0.0081$ is Phillip’s constant,
 g the earth acceleration,

$\omega_o = g/(U_{19.5})$ and

$U_{19.5}$ = the wind speed at the height 19.5 m above still water level.

See Figure 7.13 for examples of PM spectra for some wind speeds.

For this spectrum $T_{01} = 1.086 T_{02}$ and $T_m = 1.408 T_{02} = 1.14 T_o$. The periods T_{01} and T_{02} are estimates of the zero-upcrossing period, T_z , and will be defined in the next section. T_m is the modal period or the period for the spectral peak. $T_o = 2\pi/\omega_o$.

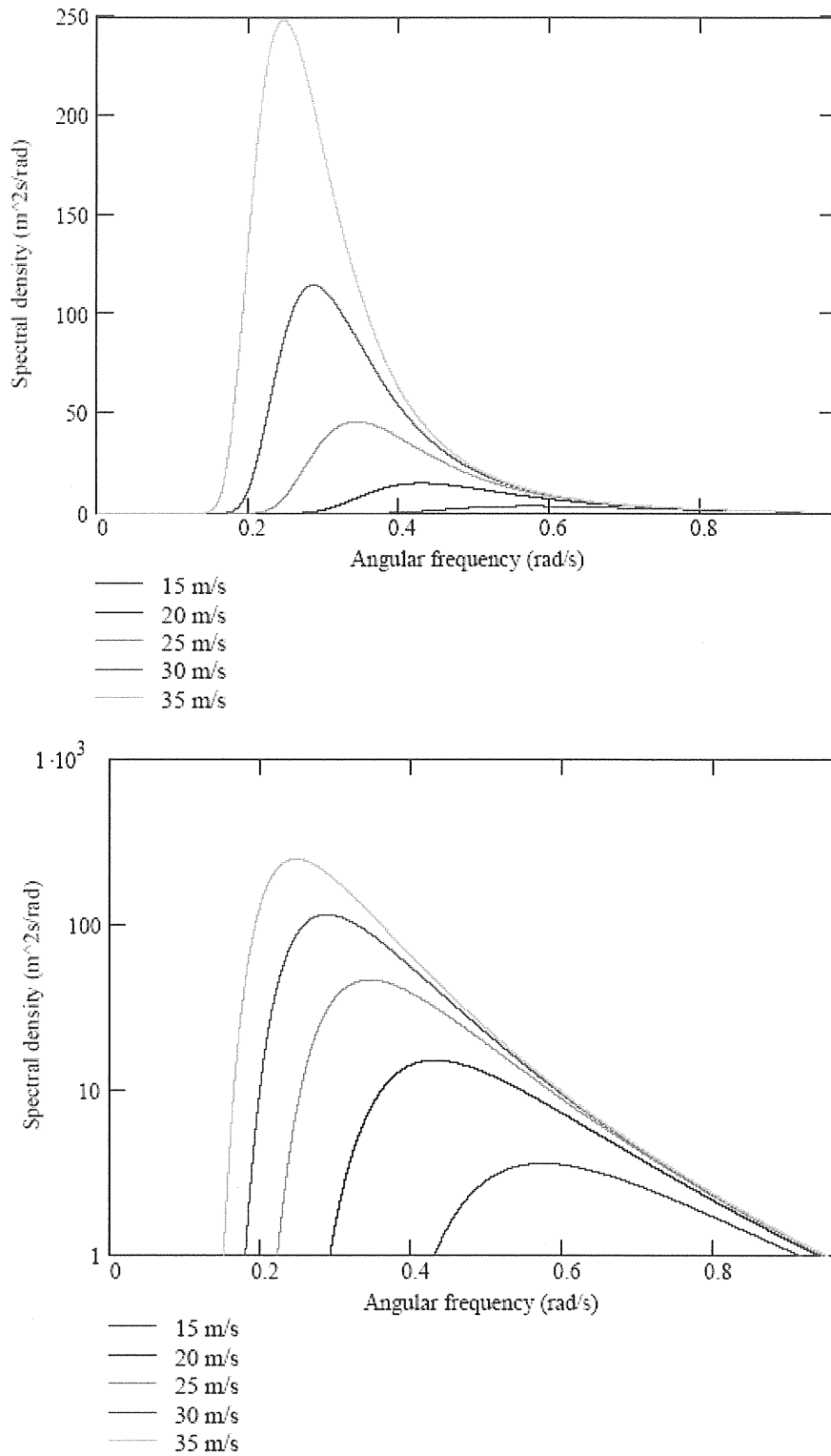


Figure 7.13 PM spectra for some wind speeds.

A variant of the one-parameter PM-spectrum is the ITTC spectrum (ITTC = International Towing Tank Conference).

$$S_{ITTC}(\omega) = \alpha g^2 \omega^{-5} e^{-\frac{3.11}{H_s^2} \omega^4} \quad \dots(7.22)$$

In this spectrum the significant wave height, H_s , is used instead of the wind speed or mean period.

Mostly the sea state is, however, not fully developed as the wind speed and direction change, the fetch is too short, or the duration is not long enough, especially for strong winds and high waves. Then two-parameter spectra for developing seas can be used, e.g. some where the wave height and frequency are the parameters. This was originally proposed by Bretschneider and offers more flexibility, because the energy of the spectra can be placed at arbitrary locations on the frequency axis.

$$S_B(\omega) = \frac{1.25}{4} H_s^2 \frac{\omega_m^4}{\omega^5} e^{-1.25 \left(\frac{\omega_m}{\omega}\right)^4} \quad \dots(7.23)$$

where ω_m is the modal angular frequency (maximum of spectrum).

Such spectra belonging to the PM-family are also, somewhat incorrectly, referred to as PM-spectra. Two other spectra are the ISSC spectra Equation (7.24a) and Equation (7.24b) (ISSC = International Ship Structures Congress, 1964). The periods T_{01} and T_{02} are estimated by moments of measured spectra and are both estimates of the zero-crossing period. Spectral moments and the periods T_{01} and T_{02} will be defined in the next section.

$$S_{ISSCa}(\omega) = 0.11 \left[\frac{H_s}{\left(\frac{T_{01}}{2\pi}\right)^2} \right]^2 \omega^{-5} e^{-0.44 \left(\frac{T_{01}}{2\pi} \omega\right)^4} \quad \dots(7.24a)$$

$$S_{ISSCb}(\omega) = \frac{1}{4\pi} \left[\frac{H_s}{\left(\frac{T_{02}}{2\pi}\right)^2} \right]^2 \omega^{-5} e^{-\left(\frac{1}{\pi}\right) \left(\frac{T_{02}}{2\pi} \omega\right)^4} \quad \dots(7.24b)$$

An almost identical spectrum⁵ as (7.24a) was recommended by ITTC 1978 for “open sea spectral formulation”. See ITTC –Recommended Procedures and guidelines 2005^{xxxii}.

Two-parameter spectra still give too little freedom to reproduce realistic spectra of developing sea. In 1963 Hasselman *et al*^{xxxiii} published the JONSWAP spectrum, which was one outcome from the Joint North Sea Wave Project.

⁵ Notations are different but numerical difference is 1%.

$$S_{JONSWAP}(\omega) = S_{PM}(\omega) \gamma^e \frac{1}{2} \left(\frac{\omega - \omega_m}{\sigma \omega_m} \right)^2 = \alpha g^2 \omega^{-5} e^{-1.25(\omega_m / \omega)^4} \gamma^e \frac{1}{2} \left(\frac{\omega - \omega_m}{\sigma \omega_m} \right)^2, \quad \dots(7.25)$$

where $\gamma^e \frac{1}{2} \left(\frac{\omega - \omega_m}{\sigma \omega_m} \right)^2$ is the peak enhancement factor,

ω the angular frequency,

ω_m the modal angular frequency (maximum of spectrum)

$\sigma = \sigma_a$ for $\omega < \omega_m$, “standard deviation” of the peak enhancement factor to the left and

$\sigma = \sigma_b$ for $\omega > \omega_m$, “standard deviation” of the peak enhancement factor to the right.

Recommended values are, when the fetch, F , and the wind speed, U_{10} , at 10 m height is used:

$$\gamma = 3.30$$

$$\sigma_a = 0.07$$

$$\sigma_b = 0.09$$

$$\alpha = 0.076 F_o^{-0.22}$$

$$\omega_m = 7\pi(g / U_{10}) F_o^{-0.33} \text{ and}$$

$$F_o = gF / (U_{10})^2.$$

Another formulation of the spectrum (7.25a) is recommended by ITTC 1984 for “long crested limited fetch sea spectral formulation”. See ITTC –Recommended Procedures and guidelines 2005^{xxxii}. The peak enhancement factor is identical⁶, but the $S_{PM}(\omega)$ factor is different

$$S_J(\omega) = 155 \frac{H_s^2}{T_{01}^4 \omega^5} \exp \left(- \left(\frac{944}{T_{01}^4 \omega^4} \right) \right) \gamma^{\exp \left(- \frac{(0.191 \omega T_{01} - 1)^2}{2\sigma} \right)} \quad \dots(7.25b)$$

The expression (7.25b) gives identical results to (7.25a) provided T_{01} and H_s are the same.

The JONSWAP spectrum is in common use for design of drilling platforms in the offshore industry because it offers more flexibility with its five parameters, and can produce more realistic spectra. The parameters are then chosen from wave statistics combined with systematic parameter fitting.

For the JONSWAP spectrum $T_{01} = 1.073 T_{02} = 0.834 T_m = 0.924 T_1$.

Note in Figure 7.14 the different characteristics of the two spectra with the sharp peak of the JONSWAP spectrum. In Figure 7.14 the JONSWAP spectrum has a larger variance and thus significant wave height. In Figure 7.15 the JONSWAP spectrum and PM spectrum have the same variance and significant wave height but different modal periods.

⁶ Using T_1 in stead of ω_m it looks different

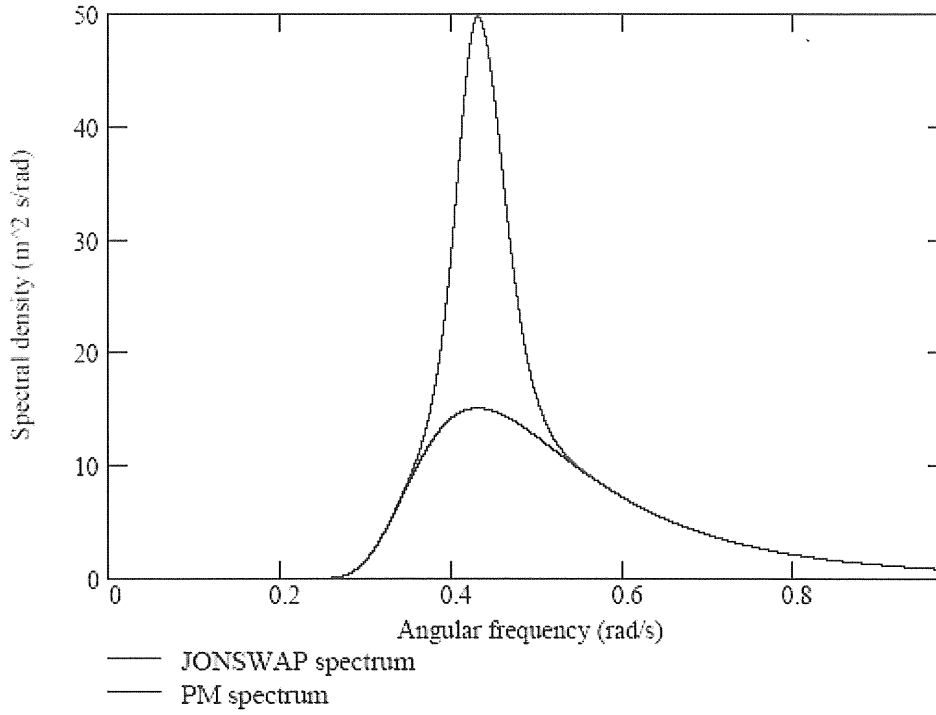


Figure 7.14 A JONSWAP spectrum and PM spectrum with the same modal frequency, $\omega_m = 0.878 \omega_b = 0.431$ rad/s.

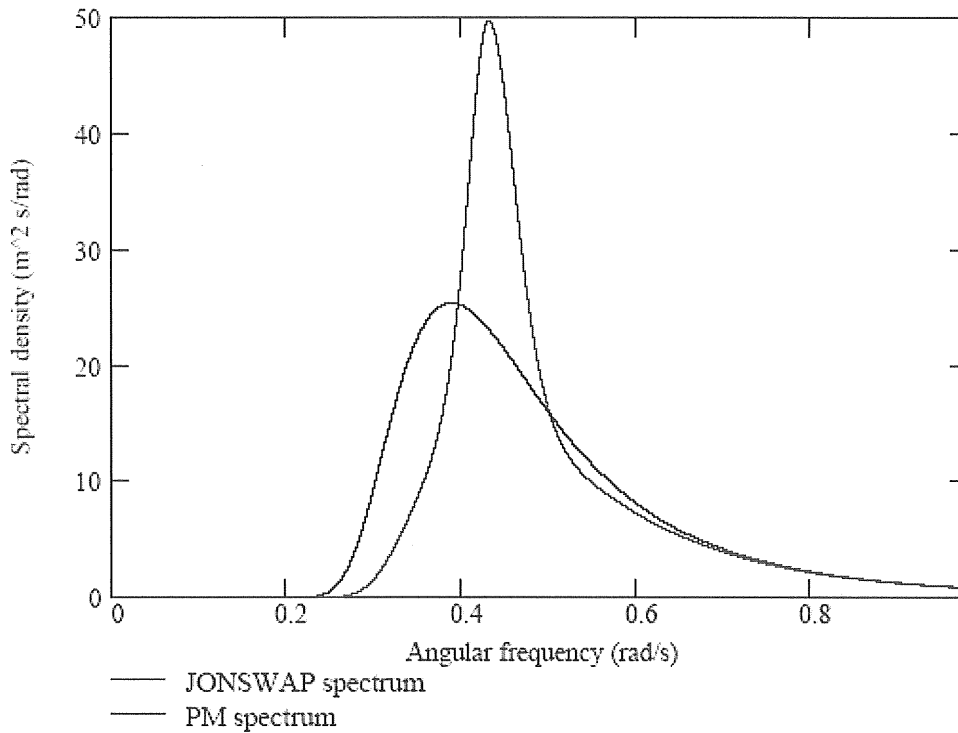


Figure 7.15 A JONSWAP spectrum and PM spectrum with the same significant wave height H_s .

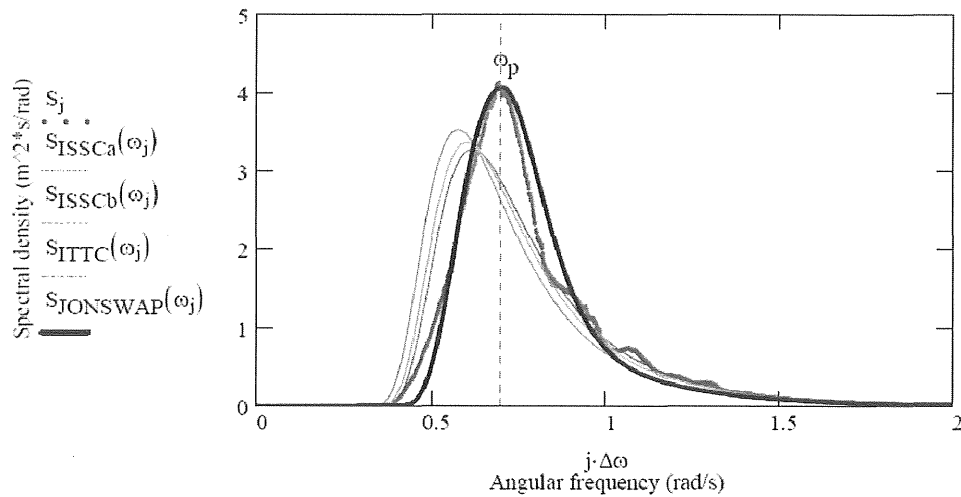


Figure 7.16 Fit of ISSCa, SISSCb, ITTC and JONSWAP spectra to the measured smooth spectrum (S_j) shown in Figure 7.12 using calculated T_{01} , T_{02} and H_s respectively for the first three and a manual fit of the five parameters of the JONSWAP spectrum.

In Figure 7.16 fits of standard spectra are shown to the measured smoothed spectrum (S_j) of Figure 7.12 using calculated T_{01} for the ISSCa spectrum, T_{02} for the SISSCb spectrum, H_s for the ITTC spectrum and a manual “best” fit of the five parameters of the JONSWAP spectrum. It is obvious that only the JONSWAP spectrum has enough parameters to make a good fit possible.

Sometimes a sea state is a result of superposition of local wind waves and swell from distant storms. Then the spectrum must have double peaks. Such spectra are the six parameter spectrum of Ochi and Hubble or the spectrum by Thorsethaugen. This will not be referred here.

Moments and wave characteristics

The wave characteristics like the significant wave height, mean period etc. are nowadays estimated indirectly from moments of the spectra and not from the time records. This yields more reproducible results. The spectral moments are defined as

$$m_n = \int_0^{\infty} \omega^n S(\omega) d\omega \quad \dots(7.25)$$

where n is an integer. A limitation with this is, however, that the fourth moment of the PM-family spectra including the JONSWAP spectrum is infinite, and for measured spectra depends on the resolution or measuring intervals. St Denis (1980, See PNA, 1989) proposes that the integration for m_4 is taken up to $5\omega_m$.

The 0th moment gives the variance, σ^2 , significant wave height, H_s , and root mean square wave height, H_{rms} , as

$$Var\{\zeta(t)\} = m_0 = \sigma^2 \quad \dots(7.26)$$

$$H_s \approx H_{m0} = 4\sqrt{m_0} = 4\sigma = \sqrt{2}H_{rms}, \quad \sigma = \sqrt{m_0} \approx H_s / 4 \quad \dots(7.27)$$

The *zero-crossing period*, T_z , is for a broad spectrum best estimated as

$$T_z \approx T_{01} = 2\pi m_0 / m_1 \quad \dots(7.28)$$

and for a more common narrower spectrum to

$$T_z \approx T_{02} = 2\pi\sqrt{m_0/m_2} \quad \dots(7.29)$$

Sometimes, in the context of the significant wave, the notion of significant wave-period is used. This is a little shorter than T_{01} .

The *crest period*, T_c , is estimated as

$$T_c \approx T_{24} = 2\pi\sqrt{m_2/m_4} \quad \dots(7.30)$$

The *spectral width* or *broadbandedness* is estimated by (Longuet-Higgins)

$$\epsilon^2 = 1 - \left(\frac{T_c}{T_z}\right)^2 \approx 1 - \left(\frac{T_{24}}{T_{02}}\right)^2 = 1 - \left(\frac{m_2^2}{m_0 m_4}\right) \quad \dots(7.31)$$

Another proposal was made by Mollison (1985):

$$\epsilon_0 = \sqrt{\frac{m_0 m_{-2}}{m_{-1}^2} - 1}$$

Mean period of component waves

$$T_{-1,0} = \frac{\int_0^\infty TS(\omega)d\omega}{\int_0^\infty S(\omega)d\omega} = \frac{\int_0^\infty \frac{2\pi}{\omega} S(\omega)d\omega}{\int_0^\infty S(\omega)d\omega} = \frac{2\pi \int_0^\infty \omega^{-1} S(\omega)d\omega}{\int_0^\infty S(\omega)d\omega} = 2\pi m_{-1} / m_0 \quad \dots(7.32)$$

Average wave length between zero up-crossings

$$\langle \lambda \rangle = \frac{g}{2\pi} T_z T_c \approx \frac{g}{2\pi} T_{02} T_{24} = 2\pi g \sqrt{m_0 / m_4} \quad \dots(7.33)$$

Variance of the slope of the wave surface

$$\left\langle \left(\frac{\partial \zeta}{\partial x} \right)^2 \right\rangle = m_4 / g^2 \quad \dots(7.34)$$

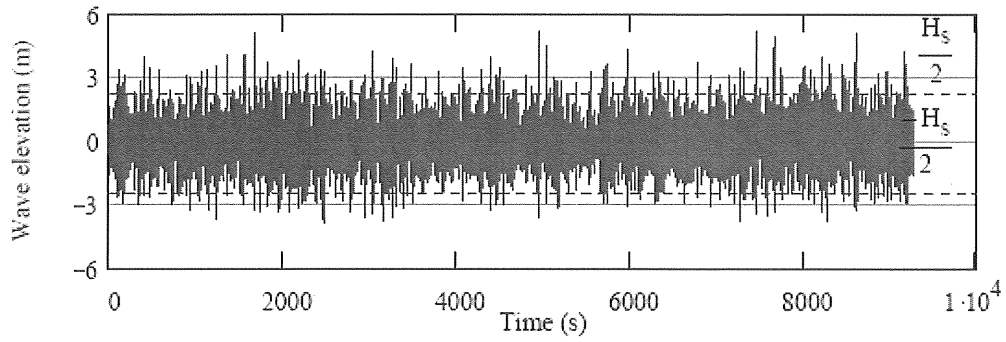


Figure 7.17 The sample wave elevation with $\pm \frac{1}{2}$ the significant wave $H_s \approx H_{m0}$ height for comparison.

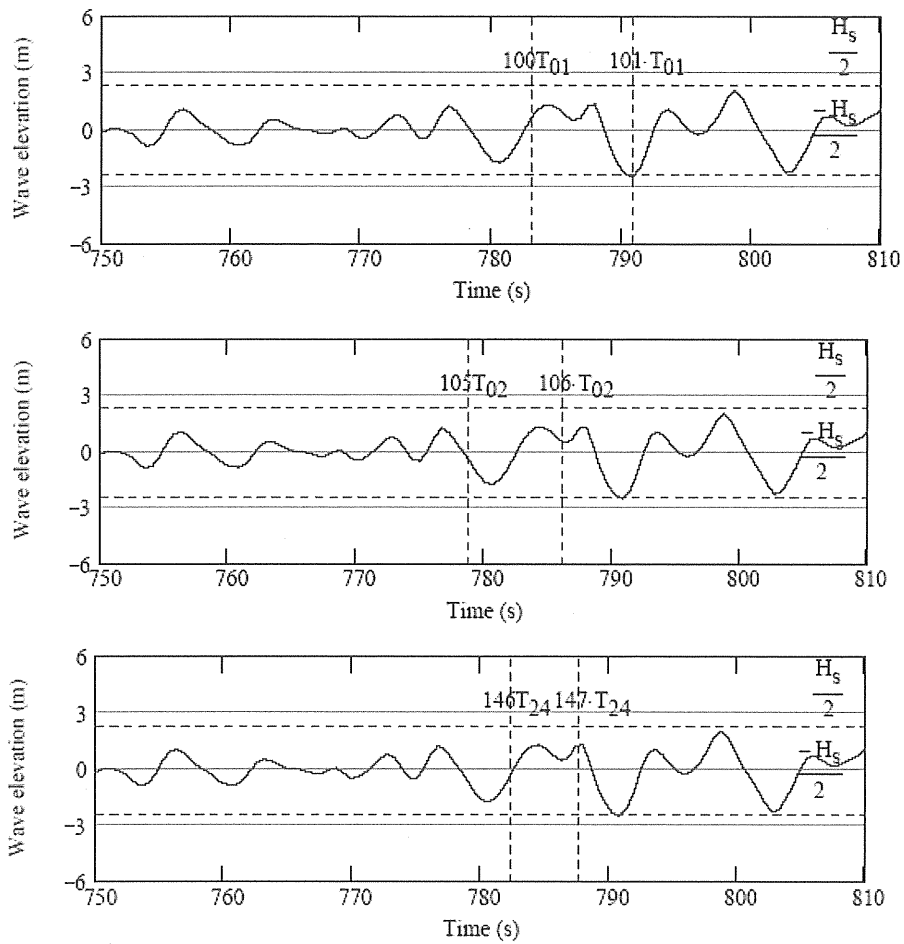


Figure 7.18 The sample wave elevation with characteristic periods estimated from its spectrum.

7.4 Synthesised Waves

The observation of a wavy lake or ocean surface reveals that the surface normally is pretty confused with significantly varying wave heights, periods and wavelengths, as well as waves progressing in various directions. By using a the spectral Fourier model described in the previous section, i.e. assuming that the wavy surface is built up by an addition (superposition) of linear waves one can describe records of such wavy surfaces and reproduce or synthesise them.

The water-surface elevation in a point x is then approximated by a sum

$$\zeta(t) = \sum_{i=1} a_i \cos(\omega_i t - k_i x + \varepsilon_i), \quad \dots(7.35)$$

where a_i , ω_i , k_i and ε_i are the amplitude, circular frequency, wave number and phase of the i^{th} component. A fundamental prerequisite for the waves to be modelled in such a way is that they should be part of a stationary process whose statistical properties may not change abruptly with time.

Further, the sum above is usually considered to be a Fourier series with orthogonal components on a finite time interval, e.g. $T_r = 20$ minutes. This has the consequence that the elevation is repeated exactly every time interval. The repeating time, T_r , implies the frequency division, $\Delta f = 1/T_r$. Now, choosing amplitudes of the components from some established standard spectrum and assigning random phases distributed evenly between 0 and 2π radians (Figure 7.18), a synthetic irregular wave can be formed. In Figure 7.17 to Figure 7.19, the steps leading to such a wave is illustrated. We have used a PM spectrum.

The amplitudes are normally chosen as

$$a_i = \sqrt{2S(\omega_i)\Delta\omega}, \quad \dots(7.36)$$

which will produce a discrete spectrum of the same shape as the original PM spectrum, Figure 7.19. The choice can be criticised because it does not produce a realistic amplitude spectrum as the one in Figure 7.7, and consequently the randomness of the resulting synthesised record will be too small. Instead random amplitudes from a Gaussian distribution with mean, a_i , and standard deviation $\sqrt{1/2}a_i$ should be used according to (Tucker, 1984^{xxxiv})

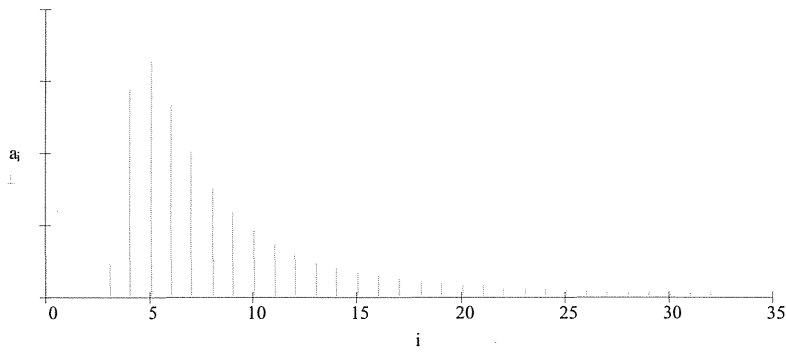


Fig. 7.19 Thirty-two component amplitudes chosen by help of a PM spectrum

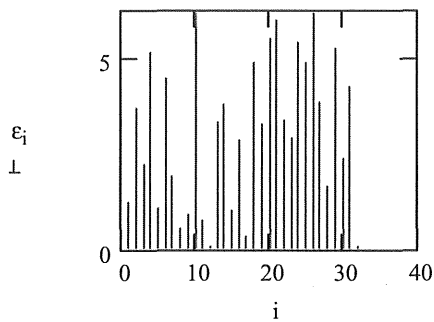


Fig. 7.20 Thirty-two random component phase angles between 0 and 2π radians

The assigned amplitudes and phase angles inserted into equation (7.35) will then produce the wave “record” shown in Figure 7.21, where the randomness seem to be OK within each time interval, T_R . The simulated synthetic wave is shown to repeat itself, which is a consequence of using components evenly distributed over the frequency range with the division Δf . In fact the repetition time $T_R = 1/\Delta f$, and *vice versa* if T_R is the length of a record or observation the highest frequency resolution would be $\Delta f = 1/T_R$. (See Bendat and Piersol, 1986)

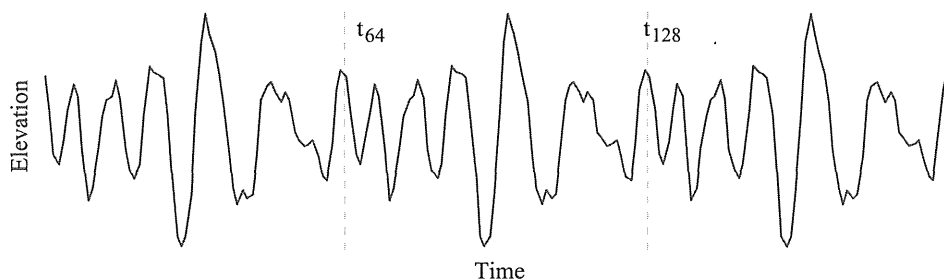


Fig. 7.21 Simulated water surface elevation. Note the repeated pattern.

Directional sea

The spectral model can be extended to include wave components propagating in different directions by

$$\zeta(x, y, t) = \sum_{i=1}^N \sum_{j=1}^K a_{ij} \cos[k_i(x \cos \theta_j + y \sin \theta_j) - \omega_i t + \varepsilon_{ij}], \quad \dots(7.37)$$

with

$$a_i = \sum_{j=1}^K a_{ij} . \quad \dots(7.38)$$

where θ_j is the angle between the x-axis and the direction of propagation of the component.

The variance of the directional waves are distributed according to some spreading function, $D(\theta)$, fulfilling the demand that the integral around the horizon

$$\int_0^{2\pi} D(\theta) d\theta = 1 , \quad \dots(7.39)$$

so that the directional spectrum becomes

$$S(\omega, \theta) = S(\omega)D(\theta) , \quad \dots(7.40)$$

Usually the spread is restricted to $\pm 90^\circ$ around the main direction of propagation.

The simplest spreading functions are independent of the wave frequency, and a commonly used one is the cosine square distribution

$$D(\theta) = \begin{cases} \frac{2}{\pi} \cos^2 \theta, & |\theta| < \pi / 2 \\ 0 & |\theta| > \pi / 2 \end{cases} . \quad \dots(7.41)$$

See Figure 7.22.

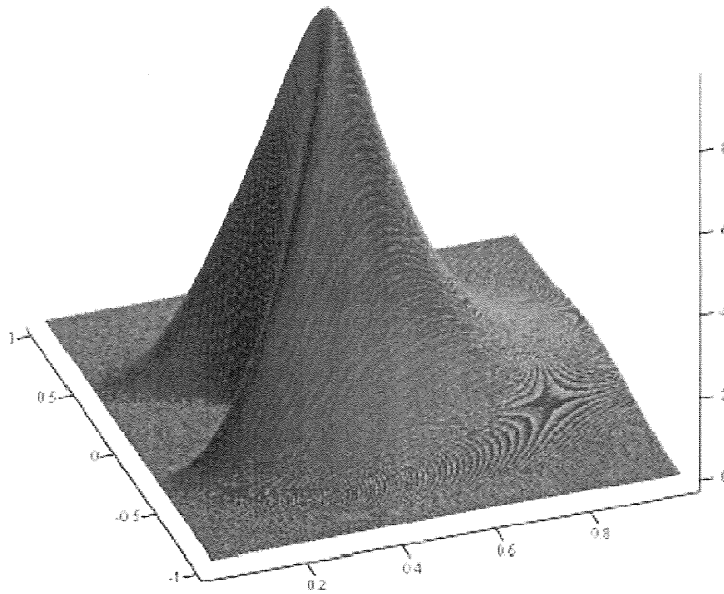


Fig. 7.22 A 3D wire plot of a \cos^2 PM spectrum.

Real waves exhibit a more complicated pattern with longer, long-period waves having less directionality than shorter, short period waves. One directionality function taking care of that is the SWOP distribution (Pierson et al., 1960):

$$D(\theta) = \begin{cases} \frac{1}{\pi} (1 + (0.5 + 0.82R)\cos(2\theta) + 0.32R \cos(4\theta)), & |\theta| < \pi/2 \\ 0 & |\theta| > \pi/2 \end{cases} \dots(7.41)$$

with $R = \exp(-0.5(\omega U_{19.5} / g)^4)$ and
 $U_{19.5}$ the wind speed at 19.5 m height.

Often the directionality of the sea is ignored, especially for severe sea states as the directionality then is smaller.

7.5 Short Term Statistics

The water level in an irregular wave as a function of time constitutes a stochastic process. We will show that its variation around the still water level is a Gaussian process with zero mean, as a result of the addition of many harmonic components $\zeta_i(t)$ with uniformly distributed phase angles ε_i .

$$\zeta_i(t) = a_i \cos(\omega_i t + \varepsilon_i), \dots(7.42)$$

The means of these component processes are all zero;

$$\mu_i = \frac{1}{T} \int_0^T \zeta_i(t) dt = \frac{1}{T} \int_0^T a_i \cos(\omega_i t + \varepsilon_i) dt = 0, \dots(7.43)$$

and the variances around the means are;

$$Var(\zeta_i(t)) = \sigma_i^2 = \frac{1}{T} \int_0^T (\zeta_i(t))^2 dt = \frac{1}{T} \int_0^T (a_i \cos(\omega_i t + \varepsilon_i))^2 dt = \frac{1}{2} a_i^2 \dots (7.44)$$

The distribution of one harmonic component

If the phase angle ε_i of $\zeta_i(t)$ is randomly distributed on the interval $[0, 2\pi)$ then, according to a theorem in statistics, its frequency function is

$$p(\zeta_i(t)) = p(\varepsilon_i) \frac{d\varepsilon_i}{d\zeta_i} \dots (7.45)$$

If further ε_i is uniformly distributed on the interval

$$p(\varepsilon_i) = \frac{1}{2\pi} \dots (7.46)$$

Solving ε_i from Equation (7.42)

$$\varepsilon_i = \arccos\left(\frac{\zeta_i}{a_i}\right) - \omega_i t \dots (7.47)$$

and thus

$$\frac{d\varepsilon_i}{d\zeta_i} = \frac{1}{\sqrt{a_i^2 - \zeta_i^2}} \dots (7.48)$$

which, however, only is defined on the interval $[0, \pi)$ and therefore $p(\varepsilon_i)$ has to be doubled on this interval. Finally substituting Equations (7.46) to (7.47) into (7.48) the frequency distribution of ζ_i is

$$p(\zeta_i) = \frac{1}{\pi \sqrt{a_i^2 - \zeta_i^2}} \quad -a_i \leq \zeta_i \leq a_i \dots (7.49)$$

This frequency function is shown in Figure 7.23 and its distribution function in Figure 7.24. In the same figures also the corresponding functions of a Gaussian process with the same mean and standard deviation are shown. One can note that the frequency function is far from similar to the Gaussian frequency function, while the distribution functions are more similar.

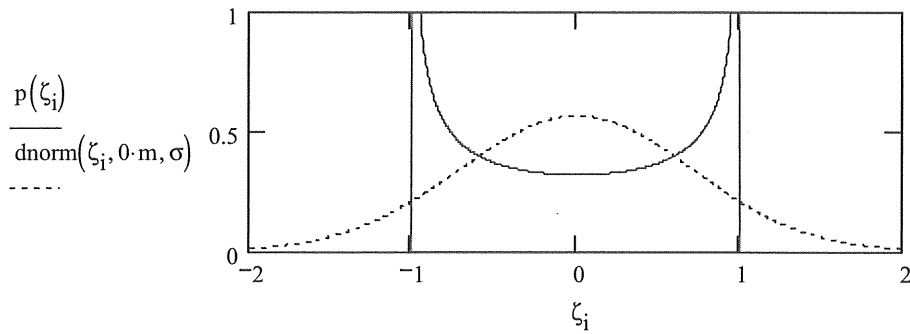


Figure 7.23 Comparison between the frequency distribution of the level of a harmonic function and the frequency distribution of a Gaussian process with the same standard deviation

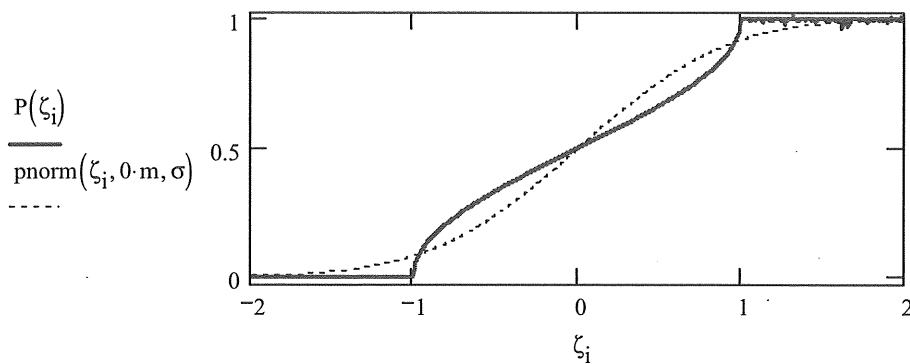


Figure 7.24 Comparison between the accumulative distribution of the level of a harmonic function and the accumulative distribution of a Gaussian process with the same standard deviation

The mean of the frequency-distribution function is

$$\mu_i = \int_{-a_i}^{a_i} \zeta_i p(\zeta_i) d\zeta_i = 0 \quad \dots(7.50)$$

and its variance

$$\sigma_i^2 = \int_{-a_i}^{a_i} \zeta_i^2 p(\zeta_i) d\zeta_i = \frac{1}{2} a_i^2 \quad \dots(7.51)$$

which, of course are the same as for the time function itself.

The distribution of the water level in an irregular wave

The water level variation around the mean can, as stated before, be written as a sum of cosine functions with varying frequencies, ω_i , and random phase angles, ε_i .

$$\zeta(t) = \sum_i \zeta_i(t) = \sum_i a_i \cos(\omega_i t + \varepsilon_i). \quad \dots(7.52)$$

Each component is a stochastic variable with mean, μ_i , and variance, σ_i^2 . Then, according to the central limit theorem the sum of many components, $\sum_i \zeta_i(t)$, approaches a Gaussian process with the mean

$$\mu = \sum_i \mu_i = 0 \quad \dots(7.53)$$

and the variance

$$\sigma^2 = \sum_i \sigma_i^2 = \sum_i \frac{1}{2} a_i^2 = m_0, \quad \dots(7.54)$$

where m_0 is the area under the wave spectrum or 0th moment and σ the standard deviation.

Thus the water level in an irregular wave is Gaussian distributed with the frequency function

$$p(\zeta) = \frac{1}{\sigma\sqrt{2\pi}} e^{-\zeta^2/(2\sigma^2)} = \frac{1}{\sqrt{2\pi m_0}} e^{-\zeta^2/(2m_0)}. \quad \dots(7.55)$$

This is also the case for all derived responses.

Using this knowledge of the stochastic Gaussian process in a sea state, e.g. the fraction of time during which the water level is above a certain level can be estimated, the fraction of time green water is flowing in over the deck or the fraction of time the ship bottom is above the water surface.

Example

How large part of the time will the surface level be above 1 m around a platform leg in a sea state with the significant wave height, $H_s = 3$ m?

Solution

Assuming the duration of the sea state is T and the sum of all times the water level is above $\zeta = 1$ m is t the fraction of time is

$$\frac{t}{T} = P(\zeta > 1 \text{ m}) = \int_{1 \text{ m}}^{\infty} \frac{1}{\sigma\sqrt{2\pi}} e^{-\zeta^2/(2\sigma^2)} d\zeta = \frac{1}{\sqrt{2\pi m_0}} \int_{1 \text{ m}}^{\infty} e^{-\zeta^2/(2m_0)} d\zeta. \quad \dots(7.56)$$

As $H_s = 4\sqrt{m_0}$ and $\sigma = H_s/4$ Equation (7.56) will give 0.0912 e.g. by help of the standard normal distribution with $(1 \text{ m})/\sigma = 1.33$ as found in table in Standard Mathematical Tables:

$$1 - F(1.33) = P(\zeta > 1 \text{ m}) = 0.0912 \text{ or } 9 \% \text{ of the time}$$

or by an inbuilt function in Mathcad:

$$1 - \text{cnorm} \frac{1}{0.75} = 0.0912$$

7.6 Extremes in a Sea State

For a reasonably narrow-banded Gaussian sea state the probability density for the level of wave crests or local maxima, ζ_{\max} , is approximately Rayleigh distributed with the frequency function

$$p(\zeta_{\max}) = \frac{\zeta_{\max}}{m_0} e^{-(\zeta_{\max}^2 / (2m_0))}, \quad \dots(7.57)$$

which has the variance of the sea surface elevation or 0th moment of the spectrum as its sole parameter. This expression can be used for maxima of all other derived processes too.

The probability density for the wave heights, H , is also approximately Rayleigh distributed with the frequency function

$$p(H) = \frac{H}{4m_0} e^{-(H^2 / (8m_0))}. \quad \dots(7.58)$$

Its distribution function or probability that the wave height $H < H_q$ is then

$$P(H < H_q) = \int_0^{H_q} \frac{H}{4m_0} e^{-(H^2 / (8m_0))} dH = 1 - e^{-(H_q^2 / (8m_0))} \quad \dots(7.59)$$

The probability Q that the wave height should be higher than H_q is then

$$Q(H > H_q) = 1 - P(H < H_q) = e^{-(H_q^2 / (8m_0))} \quad \dots(7.60)$$

From this follows that the wave H_q that is exceeded with the probability Q is

$$H_q = \sqrt{8m_0 \ln(1/Q)}. \quad \dots(7.61)$$

Example

How many waves will be greater than 5 m during 6 hours in a sea state with the significant wave height, $H_s = 3$ m and mean wave period 10 s?

Solution

The number of waves during 6 hours is

$$N = \frac{6 \cdot 3600 \text{ s}}{10 \text{ s}} = 2160$$

The relative number of waves exceeding $H_q = 5$ m of these is, with $16m_0 = H_s^2$

$$Q(H > H_q) = e^{-(H_q^2 / (H_s^2 / 2))} = e^{-(5^2 / (3^2 / 2))} = e^{-2(5/3)^2} = 0.00387$$

The number of waves n_q larger than 6 m is finally

$$n_q = QN = 8.35 \approx 8$$

Of course one cannot expect that the number of waves larger than 5 m should be just 8 in all such sea states, but the number should be seen as an expected number in such sea states. Many sea states should give the arithmetic mean around 8.4.

According to the given example an approximate value of Q is:

$$Q = n_q / N \quad \dots(7.62)$$

and consequently

$$H_q = \sqrt{8m_0 \ln(N/n_q)} \quad \dots(7.63)$$

is the wave height that is exceeded n_q times of N waves.

Extreme wave height

The expected value of the wave height that is exceeded once of N waves is then

$$H_{\max} = \sqrt{8m_0 \ln(N)} \quad \dots(7.64)$$

because this probability is approximately $Q_N = 1/N$.

The wave height that is exceeded by 10, 1, 0.1 and 0.01 % of the number of waves in a sea state can also be assessed by Equation (7.61) and are sometimes given in literature as references. See Table below

| Q (%) | $H_q / \sqrt{m_0}$ | H_q / H_{rms} | H_q / H_s |
|-------|--------------------|-----------------|-------------|
| 10 | 4.29 | 1.52 | 1.07 |
| 1 | 6.07 | 2.15 | 1.52 |
| 0.1 | 7.43 | 2.62 | 1.86 |
| 0.01 | 8.58 | 3.03 | 2.15 |

The maximum wave, H_{\max} , in a sea state is often given as the most probable maximum wave height of a thousand waves, that is, corresponding to 0.1 % above. In a sea state with the mean period 10 s this corresponds to a duration of 10 000 s or 2.8 hours. In a certain sea state the largest wave can of course be higher or lower but the mean of many measurements or simulations should be $1.86H_s$.

The same methods for estimating periods, variances and extremes, that have been used for the waves in this chapter can be applied to all derived motions, accelerations, loads, etc.

8 WAVE STATISTICS

Up till now we have only discussed how to describe sea states and the statistical properties of the water surface elevation in these. This is often called short-term statistics. However, to be able to design structures and ships, we need know the probability of the appearance of sea states of different wave heights and periods or the probability of extreme individual waves during the expected life time of the structures. This is often called long-term statistics. Founded on the long-term statistics, the probability of extreme loads on fixed stiff structures, and extreme responses of flexible structures or floating bodies. For a flexible or floating structure it is not certain that the “worst sea state” or the “worst wave” will give the largest stress or motion. The response probabilities are also of interest for estimation of fatigue, downtime of floating offshore production or drilling platforms, frequency of green water, slamming, accelerations etc. for ships.

A basic term used in design codes and guidelines is the return period or recurrence interval. It is an estimate of the mean interval of time between events like an earthquake, flood or river discharge flow of a certain intensity or size. It is a statistical measurement denoting the average recurrence interval over an extended period of time, and is usually required for risk analysis (i.e. whether a project should be allowed to go forward in a zone of a certain risk) and also to dimension structures so that they are capable of withstanding an event of a certain return period (with its associated intensity of a design quantity. (Wikipedia Nov 2008)

In the guidelines concerning loads and load effects on load-bearing structures in the petroleum activity in Norwegian waters (Norwegian Petroleum Directorate, 1992^{xxxv}) it is stated that one should use a design sea state given by a JONSWAP spectrum with one-hundred-year-return significant wave height, $H_{m0}^{100,yr}$, combined with the peak period, $T_p^{100,yr}$, or other spectra with larger probability and other shape if such spectra give larger load effects. There is also an option to use a one-hundred-year design wave, $H_{max}^{100,yr} = 1.9H_{m0}^{100,yr}$ combined with the period $T_{max}^{100,yr} = 0.92T_p^{100,yr}$. For floating structures, especially, the wave period should be varied in order to investigate the responses for shorter waves with maximum steepness. The factor 1.9 above is founded on the assumption that the duration of the sea state is taken as 3 h. One can note that the 100 year maximum wave height derived in this way is a little smaller than if the maximum probable wave height is taken as the most probable largest of all individual waves. Compare results in Table 8.9 and Table 8.11 for the North Atlantic.

In Paragraph 8.1 we discuss the concept of risk. Paragraph 8.2 is a short account of design with safety factors versus with load and material coefficients. Then in Paragraph 8.3 follows long-term statistics of waves.

8.1 The Concept of Risk

Before we look at the limit states for design we will acquaint ourselves with the concept of risk. A hazard is a source of danger but does not contain any likelihood or actual impact it will have on people, environment or economics. Risk combines both likelihood and impact, and “a risk analysis tries to answer the questions:

- (i) What can happen?

- (ii) How likely is it to happen?
- (iii) Given that it occurs, what are the consequences?''xxxvi

Risk can then be expressed as a combination of the probability, E , of the event and its consequence. Some authors simply give the risk, R , as the product of the probability, E , and some measure of the consequence, C , i.e. $R = EC$. The consequence can be e.g. the number of killed or wounded people due to the undesired event or the economic cost i.e. lost income, repair cost etc. In the latter case R can be named the risk cost. See Graham, 1995^{xxxvii} for a more thorough discussion.

Design event at given risk

Denote the probability that an event with the return period, T_R , shall occur or be exceeded a certain year by Q . An estimate of this probability is $Q = 1/T_R$. The probability for not exceeding is then $P = 1 - Q$ in average per year, and the probability for the event not to be exceeded any year during a lifetime, L , of the design object is the product of the probabilities for each year i.e.:

$$P(\text{no year}) = (1 - Q)^L \quad \dots(8.1)$$

and consequently the probability, E , that it would be exceeded at least once during the L years:

$$E = P(\text{at least once}) = 1 - (1 - Q)^L = 1 - (1 - \frac{1}{T_R})^L \quad \dots(8.2)$$

This function is shown in Table 8.1 below. For $L = T_R$ it asymptotically approaches $1 - e^{-1} = 0.632$ when T_R increases. The probability, E , for exceeding the hundred-year wave is thus 63 % in 100 years.

Table 8.1 The probability, E , of an event with the return period T_R (years) to be exceeded at least once during the lifetime L (years)

| L (yrs) T_R (yrs) | 1 | 5 | 10 | 50 | 100 | 500 | 1000 | 5000 | 10000 |
|--------------------------|-------|--------------------|-------|-------|-------|-------|-------|-------|-------|
| 1 | 1 | 1 | 1 | 1 | 1 | 1 | 1 | 1 | 1 |
| 5 | 0.2 | 0.672 | 0.893 | 1 | 1 | 1 | 1 | 1 | 1 |
| 10 | 0.1 | 0.41 | 0.651 | 0.995 | 1 | 1 | 1 | 1 | 1 |
| 50 | 0.02 | 0.096 | 0.183 | 0.636 | 0.867 | 1 | 1 | 1 | 1 |
| 100 | 0.01 | 0.049 | 0.096 | 0.395 | 0.634 | 0.993 | 1 | 1 | 1 |
| 500 | 0.002 | 0.01 | 0.02 | 0.095 | 0.181 | 0.632 | 0.865 | 1 | 1 |
| 1000 | 0.001 | 0.005 | 0.01 | 0.049 | 0.095 | 0.394 | 0.632 | 0.993 | 1 |
| 5000 | 2E-4 | 0.001 | 0.002 | 0.01 | 0.02 | 0.095 | 0.181 | 0.632 | 0.865 |
| 10000 | 1E-4 | 5·10 ⁻⁴ | 0.001 | 0.005 | 0.01 | 0.049 | 0.095 | 0.393 | 0.632 |

Example

In many rules it is stated that the weighted probability per year of a combination of design events should be 10^{-4} . This means a return period of 10 000 years. One can then ask: How large is the risk, E , that it would occur during a lifetime of 50 years.

Solution: For $T_R = 10\ 000$ years and $L = 50$ years the table gives $E = 0.005 = 0.5\%$.

One can invert the problem and ask: If you accept a risk, E , during a lifetime, which return period should be used? This can be solved from Equation (8.2)

$$T_R = [1 - (1 - E)^{1/L}]^{-1} \quad \dots(8.3)$$

Example

A risk, E , of 1 % is accepted for a design event to be exceeded in the lifetime 50 years. Which return period should be used?

Solution: For $E = 0.01 = 10^{-2}$ and $L = 50$ the Table 8.1 gives $T_R = 5\ 000$ years or 4975 from Equation (8.3).

Observe that the real risk of damage certainly is different, as one uses safety factors or load and material coefficients at the design to safeguard the limitation in knowledge of statistical distributions of events, loads, load effects, material properties as well as the quality of construction work. Finally it is actually so that damage often appears due to unforeseen types of events and human mistakes.

8.2 Design Approaches

There are typically two approaches for designs. One is to use *safety factors* i.e. to calculate the load effect, e.g. a stress, for given design loads and compare the load effect with a given criteria, e.g. the breaking strength, divided by a safety factor $S > 1$ depending of construction loads etc. The other is to use a safety format with *load and material coefficients* and assign coefficients $\gamma_f > 1$ to each load, and material coefficients $\gamma_m < 1$ to each component. Then check that the total load effect calculated with the load coefficients is smaller than the design capacity calculated with the material coefficients.

Design with Safety Factors

In many rules e.g. from DnV^{xxxviii}, the British Health and Safety Executive^{xxxix}, the Norwegian Marine Directorate^{xl}, design with safety factors are applied. Then the safety factor or ratio, S , between permissible load effect, R , and calculated load effect, F , exceed certain minimum values for specified load cases. Examples of load effects are motions, clearance distance or tension.

As an example of safety factors in Table 8.2 the safety factors for the forces in mooring lines according to DnV's POSMOOR rules for floating units not placed close to other installations.

Table 8.2 Safety factors According to DnV's mooring rules for mobile offshore units (POSMOOR)

| Operation condition | | Quasi-static analysis | Dynamic analysis |
|---------------------|---|-----------------------|------------------|
| | | POSMOOR | POSMOOR |
| Survival | Intact system | 1.80 | 1.50 |
| | Transient motion after single-line failure | 1.10 | 1.00 |
| | Temporary mooring after single-line failure | 1.25 | 1.10 |
| Operation | Intact system | 2.70 | 2.30 |
| | Transient motion after single-line failure | 1.40 | 1.20 |
| | Temporary mooring after single-line failure | 1.80 | 1.50 |

The extreme weather condition to be considered is the most unfavourable of

- 1) 10 min average wind speed and sea state corresponding to a 100-year return period combined with a 10 year-return-period current.
- 2) Current velocity and sea state with 100-year return period combined with a 10 min average wind speed with a 10-year-return period

Safety format with load and material coefficients

The general requirement to achieve sufficient safety is that the design load effect, S_d , not exceed the design capacity, R_d :

$$S_d \leq R_d \quad \dots(8.4)$$

The equality, $S_d = R_d$, defines a limit state.

The design load is normally formed by the product of a characteristic load, F_k , and a load coefficient, γ . The load effect, S , is a function of the design load, so that adding the load effects (in a linear system) you get the design load effect as:

$$S_d = \sum S(\gamma F_k) \quad \dots(8.5)$$

The characteristic loads shall be established for each load category, Table 8.3, and limit state, Table 8.4

Table 8.3 Load categories:

| | | |
|---|---------------------------|--|
| P | Permanent load | |
| L | Variable functional loads | Payload, ballast, mooring etc. |
| D | Deformation load | incl. pretension, temperature, subsidence |
| E | Environmental loads | wind, waves, currents, tides, varying water levels, ice and snow |
| A | Accidental loads | fire, collision by ships, breakage of mooring line, flooding of flotation body or hull compartment |

Table 8.4 Limit states

| | |
|-----|---------------------------------------|
| ULS | Ultimate Limit State |
| FLS | Fatigue Limit State |
| ALS | Progressive or Accidental Limit State |
| SLS | Serviceability Limit State |

Load effects can be:

- Motion
- Acceleration
- Stress
- Deformation

An example of is given in Table 8.5.

Table 8.5 Load coefficients, γ_f , and their combinations in the ultimate limit state, ULS, According to DnV's tentative rules for fish farms.

| The most unfavourable load combination of a) and b) below shall be applied | | Load categories | | | |
|---|----|-----------------|-----|-----|------|
| | | P | L | D | E |
| Combination of design loads | a) | 1.3 | 1.3 | 1.0 | 0.7 |
| | b) | 1.0 | 1.0 | 1.0 | 1.3* |
| * For unmanned floaters this coefficient can be taken as 1.15. For permanent loads the coefficient shall be taken as 1.0 if this is less favourable. The coefficients should be the same for the whole structure. | | | | | |

In the accidental limit state, ALS, all load coefficients are set to 1.0.

Characteristic loads:

The environmental loads for ULS and ALS shall have a yearly probability of 0.01 or less.

The fatigue limit state

The fatigue limit state, FLS, shall be investigated. All load coefficients are set to 1.0.

Example of material coefficients are given in Table 8.6

Table 8.6 Material coefficients γ_m

| Limit state | Steel structures | Concrete struct. | | Chain | Wire rope | Synthetic rope |
|-------------|------------------|------------------|--------|-------|-----------|----------------|
| | | Concr. | Reinf. | | | |
| ULS | 1.15 | 1.40 | 1.25 | 1.5 | 1.3 | 3.0(2.5)* |
| FLS | 1.00 | 1.20 | 1.10 | | | |
| ALS | 1.00 | 1.20 | 1.10 | 1.3 | 1.15 | 2.5(1.3)* |
| SLS | 1.00 | 1.00 | 1.00 | | | |

* Coefficients within brackets apply if there is satisfying documentation of the rope

8.3 Long term wave statistics

Wave statistics

In Chapter 7 we treated the statistical distribution of wave heights within a sea state and found that these wave heights were Rayleigh-distributed with the frequency distribution

$$p(H) = \frac{H}{4m_0} e^{-(H^2/(8m_0))}, \quad \dots(7.58)$$

if the water level constitutes a stationary Gaussian process.

In the context of this chapter it would be practical to exchange the parameter m_0 for H_s using $H_s = 4\sqrt{m_0}$ so that

$$p(H) = \frac{4H}{H_s^2} e^{-2(H/H_s)^2}. \quad \dots(8.6)$$

The significant wave height varies in its turn between the recorded sea states represented by point measurements of water elevations. Often the measurements are performed at regular intervals and recorded and analysed for a set period of time, during which it is assumed that the sea state is stationary. Often measurements are done for 20 minutes every three hours, but as computer capacity increases it may be done more often, although the period of analysis should not contain large changes in significant wave height or mean period invalidating the stationary assumption.

Table 8.7 Scatter diagram from the North Atlantic, Area 16, All directions: From Hogben et al. (1986)^{xli}, with the change that 1 % observations are added for 10-11 m at 12-13 s to make the table sum 1000 ‰. The sum column and row column denoted Hogben are taken directly from Hogbens table, while the other sum column and row column are results of summing the figures in the table.

| $T_z(s)$ $H_s(m)\backslash$ | <4 | 4-5 | 5-6 | 6-7 | 7-8 | 8-9 | 9-10 | 10-11 | 11-12 | 12-13 | >13 | Hogben | Row sum | Cumulated sum |
|--------------------------------|----|-----|-----|-----|-----|-----|------|-------|-------|-------|--------------|-------------|-------------|---------------|
| <1 | 0 | 2 | 13 | 22 | 14 | 5 | 1 | 0 | 0 | 0 | | 57 | 57 | 57 |
| 1-2 | 0 | 0 | 11 | 53 | 78 | 51 | 18 | 4 | 1 | 0 | | 218 | 216 | 273 |
| 2-3 | 0 | 0 | 4 | 31 | 77 | 80 | 44 | 15 | 4 | 1 | | 255 | 256 | 529 |
| 3-4 | 0 | 0 | 1 | 13 | 45 | 64 | 47 | 21 | 6 | 2 | | 197 | 199 | 728 |
| 4-5 | 0 | 0 | 0 | 4 | 21 | 37 | 34 | 18 | 7 | 2 | | 124 | 123 | 851 |
| 5-6 | 0 | 0 | 0 | 1 | 9 | 19 | 20 | 13 | 6 | 2 | | 70 | 70 | 921 |
| 6-7 | 0 | 0 | 0 | 1 | 3 | 9 | 11 | 8 | 4 | 1 | | 37 | 37 | 958 |
| 7-8 | 0 | 0 | 0 | 0 | 1 | 4 | 6 | 5 | 3 | 1 | | 20 | 20 | 978 |
| 8-9 | 0 | 0 | 0 | 0 | 1 | 2 | 3 | 3 | 2 | 1 | | 11 | 12 | 990 |
| 9-10 | 0 | 0 | 0 | 0 | 0 | 1 | 2 | 1 | 1 | 0 | | 6 | 5 | 995 |
| 10-11 | 0 | 0 | 0 | 0 | 0 | 0 | 1 | 1 | 1 | 0 | | 3 | 3 | 998 |
| 11-12 | 0 | 0 | 0 | 0 | 0 | 0 | 0 | 1 | 0 | 0 | | 2 | 1 | 999 |
| 12-13 | 0 | 0 | 0 | 0 | 0 | 0 | 0 | (1) | 0 | 0 | | 1 | 1 | 1000 |
| 13-14 | 0 | 0 | 0 | 0 | 0 | 0 | 0 | 0 | 0 | 0 | | 1 | 0 | |
| >14 | 0 | 0 | 0 | 0 | 0 | 0 | 0 | 0 | 0 | 0 | | 1 | 0 | |
| | | | | | | | | | | | Total | 1003 | 1000 | |
| Hogben | 0 | 3 | 28 | 124 | 249 | 271 | 186 | 90 | 34 | 10 | 3 | | 998 | |
| Column sum | 0 | 2 | 29 | 125 | 249 | 272 | 187 | 91 | 35 | 10 | | | 1000 | |

Probability distributions of significant wave heights

The statistical distribution of the significant wave height can often be approximated by a two-parameter Weibull distribution

$$P(H_s > x) = e^{-(x/H_c)^\gamma} \quad \dots(8.7)$$

where H_c and γ are parameters that must be derived from measured significant wave heights, H_s .

As an example in Table 8.7 a joint frequency table of significant wave height and zero-crossing period or “scatter diagram” for the North Atlantic is given. The table is taken from the publication by Hogben et al. (1986), the most comprehensive publication of wave data covering 104 ocean areas, denoted Marsden areas. Jensen (2001) discusses the limitation and use of this data.

In order to fit the Weibull distribution, equation (8.7), to the measurements of the North Atlantic in Table 8.7 one can plot the cumulated sums from the table in a Weibull paper, which is constructed such that a perfect distribution plots as a straight line⁷, and then fit a line by linear regression. The wave height classes are divided in $\Delta H_s = 1$ m intervals. The sample probability of H_s being smaller than upper class limits is plotted as

$$P_i = P(H_s < i\Delta H_s) = \frac{\sum_{j=1}^i n_j}{N+1} \quad \text{or} \quad P(H_s > i\Delta H_s) = 1 - P_i \quad \dots(8.8)$$

where n_j is the number of observations Class j out of the total number N . N is here arbitrarily set to 1000 in conformity with Table 8.8.

In Figure 8.1 the sample probabilities, $1 - P_i$, Equation (8.8) and the fitted distribution Equation (8.7) with $\gamma = 1.74$ and $H_c = 3.94$ m are plotted.

⁷ One can write Equation (8.7) $\ln(P(H_s)) = -(H_s/H_c)^\gamma$, then $\ln(-\ln(P(H_s))) = \gamma(\ln(H_s) - \ln(H_c))$ which is a straight line of the form $y = kx+l$ in Figure 8.1 with slope $k = \gamma$ and gives $x = \ln(H_c)$ for $y = \ln(-\ln(P(H_s))) = 0$.

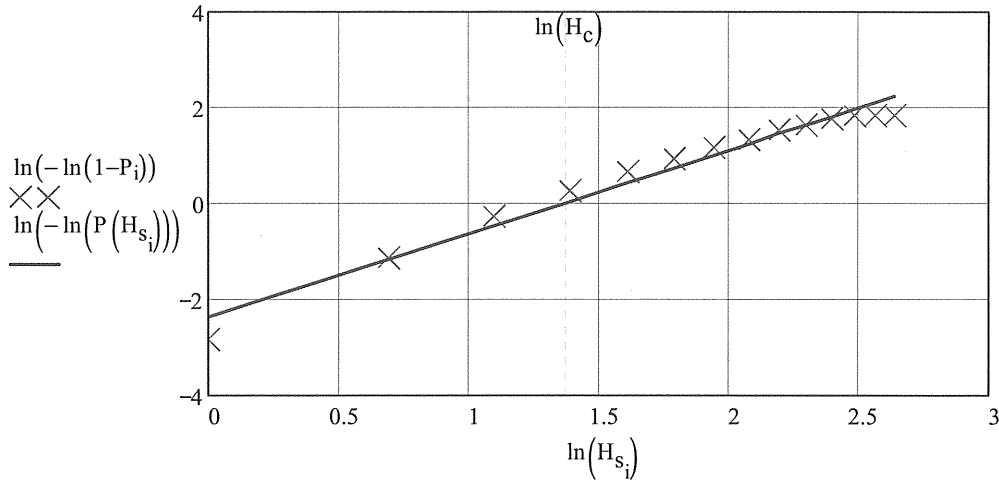


Figure 8.1 Sample probability distribution P_i and fitted Weibull distribution.

Table 8.8 Sample probabilities of $P(H_s < x) = 1 - P(H_s > x) = 1 - e^{-(x/H_c)^\gamma}$ constructed from Table 8.7 and Equation 8.8.

| Wave height classes $H_s(m) \setminus$ | Class No i | Permille of observations in each class (%) | Permille of observations below upper limit of each class (%) | Probability of H_s being smaller than upper class limit $P_i = P(H_s < i\Delta H_s)$ |
|--|--------------|--|--|--|
| <1 | 1 | 57 | 57 | 0.057 |
| 1-2 | 2 | 216 | 273 | 0.273 |
| 2-3 | 3 | 256 | 529 | 0.529 |
| 3-4 | 4 | 199 | 728 | 0.728 |
| 4-5 | 5 | 123 | 851 | 0.851 |
| 5-6 | 6 | 70 | 921 | 0.921 |
| 6-7 | 7 | 37 | 958 | 0.958 |
| 7-8 | 8 | 20 | 978 | 0.978 |
| 8-9 | 9 | 12 | 990 | 0.990 |
| 9-10 | 10 | 5 | 995 | 0.995 |
| 10-11 | 11 | 3 | 998 | 0.998 |
| 11-12 | 12 | 1 | 999 | 0.999 |
| 12-13 | 13 | 1 | 1000 | 1 |
| Column sum | | 1000 | | |

Now the fitted distribution can be used directly to assess the probability of significant wave heights. If the probability is $P(H_s > x)$ that an observed significant wave height is larger than or equal to x then the inverse is called the return period

$$R_p = \frac{1}{P(H_s > x)},$$

which should be interpreted as the mean number of observations needed to observe one value larger or equal to x . If we assume that the observations are equidistant in

time, τ , then we can express the return period as a time span needed for such an observation as

$$R = \frac{\tau}{P(H_s > x)} \quad \dots(8.9)$$

Wave observations are usually based on 20 minutes time series of measured waves. The observations are often not performed every 20 minutes but rather every 3 hrs or 6 hrs, but are assumed to be representative also for all periods between the observations, and then we can set $\tau = 20$ min. By solving H_s from Equation (8.7) we can now calculate e.g. the 10-year, 20-year, 50-year, 100-year, 500-year or 1000-year significant wave height. The statistics given here give the results in Table 8.9.

Table 8.9 Significant wave heights and maximum wave heights in the North Atlantic for various return periods.

| $R(\hat{a}r)$ | H_s^R | H_{max}^R |
|---------------|---------|-------------|
| 10 | 16.84 | 31.84 |
| 20 | 17.37 | 32.84 |
| 50 | 18.06 | 34.14 |
| 100 | 18.57 | 35.10 |
| 500 | 19.71 | 37.25 |
| 1000 | 20.18 | 38.15 |

If we further assume that the expected “maximum” individual wave height for various return periods are given by sea states with the same return period and if these are set as the three-hour extreme wave height Equation (7.64)

$$H_{max} = \sqrt{8m_0 \ln(N)} = H_s \sqrt{\frac{1}{2} \ln(N)}$$

In Table 8.8 one can see that the most common mean period is $T_z = 8.5$ s then three hours contain $N = 1,271$ waves and thus $H_{max} = 1.89H_s$ and e.g. $H_{max}^{20\hat{a}r} = 32.8$ m and $H_{max}^{100\hat{a}r} = 35.1$ m. (Note that the weighted average of all T_z in Table 8.8 happen to be 8.42 s. To be used below)

Probability distributions of individual wave heights

The method to estimate the maximum individual wave height used in the previous paragraph is used by e.g. Norwegian authorities in the context of petroleum exploration. Traditionally however one used to estimate it by finding the distribution for all individual wave heights. E.g. a numerical distribution of individual waves can be formed by adding the Rayleigh distributions for all observations in Table 8.8.

$$P(H < x) = 1 - \sum_{j=1}^M e^{-2(x/H_j)^2} n_j / N \quad \dots(8.10)$$

where $P(H < x)$ is the long term sample probability that a wave height does not exceed x . See Jensen (2001) or Faltinsen (1990). The method described below was proposed by Nordenström^{xliii} (1973).

Under the assumption that the individual wave heights in a sea state obey the Rayleigh distribution Equation (7.59) the long term distribution of individual wave heights can be written as a Weibull distribution given by

$$P_L(H > x) = e^{-\left(\frac{x}{CH_c^{1/d}}\right)^D} \quad \dots(8.11)$$

where H_c is one of the parameters of the Weibull distribution of the significant wave heights and the coefficients C and D are functions of the other parameter the slope, γ . The coefficient, d , depends on whether measured H_s data or visual wave heights H_v are used. For visual data $d = 4/3$ and for significant wave heights $d = 1$. Compare Equation (7.6), which gives $H_v \approx 0.501H_s^{4/3}$.

Table 8.10 The parameters C and D of the long term distribution of individual wave heights Equation (8.6).

| $\gamma \times d$ | C $d = 4/3$ | C $d = 1$ | D |
|-------------------|------------------|----------------|-------|
| | 1.189 | 0.707 | 2.000 |
| 10.00 | 1.056 | 0.628 | 1.780 |
| 8.00 | 1.029 | 0.612 | 1.712 |
| 6.00 | 0.992 | 0.590 | 1.614 |
| 4.00 | 0.930 | 0.553 | 1.444 |
| | | | |
| 3.33 | 0.901 | 0.536 | 1.354 |
| 2.86 | 0.876 | 0.521 | 1.276 |
| 2.50 | 0.855 | 0.508 | 1.208 |
| 2.22 | 0.837 | 0.497 | 1.144 |
| 2.00 | 0.820 | 0.488 | 1.086 |
| | | | |
| 1.82 | 0.807 | 0.480 | 1.034 |
| 1.67 | 0.794 | 0.472 | 0.988 |
| 1.54 | 0.783 | 0.465 | 0.944 |
| 1.43 | 0.772 | 0.459 | 0.904 |
| 1.33 | 0.762 | 0.453 | 0.868 |
| | | | |
| 1.25 | 0.754 | 0.448 | 0.834 |
| 1.18 | 0.746 | 0.444 | 0.802 |
| 1.11 | 0.739 | 0.439 | 0.744 |
| 1.05 | 0.732 | 0.435 | 0.746 |
| 1.00 | 0.726 | 0.432 | 0.722 |
| | | | |
| 0.67 | 0.689 | 0.410 | 0.538 |
| 0.50 | 0.666 | 0.396 | 0.428 |
| 0.40 | 0.656 | 0.390 | 0.356 |

For the given data for the North Atlantic $\gamma = 1.74$ and $H_c = 3.94$ m were found above and $d = 1$ because significant wave data is used. Then $C = 0.476$ and $D = 1.009$ are found by interpolation in Table 8.10. Further the return period of individual waves exceeding x is written

$$R = \frac{\tau}{P_L(H > x)}, \quad \dots(8.12)$$

where τ is the average wave period during the return period, R , or equivalently the number of waves are R/τ . The mean wave period derived from Table 8.7 is $T_z = 8.42$ s which can be set to τ . Then the following maximum expected individual wave height for some return periods will be given as in Table 8.11. These maximum wave heights are a little higher than those derived from the significant R -year return wave heights as would be expected.

Table 8.11 Maximum wave heights in the North Atlantic for various return periods.

| $R(\text{år})$ | H_{max}^R |
|----------------|--------------------|
| 10 | 31.89 |
| 20 | 33.14 |
| 50 | 34.80 |
| 100 | 36.06 |
| 500 | 38.97 |
| 1000 | 40.23 |

Jensen (2001) derives the 20 year maximum wave to 36 m from the same data as here. He uses a one sided normal distribution for the distribution of significant wave heights which then gives a Gumbel distribution of individual wave heights.

Joint probability of wave heights, winds and currents

In Norwegian guidelines for the design of offshore platforms the extreme weather condition to be considered is the most unfavourable combination of

- wind speed and sea state corresponding to a 100-year return period combined with a 10 year-return-period current.
- current velocity and sea state with 100-year return period combined with a wind speed with a 10-year-return period.

If these conditions are supposed to be independent the combined return period would be 10^{-5} per year, which obviously is incorrect as the wind, waves and maybe also the current are not independent. The target probability is stated as 10^{-4} per year.

A recent treatise of the joint probability of wind and waves in the Northern North Sea is given by Johannessen et al. (2002). In this the marginal distribution of the wind speed is taken as a two-parameter Weibull distribution. In each wind-speed class the significant wave heights are found to follow a two-parameter Weibull distribution and the peak periods a log-normal distribution.

Design wave for a ship

For the design of a ship's hull girder the most critical wave event may be taken as a head or bow, regular, plane wave having a wave length, λ , equal to the length, L_{pp} , of the ship. A ship in such wave will alternatively have the wave crests at the bow and stern and the wave trough amidships (sag), or troughs at the bow and stern and a wave crest amidships (hog). The wave should have a reasonable wave amplitude, a , and steepness, $2a/\lambda$ as is described in the following.

The most probable maximum wave amplitude during 3 h is given by

$$a = \frac{H_s}{4} \sqrt{2 \ln \left(\frac{3 \text{ h}}{T_z} \right)} \approx H_s. \quad \dots(8.13)$$

where the last approximation is somewhat conservative. The maximum possible wave steepness is 0.142 giving the maximum wave amplitude as

$$a < L_{pp} / 14 = 0.071L_{pp} . \quad \dots(8.14)$$

According to Table 8.9 the 20 year significant wave height can be set to 17.37 m in the North Atlantic. Then for a 200 m long ship the ship-girder design wave will have the amplitude $a = H_s = 17.37$ m or $a = 200 \text{ m}/14 = 14.2$ m, whichever is smallest. So in this case $a = 14.2$ m, i.e. the wave height 28.6 m. The corresponding wave period is $T = \sqrt{2\pi L_{pp} / g} = 11.3$ s, in deep water without current that is. Compare this with the information given in the scatter diagram Table 8.7. For a more elaborate discussion, see Jensen (2001) or Tromans et al (1991) for an alternative form of the design wave.

9 RESPONSES OF A SHIP IN IRREGULAR WAVES

9.1 The ship as a mechanical filter

In Chapter 6 we studied the forces and motions of a ship in a regular sinusoidal wave, in Chapter 7 the modelling of wind waves without and with directional spread and in Chapter 8 the statistics of waves and sea states. For many years the seakeeping performance was only assessed for regular design waves. But, as was first proposed by St Denis and Pierson (1953), the ship can be looked upon as a mechanical filter, which filters the irregular sea into a ship motion, very much like the electronic filter in a radio receiver filters radio waves.



Figure 9.1 The ship as a mechanical filter

9.2 The Heave Motion in Irregular Waves

Heave transfer function

In Chapter 6 the heave motion at zero speed in a plane regular wave with the amplitude, a , and the propagation direction, θ , was deduced. For a box-like ship the wave excited heave motion was then represented by a complex heave motion:

$$\eta_{3c} = \hat{\eta}_{3c} e^{-j\alpha} = a e^{-kT} \frac{(\rho g B - \omega^2 a_{33} - j\omega b_{33})}{(\rho g B L - (\rho T B L + a_{33} L)\omega^2 - j\omega b_{33} L)} 2 \frac{\sin(k(\cos\theta)L/2)}{k \cos\theta} e^{-j\alpha}. \quad (9.1)$$

Compare Equation (6.43). Here the modulus $|\hat{\eta}_{3c}|$ of the complex amplitude represents the heave amplitude, the argument, $\arg(\hat{\eta}_{3c})$, the phase lag to the wave motion and the real part, $\text{Re}(\eta_{3c})$, the real heave motion.

By dividing the complex amplitude by the wave amplitude, a , we get a complex transfer function between the wave motion and the heave motion as

$$T_{3c}(\omega, \theta) = \frac{\hat{\eta}_{3c}}{a} = e^{-kT} \frac{(\rho g B - \omega^2 a_{33} - j\omega b_{33})}{(\rho g B L - (\rho T B L + a_{33} L)\omega^2 - j\omega b_{33} L)} 2 \frac{\sin(k(\cos\theta)L/2)}{k \cos\theta} \dots (9.2)$$

Now forming the product of the transfer function Equation (9.2) and the wave function (9.3) in $x = 0$ m.

$$\zeta_c(\omega, t, \varepsilon) = a e^{j(-\alpha t + \varepsilon)} = a [\cos(-\alpha t + \varepsilon) + j \sin(-\alpha t + \varepsilon)] \quad \dots (9.3)$$

we get the complex heave motion in the time domain as

$$\eta_{3c}(\omega, \theta, t, \varepsilon) = T_{3c}(\omega, \theta) \zeta_c(\omega, t, \varepsilon). \quad \dots(9.4)$$

Compare Equation (3.32). The wave function (9.3) is the same as Equation (5.13), but complemented with a phase angle, ε .

The transfer function (9.2) transfers both the amplitude, $|T_{3c}(\omega, \theta)|$, and the phase lag, $\arg(T_{3c}(\omega, \theta))$, to the wave motion, and the real heave motion can thus be written

$$\text{Re}(\eta_{3c}(\omega, \theta, t, \varepsilon)) = \text{Re}(T_{3c}(\omega, \theta) \zeta_c(\omega, t, \varepsilon)) = a |T_{3c}(\omega, \theta)| \cos(-\omega t + \varepsilon - \arg(T_{3c}(\omega, \theta))) \quad \dots(9.5)$$

The amplification factor, $|T_{3c}(\omega, \theta)|$, or frequency response function is the heave amplitude divided by the wave amplitude (m/m) and is often called the heave-response amplitude operator or *RAO*⁸ and has its equivalents in other degrees of freedom as well as for derived responses.

Heave motion in the time domain

An irregular plane with the direction of propagation, θ , in relation to a ship heading along the x -axis projected on the ship, can be represented by a complex sum written as

$$\zeta_c(t) = \sum_{i=1} a_i e^{j(k_i(\cos(\theta))x - \omega_i t + \varepsilon_i)}, \quad \dots(9.6)$$

where ε_i are the random phase angles

a_i the amplitudes

k_i the wave numbers and

ω_i the angular frequencies of the component waves.

In the origin of the co-ordinate system $x = 0$ m, so the elevation there is

$$\zeta_c(t) = \sum_{i=1} a_i e^{j(-\omega_i t + \varepsilon_i)}. \quad \dots(9.6b)$$

Compare Equation (7.35). From Equation (9.5) and (9.6) now follows by superposition that the heave motion in the time domain can be written

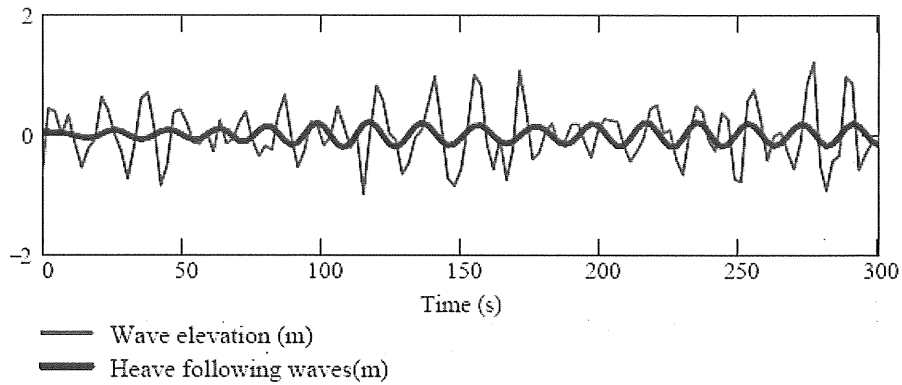
$$\eta_{3c}(t) = \sum_{i=1} a_i T_{3c}(\omega_i, \theta) e^{j(-\omega_i t + \varepsilon_i)}. \quad \dots(9.7)$$

This time-domain heave is shown in Figure 9.2 for the box-like ship in three wave directions. Length \times beam \times draught = $L \times B \times T = 100 \text{ m} \times 20 \text{ m} \times 10 \text{ m}$. The above simulation was done in the frequency domain starting out with a wave spectrum,

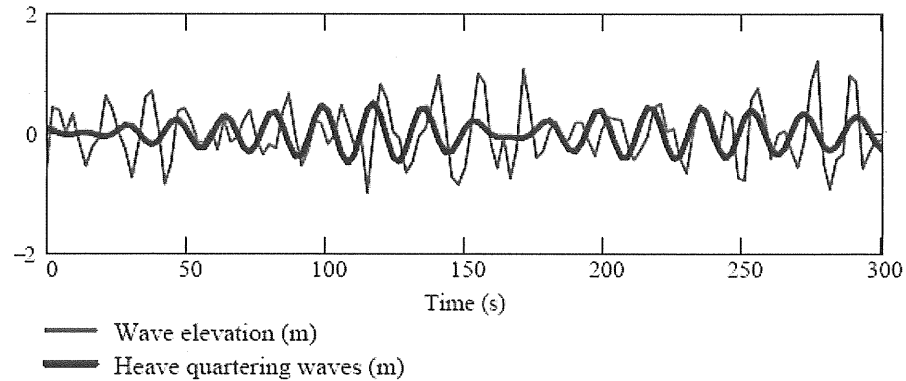
⁸ In some literature the square of $|T_{3c}(\omega, \theta)|$ is called *RAO* because the square is used in the multiplication by the wave spectrum to form the motion spectrum.

multiplying with a transfer function to produce a response spectrum and from this response spectrum simulating a time trace of response by an inverse fast-Fourier transformation, IFFT. Compare the flow chart of “Alternative roads of action” Figure 3.12. By preserving the random phase angles, ε_i , of the component waves and “adding” the phase lags of the response components by the complex transform multiplication the time trace of response shows the correct time response, to first order that is.

a)



b)



c)

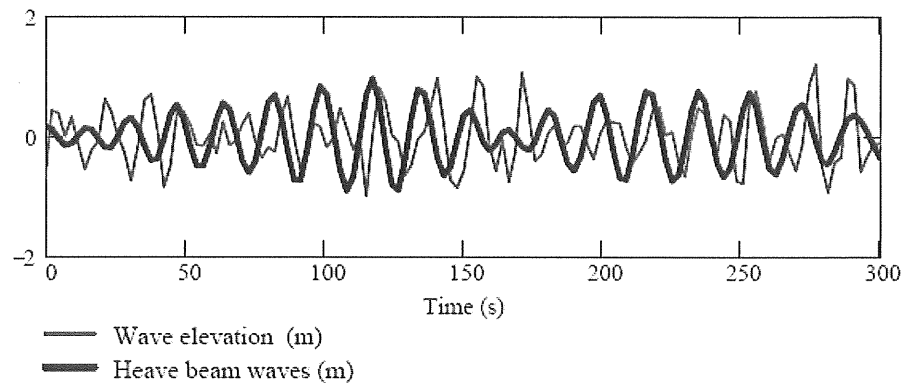


Figure 9.2 Heave motion in 300 seconds of simulated plane waves with $H_s = 2$ m and $T_{02} = 5$ s ISSCb spectrum.

- a) Following waves
- b) Quartering waves
- c) Beam waves

Forming the heave motion spectrum

The discrete heave spectrum can be formed from the time domain simulation by

$$S_{3i}(\omega_i, \theta) = \sum_{i=1} \frac{1}{2} |a_i T_{3c}(\omega_i, \theta)|^2 \quad \dots(9.8)$$

The continuous heave spectrum is formed analogously by the simple operation

$$S_3(\omega, \theta) = |T_{3c}(\omega, \theta)|^2 S(\omega) \quad \dots(9.9)$$

Below in Figure 9.3 the heave spectrum for following (or meeting) waves in two different sea states from Table 8.7 are shown using the ISSC wind-sea spectrum Equation (7.25). It is seen how the sea state with shorter mean period does not excite the ship much within the frequency range where the transfer function is appreciable. In Figure 9.4 the response spectra for three headings are shown. There it is clearly seen that beam sea is unfavourable for the heave motion.

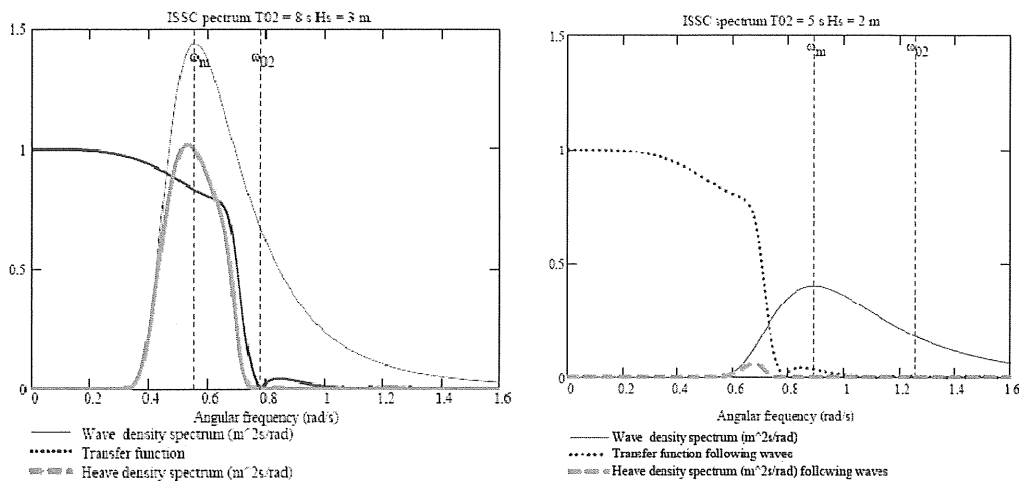


Figure 9.3 Heave-response spectra of the box-like ship in the same heading ($\theta = 0$ deg) at two different sea states.

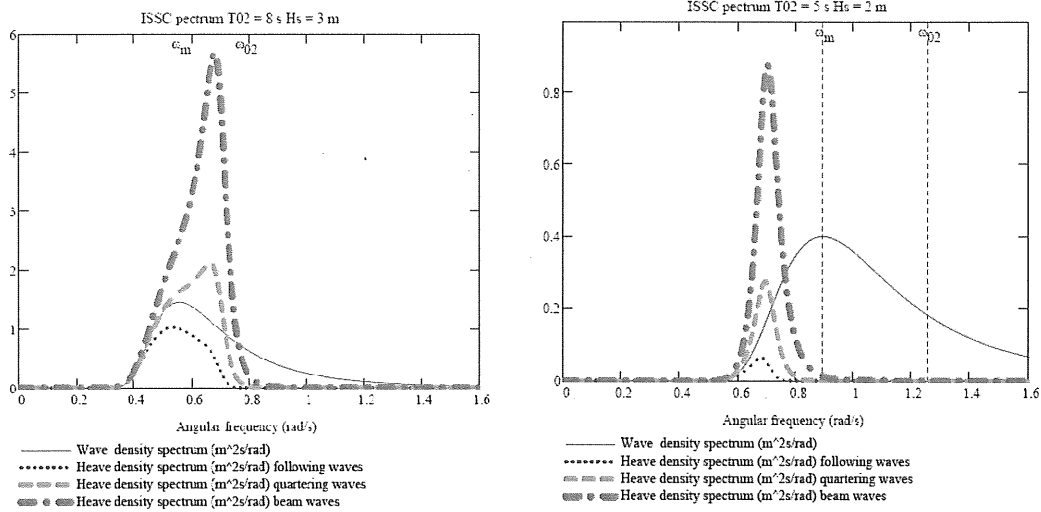


Figure 9.4 Response spectra of the box-like ship in three headings at two different sea states.

The characteristics of the responses as zero-crossing period, crest period, significant response and standard deviation can now be calculated from the moments of the response spectra, because the responses or derived responses are also – like the wave motion – normal-distributed Gaussian processes as they were produced by a linear filter or transfer function. The most interesting characteristics are the mean zero-crossing period evaluated as T_{02} and the standard deviation, σ . The significant double amplitude $H_s = 4\sigma$. See Chapter 7 page 131 and 132. Also the short term statistics and maxima or peaks can be assessed as was outlined for the waves in paragraphs 7.5 and 7.6. Long-term statistics can be assessed by operating the RAOs on the wave statistics of Table 8.7 for example. A choice of type spectrum must of course be made.

In Table 9.1 one can see that the zero-crossing periods of the responses are longer than the zero-crossing periods of both exciting sea states; that the significant double-amplitude motions are smaller than the significant wave heights in all headings except in beam sea. In the larger beam sea state the heave response of the ship is amplified by a factor 1.32 (32 % larger) compared to the heave motion of the sea. The natural frequency of the box like ship heaving in calm water is 9 s. What is the deep-water wave length corresponding to T_{02} ? Compare also Figure 6.13 and Figure 6.15.

Table 9.1 Some characteristics of the two wave spectra and their heave responses

| H_S (m) | T_{02} (s) | θ (°) | $4\sigma_r$ (m) | T_{02r} (s) | $4\sigma_r/H_s$ |
|-----------|--------------|--------------|-----------------|---------------|-----------------|
| 2 | 5 | 0 | 0.62 | 9.4 | 0.32 |
| | | 45 | 0.66 | 9.1 | 0.33 |
| | | 90 | 1.20 | 8.8 | 0.60 |
| 3 | 8 | 0 | 1.94 | 11.2 | 0.64 |
| | | 45 | 2.76 | 10.5 | 0.92 |
| | | 90 | 3.96 | 10.0 | 1.32 |

9.3 The Pitch Response

The pitch response can be treated exactly as the heave response with the complex transfer function

$$T_{5c}(\omega, \theta) = \frac{\hat{\eta}_{5c}(\omega, \theta)}{a} \quad \dots(9.10)$$

which has the unit rad/m. The complex pitch amplitude $\hat{\eta}_{5c}(\omega, \theta)$ is given by Equation (6.55). One can also choose to form a wave-slope spectrum from the wave amplitude spectrum first and use a dimensionless transfer function

$$T_{5slope}(\omega, \theta) = \frac{\hat{\eta}_{5c}(\omega, \theta)}{k(\omega)a} \quad \dots(9.11)$$

This is, however, unnecessarily complicated.

Thus the continuous pitch spectrum is simplest formed by the operation

$$S_5(\omega, \theta) = |T_{5c}(\omega, \theta)|^2 S(\omega) \quad \dots(9.12)$$

Some results of pitch-response spectra for the same two sea states as for the heave response are shown in figures below.

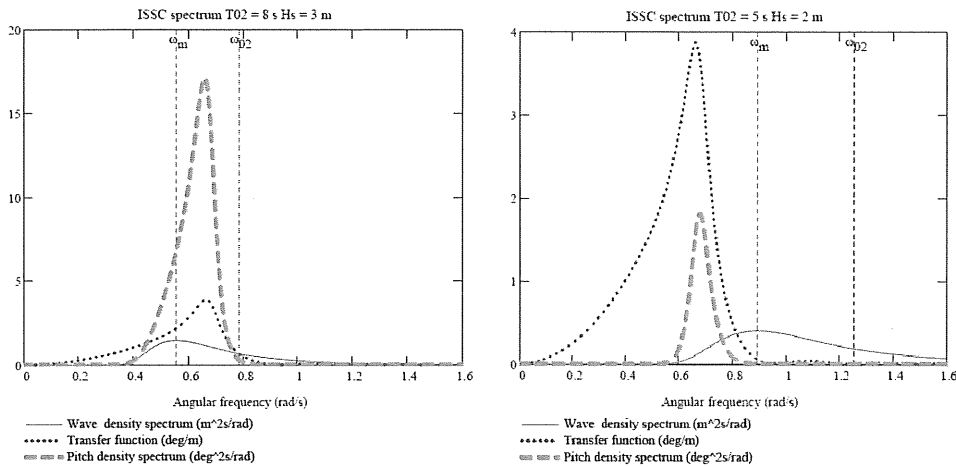


Figure 9.5 Pitch-response spectra of the box-like ship in the same heading ($\theta = 0$ deg) at two different sea states.

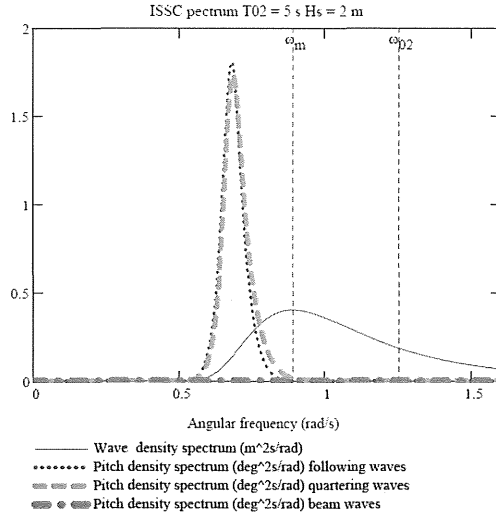


Figure 9.6 Pitch-response spectrum of the box-like ship in three headings at one sea states.

Time domain pitch can be simulated as was done with heave. If the same arbitrary phase angles are used for the wave, heave and pitch the pitch, heave and wave will be contemporary.

9.4 The Response of Vertical Motion at Station x

To be able to calculate “green water”, propeller or bottom emergence, slamming and acceleration we need the response of vertical motion at any station x along the ship. The 3D motion, velocity and acceleration at a point (x,y) are described by Equations (6.75-77):

$$s_3 = \eta_3 + y\eta_4 - x\eta_5 \quad \dots(6.75)$$

$$\dot{s}_3 = \dot{\eta}_3 + y\dot{\eta}_4 - x\dot{\eta}_5 \quad \dots(6.76)$$

and
$$\ddot{s}_3 = \ddot{\eta}_3 + y\ddot{\eta}_4 - x\ddot{\eta}_5 \quad \dots(6.77)$$

Neglecting roll motion, which is difficult to assess and small in head sea ($\theta = \pi$), the expressions for the vertical motion, velocity and acceleration at a station (x) along the ship are reduced to the following equations in complex form:

$$s_{3c} = \eta_{3c} - x\eta_{5c} \quad \dots(9.13)$$

$$\dot{s}_{3c} = \dot{\eta}_{3c} - x\dot{\eta}_{5c} \quad \dots(9.14)$$

and
$$\ddot{s}_{3c} = \ddot{\eta}_{3c} - x\ddot{\eta}_{5c} \quad \dots(9.15)$$

The vertical motion, velocity and accelerations responses can be treated as the heave and pitch responses with the complex transfer functions

$$T_{s3c}(\omega, \theta, x) = \frac{\hat{\eta}_{3c}(\omega, \theta)}{a} - x \frac{\hat{\eta}_{5c}(\omega, \theta)}{a} = T_{3c}(\omega, \theta) - xT_{5c}(\omega, \theta) \quad \dots(9.16)$$

$$T_{s3velc}(\omega, \theta, x) = -j\omega \left(\frac{\hat{\eta}_{3c}(\omega, \theta)}{a} - x \frac{\hat{\eta}_{5c}(\omega, \theta)}{a} \right) = -j\omega(T_{3c}(\omega, \theta) - xT_{5c}(\omega, \theta)) \dots(9.17)$$

$$T_{s3acc}(\omega, \theta, x) = -\omega^2 \left(\frac{\hat{\eta}_{3c}(\omega, \theta)}{a} - x \frac{\hat{\eta}_{5c}(\omega, \theta)}{a} \right) = -\omega^2(T_{3c}(\omega, \theta) - xT_{5c}(\omega, \theta)) \dots(9.18)$$

which have the units m/m, m/(sm) and m/(s²m) respectively.

Examples of vertical motion spectra, velocity spectra and acceleration spectra formed by transformations equivalent to Equation (9.12) are given in the figures 9.7 to 9.9 below.

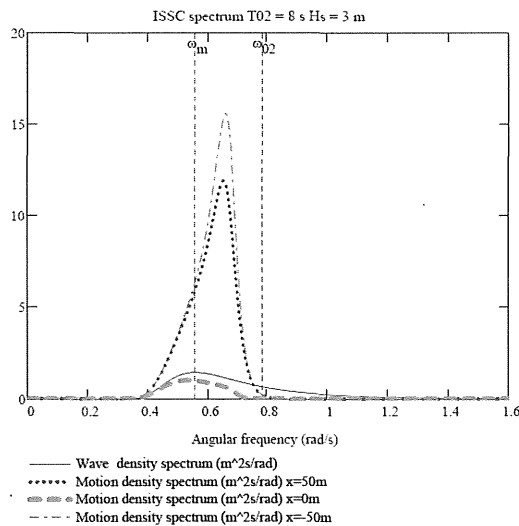


Figure 9.7 Vertical motion response of the box-like ship in three stations.

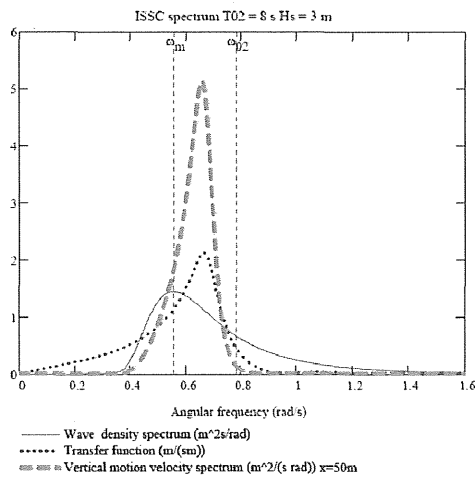


Figure 9.8 Vertical velocity response of the box-like ship at bow in following waves.

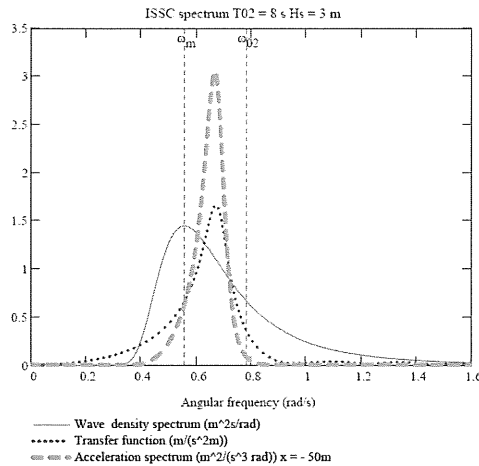


Figure 9.9 Vertical acceleration response of the box-like ship at bow in following waves.

9.5 Accelerations, seasickness and human performance

It is difficult to work if the accelerations onboard are too large. This is important for the safety on ships and in the offshore industry, where also downtime of operations should be avoided. In the passenger and cruising trade the comfort is important. In freighters cargo may get loose so fastenings must be attached and designed. In tankers the sloshing in incompletely filled tank compartments may cause structural problems.

Seasickness

Vertical acceleration is probably the prime reason for seasickness (motion sickness, kinetosis). For instance in Figure 9.9 a motion-sickness index, MSI, is given as the share of exposed persons throwing up within a given time at combinations of mean frequency and standard deviation⁹ of acceleration.

As an application we can – from the acceleration spectrum above – calculate the spectral moments and estimate the mean period of acceleration to $T_{02acc} = 9.7$ s and the standard deviation to 0.6 m/s^2 . Then assessing seasickness in Figure 9.9, we find that between 10 and 20 % of passengers will through up within 20 hours under such conditions.

⁹ RMS in Figure 9.9 and Table 9.2 is defined for the acceleration itself. As the mean is zero it is identical to the standard deviation. The RMS value used in other contexts in this compendium is defined for the amplitudes or double amplitudes of the quantities e.g. H_{rms} .

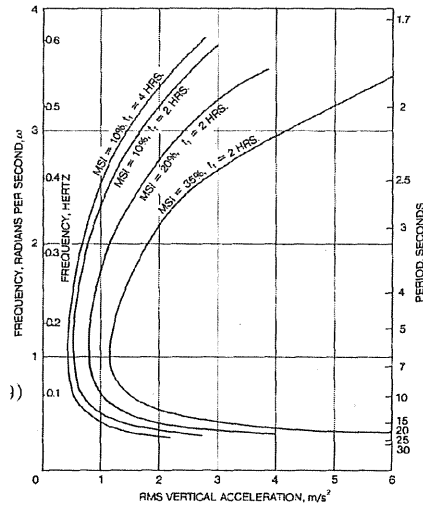


Figure 9.9 Motion-sickness index, MSI, is the share of exposed persons throwing up within the given time at combinations of RMS (standard deviation) acceleration and mean frequency (Mandel1979).

Human performance

For the performance of the crew the standard deviation 0.1 g for vertical acceleration at the bridge can be adopted, a criterion denoted by “*Intellectual work*” by a Nordforsk study^{xliii}. In cabins and restaurants the criterion of “*Transit passengers*” is stricter and given as 0.05 g for vertical acceleration. Also criteria for transversal (horizontal) acceleration are given. See Table 9.2.

In addition to the acceleration criteria, crew performance and passenger comfort is governed by the ability to move around the ship. This criterion can be formulate in terms of “*motion induced interruptions*” or *MMI* (Graham, 1990^{xliv}). *MMI* gives an indication of the number of events per minute in which a standing person will look for support to maintain balance. According to Graham’s work, the allowed *MMI* is 1/min. Above this limit crew performance is substantially degraded. For the passenger areas the allowed *MMI* is 0.5/min. For practical application of *MMI* it is referred to Graham’s work.

Table 9.2 Examples of human performance criteria

| | Motion induced interruption | Standard deviation (RMS of quantity) | | Significant double amplitude (SDA) | |
|-------------------------------|------------------------------------|--------------------------------------|--------------------------|------------------------------------|--------------------------|
| | | Verical acceleration | Transversal acceleration | Verical acceleration | Transversal acceleration |
| | <i>MMI</i> (min ⁻¹) | (g) | (g) | (m/s ²) | (m/s ²) |
| Navigation bridge | 1 | 0.10 | 0.05 | 4.0 | 2.0 |
| Cabins and restaurants | 0.5 | 0.05 | 0.04 | 2.0 | 1.6 |

9.6 Motions of moored ships in harbours

To calculate wave excited first order motions for moored ships in the open sea or moored offshore platforms is a straightforward matter nowadays - with the exception of roll motions of ships. To calculate motions for a ship at berth in a harbour introduces the complications of the wave penetration into and possible resonance of the harbour to the waves, the non-linear mooring arrangements, but also the necessity to take the proximity of the quay walls, shore slopes and sea floor into account, when assessing the hydrodynamic properties of the ship. This is all automatically "included" when making physical model tests with regular or pseudo random waves, albeit with model scale deficiencies. Field measurements are also useful, but cannot be used for testing changes of harbour and mooring layout. It is however gradually becoming possible to make "complete" numerical modelling of ships moored in harbours^{xlv}.

Recommended allowed limits of motions for safe mooring conditions

Table 9.3 Criteria for safe stay at berth (Nordic Council, 1986)

| Type of vessel | surge (m) | sway (m) | heave (m) | yaw (deg) | pitch (deg) | roll (deg) |
|------------------------------|--|--|--|--|--|--|
| |  |  |  |  |  |  |
| <u>Fishing vessel</u> | | | | | | |
| (L _{oa} = 25-60 m) | | | | | | |
| Movement | 1.2-1.5 | 1.0-2.0 | 0.6-1.0 | 6 | 4 | 8 |
| <u>Freighters/coasters</u> | | | | | | |
| (L _{oa} = 60-120 m) | | | | | | |
| Movement | 1.0-2.0 | 1.5-2.0 | 1.0-1.5 | 3-5 | 2-3 | 6 |
| <u>Velocity</u> | | | | | | |
| Size of vessel | | | | | | |
| about 1000 DWT | 0.6 m/s | 0.6 m/s | | 2.0 deg/s | | 2.0 deg/s |
| about 2000 DWT | 0.4 m/s | 0.4 m/s | | 1.5 deg/s | | 1.5 deg/s |
| about 5000 DWT | 0.3 m/s | 0.3 m/s | | 1.0 deg/s | | 1.0 deg/s |

Table 2.2 Criteria for vessel movements for safe mooring conditions at berth. The movements are peak-peak values. For the berth to be acceptable, the frequency of these movements should be less than 3 h/year.

Table 9.4 Recommended velocity criteria for Safe mooring conditions of various ships PIANC (1995).

| Ship size (DWT) | Surge (m/s) | Sway (m/s) | Heave (m/s) | Yaw (°/s) | Pitch (°/s) | Roll (°/s) |
|-----------------|-------------|------------|-------------|-----------|-------------|------------|
| 1,000 | 0.6 | 0.6 | - | 2.0 | - | 2.0 |
| 2,000 | 0.4 | 0.4 | - | 1.5 | - | 1.5 |
| 8,000 | 0.3 | 0.3 | - | 1.0 | - | 1.0 |

1) These criteria are applicable for fishing vessels, coasters, freighters, ferries and Ro-Ro vessels.

Table 9.5 Wave criteria for small craft and pleasure boats. The acceptable frequency of occurrence is one to a few times per year. PIANC (1995).

| Ship Length (m) | Beam/Quartering Seas | | Head Seas | |
|-----------------|----------------------|---------------------------|------------|---------------------------|
| | Period (s) | Height H _s (m) | Period (s) | Height H _s (m) |
| 4 - 10 | < 2.0 | 0.20 | < 2.5 | 0.20 |
| | 2.0 - 4.0 | 0.10 | 2.5 - 4.0 | 0.15 |
| | > 4.0 | 0.15 | > 4.0 | 0.20 |
| 10 - 16 | < 3.0 | 0.25 | < 3.5 | 0.30 |
| | 3.0 - 5.0 | 0.15 | 3.5 - 5.5 | 0.20 |
| | > 5.0 | 0.20 | > 5.5 | 0.30 |
| 20m | < 4.0 | 0.30 | < 4.5 | 0.30 |
| | 4.0 - 6.0 | 0.15 | 4.5 - 7.0 | 0.25 |
| | > 6.0 | 0.25 | > 7.0 | 0.30 |

Recommended allowed limits of motions for safe working conditions

Recommended allowed limits of motions for safe working conditions at loading and unloading of various ship types, from pleasure boats through fishing vessels to large bulk carriers are presented by PIANC (1995)^{xlvi}, and by the Nordic Council (1986)^{xlvii}. The working group of the Nordic Council discusses its recommendations thus: "The vessel movements accepted during loading/unloading operations are to some extent determined by local traditions. Generally, this acceptance does not consider possible reduced cost effectiveness. In relation to harbour layouts, however, it is necessary to take such factors into consideration."

The choice of motion criteria depend on

- Loading/unloading methods, gear and personnel
- Vessel type, type of goods
- Characteristics of the vessel motions

Table 9.6 Criteria for safe working conditions PIANC (1995)

| Ship Type | Cargo Handling Equipment | Surge (m) | Sway (m) | Heave (m) | Yaw (°) | Pitch (°) | Roll (°) |
|----------------------|--------------------------|------------------|----------|-----------|---------|-----------|----------|
| Fishing vessels | Elevator crane | 0.15 | 0.15 | | | | |
| | Lift-on-lift-off | 1.0 | 1.0 | 0.4 | 3 | 3 | 3 |
| | suction pump | 2.0 | 1.0 | | | | |
| Freighters, coasters | Ship's gear | 1.0 | 1.2 | 0.6 | 1 | 1 | 2 |
| | Quarry cranes | 1.0 | 1.2 | 0.8 | 2 | 1 | 3 |
| Ferries, Ro-Ro | Side ramp ² | 0.6 | 0.6 | 0.6 | 1 | 1 | 2 |
| | Dew/storm ramp | 0.8 | 0.6 | 0.8 | 1 | 1 | 4 |
| | linkspan | 0.4 | 0.6 | 0.8 | 3 | 2 | 4 |
| | Rail ramp | 0.1 | 0.1 | 0.4 | - | 1 | 1 |
| General cargo | - | 2.0 | 1.5 | 1.0 | 3 | 2 | 5 |
| Container vessels | 100% efficiency | 1.0 | 0.6 | 0.8 | 1 | 1 | 3 |
| | 50% efficiency | 2.0 | 1.2 | 1.2 | 1.5 | 2 | 6 |
| Bulk carriers | Cranes | 2.0 | 1.0 | 1.0 | 2 | 2 | 6 |
| | Elevator/bucket-wheel | 1.0 | 0.5 | 1.0 | 2 | 2 | 2 |
| | Conveyor belt | 5.0 | 2.5 | | 3 | | |
| Oil tankers | Loading arms | 3.0 ³ | 3.0 | | | | |
| Gas tankers | Loading arms | 2.0 | 2.0 | | 2 | 2 | 2 |

- Remarks:
- 1) Motions refer to peak-peak values (except for sway: zero-peak).
 - 2) Ramps equipped with rollers.
 - 3) For exposed locations 5.0 m (regular loading arms allow large movements)

9.7 Green water and propeller or bottom emergence

As was told in Chapter 6, if the wave elevation comes above the instantaneous position of the railing or above the freeboard at any point of the ship this will result in water on deck, so called green water. To treat this problem in the frequency domain we form the transfer function for the relative vertical motion between the ship and water elevation for any heading and at any station, x , but only along the longitudinal axis of the ship, $y=0$:

$$\hat{s}_{3relc}(\omega, \theta, x) = \hat{\eta}_{3c}(\omega, \theta) - x\hat{\eta}_{5c}(\omega, \theta) - \hat{\zeta}_c(x, \theta) \quad \dots(9.19)$$

Where $\hat{\zeta}_c(x, \theta) = ae^{j(kx\cos(\theta)+\epsilon)}$ is the complex amplitude of wave elevation at station x .

The transfer function becomes

$$T_{s3relc}(\omega, \theta, x) = \frac{\hat{\eta}_{3c}(\omega, \theta) - x\hat{\eta}_{5c}(\omega, \theta) - \hat{\zeta}_c(x, \theta)}{a} \quad \dots(9.20)$$

and the response spectrum

$$S_{s_{3rel}}(\omega, \theta, x) = |T_{s_{3relc}}(\omega, \theta, x)|^2 S(\omega). \quad \dots(9.21)$$

Examples of response spectra for the vertical relative motion are shown in Figure 9.10.

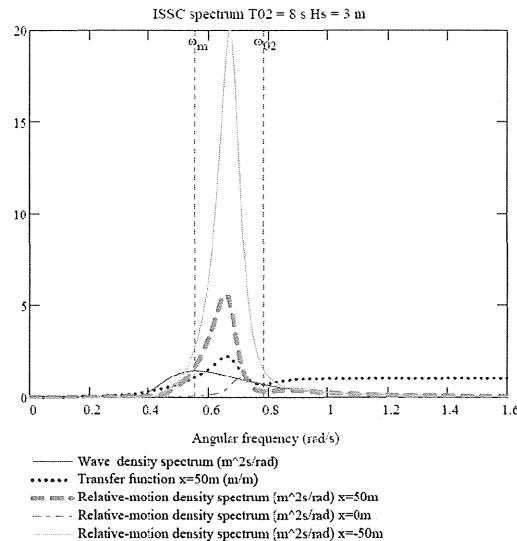


Figure 9.10 Response spectra of relative motion at bow, amidships and aft.

Probability of green water on deck.

Green water will appear on deck if the relative motion is larger than the freeboard, $F_b(x)$. The process of relative motion will be normal distributed because its constituent processes, heave and pitch, are normal distributed. As then the relative motion is a normal distributed process with zero mean and standard deviation, $\sigma_{s_{3rel}}(x)$, the maxima or minima of the relative motion will be Rayleigh distributed. Therefore the probability of an individual *minimum* of relative motion being deeper than the freeboard or the probability of green water will be

$$P_{gw}(x) = P(s_{3rel}(x) > F_b(x)) = 1 - P(s_{3rel}(x) < F_b(x)) \approx \exp\left(-\frac{1}{2}\left(\frac{F_b(x)}{\sigma_{s_{3rel}}(x)}\right)^2\right) \dots(9.22)$$

The number of green-water occurrences within a time period, t , can be assessed by

$$N_{gw} = \frac{t}{T_{02s_{3rel}}} P_{gw}(x). \quad \dots(9.23)$$

For $H_s = 8$ m, $T_{02} = 10$ s, $F_b = 10$ m, $x = -50$ m and zero heading, the standard deviation is $s_{3rel} = 3.27$ m and the response mean upcrossing period $T_{02s_{3rel}} = 9.4$ s. This gives the number of green water occurrences per hour $N_{gw}/t = 3.54/\text{hr}$ or equivalently one occurrence every 17 minutes. One can also ask how will the No of occurrences change with freeboard. This is illustrated in Figure 9.10.

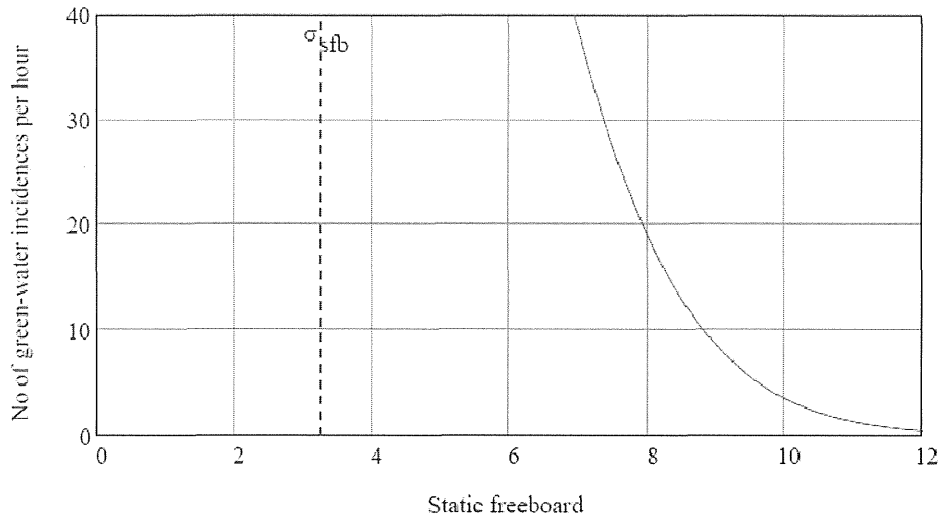


Figure 9.11 No of green water occurrences per hour as a function of static freeboard.

The probability of propeller or bottom emergence

The risk for the propeller to emerge out of the water and the risk that the bottom will rise above the water and experience slamming at re-entry can be assessed in complete analogy to what was done for green water. If the draught is T or the propeller is T below the mean-water surface.

$$P_T(x) = P(s_{3rel}(x) > T(x)) = 1 - P(s_{3rel}(x) < T(x)) \approx \exp\left(-\frac{1}{2}\left(\frac{T(x)}{\sigma_{s3rel}(x)}\right)^2\right) \dots (9.24)$$

The number of emergencies within a time period, t , can then be assessed by

$$N_T = \frac{t}{T_{02s3rel}} P_T(x) \dots (9.25)$$

Thus if $T = F_b = 10$ m, and all other conditions also are the same as above, then it must follow that $N_T = N_{gw}$.

9.8 Probability of Slamming

As told in Paragraph 6.8 slamming will appear when the ship's bottom has risen out of the wave and hits back at re-entry. For slamming to occur the relative velocity at re-entry must exceed a threshold velocity, v_0 . The first probability is given by (9.24) the second probability must be assessed by the relative velocity response. To treat this problem we form the transfer function for the relative vertical velocity between the ship and the water elevation at any station, x :

$$\hat{s}_{3relvelc}(\omega, \theta, x) = -j\omega(\hat{\eta}_{3c}(\omega, \theta) - x\hat{\eta}_{5c}(\omega, \theta) - \hat{\zeta}_c(x, \theta)) \dots (9.26)$$

Where as before $\hat{\zeta}_c(x, \theta) = ae^{j(kx \cos(\theta) + \varepsilon)}$ is the complex amplitude of wave elevation at station x .

The transfer function becomes

$$T_{s3relvel}(\omega, \theta, x) = -j\omega \left(\frac{\hat{\eta}_{3c}(\omega, \theta) - x\hat{\eta}_{5c}(\omega, \theta) - \hat{\zeta}_c(x, \theta)}{a} \right) \quad \dots(9.27)$$

and the response spectrum

$$S_{s3relvel}(\omega, \theta, x) = |T_{s3relvel}(\omega, \theta, x)|^2 S(\omega). \quad \dots(9.28)$$

Examples of response spectra for the vertical relative velocity are shown in Figure 9.12.

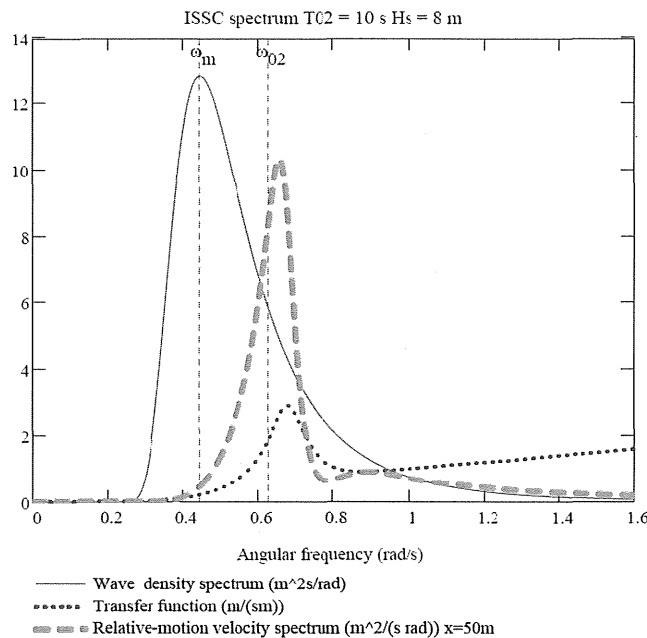


Figure 9.12 Response spectrum of relative vertical velocity at bow.

As the relative vertical position and the vertical relative velocity can be shown to be statistically uncorrelated processes (Jensen^{xlviii}, 2001) the probability of slamming is

$$P_{slam}(x) = [P(s_{3rel}(x) > T(x))][P(s_{3relvel}(x) > v_0)] \approx \exp \left\{ -\frac{1}{2} \left[\left(\frac{T(x)}{\sigma_{s3rel}(x)} \right)^2 + \left(\frac{v_0}{\sigma_{s3relvel}(x)} \right)^2 \right] \right\} \quad \dots(9.29)$$

The number of slamming occurrences within a time period, t , can be assessed by

$$N_{slam} = \frac{t}{T_{02s3rel}} P_{slam}(x). \quad \dots(9.30)$$

For $H_s = 8$ m, $T_{02} = 10$ s, $T = 10$ m, threshold velocity $v_0 = 2$ m/s, $x = 50$ m and zero heading, the standard deviation is $s_{3relvel} = 2.17$ m/s and the response mean upcrossing period $T_{02s3rel} = 9.4$ s. This gives the number of slamming occurrences per hour $N_{slam}/t = 2.31/\text{hr}$ or equivalently one occurrence every 26 minutes. One can also ask how the No of occurrences will change with draught. To do that correctly the motion and velocity transfer functions should be reassessed for each draught, which has not been done here. Approximately it has been illustrated in Figure 9.13 for draughts $\pm 20\%$ of the given draught.

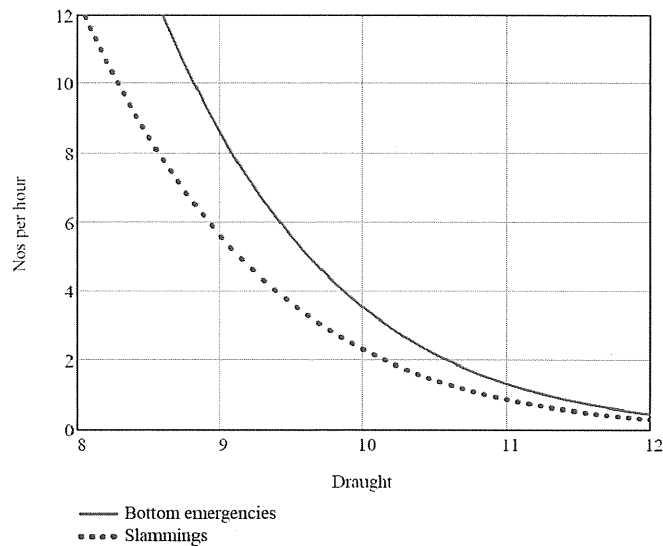


Figure 9.13 No of bottom emergencies and slammings per hour as a function of static draught. Threshold velocity arbitrary set to $v_0 = 2$ m/s.

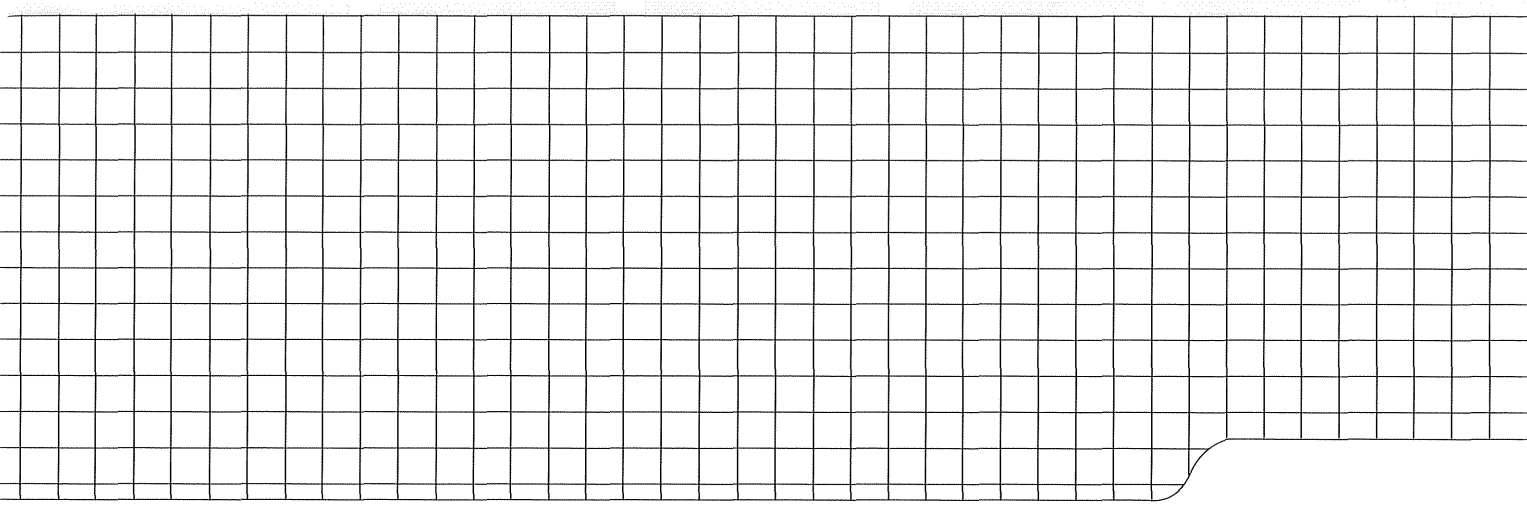
10 REFERENCES

-
- ⁱ Faltinsen, O.M and Michelsen, F.: Motions of large structures in waves at zero Froude number, *International Symposium of Dynamics of Marine Vehicles and Structures in Waves*, ed. R:E:D: Bishop and W:G: Price, pp 91-106, London, Mechanical Engineering Publications Ltd, 1974
- ⁱⁱ Korvin-Kroukovsky, B.V. and Jacobs, W.R.: Pitching and heaving motions of a ship in regular waves, *Transactions SNAME*, 1957
- ⁱⁱⁱ Jensen, J.J., Mansour, A.E. and Olsen, A.S.: Estimation of ship motions using closed-form expressions, *Ocean Engineering* 31 (2004) 61-85
- ^{iv} Jensen, J.J. and Pedersen, T.P.: Wave-Induced Bending Moments in Ships – A Quadratic Theory, *Trans. The Royal Institute of Naval Architects*, 1978
- ^v Roy R. Craig, Jr.: *Structural Dynamics*, John Wiley & Sons, New York, 1981
- ^{vi} J. B. Roberts and P. D. Spanos: *Random vibration and statistical linearization*, John Wiley & Sons, Chichester, 1990
- ^{vii} William T. Thompson: *Theory of Vibration with Applications*, Prentice-Hall Inc., Englewood Cliffs, 1972
- ^{viii} Bathe, K.J. and Wilson E.L.: *Numerical Methods in Finite Element Analysis*. Prentice-Hall, Inc., Englewood Cliffs, New Jersey (1976).
- ^{ix} Cummins 1962
- ^x van Oortmerssen
- ^{xi} Bergdahl och Johansson 1988
- ^{xii} Rouse, Daily-Harleman
- ^{xiii} Rouse, Daily-Harleman
- ^{xiv} Rouse, Daily-Harleman
- ^{xv} Wiegel, R. (1964): *Oceanographical Engineering*, Prentice Hall, Englewood Cliffs, N.J., USA
- ^{xvi} Dean, R.G. and Dalrymple, R.A., 1991: *Water wave mechanics for engineers and scientists*, *World Scientific*
- ^{xvii} LeMéhauté
- ^{xviii} Skjelbreja and Henriksen
- ^{xix} Airy, B.G. (1845): *Tides and waves*, *Encycl. Metrop.*, London

- ^{xx} Krogstad and Arntsen (2002): Linear wave theory www.ntnu.no Visited 2004-03-05.
- ^{xxi} Chakrabarti, S.K. (1987): *Hydrodynamics of offshore structures*, Computational Mechanics Publications, Springer-Verlag
- ^{xxii} CERC (1984): *Shore protection manual*, U.S. Army Coastal Engineering Research Center
- ^{xxiii} William, J.M. (1985): *Tables of progressive gravity waves*, Pitman Publishing Ltd, ISBN 0-273-08733-9
- ^{xxiv} Dean, R.G. (1974): *Evaluation and development of water wave theories for engineering application*, Volume I, Presentation of research results, US Army, Corps of Engineers, Coastal Engineering Research Center, Special Report No 1, Nov 1974
- ^{xxv} Kinsman, B. (1965): *Wind Waves*, Prentice Hall, Englewood Cliffs, N.J., USA
- ^{xxvi} Silvester, R. (1974): *Coastal Engineering, 1*, Developments in Geotechnical Engineering, Vol. 4A, Elsevier, Amsterdam
- ^{xxvii} Faltinsen, O.M. (1990): *Sealloads on ships and offshore structures*, Cambridge University Press, ISBN 0 521 37285 2
- ^{xxviii} Johansson, Mickey, *Barrier-type breakwaters, Transmission, reflection and forces*, PhD Thesis, Report Series A:19, Department of Hydraulics, Chalmers University of Technology, ISSN 0348-1050
- ^{xxix} *Principles of Naval Architecture* (1967), Ed. John P. Comstock, The Society of Naval Architecture and Marine Engineers, Library of Congress Catalog Card No. 67-20738. Ch. IX, p 642 & 645
- ^{xxx} Salvesen, N., Tuck, E.O. and Faltinsen O.M. (1970), Ship motions and sea loads, *Trans. SNAME*, 78, 250-87
- ^{xxxi} Jensen, J.J., Mansour A.E. and Olsen A.S. (2004): Estimation of ship motions using closed-form expressions, *Ocean Engineering*, 31, 61-85
- ^{xxxii} *ITTC – Recommended Procedures and guidelines*. Testing and extrapolation methods for responses, sea keeping, sea keeping experiments, 7.5-02, 07-02.1 2005
- ^{xxxiii} Hasselmann, K. et al. (1973): Measurements of wind-wave growth and swell decay during the joint North sea wave project (JONSWAP), *Ergänzungsheft zur Deutschen Hydrographischen Zeitschrift*, Reihe A(8°), Nr 12, Deutsches Hydrographisches Institut, Hamburg

- ^{xxxiv} Tucker, M.J., Cahallenor, P.G. and Carter, D.J.T., (1984): Numerical simulation of a random sea: a common error and its effect upon wave group statistics, *Applied Ocean Research*, 1984, Vol. 6, No. 2
- ^{xxxv} Oljedirektoratet (NPD, Norwegian Petroleum Directorate): *Vejledning om laster og lastvirkninger til forskrift om bærende konstruksjoner i petroleumsvirksomheten*, utgitt av Oljedirktoratet 7.2 1992
- ^{xxxvi} Bedford, T. and Cooke, R., 2001: *Probabilistic Risk Analysis, Foundations and Methods*, Cambridge University Press
- ^{xxxvii} Graham, L. Phil, 1995: *Safety Analysis of Swedish Dams: Risk Analysis fo the Assessment and Management of Dam Safety*, Licentiate Thesis, Division of Hydraulic Engineering, Department of Civil and Environmental Engineering, Royal Institute of Technology. Stockholm.
- ^{xxxviii} Det norske Veritas: *Position Mooring (POSMOOR), Rules for the Classification of Mobile Offshore Units*; Part 6, Chapter 2, July 1989.
- ^{xxxix} Health and Safety Executive (UK): *Offshore Installations: Guidance on Design, Construction and Certification*, Section 32, Station Keeping, Draft, November 1991.
- ^{xl} Sjøfartsdirektoratet (NMD, Norwegian Maritime Directorate): *Forskrift av 10. januar 1994 for flyttbare innretninger med produksjonstekniske installasjoner om bord*. (Regulations of 10 January 1994 for Mobile Units with Technical Installations for Production on board)
- ^{xli} Hogben, N.,Dacunha, N.M.C. and Olliver, G.F. (1986): *Global wave statistics*, British Maritime Technology, Unwin Brothers Ltd., UK
- ^{xlii} Nordenström, N. (1973): *A method to predict long-term distributions of waves and wave-induced motions and loads on ships and offshore structures*, DnV Publication No. 81, April 1973.
- ^{xliii} The Nordic Cooperative Project, *Assessment of Ship performance in a Seaway*, ISBN 87-982637-1-4, 1987
- ^{xliv} Graham, R. (1990): Motion-Induced Interruptions as Ship Operability Criteria, *Naval Ship Engineers Journal*, p65-71, 1990
- ^{xlv} Bingham, H. (2000): A hybrid Boussinesq-panel method for prediction the motion of a moored ship, *Coastal engineering*, 40(2000) 21-38
- ^{xlvi} Criteria for movements of moored ships in harbours, A practical guide, PIANC, PTC II, Report of working group no. 24, Supplement to Bulletin no. 88, 1995.
- ^{xlvii} Skibsbevægelser i havne. (Ship motions in harbours), Nordisk ministerråds embedsmandskomité for transportspørsmål (Official Committee of the Nordic Council on Transport Questions), Nov 1986

^{xlviii} Jensen, J.J. (2001): *Load and global response of ships*, Elsevier Ocean Engineering Book Series, Vol. 4



20

CHALMERS UNIVERSITY OF TECHNOLOGY
SE 412 96 Göteborg, Sweden
Phone: + 46 - (0)31 772 10 00
Web: www.chalmers.se